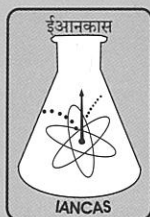
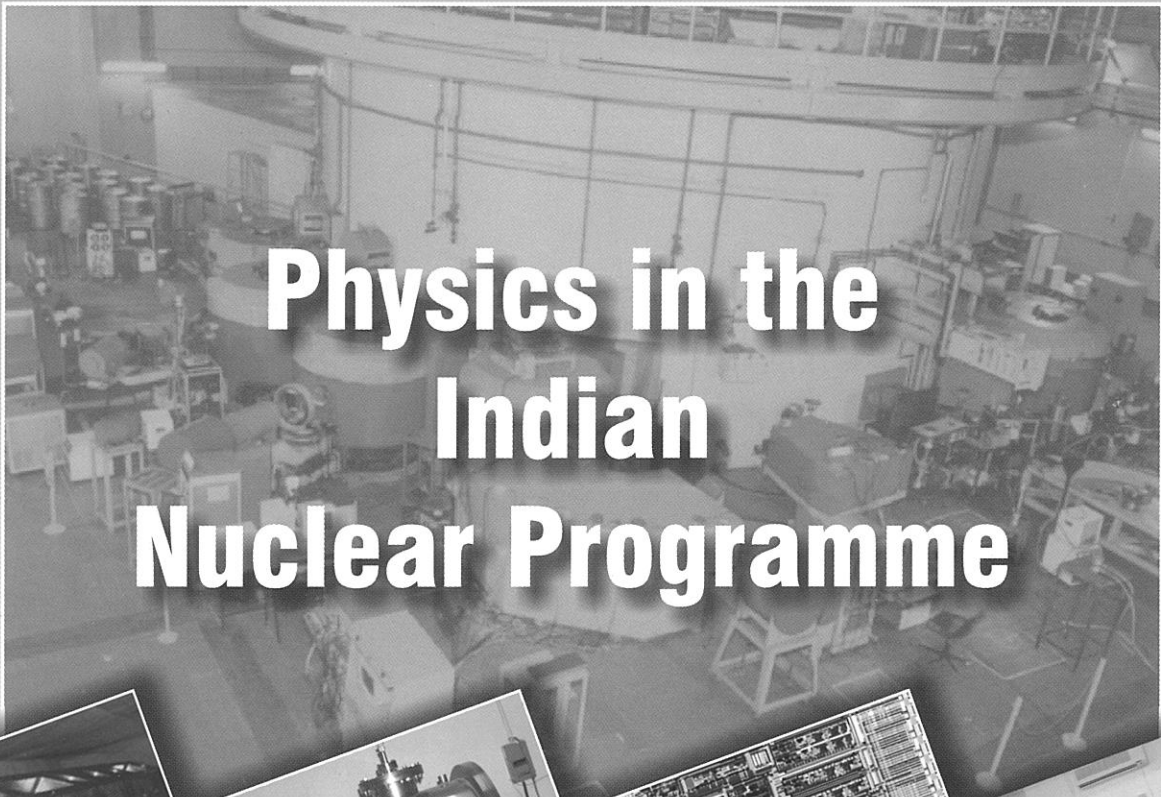


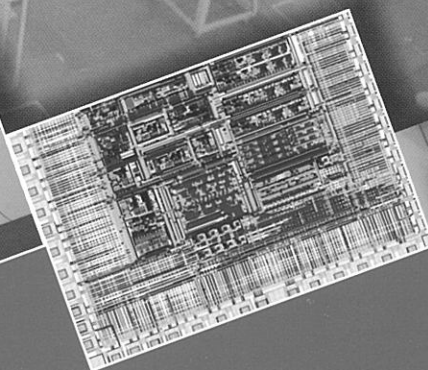
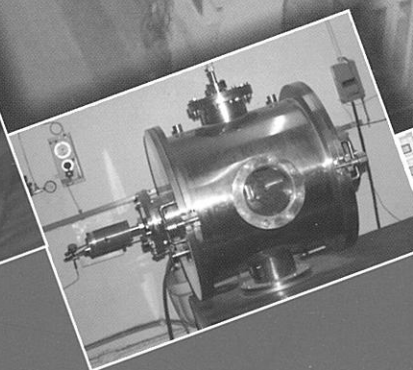
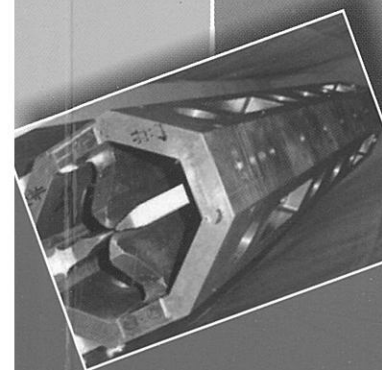
IANCAS Bulletin



INDIAN ASSOCIATION OF NUCLEAR CHEMISTS
AND ALLIED SCIENTISTS



Physics in the Indian Nuclear Programme



Editorial

Physics is the backbone of science. Indian physicists have contributed immensely to the mission-oriented programs of the Department of Atomic Energy (DAE) and helped it to occupy a pre-eminent place in the science and technology scene of our country. The current bulletin was planned to showcase the role of physics in the Indian nuclear program. The task being difficult, required meticulous planning and coordination from a very eminent physicist. On behalf of IANCAS, I express my sincere gratitude to Dr. S. Kailas for readily agreeing to be the Guest Editor for this bulletin and for the dedicated follow up for shaping the articles in proper perspective. As this bulletin is covering a wide range of topics from eminent physicists the total number of pages has doubled. The editorial board took a decision to publish this issue in color, as a special bulletin covering 2 quarters. I hope this special issue will be greatly enjoyed by our readers.

CONTENTS

From the Secretary's Desk	2
IANCAS Awards	3
Dr. Tarun Datta Memorial Award	9
IANCAS - Prof. H.J. Arnikaar - Best Thesis Award	11
Guest Editorial	15
Some Condensed Matter and Materials Science Research in DAE	17
<i>S.K. Sikka</i>	
Nuclear Data Physics Needed to Develop Advanced Nuclear Energy Systems	25
<i>S. Ganesan</i>	
High Energy Density Systems – Physics & Modelling	35
<i>S.V.G. Menon, Aditi Ray, Bishnupriya Nayak, Chandrani Bhattacharya, Karabi Ghosh, G. Kondayya, Madhusmita Das, A. Sai Venkata Ramana, M.K. Srivastava, Vinod Kumar</i>	
Lasers in Nuclear Energy Programme	45
<i>B.N. Jagatap</i>	
Plasma Physics and Technologies in DAE	56
<i>A. K. Das</i>	
DAE's Accelerator Physics Programme Relevant to Nuclear Energy	68
<i>V.C. Sahni</i>	
Modern Nuclear Instrumentation: Advances in Sensors and Electronics Development	75
<i>V.B. Chandratre, Menka Sukhwani, R.S. Shastrakar, K.M. Sudheer, V. Shedam, Sourav Mukhopadhyay, V.D. Srivastava, S. Khole, Shiv Kumar, Anubha Keni, Veena Salodia, Aditya Darad</i>	
Imaging Techniques using X-rays, Gamma and Neutron	89
<i>Amar Sinha, Yogesh Kashyap, P.S. Sarkar, Tushar Roy</i>	
Nuclear Reaction Analysis: Principles and Applications	101
<i>V.S. Raju and Sanjiv Kumar</i>	
An Overview of Radiological Safety in Nuclear Installations	110
<i>P.K. Sarkar</i>	

Some Condensed Matter and Materials Science Research in DAE

S.K. Sikka

Homi Bhabha Chair Professor, Bhabha Atomic Research Centre, Mumbai 400 085

Abstract

Searching for new materials, understanding their properties and then tailoring them for use for a specific purpose is the basic aim of condensed matter and materials science research and development. This paper describes some examples of such research carried out in the constituent units of DAE.

Introduction

There is an intimate relationship between Condensed Matter Physics and Materials Science. The former attempts to understand the properties of large collections of atoms in condensed form, by using a combination of experimental, theoretical and computational techniques. Materials Science combines research with innovation, to optimize and tailor a material for a specific application. Both these sciences have resulted in a far-reaching impact on the way we live on this planet, and have had a huge influence on other disciplines) chemistry, biology, earth and planetary sciences, nuclear and defence sciences etc. This write-up will describe some of the research results, of condensed matter and materials sciences (CMMS) in Department of Atomic Energy (DAE).

DAE is a mission-oriented agency with the main mandate to help India achieve energy and national security. To fulfill this mission, it has built various kinds of nuclear power plants and supporting infrastructure, and gained mastery over the entire fuel cycle. It is obvious that this has required research and development of special materials, which would have to withstand the harsh in-service environments: high temperatures, neutron irradiation, interaction with coolant, fission products and hydrogen gas etc. These may lead to hardening, embrittlement and dimensional changes in a material. There may also be precipitation, agglomeration and hydride formation. All these have strong connection to the safety requirements and whole life behaviour. Thus, right from beginning, CMMS activity has been accorded a special status in DAE. Towards this end, DAE has set up some major facilities for research. These include DHRUVA and CIRUS reactors at BARC, INDUS 1 & 2 synchrotrons at RRCAT and particle accelerators at BARC, IGCAR and VECC. There are also extensive local level amenities like electron microscopy, spectroscopy, diffraction, laser processing, and also the amenities for research, employing magnetic fields and at elevated and low temperatures. Wide-ranging fabrication and characterization tools and high performance computational resources back these. Some of the research areas are one of a kind in India. A prime example of this, is the neutron beam research using nuclear reactors. Sometimes, the mission-related activities of DAE have needed basic research to be started in a particular field. For example, high-pressure and shock-wave physics for design of nuclear weapons (termed as directed basic research by Chidambaram [1]).



Fig. 1 Some neutron scattering instruments around the Dhruva reactor at BARC. The Solid State Physics Division of BARC operates a national facility for neutron beam research around these instruments.

There have been also some spin offs. These may be illustrated by some examples. In neutron beam research, the diffractometers and spectrometers were all designed and built locally. As this activity shifted from APSARA to CIRUS and then to DHRUVA to make use of higher neutron fluxes for experiments, the instruments, which were in the beginning manually operated, were converted into well-engineered, high precision, fully automatic computer controlled ones. Fig. 1 shows some of these neutron scattering instruments around the reactor in DHRUVA [2]. This, in fact, laid the foundation of the instrumentation building culture in DAE, and proved very handy when there was a foreign-exchange crunch, or embargos imposed after our nuclear tests. When, it was required to build beam-line instrumentation for use of INDUS1 and INDUS2 synchrotron radiation sources, this experience, again, proved very valuable (see Fig.2 for one such beam-line and the measured diffraction pattern as a function of pressure of uranium [3] - note this sample would not have been permitted for an Indian in a source abroad). Many of the designed components were manufactured in the Central Workshops in various units of DAE. Similarly, for nuclear weapon design, high performance computers were required and which the foreign vendors denied to DAE establishments. Our computer engineers and scientists rose to the occasion, to build faster and more powerful computers over a period of time. Now, in BARC, the available computing power is near 10 TFLOPS [4].

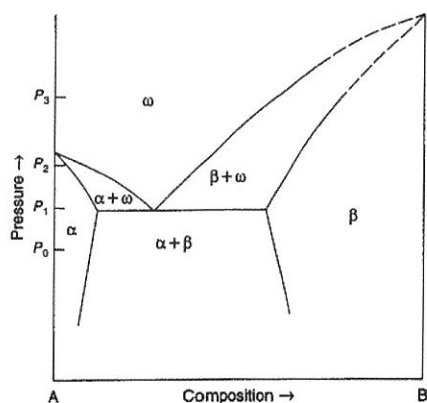


Fig. 3 Metastable pressure – composition (P - X) phase diagram of group IV elements Ti, Zr, Hf and their alloys with d rich transition elements.

Initially, this was done by empirical means [17]. Over a period of time, both experimental techniques as well as theoretical tools were set up. Diamond anvil cells for static pressure generation, gas gun, high explosives and laser-based techniques for shock-wave generation were developed. Fig. 4 displays one such application for the pink granite rock in the India's thermonuclear test emplacement hole in 1998. First principles electron structure methods were also used to compute the equation of state, phase stability and opacities of materials used in nuclear devices. All these led to the development of the state-of-art computer-codes for design, simulation and yield estimates of nuclear explosives. A large number of materials have now been studied [18]. Here, we will confine to applications for some actinides.

In the series of actinide metals, there is a progressive filling up of $5f$ electrons. Physical properties data show that this series must be split into two. At 0.1 MPa, the $5f$ electrons are itinerant in Pa, U and Np and participate in bonding, like the d electrons in transition elements. The elements from Am onwards, contain localized $5f$ electrons. Pu is at the boundary between the two sets. In Th, in which there are no $5f$ electrons at 0.1 MPa and only at high pressure, the $5f$ levels fall below the Fermi level, Rao et al [19] showed that hybridization effects between $5f$ and other levels are still required to reproduce the experimental measured EOS (see Fig.5). The shock equation of state of U, up to 15 Mbar, to which p - v data was measured by various techniques at Trombay, could also be reproduced by first principles DFT calculations [20]. It was also shown that the $5f$ electrons become fully delocalized only above 40 GPa in α -Pu, after a phase change to the distorted α -U structure [21]. For ambient and high temperature phases of Pu, it is now known, for some time, that the conventional DFT theories do not work. The use of LDA+U (U = Hubbard like Coulomb repulsion between $5f$ electrons) method [22] for δ -Pu and α -Pu, however, reproduces the structural parameters, bulk modulus, the Debye temperatures etc. measured recently by the Los Alamos group [23].

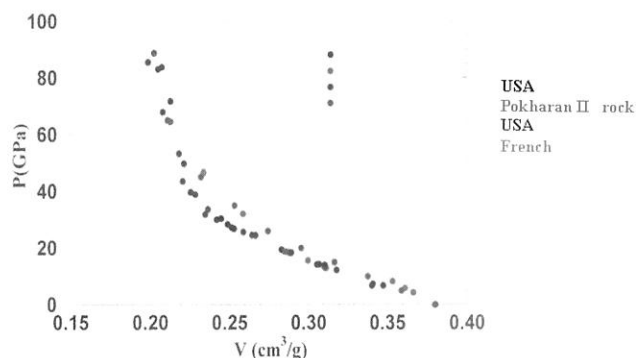


Fig. 4 Shock Pressure vs. volume data for a POK-II pink granite rock compared to USA and French Sahara granite rocks.

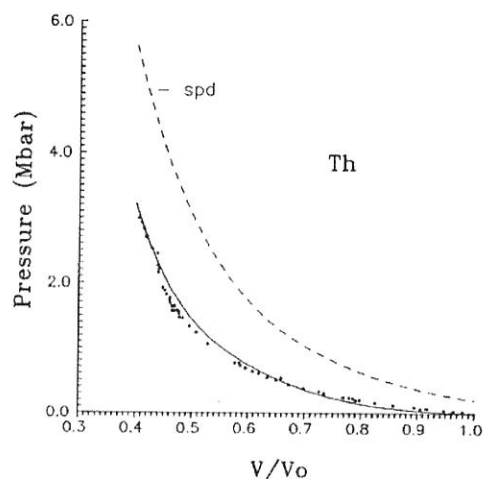


Fig. 5 The computed 0 K isotherm of thorium compared to the experimental data. The curve marked *spd* is for the case when the f -electron contribution is suppressed in the calculations.

Small-angle Neutron Scattering Study of a Maraging Steel

Because of high strength and toughness, coupled with good corrosion resistance, maraging steels (iron alloys with Cr, Ni, Mo with small amounts of Ti, Al and almost C free), are used for many challenging applications, including nuclear. The presence of strong carbide formers such as Mo and Cr does not exclude the possibility of the incidence of un-dissolved carbides in their quenched structures. It is known that the occurrence of carbides can significantly influence their fatigue properties. At Trombay, Sen et al [24] have used small angle neutron scattering (SNS) to look for these precipitates. Fig. 6 shows SNS profiles for the specimens of a solution quenched PH13-8 Mo steel sample. It points to the isotropic distribution of the precipitates, as the measured structure factor $S(q)$ remains invariant with the orientation of the specimen. The size distribution of the precipitates, has been characterized by assuming different poly-dispersive (cylindrical or parallelepiped) models.

6. I.K. Gopalakrishnan, P.V.P.S.S. Sastry, K. Gangadharan, J.V. Yakhmi, G.M. Phatak and R.M. Iyer, Appl.Phys.Lett.53 (1988) 414
7. R. Mittal, S.L. Chaplot, S.K. Mishra and P.P. Bose, Phys. Rev. B75 (2007) 174303
8. T. R. Ravindran, A.K. Arora and T.A. Mary, Phys. Rev. Lett. 84 (2000) 3879
9. S.M. Sharma and S.K. Sikka, Prog. Mater. Sci., (1996) 1.
10. S.M. Sharma, P.V. Taradesai, S. Karmakar, S.K. Sikka, A.K. Sood, A. Govindraj and C.N.R. Rao, Phys.Rev. B63 (2001) 205417
11. S. Banerjee, P. Mukhopadhyay, in "Phase Transformation in Alloys Examples from Titanium and Zirconium", Pergamon, U.K. (2007)
12. R. Tewari, D. Srivastava, G.K. Dey, J.K. Chakravarty, and S. Banerjee, J. Nucl. Mat. 383 (2008) 153
13. J.S. Gyanchandani, S.C. Gupta, S.K. Sikka and R. Chidambaram, High Press. Res. 4 (1990) 472
14. G. Jyoti, K.D. Joshi, S.C. Gupta, S.K. Sikka, G.K. Dey and S. Banerjee, Philos. Mag. Lett. 75 (1997) 291.
15. Y.K. Vohra, E.S.K. Menon, S.K. Sikka and R. Krishnan, Acta Met. 29 (1981) 457
16. S.K. Sikka, Y.K. Vohra and R. Chidambaram, Prog. Mater. Sci., 27 (1982) 245.
17. R. Chidambaram and S.K. Sikka, BARC internal report (unpublished)
18. S.K. Sikka, B.K. Godwal and R. Chidambaram, In High Pressure Shock Compression of Solids III, ed. By L. Davison M Shahinpoor, (1997) Springer (NY).
19. R.S. Rao, B.K. Godwal and S.K. Sikka, Phys. Rev. B46 (1992) 5780
20. B.K. Godwal, R.S. Rao, A.K. Verma, M. Shukla, H.C. pant and S.K. Sikka Laser and Particle Beams 21 (2003) 523
21. S.K. Sikka, Solid State Communications 133 (2005) 169
22. A.K. Verma, private communication.
23. I. Stroe, J.B. Betts, A. Trugman, C.H. Mielke, J.N. Michell, Mramos, F.J. Freobert, H. Ledbetter, A Migliori, J. Accoust. Soc. Am. 127 (2010) 741
24. D. Sen, A.K. Patra, S. Mazumder, J. Mitra, G.K. Dey and P.K. De, Mater. Sci. Engg, A397 (2005) 370
25. S. Mazumder, D. Sen, A.K. Patra, S.A. Khadelkar, R.K., R.M. Cursetji, R. Loidl, M. Baron and H. Rauch, Phys. Rev. Lett. 93, (2004) 255704
26. Baldev Raj, S.L. Mannan, P.R. Vasudeva, and M.D. Mathew, Sadhna,27 (2002) 527
27. C. David B.K. Panigrahi, G. Amarendra, S. Abhaya, S. Balaji, A.K. Balamurugan, K.G.M. Nair, B. Viswanathan, C.S. Sunder and Baldev Raj, Surface and Corrosion Technology 203 (2009) 2363
28. C. David, B.K. Panigrahi, S. Balaji, A.K. Balamurugan, K.G.M. Nair, G. Amarendra, C.S. Sundar and Baldev Raj, J. Nucl. Mat. 383 (2008) 132
29. B. P. Mandal and A.K. Tyagi, BARC Newsletter, March – April (2010) 6
30. S. Saha, D.V.S. Muthu, C. Pascanut, N. Dragve, R. Suryanaryan, G. Dhalenne, A. Revochevschi, S. Karmakar, S.M. Sharma and A.K. Sood, Phys. Rev. B74 (2006) 064109
31. C. B. Basak, R. Keswani, G.J. Prasad, H.S. Kamath and N. Prabhu, J.Alloy and Comp. 471 (2009) 544
32. M. Kiran Kumar, S. Aggarwal, V. Kain.T. Saario, and M. Bojinov, Nucl. Eng. And Design, 240 (2010) 985
33. S. Kailas, in "Accelerator Driven System in the Nuclear Power Programme", Indian Nucl. Soc. News, 6 (2009), 3
34. Chintamani Das and R. Fotedar, Internal Report, Materials Processing Division, BARC 2008
35. S.C. Gadkari, Crystal Technology Section. Technical Physics Division, BARC -personal communication
36. S. Mohan, S. Mishra, K. Bhanja, S. Naik, and R. Kumar- submitted for publication
37. H.K. Poswal, S.M. Sharma and S.K. Sikka, High Press. Res. 30 (2010) 198
38. P. Goel, N. Choudhury, S.L. Chaplot, J. Nucl. Mat. 377 (2008) 438
39. S.L. Chaplot and S.K. Sikka, Phys. Rev. B61 (2000) 11205
40. P.V. Durgaprasad, B.K. Dutta, H.S. Kushwaha and S. Banerjee, Nuc. Eng. Des (2010) in press
41. B.K. Dutta, N.Naveen Kumar and P.V. Durgaprasad- under publication
42. Nuclear Technology Development- Atoms with Mission, ed. Baldev Raj, Chapter 4 "From ore to core-competence in materials technology" (2004) p.161
43. BARC highlights 'Materials Science and Engineering' ed. A.K. Suri (2006)



Dr. Satinder Kumar Sikka (1942 born) is from the 4th Batch of the Training School of Bhabha Atomic Research Centre. From August 1961 to November 2002, he worked at BARC in the fields of neutron and x-ray crystallography, high pressure and shock wave physics and participated in conducting the Indian nuclear explosions of 1974 & 1998. He was the leader of the design team for the 1998 nuclear test series. He has published 150 papers in referred journals. At BARC, he was Director of Atomic and Condensed Matter Physics Group. From 2002-2008, he was the Scientific Secretary to the Principal Scientific Advisor to the Government of India. Presently, he is Homi Bhabha Chair Professor at BARC. He has been a Member of the Editorial Board of the journal 'High Pressure Research' from 2002 and was a Consultant to the Commission on High Pressure of International Union of Crystallography from 2002-2006. He has also been Chairman of National Committees of INSA for IUCr and CODATA. Dr. Sikka was awarded 'Padma Shri' in 1999. He is a Fellow of all the three national science academies. Among the other prominent awards received by him are: H.K. Firodia Award for Excellence in Science & Technology (1998), MRSI-ISCS Superconductivity and Materials Science Annual Prize (2001), M.M. Chugani Award for Excellence in Applied Physics (2002), The Homi Jehangir Bhabha Medal for Experimental Physics of INSA (2005) and Indian Nuclear Society 'Homi Bhabha Lifetime Achievement' Award (2007).

Nuclear Data Physics Needed to Develop Advanced Nuclear Energy Systems

S. Ganesan

Nuclear Data Section, Reactor Physics Design Division, Bhabha Atomic Research Centre, Trombay, Mumbai 400085;
E-mail: ganesan555@gmail.com

Abstract

The article attempts to highlight the great importance of nuclear-data-physics activities to support a robust nuclear energy programme, with particular emphasis in the Indian context.

Introduction

Basic nuclear physics research continues to greatly influence the evolution of nuclear energy and its operation [1-5]. Development of knowledge-base providing accurate description of basic nuclear interactions, is a fundamental and natural part of the evolution of nuclear science and technology. Nuclear energy has been introduced to mankind without adequate knowledge of nuclear data physics that would be demanded by advanced reactor designs. This statement may sound strange, with hundreds of GEN-I, GEN-II and GEN-III reactors operating today, but in this article an attempt will be made to illustrate this understanding with several interesting examples.

The safety and operational requirements of existing power plants have been engineered with a number of one-to-one mockup experiments providing adequate and conservative safety margins. Basic physics understanding and better data physics of nuclear interactions are continuing to be rigorously sought by nuclear design communities in order to extrapolate to states of the power plant, in conditions not covered in one-to-one mock experiments. In the subject area of nuclear data physics, for instance, there is a lot of interest (and challenges) in attempting to quantify nuclear data uncertainties in the form of co-variances to enable error propagations to be assessed in complex simulations.

When physics is ignored or taken for granted in designs and in operations, incidents or accidents are likely to happen, as illustrated in the interesting article of B. L. Cohen [4]. The worst reactor accident of all time that occurred at Chernobyl, USSR, in April of 1986 makes reactor designs to go for physics designs with a negative feedback coefficient of reactivity for all operating conditions, over the entire life of the plant (that is 100 years for GEN-IV and INPRO systems). The educative and interesting physics contents available in detail in Cohen's article [4] are not repeated here to save space.

The research in frontier areas of basic nuclear data physics, associated knowledge management and critical evaluation of associated uncertainties are being rigorously sustained, well supported and pursued further in BARC. The existing strength of currently available, state-of-art nuclear databases in use for various applications is highly commendable but inadequate to meet the nuclear data needs of new reactor concepts, as different neutron energy spectra, materials and compositions are involved. Ready plug-in

libraries from international sources are not sufficient to meet all our needs. For instance, the fusion evaluated nuclear data (FENDL) libraries [6] created through successful international co-ordination by the IAEA and tailored to meet the design needs of the International Thermonuclear Experimental Reactor do not cover) by design) actinides and hence cannot be straightaway utilized for design studies of fusion-fission hybrids. The experience in creating databases such as FENDL revealed that a large amount of work would also be essential in order to create ENDF/B formatted evaluated nuclear data files using new experimental data. These tasks included EXFOR [7] compilations, follow up with critical evaluation, production of new ENDF/B formatted libraries extending to higher energies, and quality assured nuclear data processing activities to provide the designers/users/ of innovative systems with "ready to plug-in" processed data, that are integrally validated, for use in applications.

General Remarks on Nuclear Data Physics

"Nuclear data" is a technical term that stands for quantitative results of scientific investigations of the nuclear properties of matter. These numerical data describe quantitatively the physics properties of atomic nuclei and the fundamental physical relationships governing their interactions, thereby characterizing the physical processes underlying all nuclear technologies.

The scope of nuclear data collections includes all 85 natural elements with 290 stable isotopes and more than 2500 radioactive nuclides. There are hundreds of different nuclear and atomic physics databases evolved over years of efforts and measurements. The online nuclear data services (<http://www-nds.indcentre.org.in>) that mirror the nuclear data website of the International Atomic Energy Agency (IAEA), Vienna (<http://www-nds.iaea.org>) commissioned in Mumbai in November 2004 provide the best recommended data for the user community.

For technical handling and convenience, the nuclear data are commonly categorized into two main groups:

1. Nuclear reaction data, describing the interactions of various energetic projectiles such as neutrons, protons or photons with target nuclei, and
2. Nuclear structure and decay data, which provides numerical values of nuclear energy levels, half-lives and radioactive decay radiations.

Obviously, new concepts of reactor designs will have a sound scientific basis if the nuclear data used are accurate.

Applications of nuclear data include all areas of nuclear science and technology, covering energy applications (fission reactor design; nuclear fuel cycles; nuclear safety; reactor monitoring and fluence determination; waste disposal and transmutation; accelerator-driven systems; fusion device design and plasma processing technologies) as well as non-energy applications (cancer radiotherapy; production of radioisotopes for medical and industrial applications; personnel dosimetry and radiation safety; nuclear safeguards; environmental monitoring and clean-up; materials analysis and process control; radiation damage studies; detection of concealed explosives and illegal drugs; exploration for oil and other minerals) and basic research (e.g. nuclear astrophysics) and education. See Ref. [8, 9] for more details.

What are the Topics in Nuclear Data Physics?

Many of the concepts such as “evaluation of basic data”, “EXFOR compilations”, Integral criticality benchmarking” etc., are new initiatives in India since historically reactor physics studies in India started from the point of using ready “plug-in” (and processed) nuclear data libraries.

The topics in nuclear data physics in India, as presented below, cover a wide range of power and non-power applications in the Indian context, with a balance of basic and applied nuclear data physics activities by a well-defined team of nuclear physicists, nuclear engineers (that include reactor physicists), mathematicians, radiochemists and software information management.

- Indian experimental generation of basic physics data. See, for instance, refs [10-13]. Indian leadership recognizes that experimental studies require good quality research facilities to determine nuclear cross sections covering neutron and charged-particle reactions, and nuclear structure and decay data (all with well-defined uncertainties and to high accuracy), with the ability to cover the nuclear data physics needs for advanced fission and fusion systems (that also has thorium fuel and closed fuel cycle), analytical science and nuclear medicine. This involves, because of the need for neutron sources and particle accelerators, significant costs and capital outlay, and all nuclear physicists by default would provide the expertise to undertake facility development tailored to nuclear data physics measurements.
- Compilations of nuclear physics data generated by experiments in India and training workshops in EXFOR (More than 125 Indian EXFOR entries based upon Indian nuclear physics experiments since 2006 have been made and accepted by the IAEA. The Indian EXFOR data compilation activity has increased international visibility to India’s work in nuclear physics data generation. India offers to collaborate with other network of reaction data centres and help host more such training workshops on

international co-ordination of EXFOR compilation activity in the coming years. Presently, as a member of NRDC, BARC (NDPCI) plans to continue the EXFOR compilation activity and take up more responsibilities in co-ordination with the IAEA and NRDC network.). [14].

- Computerized visualizations [15].
- Large nuclear data files information management [16], IAEA mirror website (<http://www-nds.indcentre.org.in>) at Mumbai and India NDPCI website (to be created soon)
- Evaluations of basic nuclear data which include nuclear model based predictions and generation of covariances.
- Creation of computerized Indian evaluated nuclear data files in ENDF/B format
- Physics-laws-based nuclear data processing for multi-group and Monte Carlo applications to produce “plug-in” nuclear data libraries (seen by reactor physicists as the “nuclear data tables”)
- Integral measurements and validations by use of experimental benchmarks and critical facilities. The task involves performing a number of sensitivity studies, assessment of uncertainties in system characterization and benchmarking to match the QA of the International Criticality Benchmark Evaluation Project of the US-DOE (<http://icsbep.inl.gov>). India has internationally benchmarked criticality of KAMINI [16] and PURNIMA-II [17] research reactors.

Perspectives on Needs of Nuclear Data Physics Research for Advanced Reactor Systems

Developments of new reactor designs in India [18-20] for utilization of thorium, such as the Advanced Heavy Water Reactor (AHWR), especially demand creation of new nuclear data for all the isotopes of thorium fuel cycle. Improved nuclear data are essential to support new initiatives such as the international project on innovative nuclear reactors and fuel cycles (INPRO) that aims to support the safe, sustainable, economic and proliferation-resistant use of nuclear technology to meet the global energy needs of the 21st century. The detailed pursuit of development of Generation IV nuclear energy systems that offer advantages in the areas of economics, safety, reliability and sustainability require significantly improved nuclear data. The development of Accelerator Driven Sub-critical Systems proposed by Carlo Rubbia and others require significant amount of new nuclear data in extended energy regions and improvement of the presently available nuclear data. The quality assurance in design and safety studies in nuclear energy in the next few decades and centuries require new and improved nuclear data with high accuracy and energy resolution.

The basic nuclear-data-physics research has been essential in shaping concepts of nuclear power reactor designs. Nuclear physics is not yet matured enough, for instance, to quantitatively predict neutron induced resolved resonance cross sections in nuclei which can only be determined by high resolution cross section experiments by neutron time of flight methods. Even after more than six

decades since the discovery of nuclear fission process, the basic nuclear physics experimental data is continuing to remain more uncertain than the target accuracies needed by reactor designers who rigorously desire to propagate error in simulations. Therefore, experimental critical facility programme to enable integral validation studies is also an essential part of any serious nuclear programme to speed up implementation of nuclear energy.

Conceptual studies [21] of Accelerator Driven Sub-critical Systems (ADSS) have given a fresh look at the use of thorium fuel cycle in a lead-bismuth coolant environment. The nuclear data requirements for ADSS [3] span energies up to GeV, much beyond the 10 MeV limit used for neutron energies in the design and operation of thermal reactor systems in India and the 15MeV limit used for fast reactors. The basic data files available from the Indian Mirror site for fusion, fast and thermal reactor applications in a majority of cases go up 20 MeV. A number of additional reaction channels open at higher energies. The mirror site maintained in India is expected to provide updates on all data requirements of ADSS systems designed for energy amplification, ultimate disposal of nuclear waste by incineration and thorium utilization extending to energies up to GeV. The need for precise, experimental, neutron-induced and charged particle-induced nuclear data, remains indeed very strong to enable potential economies related, for instance, new fuel designs such as using thorium and higher burn-up (few hundreds of GWD/Te) to be made. The nuclear data of isotopes of thorium fuel cycle, which have not been paid [22] enough attention in the past, until 2000, have been significantly improved in the last decade as a result of international efforts such as the recently concluded IAEA-CRP, entitled "Evaluated nuclear data for Thorium-Uranium fuel cycle". The details of the CRP, the basic and the associated processed "plug-in" nuclear data libraries are available at the website [23].

Nuclear data of minor actinides and fission products are also crucial in international formulation of radioactive transport regulations. These requirements demonstrate the immediate need for experimental research, the results of which would be incorporated with the basic nuclear data.

In late sixties/early seventies, the concept of steam-cooled fast breeder reactors was abandoned as the newly discovered values of "alpha" (ratio of capture to fission cross section) of ^{239}Pu were 2 to 3 times the earlier known values in the keV energy region. The high alpha values in keV region was discovered experimentally by improved measurements and explained qualitatively by the double humped fission barrier model of the nucleus and the associated intermediate structure in the neutron induced fission cross section of ^{239}Pu , arising due to the rapid fluctuations in neutron induced fission width of the 1^+ spin state. This striking example showed that nuclear data physics influences evolution of reactor concepts. More details are available in Ref. [24].

The initial choice of pure ^{233}U as fuel was abandoned in the Indian Compact High Temperature Reactor (CHTR) designs, as its use resulted in calculated positive Doppler reactivity effect in the initial stages.

Why and how does the old WIMSD multigroup library "works well" in many cases? In the early sixties and later, for instance, corresponding to, for instance, the 1971-81 WIMSD multigroup nuclear data libraries, the effective neutron-nuclear interaction cross sections of major fissile and fertile isotopes (^{235}U , ^{238}U and ^{239}Pu) were adjusted to fit the results of several hundreds of integral experiments. During those times, not only the nuclear data had large uncertainties but the computing resources were also limited. In many cases the nuclear data seemed to have been available in greater detail than what the computing resources could accommodate with the approximations in number of multigroups, resonance treatment etc. Not all the adjustments in basic data were justified when improved differential measurements were conducted and results of new basic data became available several years later. It is realized that there are considerable cancellations of errors in using old WIMSD multigroup data sets with the approximations in calculations with limitations in computing power at that time. These "working" procedures in sixties were applicable in a restricted way to only specific systems for the limited burnup and operating parameters that were studied. Today, after more than four decades since the 1971-81 libraries, many of the same experiments can be simulated using the new WLUP IAEA libraries without any adjustment of any of the cross sections. For U-235 for instance, we produce below a plot of "eta" using the XnWLUP software [15]. The values of eta correspond to the infinite dilution cross sections, comparing the 1981 set with ENDF/B-VII.0 based 69 group multigroup cross sections. From physics point of view "eta" represents the net number of neutrons released per neutron absorbed and the effective "eta" over the neutron spectrum is essentially the infinite medium multiplication factor, K_{inf} . The target accuracy in K_{inf} is 1mk and this gives the needed target accuracy for "eta" parameter as 0.1%. We see that the 1981 set and the ENDF/B-VII.0 data set differ by about -11% to 25% in some energy groups. Around the energy of 0.025 eV, the 2006 data is 0.5% larger than the 1981. This is the situation even with the main fissile material that is well investigated. See Fig. 1 and Fig. 2.

It may be noted that even in the case of the main fissile isotope, U-235, the shape of the curve of "eta" was required to be revised in the sub-thermal range, for which no experimental data previously existed, in order to provide better agreement [25] between calculated and measured values of moderator temperature coefficient of reactivity in operating PWRs. Such a recommendation was indeed confirmed based upon improved measurements and implemented in evaluations.

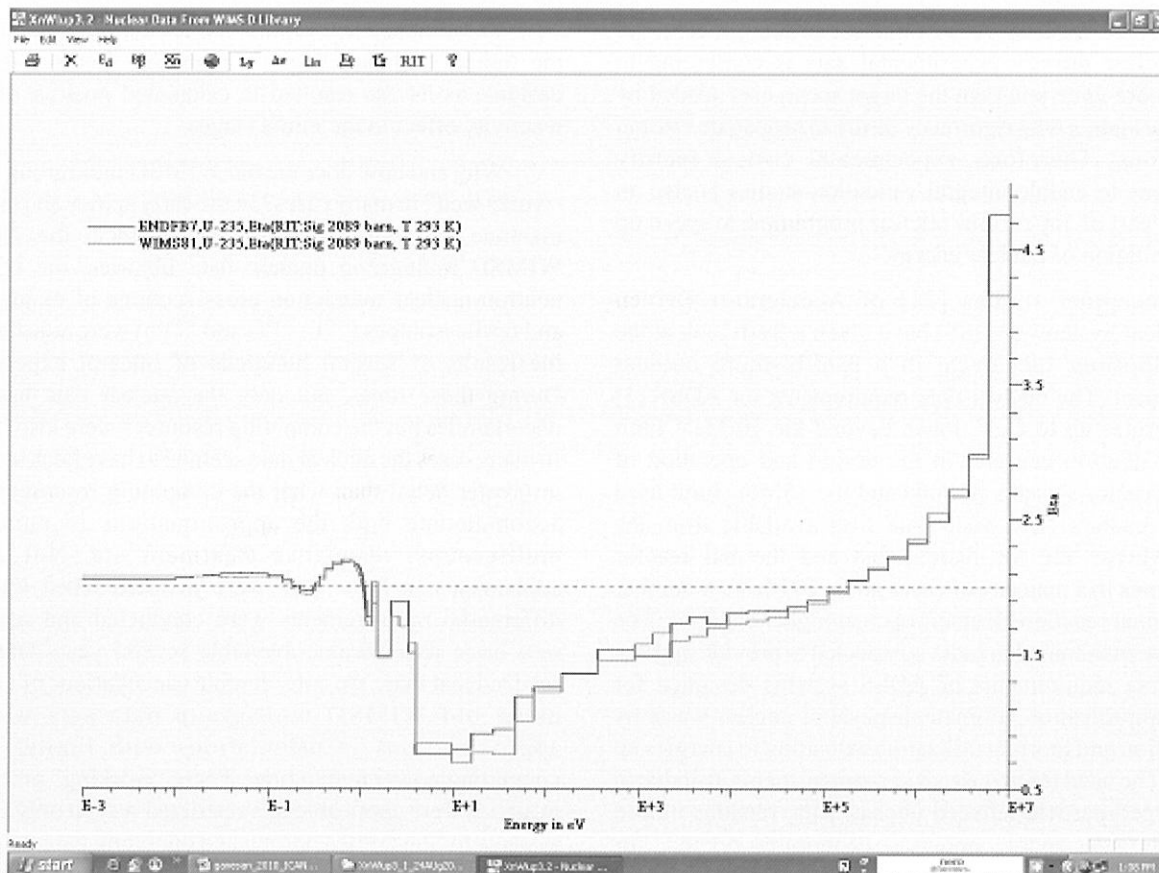


Fig. 1 Comparison of η of ^{235}U

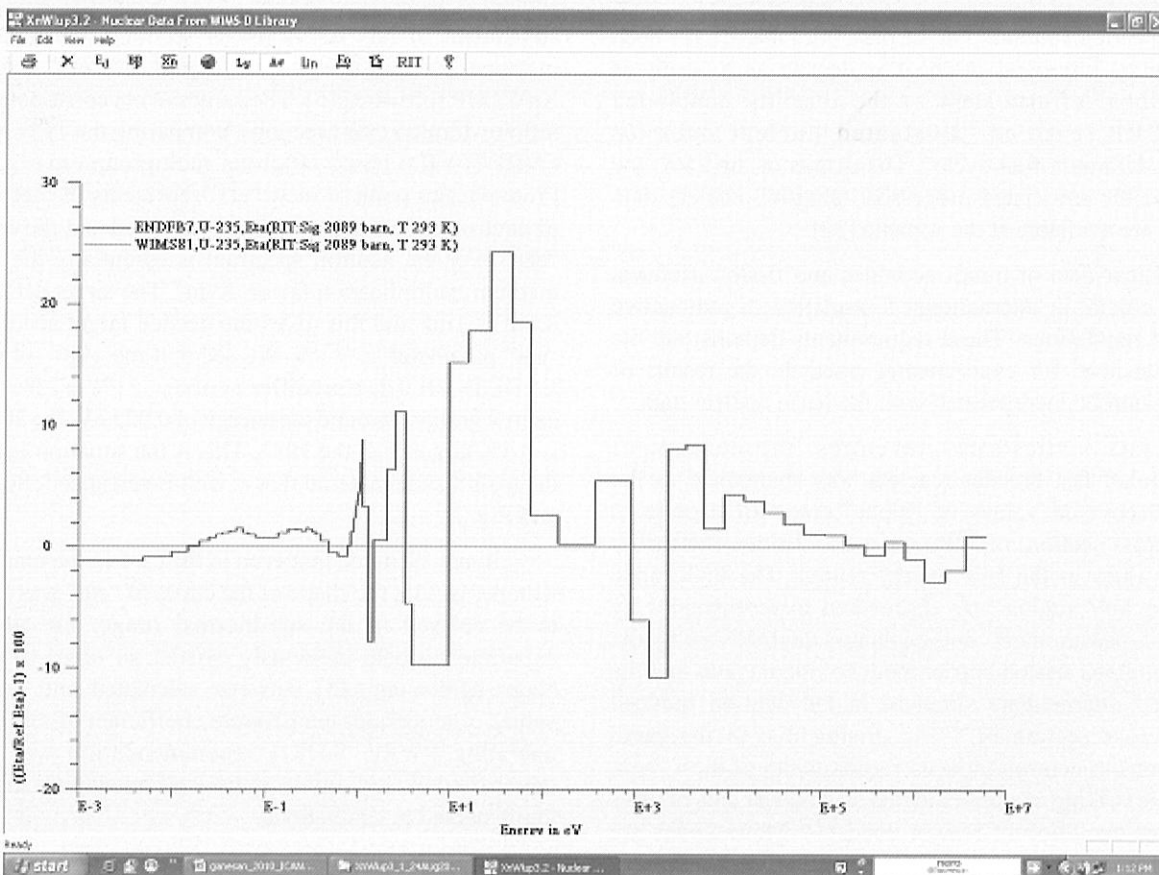


Fig. 2 Comparison of η of ^{235}U shown as ratio of WIMSD (ENDF/B-VII.0) to that of WIMDS1981.

CERN N_TOF Facility

Preliminary research for ADSS use existing nuclear data developed for thermal, fast and fusion reactors and those generated for fundamental physics understanding as in astrophysics.

A new initiative involving more than 40 Institutes including BARC is the on-going Phase-2 experimental campaign at the CERN n_TOF facility [26]. Recently, measurements to accurately determine the (n,γ) cross sections of all stable Fe and Ni isotopes in the neutron energy region between 0.1 keV and 1 MeV has been started at the CERN n_TOF facility. A large “instantaneous” number of neutrons from spallation reactions are produced by the impact of intense proton bunches from the CERN PS (7×10^{12} protons in a 7 ns wide bunch) with an energy of 20 GeV on a massive lead target. The initial neutron bursts are further moderated in a water volume at the exit towards the evacuated neutron beam pipe, which connects the target with the experimental area at a distance (neutron flight path) of about 185 m. The long flight path provides high resolution in neutron energy, which enables resolving s, p, d waves etc., neutron resonances that are closely spaced in energy space. The excellent energy resolution of 0.1% at 30 keV and a neutron intensity of more than 105 neutrons/pulse in the 1 keV-100 keV range make the facility quite unique.

It may be noted that neutron capture (followed by β -decay) is the main nuclear reaction process leading to the formation of elements heavier than iron in the universe. It is known that the “slow neutron capture” or the so called “s” process, which occurs in the interior of stars during the Red Giant phase, is characterized by neutron capture times of about a year, much longer than typical β -decay times. Accordingly, the reaction path of the s process runs along the valley of β -stability and the resulting abundances are directly correlated with the respective capture cross sections. ADSS related evaluations of basic nuclear physics database are immensely benefited by basic neutron data physics measurements performed to understand the origin of nature.

When Nuclear Reactors are Already Operating do we Need to Improve or Add New Nuclear Data Physics?

The answer is indeed a solid “Yes”. Nuclear reactor designs have not been yet experimentally verified for long burnups and multiple fuel cycles. Even in limited burnups (6 GWe/te), the predictions of fissile materials and isotopes produced in the operating research and power reactors (PHWRs) in India are much better with the use of new IAEA WLUP libraries as compared to the use of 1971-81 WIMSD libraries used originally in the design. We illustrate, by the following striking instance, of great practical importance in terms of safe operation of the reactor, the need to continuously update nuclear physics data in reactor analyses even when the reactors are already operating.

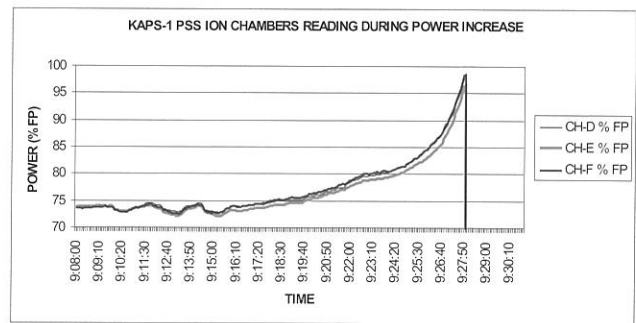


Fig. 3 An over-power transient incident of magnitude INES level 2 in 220 MWe PHWR reactor.

For Safe Operation of Existing Reactors: A Practical Example

Recently, an incident involving power rise took place in KAPS, Unit 1. A public release dated April 22, 2004 by the Atomic Energy Regulatory Board provides the details of this incident. On March 10, 2004, KAPS-1 experienced an incident involving incapacitation of reactor regulating system, leading to an unintended rise in reactor power from 73% Full Power (FP) to near 100%FP, with trip occurring on Steam Generator DELTA T High Level 2 on INES Scale. See Fig. 3.

In the simulation of the over-power transient incident, one of the important feedback coefficients is the FTC. The initial assessment for KAPS-1 was carried out using the feedback reactivity coefficients based on the WIMS 27 group neutron cross section library, which is a condensed version of the 69 group WIMS library of the early sixties. The predicted power rise was much less steeper than the observed power rise. The various feedback reactivity coefficients were estimated again using the recent WIMSD library derived from the ENDF-B/VI.8 cross section library as part the Coordinated Research Programme (CRP) of the International Atomic Energy Agency entitled, “Final Stage of the WIMSD Library Update Project (WLUP)” which ended in 2001. The feedback reactivity coefficients like the power coefficient was worked out and found to be lower than the earlier values. Using the re-calculated power coefficient and taking account the operational history, this transient analysis was performed and the over-power transient was explained.

The reactor physics results discussed in this Section were obtained in reactor simulations using the new WIMS-D libraries of the IAEA Co-ordinated Research Programme entitled, “Final Stage of the WIMS-D Library Project” [which ended in 2001. The discussions, though limited in physics by WIMS-D conventions, are illustrative to throw light on the use of different nuclear data sets.

It has been found that the fuel temperature coefficient (FTC) calculated by the new 69-group “iaea.lib” library gives significantly different results at higher burn-ups and explains as a preliminary observation the unexpected power rise that occurred in the KAPS-1 unit. In a PHWR, the

precise crossover point in burnup where the FTC becomes positive depends on many parameters such as the temperature range and 19 versus 37-rod cluster. The FTC is due to the combined effect of Doppler effect and fuel re-thermalization effect. Recent calculations of FTC of PHWR lattices, performed independently by several researchers, illustrate the following: The average burnup in PHWRs in India is typically 6 GWD/te. The 27 group “wims1981” library has a cross over point, for FTC at about 12 GWD/Te burnup (which was recognized in the early design manuals); at about 9.4 GWD/Te with the same but 69-group library, at about 6 GWD/Te for a 19 rod cluster with the new “iaea.lib” library and at about 4.5 GWD/Te for 37 rod cluster of PHWR with the “iaea.lib” library. Actually the cross over point of the FTC is not just the issue but how negative it should be in order to overcome positive reactivity that includes the xenon kill feedback that is positive whenever power transient occurs. We have also observed that the calculated coolant void reactivity using the new “iaea.lib” library is lower than the earlier results obtained using the 1971 library. The KAPS-1 overpower transient could be explained only with the use of new WLUP libraries [27].

The Indian Atomic Energy Programme and Nuclear Data PHYSICS Requirements

The thorium fuel cycle is of great importance for our country, as we possess one third of world’s thorium reserves. The Indian Atomic Energy Programme follows a carefully planned strategy comprising of a three stage programme (www.dae.gov.in) bearing in mind the limited uranium resources and vast thorium reserves in India.

Using improved nuclear data and methods in simulation of nuclear systems is an important aspect of any serious nuclear programme. The generation and use of accurate nuclear data are considered fundamentally important, as accurate nuclear data are essential inputs to simulate nuclear interactions to obtain engineering parameters. New concepts can be studied with greater confidence if the scientific basis is sound. Nuclear power is an inevitable option for India. India has a national policy to implement a closed fuel cycle programme involving multiple fuels, (e.g., U-Pu, Th-U). With the option of closing the fuel cycle, the nuclear data requirements needed to develop the new systems with high burnup are exceptionally demanding and include all the range of actinides and fission products for multiple fuels. There is considerable overlap between the Indian programme with respect to thorium as a fuel and the on-going international efforts to develop innovative, inherently safe, proliferation-resistant and long-life-cores, with features using thorium as in INPRO and Generation IV systems.

An Advanced Heavy Water Reactor Project (AHWR)

The detailed pursuits of development of Generation IV and INPRO nuclear energy systems that offer advantages in the areas of economics, safety, reliability and sustainability

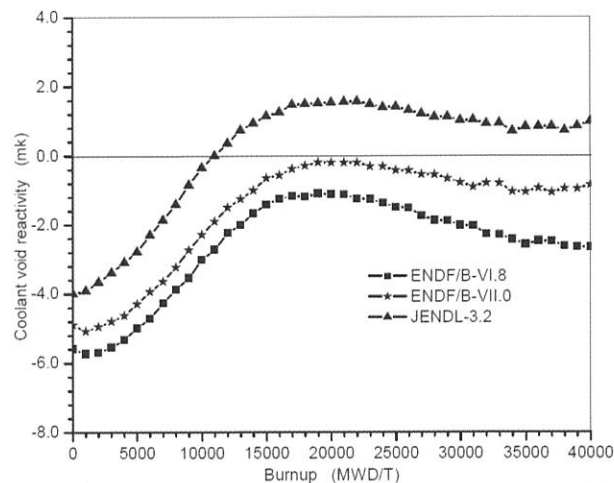


Fig. 4 Sensitivity of CVR (Voiding from normal operating conditions) to the use of three different nuclear data sets: ENDF/B-VI.8 (USA; 2000), ENDF/B-VII.0 (USA, 2006) and JENDL-3.2 (2000, Japan). More details can be found in Ref. [28].

require significantly improved nuclear data. The IAEA has selected the AHWR concept as a case study under INPRO.

An AHWR project has been taken up in BARC, for large-scale commercial utilization of thorium fuel cycle. The nuclear design of the lattice and of the core has been finalized. The design envisages the use of a novel 54-pin MOX cluster with different enrichment of ^{233}U and Pu in Thoria fuel pins and displacer rod with dysprosium cluster and central water hole at the centre. It is designed to have negative void coefficient of reactivity. The 300 MWe AHWR is foreseen with the fuel: $^{233}\text{U}/^{232}\text{Th}$ MOX + $^{239}\text{Pu}/^{232}\text{Th}$ MOX. Fuel assembly characteristics are evaluated by using transport theory codes with 69 or 172 group WIMS-D library and compared with MCNP based calculations. The core calculations are done with few group diffusion theory methods. As an illustration [28] shown in Fig. 4 is the large sensitivity of coolant void reactivity to the use of different nuclear data sets. The mandatory design requirement is that CVR should be negative by design under all operating conditions.

Another interesting point is the physics understanding of Fuel Temperature Coefficient and its behavior as a function of burnup. In the beginning and at low burnup, the FTC is dominated by ^{239}Pu , ^{233}U and ^{232}Th . At high burnup this is dominated by ^{232}Th and ^{233}U rather than that of ^{239}Pu . Thus the FTC becomes more negative with burn-up in AHWR. This is in contrast to the behaviour of FTC in PHWR where the FTC becomes positive after a certain burn-up. Our recent paper [29] presents the isotopic and energy group wise contributions to the Fuel Temperature Coefficient (FTC) in AHWR using first order perturbation analysis code. In AHWR, the contribution of ^{239}Pu to FTC decreases with burn-up and the contribution of ^{233}U in FTC becomes more negative with burn-up. Also ^{232}Th gives a significant

negative contribution, which makes the FTC become more negative with burn-up in AHWR.

An Example of Minor Actinides Criticality Data-Effect of Using Different Nuclear Data Sets

The minor actinides data are receiving increased attention these days because their data needs to be known more accurately to design actinide incineration systems. The interesting results of large discrepancies obtained by the author in the calculated criticality properties of minor actinides, such as, ^{241}Am , ^{243}Am , ^{231}Pa , ^{232}U and ^{233}Pa shed light on the inadequacy of nuclear data of these minor actinides in the fast energy region. The scatter in the author's reported [30] critical mass of ^{241}Am isotope in the literature is from 52 kg to 250 kg. In the work unpublished by the author in 2002, in the case of ^{243}Am , the scatter is from 54 kg to 2660 kg due to use of different standard nuclear data sets. In this scatter, there has been a significant scatter also due to errors in processing of the same ENDF/B data files. The nuclear data of minor actinides and fission products are also crucial in international formulation of radioactive transport regulations [31]. All these requirements demonstrate the immediate need for the research carried out in basic nuclear physics experiments and integral neutron physics experiments.

A Multi-purpose Critical Facility (CF)

As a general rule, all designs of innovative reactor systems need integral validation studies, ideally for each state of the reactor. The new concepts involving thorium systems require specially detailed basic nuclear data measurements and integral validation studies, as thorium has not received the required attention in the past. Like in other new concepts, the AHWR simulations have many assumptions and modeling approximations and are sensitive to nuclear data uncertainties especially because of thorium fuel cycle. The evaluation of the lattice characteristics requires experimental validation to freeze the design and obtain regulatory clearance, before we embark on fuel fabrication. A multi-purpose Critical Facility (CF) has been designed [6] and in advanced stage of construction. Our sensitivity calculations performed in RPDD illustrate that the critical height of the CF with AHWR representative core increases by 5 cm and 7 cm respectively when the "iaea.lib" and "jendl3.lib" libraries replace "endfb6.lib" WIMS-D library. For natural uranium core this is about 2 cm. The replacement of multigroup data of ^{232}Th alone in "jendl3.lib" by "endfb6.lib" changes the k-infinity by 10.24 mk, "jendl3.lib" yielding a higher calculated value of k-infinity. These results are similar to the sensitivity results reported by the Kyoto team. These results are consistent with the differences seen in the comparisons of multigroup data of the two sets. The self-shielded capture resonance integrals for ^{232}Th are higher in "jendl3.lib" by several tens of percent as compared to 0.1% target accuracy.

It may be noted that the experimental validation efforts in critical facilities can never exactly verify the simulated

states of higher burn-up at operating conditions. Therefore extrapolations in simulations involving improved nuclear data physics and reactor physics treatments are necessary. For instance, in developing advanced reactor systems, such as actinide burner systems and high burn-up reactors of 100 years life, it is essential to have a proper inclusion of nuclear data of fission products and minor actinides.

A Compact High Temperature Reactor (CHTR)

A Compact High Temperature Reactor (CHTR) using $^{233}\text{UC}_2$ (2.3 kg) + ThC_2 (5.7 kg) is under development [19]. The fuel is in the form of compacts of TRISO Coated fuel particles. Pb/ Pb-Bi Eutectic alloy has been proposed as the CHTR coolant. The CHTR has been designed with the objective of development and demonstration of technologies for very high temperature reactors for producing high temperature process heat for hydrogen generation. The basic design and technology development work is in progress. The CHTRs will be compact and portable, low power, long life core (more than 15 years) for producing non-grid based electricity in remote regions. Achieving a very high degree of passive safety in compact, high temperature, liquid metal cooled designs, to the extent needed for practically eliminating the need for highly skilled operators.

The design of CHTR, which exhibits intermediate neutron spectrum, was strongly influenced by considerations of nuclear data and associated uncertainties during its evolution. The cross sections for several new materials, such as Er, Bi and Ga that were considered for CHTR show large discrepancies in different cross section libraries. Another interesting issue, for instance, was related to the fact that it is mandatory to have a negative Doppler feedback effect in design. The initial choice of pure ^{233}U as fuel was abandoned, as its use resulted in calculated positive Doppler effect. Further, the calculated Doppler effect of ^{233}U has a large uncertainty as the nuclear data of resolved and unresolved resonance region are highly uncertain. As the spectrum covers regions above the thermal range, accurate knowledge of various transport and inelastic cross-sections of various constituents, such as ^{233}U , ^{232}Th , Be, Er, Th, which affect the design significantly at high temperatures are required. Experimental work to demonstrate these systems is planned.

Analyses of Irradiation of Thorium Bundles in PHWRs

Identical loading of thorium bundles was used in KAPP-1 & 2, KAIGA-1 and 2 and RAPS-3 and 4 to attain flux flattening in the initial core. The thorium oxide used is about 400 kg in all the 35 bundles put together in a reactor. The bundles loaded in KAPP-1 & 2, KAIGA-1 and 2 and RAPS-3 and 4 have already been discharged from the core. Samples were obtained from one of the irradiated ThO_2 bundles and have been analyzed experimentally by alpha spectrometry for ^{232}U and by thermal ionization mass spectrometry for ^{233}U , ^{234}U , ^{235}U and ^{236}U by two different groups in BARC. The previous analyses by two teams in BARC gave a factor of 6 to 8 under-predictions in the production of ^{232}U . We have successfully attempted to

High Energy Density Systems – Physics & Modelling

S.V.G. Menon, Aditi Ray, Bishnupriya Nayak, Chandrani Bhattacharya, Karabi Ghosh, G. Kondayya, Madhusmita Das, A. Sai Venkata Ramana, M.K. Srivastava, Vinod Kumar

Theoretical Physics Division, Bhabha Atomic Research Centre, Trombay, Mumbai 400 085, E-mail: svgmenon@barc.gov.in

Abstract

Physics of high energy density (HED) systems finds applications in several fields of current research: astrophysics, Inertial Confinement Fusion (ICF), pulsed power systems, impact phenomena, etc. Theoretical study of this field involves modelling various physical processes such as fission and fusion physics, hydrodynamics and shock-waves, radiation- and explosive-driven phenomena, transport of neutral and charged particles, radiation transport, and growth of hydrodynamic instabilities. To achieve this, one requires various databases of material properties, which are to be supplemented by accurate theoretical modelling. The databases include thermodynamic properties of matter in wide ranges of conditions, radiation transport properties of materials, neutral and charged particle interaction cross-sections, and detonation properties of high explosives.

HED systems occurring in ICF are of particular interest. A comprehensive approach to ICF requires integration of all the physical processes in simulations, and development of methods validated with experiments. As experiments in this field are severely limited to narrow ranges of thermodynamic conditions, detailed simulations can only provide sufficient insight. This article presents theoretical models and simulation studies of some of the processes involved.

Introduction

Matter under extreme conditions of temperature and pressure, occurs in several fields (see Table 1). Recent scientific and technological advances are making it possible to study these systems at a fundamental level in the laboratory. This article is concerned about the underlying physical phenomena at rather high energy density (HED) occurring in these systems, theoretical modelling, and the need for computer simulations.

TABLE 1. High Energy Density Systems

1.	Inertial Confinement Fusion Devices
2.	Explosive & Impact Loading of Materails
3.	Nuclear Weapons
4.	High Current Driven Devices
5.	Geophysics & Planetary Interiors
6.	Astrophysics – Stellar Objects

HED systems are typically those subjected to pressures in excess of 1 Mbar (1 million atmospheres). This range of pressure is equivalent to 10^5 J/cm³ of internal energy density. Energy density of this order corresponds to dissociation of a hydrogen molecule. At these conditions, all matter becomes compressible as well as ionisable and hence would exist in the plasma state. In most situations, the plasma is very dense and has properties quite different from those of dilute plasmas, which are described by classical plasma theory.

High energy density physics (HEDP) deals with the properties of matter existing in systems as shown in Table 1. In the first four cases, matter passes different states through various phase transitions during the dynamical course of reaching the final condition. Detailed knowledge of

thermodynamic properties is necessary to understand the evolution of these systems. Experiments required to generate HED conditions are quite difficult due to limited spatial, temporal and energy scales achievable in the laboratory. In other words, the ranges of parameters, which can be covered in experiments, are rather narrow. Therefore, modelling and simulations are integral parts of HEDP.

Inertial confinement fusion/fission (ICF) devices are, perhaps, the most prominent of all HED systems. This is so, due to their potential for utilization of nuclear energy. ICF physics has significant overlap with nuclear weapons physics. Though the states of matter produced and physical processes involved are similar, the characteristic scales in the two cases are quite different. In this article, we will be mainly concerned with the physics of ICF devices.

Current research in ICF are focused on interaction of laser and particle beams with matter, dynamics of X-rays in hohlraums, hydrodynamic instabilities in implosions, ablator physics, different schemes of thermonuclear ignition and burn. We are developing theoretical and computational models for simulation of these phenomena. This is being pursued via four complementary paths: (i) inclusion of the fine details of physical process; (ii) development of fast and efficient numerical algorithms; (iii) use of modern visualization tools, and finally, (iv) parallelization of some of the codes for utilizing large computer resources.

The article proceeds with a definition of HED regime, physics of ICF devices, methods of generating HED conditions and brief discussion of various physical processes involved.

Defining HED Regime

The energy densities occurring in commonly known systems like capacitors to fission and fusion devices are compared in Table 2. These can be classified as steady state and dynamical systems. The table gives an idea of the energy densities involved in HED systems. Since the time scales involved in these devices are quite different, it is also

necessary to compare the typical power levels at which these systems operate.

TABLE 2. Energy Density (kJ/kg) in Various Devices

Capacitors	0.022
Explosives	5×10^3
Fission Devices	9×10^7
Fusion Devices	3×10^8
Stellar Objects	1×10^6

While complete burning of 1 kg of chemical explosive produces about 5 MJ at 10^{12} Watt, total fission of 1 kg of U^{235} provides 17.6 kT (1 kT = 10^{12} Calories) of energy at about 10^{22} Watt. Fusion of 1 kg of equal mixture of D-T gives rise to 80.4 kT of energy which is more than 4 times the specific energy in fission.

We next turn to Fig. 1 showing the HED regimes for hydrogen in terms of a density-temperature plot [1]. The scales involved are quite large, as it covers 20 orders in density and 9 orders in temperature. On the lowest density side, going up on temperature, there is a grey line separating un-ionized and ionized hydrogen. This line has a positive initial slope with density, however, it drops down later, and after about 1g/cc, hydrogen is found to be ionized at all temperatures. This is termed as pressure ionization. The horizontal lines, marked P (total) = 1 Mbar and 1 Gbar, denote contours of radiation pressure that do not depend on material density. Above these lines, radiation pressure would dominate material pressure. The slanting lines marked P (gas) = 1 Gbar and 1 Mbar are contours of total pressure. Thus, thermal pressure in hydrogen at 1 g/cc density and 1 eV temperature (1.16×10^4 K) is about 1 Mbar.

Below the line "E (Coulomb) = kT", thermal energy of plasma is less than Coulomb energy, which means that the plasma is strongly coupled. Similarly, below the line "E (Fermi) = kT", plasma is no more classical and the quantum mechanical Fermi-Dirac pressure overwhelms thermal pressure. There are lines moving from low to high density, depicting the time development of giant planets,

TABLE 3. Typical Power Generation in Systems

Steady State Systems		Dynamic Systems		
Automobile	50-200 kW	High Power Lasers	10^{14} W	time ~ 1ns
Energy from Sun	4×10^{26} W	Explosives (1Kg)	10^{12} W	time ~ 1 μ s
Nuclear Reactors	10^9 W(e)	Fission Device (10kt)	10^{22} W	time ~ 0.25 μ s

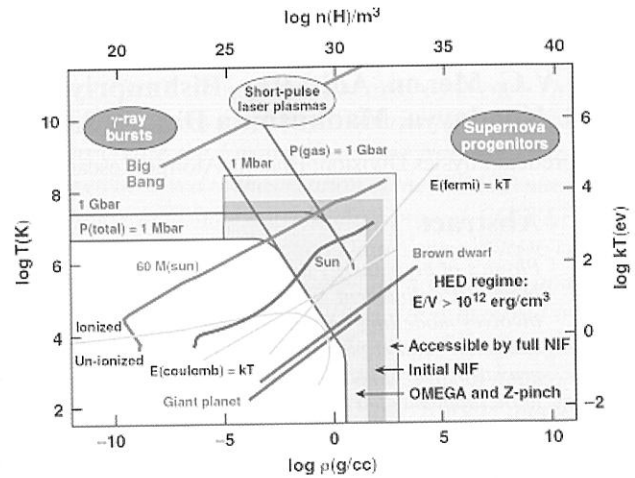


Fig. 1 Density-Temperature regimes in HED systems

brown dwarfs, Sun, a star of 60 solar mass, and big bang explosion. Regions showing γ -ray bursts and supernova progenitors are of great astrophysical significance. The area, indicated as short pulse laser plasma, are being studied using table-top lasers that generate pulses of $\sim 10^{-15}$ sec. Coloured regions accessible to laser facilities like OMEGA & Z-pinch, initial National Ignition Facility (NIF), USA, and the full NIF indicate that experimentation is feasible over very limited regions only. As mentioned earlier, this brings in the need for theoretical modelling and simulations of these systems. The models have to be robust as well as accurate. Next, we turn to the basic processes involved in ICF.

Inertial Confinement Fusion/Fission

ICF has driven much of the development of HED physics. Though there is ample literature on fusion devices, fission of micro fissile targets is also possible using the same principles. The fusion target, which is a capsule containing equal mixture of D-T, is a complex structure designed to produce energy when driver beams are shone on it. A material called ablator (for example, Be) covers the target. Laser beams are employed as driver for direct drive scheme. Several laser beams (see Fig. 2) impinge on the target and generate an ablating plasma, which implodes the fuel to conditions appropriate for initiating thermonuclear fusion.

In indirectly driven scheme, the drivers can be lasers, particle beams, or electron beams. Energy from the driver

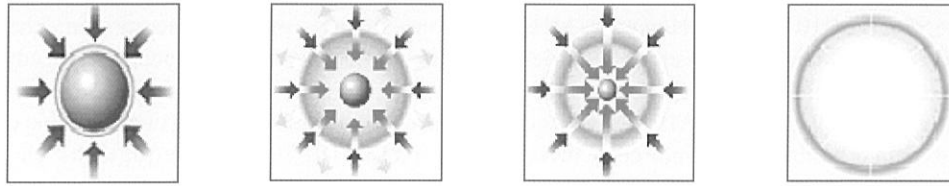


Fig. 2 Extreme pressures generated via ablation, compresses D-T fuel to ignition. (L – R): (i) ablation, (ii) implosion, (iii) ignition, and (iv) burn

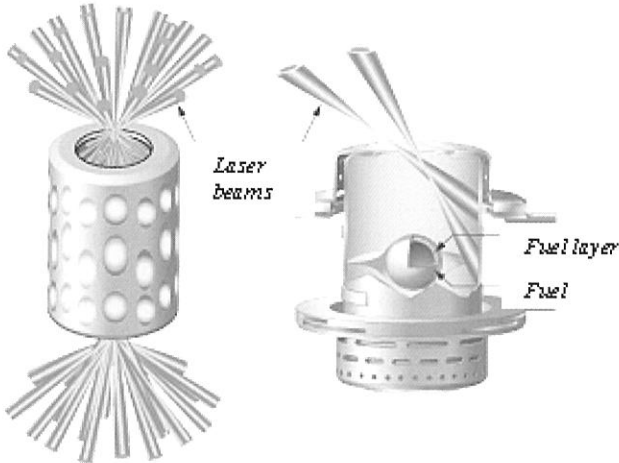


Fig. 3 In indirect drive, energy from laser beams is converted to X-rays inside the hohlraum. Uniformity of X-rays reduces asymmetries inherent in direct drive.

(see Fig. 3) is converted into thermal X-rays in a hohlraum, which is made of high-Z material like Au or U. Typical temperature of thermal X-rays is 250 eV. The X-rays absorbed by capsule generates a hot plasma, which ablates outwardly. The reaction force accelerates the remaining fuel inwards leading to compression and heating of the fuel to high temperature. Energy transport in the hohlraum via radiation is an essential feature here.

Creating Conditions of HED

Gravitational forces generate HED conditions in nature, for example, pressures at the centre of Earth and

Jupiter are about 4 Mbars and 40 Mbars, respectively. Gravity also holds stellar matter together leading to conditions suitable for thermonuclear fusion. Pressure at the core of the Sun is, approximately, in the range of trillion bars.

HED conditions have been realized in the laboratory with the advent of modern technology. Mainly five methods are pursued in different laboratories. These include: (i) explosive-driven impact phenomena, (ii) direct irradiation with laser, (iii) X-rays from laser-driven hohlraums, (iv) Z-pinch and related pulsed power devices, and (v) irradiation with electron and ion beams. All these are dynamic experiments. Driver energy is deposited in a small region, at extremely fast rate, leading to the formation and propagation of shock waves.

Experimental Systems

Laser Facilities

NIF employs neodymium-glass laser system with 192 beams which can deliver as much as 2 MJ of laser energy (of wave-length 0.35 μm) in millimetre-scale volumes in ~ 10 nanoseconds. At peak power, it generates up to 750 trillion Watts of laser light and is useful for both direct and indirect-drive experiments. It is claimed that with the full NIF, it would be possible to produce radiation dominated shocks, similar to that occurring in the secondary of a thermonuclear device. Some laser facilities are listed below (Table 4).

Z-pinch Devices

In a typical Z-pinch device, a current pulse through a plasma column compresses and heats the plasma to

TABLE 4. Main Laser facilities for HED Physics

Country	Laser	No. of Beams	Energy (kJ)	Pulse (ns)	λ (μm)
USA	NOVA	10	50	1	0.35
	NIF	192	1800	15	0.35
France	Megajoule	288	1800	15	0.35
Japan	KOYO	400	4000	6	0.35
Russia	ISKRA-5	12	15	0.25	1.3

temperatures in the range of 10-100 eV. However, MHD instabilities set limits for confinement of plasma. Cylindrical liners and wire arrays for X-ray sources are also based on the pinch effect. It is now claimed that even 15 MJ of X-rays can be delivered to a dynamic hohlraum for indirectly driven fusion.

Ion Beams

HED conditions can be realised on stopping high-velocity ions in a material like Pb. The two challenges with ion beams are: generation of short-time (ns) pulses; and deposition of energy in a small volume. Because heavier ions have larger positive charges, they can be stopped more rapidly over a given distance than lighter ions.

Basic Physics and Modelling

The fundamental physical phenomena that govern the physics of HED systems are listed in Table 5. Brief descriptions of these phenomena and typical results from our efforts in modelling and simulations will be discussed next.

TABLE 5. Physical Phenomena involved in HEDP

Hydrodynamics & Shock Waves	Radiation-driven Hydrodynamics
High Pressure EOS of Matter	Neutronics of Fission & Fusion Devices
Radiation Diffusion & Transport	Thermonuclear Ignition & Burn
Radiation Opacity of Plasmas	Hydrodynamic Instabilities

Hydrodynamics and Shock Waves

Atoms or molecules acquire kinetic energy on receiving energy from an external source. This leads to formation of pressure gradients in the medium.

Consequently, macroscopic motion, changes in density, internal energy, etc., can occur. Hydrodynamic processes may be initiated due to impact phenomena, explosive burn, lasers, ion beams or pulsed currents. It is described in terms of partial differential equations in space-time for conservation of mass, momentum and energy. An equation of state giving pressure and internal energy, in terms of density and temperature, closes the set of equations. At lower pressures, material properties like yield stress, shear stress and plastic flow models are also required. Shock waves are formed when large amplitude hydrodynamic disturbances occur. Shock waves are sharp discontinuities in the fluid variables and propagate with a speed characteristic of the pressure. The medium behind the shock front is compressed and heated, the extent of which again depends on pressure behind the shock.

ICF invariably employs dynamic compression using shock waves because the fusion rate is proportional to square of pellet density. Though static compression using diamond anvil cell is useful for laboratory studies, it is inadequate for ICF. Dynamic schemes in nanosecond scales, via strong shocks are also not useful due to strong pre-heating of the medium. For example, strong shock can increase density in monatomic ideal gas only by 4 times. But, high compression is achievable using isentropic and quasi-isentropic methods, which occur over longer (microsecond) time scales (see Fig. 4). The ramp pressure pulse produces compression of the medium at low entropy. Lasers and magnetic fields are used to generate quasi-isentropic compression. Functionally graded materials (FGM) are now being used as impacting materials in gas guns or explosive-driven systems [2, 3].

Hydrodynamics simulations need efficient and robust algorithms [4, 5]. Mesh distortions inherent in 2D and 3D Lagrangian schemes, have to be tackled with Eulerian, ALE (arbitrary Lagrangian-Eulerian) and the mesh-free Smooth Particle Hydrodynamics (SPH) schemes. In SPH, each material is modelled as a collection of large number of interacting particles obeying the Eulerian conservation

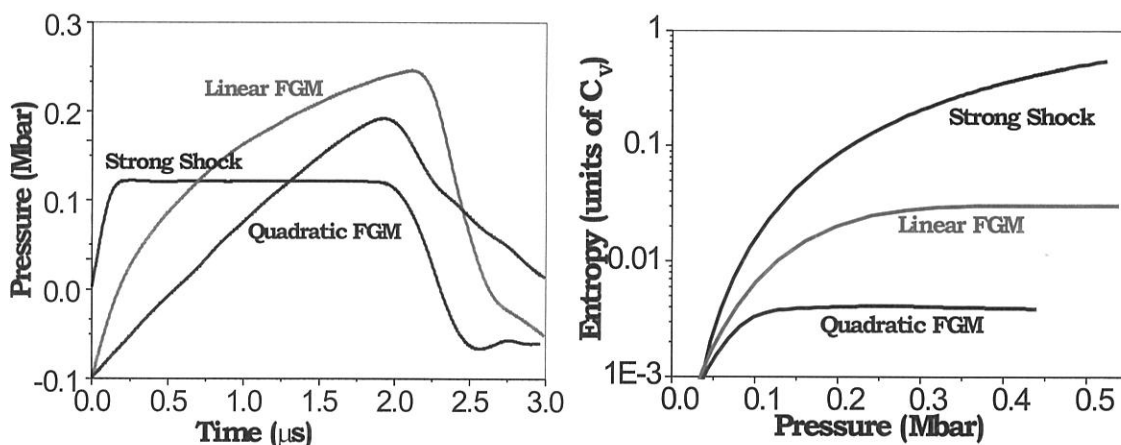


Fig. 4 Pressure and entropy variation in quasi-isentropic compression.

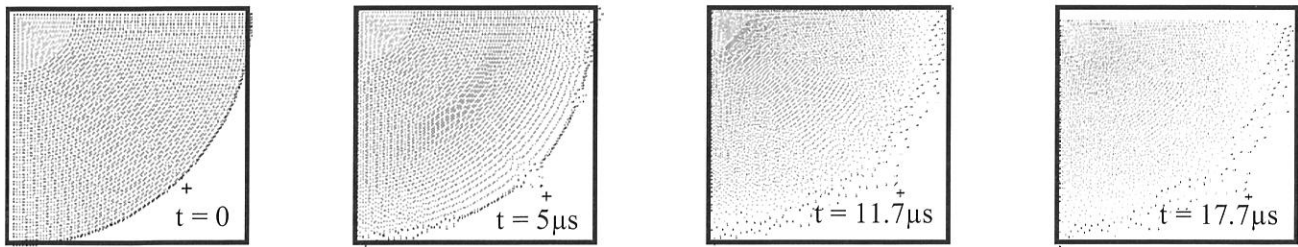


Fig. 5 SPH simulation of explosive driven Aluminum sphere

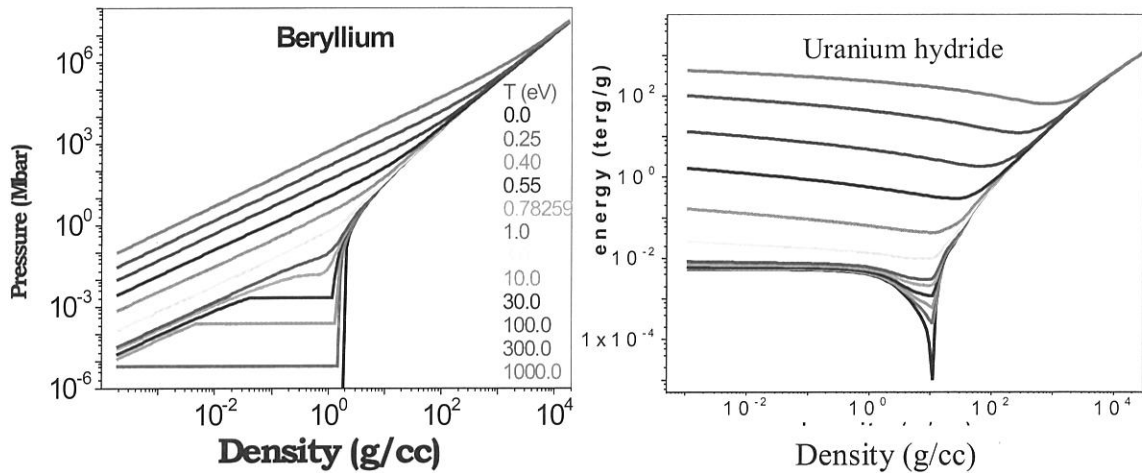


Fig. 6 Pressure isotherms of Be & Energy isotherm of UH_3

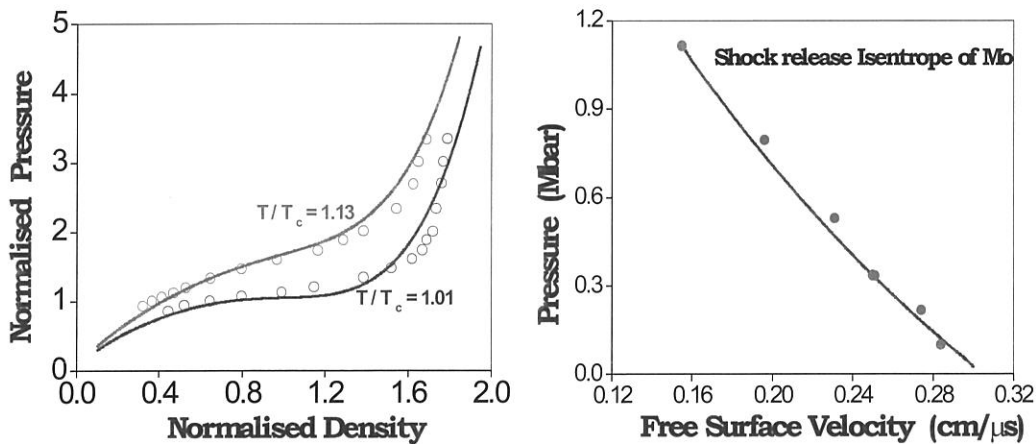


Fig. 7 EOS in liquid-vapour region – Critical point and Shock release

equations. Fig. 5 shows SPH simulation of different stages of implosion of a sphere by an explosive driven shock [6].

Equation of State

Detailed knowledge of equation of state (EOS) is necessary for hydrodynamic simulations of matter. Tables of EOS over large range of density (10^{-4} to 10^4 of normal density) and temperatures up to about 10^9 K are needed for elements, compounds and alloys. Fig. 6 shows typical pressure isotherms of Be and energy isotherms of UH_3 up to 1 keV. We have developed extensive tables for a variety of

materials, which are relevant to ICF and similar HED systems [7, 8].

The EOS models must also account for the properties of materials in the expansion phase, i.e. for densities lower than those corresponding to their respective solid phases. Materials generally undergo the liquid-vapor phase transition and it is essential to have good predictions of EOS in this region. Accuracy of the EOS models can be checked against data obtained from shock release experiments. Fig. 7 shows comparisons from our EOS models for Hg near the critical point and Mo in release experiments [9].

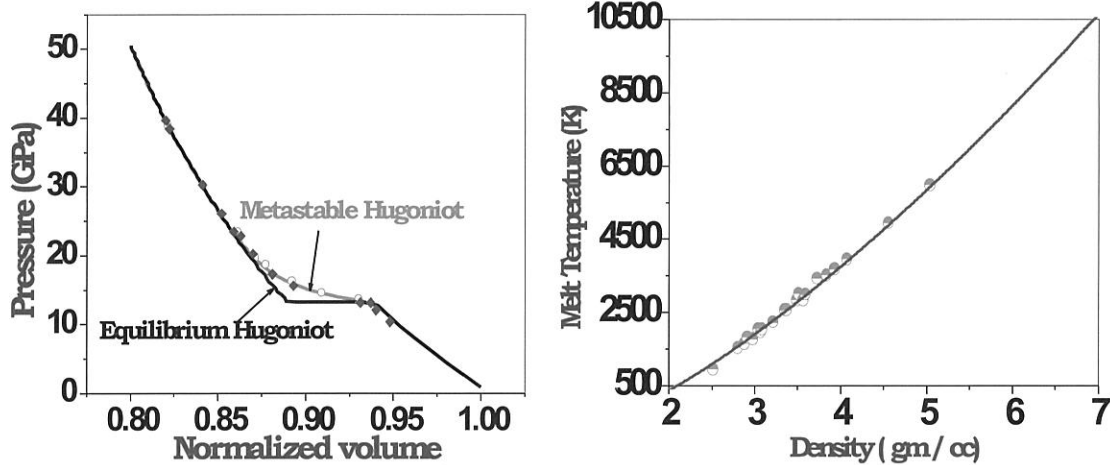


Fig. 8 Shock induced phase transition in Fe and melting of Al

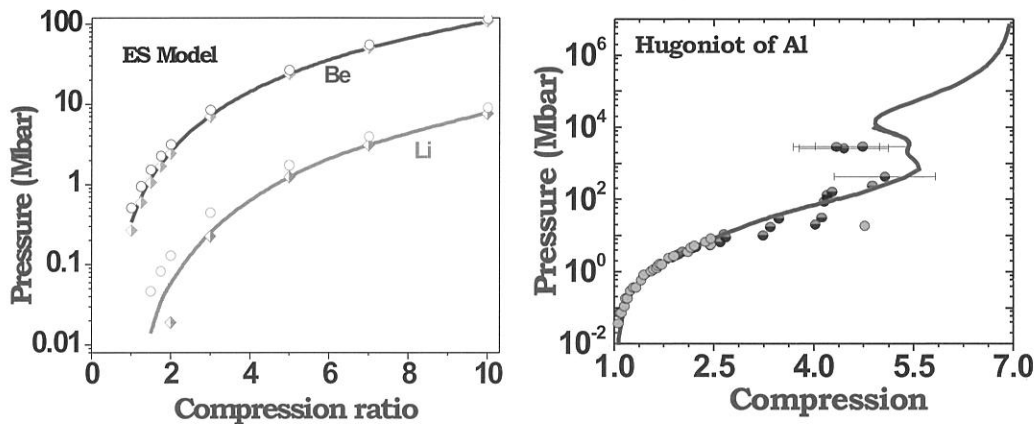


Fig. 9 Electron and radiation contributions to EOS

Materials undergo different types of phase transitions during shock wave propagation. Structural phase transitions, melting, vaporization, etc. are possible phase changes. Correct modelling of atomic motion and structural aspects are needed to predict these transitions as they occur due to small changes in energy and/or entropy. We use models based on solid and liquid state theories, which incorporate, among other features, an-harmonic atomic vibrations. Fig. 8 shows results for shock induced α - ϵ transition in Fe and melting curve for Al [10-13].

Electronic excitation induced by shock and subsequent heating, is the main contribution to EOS at high pressures. When a solid is compressed along the zero temperature isotherm (theoretically), electrons are ionized due to pressure ionization, which has origin in Pauli's exclusion principle. Our recent calculations (see Fig. 9) for Be and Li, based on Englert and Schwinger model are in excellent agreement with the TFDW model. This model includes

effects of electron exchange and quantum corrections to semi classical theory [14, 15].

Heating of materials by shocks also leads to thermal ionization. This manifests as oscillations in the high pressure Hugoniot plots. Predictions from our model and comparison with data for Al up to 10^4 Mbar are also shown in this figure [16]. We have also included radiation pressure, which exceeds material pressure around 5 keV.

Radiation Opacity

Radiation transport in HED matter requires frequency dependent absorption and emission coefficients, usually known as opacities. Because of changes in electronic structure due to pressure and thermal ionization, opacity depends on density, temperature and compositions of the materials.

Variations of ionization in Al with compression at temperatures 0.001, 0.01, 0.1, 1 and 6 keV are shown in Fig

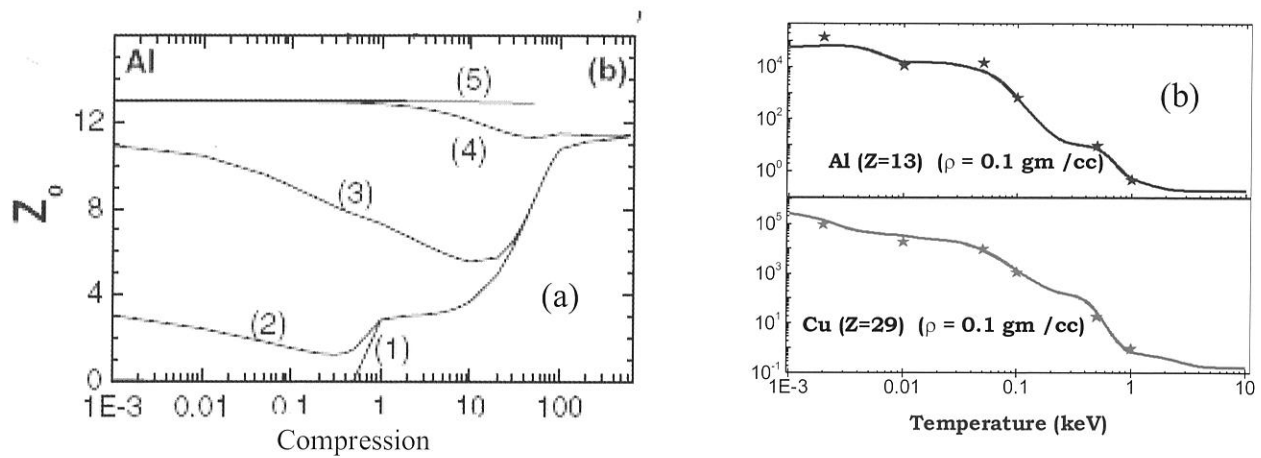


Fig 10 Ionization in Al and opacity of Al, Cu

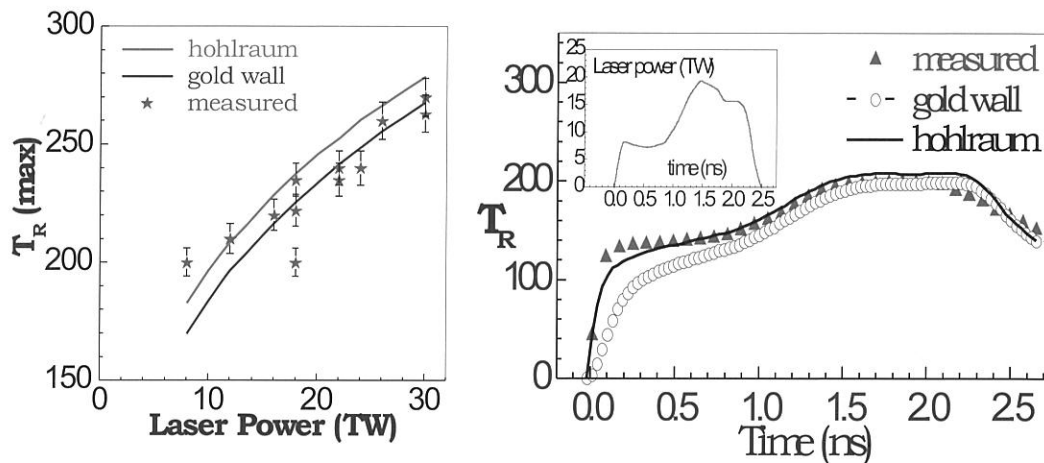


Fig. 11 Evolution of radiation temperature in hohlraum

10(a) [16]. Pressure ionization is evident in this figure for low temperatures such as 0.001 and 0.01 keV.

Extensive tables for radiation opacity are needed for simulations. These have to be computed using detailed atomic structure methods, since measurements in the entire range of parameters are impossible. Atomic theory should also include, among other details, the effects of plasma environment on electron energy levels. The concept of local thermodynamic equilibrium can be used for calculating opacities in dense matter. However, non-equilibrium effects are quite important in dilute plasmas produced by ablation. Typical results for the temperature dependent Roseland opacities [17] of Al and Cu are shown in Fig. 10(b).

Radiation Transport

Evolution of thermal X-rays in hohlraum, which is a cavity made with a high-Z material, is an important problem in indirect-drive fusion. The intensity of X-rays falling on fusion capsule and its angular uniformity determine the adequacy of the hohlraum. Modelling this problem needs multidimensional radiation transport. Fig. 11 shows peak

temperatures obtained in a gold hohlraum for different laser powers. The temporal evolution of radiation temperature, for a particular laser pulse, is also shown on in the figure [18]. Inset in the latter figure is the time history of input laser power.

Important aspects of simulating the hohlraum are absorption and re-emission of X-rays from the walls, leakages via openings and hydrodynamics of wall. In additions to radiation transport theory (based on discrete ordinates methods), we have also developed diffusion and view factor methods. The latter ones are suitable for nearly isotropic X-ray distributions [19].

Radiation Hydrodynamics

Modelling radiation-driven hydrodynamics is an essential ingredient for HEDP. In these problems, radiation transport equation in a moving medium, is solved together with hydrodynamics equations in a self-consistent manner. Fig. 12(a) displays position of the radiation shock generated in an Al foil when a X-ray pulse (see Fig. 11(b)) is incident on it. There are two distinct slopes and hence two shock speeds

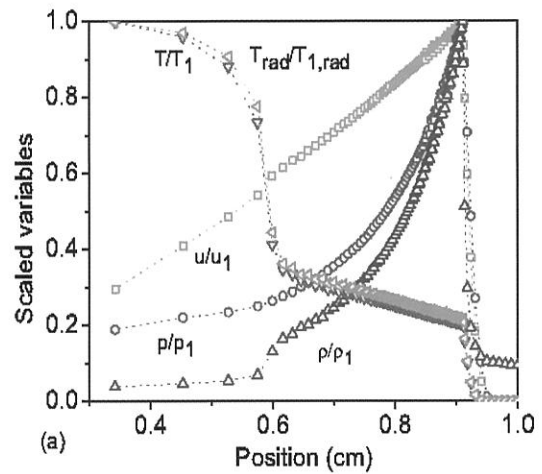
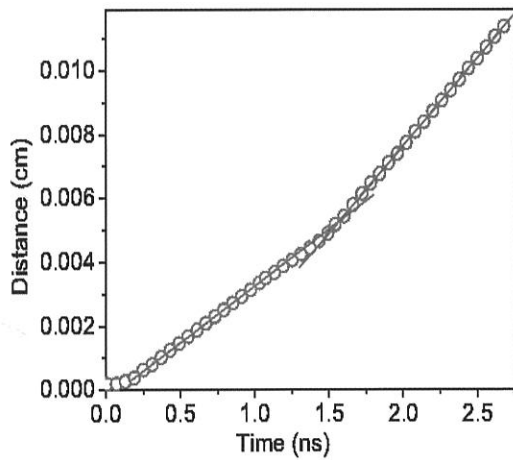


Fig. 12 Radiation driven hydrodynamics and shock waves

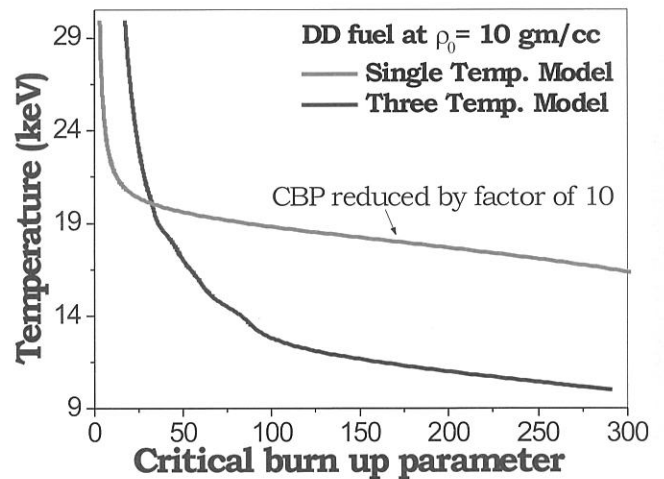
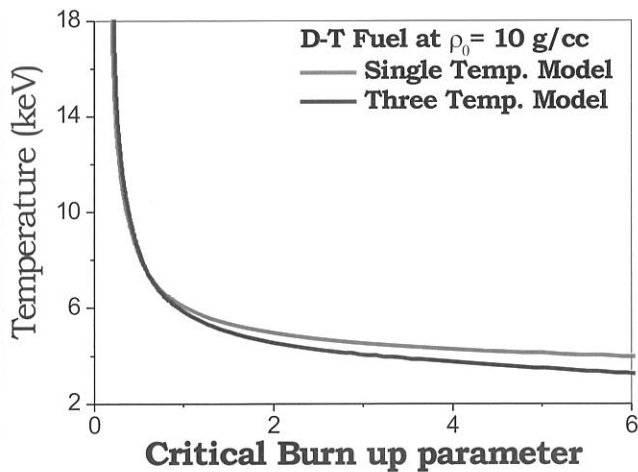


Fig. 13 Critical hot spot parameters for thermonuclear burn

corresponding to two plateaus in the incident profile. Fig. 12(b) shows the profiles of the scaled thermodynamic variables in the radiation-driven shock in a point-explosion problem [20].

Thermonuclear Burn

Most of the ICF schemes employ the concept of central ignition, wherein only a central hot spot of the capsule is heated to few keV while the remaining fuel is only compressed to high densities. For a specified temperature of the hot spot, there is a critical value of the areal density (product of mass density and its radius) for sustained burning of fuel.

We have developed a three-temperature model (ion, electron and radiation) to estimate this critical parameter for different types of fusion fuels [21]. Fig. 13 shows that for D-T fusion a single temperature model is adequate while for D-D fusion non-equilibrium effects are quite important. This is due to lower fusion cross-sections for the latter.

Tritium Breeding

It is interesting to explore the possibility of tritium breeding together with the fusion reactions. We developed a model that includes nuclear scattering and large angle Coulomb scattering of charged particles and collective plasma effects. All the radiative loss mechanisms like the bremsstrahlung, inverse Compton scattering and photon leakage from pellet are also added. Fig. 14(a) shows energy leakage probability of D ions against pellet radius in a deuterium plasma. Three cases of energy loss are shown: (i) only to electrons, (ii) electrons and ions and (iii) also including nuclear scattering. Fig. 14(b) shows tritium, normalised to its initial amount, left in the pellet at different times when various energy exchange mechanisms are included. While curve (i) is for bremsstrahlung loss only, curve (ii) also including inverse bremsstrahlung. For curve (iii), inverse Compton scattering is also considered. These results indicate the importance of the various mechanisms needed to be included [23, 24].

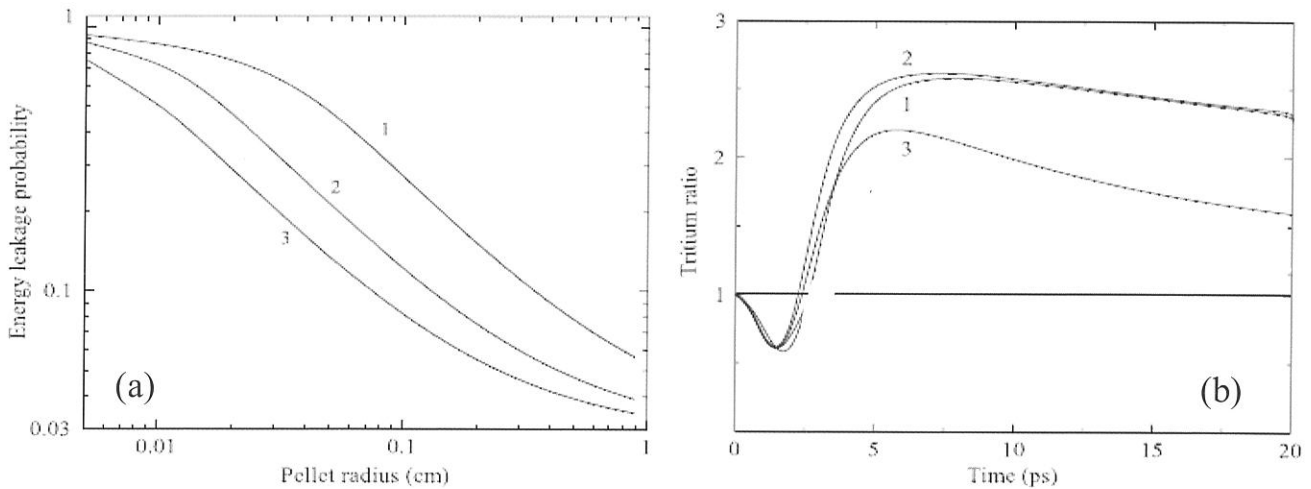


Fig. 14 Energy leakage of probability of D_2 in Fusion Plasma and Tritium Breeding

Particle Transport Theory

Energy deposition in ICF pellet by neutrons and charged particles is to be accounted in the simulations. In fact, this is what sustains burning of the fuel. Particle transport theory can be used for these calculations, if compilations of interaction cross-sections of particles with various materials are available. These data are generally converted to cross-section libraries. Details of these aspects of simulations shall not be covered in this article.

Another application of transport theory, involving neutrons, γ -rays and electrons, is in modelling the generation and propagation of the nuclear electromagnetic pulse (NEMP) from a nuclear event [24-26].

Hydrodynamic Instabilities

An ideal implosion of ICF capsule should have perfect spherical symmetry. However, this does not occur due to inherent growth of hydrodynamic instabilities during the implosion. Nonuniform irradiation, roughness of capsule surface and deviations from perfect sphericity of shells are some of the causes of instabilities. Rayleigh-Taylor instability arises when lighter ablated plasma is accelerated into denser un-ablated mass. Richtmyer-Meshkov instability occurs when a shock wave crosses an interface between two media of unequal density. Determining the effect of these instabilities is a daunting task as it needs numerical schemes of high precision and accuracy.

Conclusions

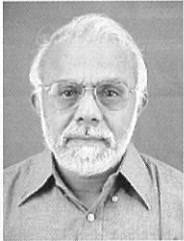
This article discussed some of the important aspects of HED systems. Our main emphasis has been on the phenomena involved in ICF, eventhough similar physics occur in other applications that we have mentioned. Brief outlines of the different topics involved are discussed together with some of our own results in these areas.

References

1. Frontiers in High Energy Density Physics, R. Davidson, et al, in Report of National Research Council, USA, 2005

2. Quasi-isentropic compression using functionally graded materials in gas-gun and explosive driven systems, Aditi Ray and S.V.G. Menon, Journal of Applied Physics, 105, 064501 (2009)
3. Optimised density profiles of functionally graded materials for quasi-isentropic implosion, Aditi Ray and S.V.G. Menon, Journal of Applied Physics, (submitted, 2010)
4. HYDRO-2D - 2-dimensional Lagrangian code for ICF studies, M.K. Srivastava, Vinod Kumar, S.V.G.Menon, BARC / I / 010 / 2003
5. Hydrodynamic modelling of imploding systems, Chandrani Bhattacharya, M.K.Srivastava, T-4-CP6, INSCA (2005)
6. Smoothed Particle Hydrodynamics in Cylindrical co-ordinates, G. Kondayya and M. K. Srivastava, BARC / ThPD / 621 / 2007.
7. High pressure EOS of materials: A HAND BOOK, M.K. Srivastava, Aditi Ray, G. Kondayya, and S.V.G. Menon, BARC/R/002/2005
8. A global equation of state for high energy density physics, M. K. Srivastava, Aditi Ray, G. Kondayya, S. V. G. Menon, BARC News Letter, February (2007)
9. Improved EOS of metals in the liquid-vapour region, Aditi Ray, M.K. Srivastava, G. Kondayya, S.V.G. Menon, Laser & Particle Beams, 24, 437 (2006)
10. Equation of state using scaled binding energy model, Chandrani Bhattacharya, M.K. Srivastava, Journal of Applied Physics, 102, 064915 (2007)
11. Ion Equation of state using scaled binding energy model, Chandrani Bhattacharya, M.K. Srivastava, Journal of Physics, Conf Series, 208, 012004 (2010)
12. Mean field theory of ionic free energy using scaled binding energies, Chandrani Bhattacharya, S.V.G. Menon, Journal of Applied Physics, 106, 064907 (2009)
13. Predicting melting curves of FCC metals using EAM potentials, Chandrani Bhattacharya, Karabi Ghosh, M.K. Srivastava, S.V.G. Menon, Journal of Physics, Condensed Matter (submitted, 2010)
14. Cold equation of state of elements using Englert-Schwinger model, A. Sai Venkata Ramana, S.V.G Menon, Proc. of 54-th DAE-Solid State Physics Symposium (2009)
15. Application of Englert-Schwinger model to cold EOS and fullerene molecule, A. Sai Venkata Ramana, S.V.G. Menon, Physica A (submitted, 2010)

16. Effect of bound electrons and radiation on shock Hugoniot, Madhusmita Das, S.V.G. Menon, Physical Review B, 79, 045126 (2009)
17. Simple models of opacities of hot dense plasma, S.V.G. Menon, Vinod Kumar, BARC / ThPD / 570 / 2003.
18. Computational methods in high-energy-density physics, Vinod Kumar, M.K. Srivastava, S.V.G. Menon, IT-18, INSCA (2005)
19. Analytical view factors and thermal radiation distribution inside a hohlraum, M.K. Srivastava, Vinod Kumar, S.V.G. Menon, Physics of Plasmas, 7, 2616 (2000).
20. Fully implicit 1-D radiation hydrodynamics – Validation and Verification, Karabi Ghosh and S.V.G. Menon, Journal of Computational Physics 229, 7488 (2010)
21. Thermonuclear burn propagation in fusion fuels using three temperature model, Bishnupriya Nayak, S.V.G. Menon, Aditi Ray, Physics of Plasmas, (submitted, 2010)
22. Slowing down of charged particles in a dense plasma, Karabi Ghosh, S.V.G. Menon, Nuclear Fusion, 47, 1176, (2007)
23. Study of the ignition requirements and burn characteristics of DT_x pellets for ICF, Karabi Ghosh, S.V.G. Menon, Journal of Physics, Conf Series, 208, 012003 (2010)
24. Compton current generated by nuclear radiation: A coupled n-γ - e transport model, G. Kondayya and Aditi Ray, Nuclear Science and Engineering, 154, 215 (2006)
25. A novel application of the multi-group method- Coupled n-γ cross-section library, G. Kondayya, Aditi Ray, Annals of Nuclear Energy, 33, 300 (2006)
26. Development of finite difference-time-domain parallel code for nuclear electromagnetic field simulation, Aditi Ray, G. Kondayya, S.V.G. Menon, IEEE Transactions on Antennas and Propagation, 54, 1192 (2006).



***Dr. S.V.G. Menon** joined BARC in 1972 from 15th batch of Training School. He is currently serving as Distinguished Scientist and is heading Theoretical Physics Division. He has contributed a lot towards BARC's strategic nuclear programmes and has received several awards. His areas of expertise are nuclear fission and fusion physics, statistical physics and computational methods.*

Lasers in Nuclear Energy Programme

B.N. Jagatap

Atomic & Molecular Physics Division, Bhabha Atomic Research Centre, Mumbai 400 085, E-mail: bnj@barc.gov.in

Abstract

Lasers and associated research areas play a prominent and decisive role in the nuclear energy programme. The range of applications cover a wide spectrum of issues, from mineral prospecting to isotope separation, from quality control to detection of nuclear events, from maintenance of nuclear plants to their decommissioning and from generation of x-rays, gamma rays, neutrons, accelerated particle beams to fusion energy. This article provides an overview of the involvements of lasers in nuclear energy programme, the current R&D trends and the future prospects.

Introduction

Since the invention of the first laser, the Ruby laser, by Theodore Maiman in 1960, there has been an explosive growth in the physics and technology of lasers, and their applications to practically all branches of science and technology. These fifty years have seen the diversified development of gas-, liquid- and solid-state lasers operating over a large wavelength range from infrared to x-rays, with powers ranging from milliwatt to petawatt (10^{15} W), and of pulse durations extending from continuous wave to femtosecond (10^{-15} s) and even lower. Armed with these incredible light sources, laser physics, intermingling with atomic, molecular and solid state physics, nonlinear and quantum optics, and more recently with plasma and nuclear physics, has given rise to amazingly new applications in the field of nuclear science and technology. Lasers, thus, have come a long way from being a tool for basic research to becoming a powerhouse of new generations of technologies. The impact of lasers on nuclear technology has been so profound that today 'laser nuclear science and engineering' is recognized as an important field of research and development world over.

The role of laser physics and ensuing technologies in the nuclear energy programme is illustrated in Fig.1. The dominant fields of work are depicted in this figure in relation to the available laser power, which has risen very steeply over the years, thanks to the sustained advances in the laser physics and technology. For the sake of simplicity of discussion, various uses of lasers are grouped into three broad classes depending on the nature of the laser-matter interactions.

The applications in the first group are driven by the monochromaticity and tunability of lasers, which permit selective excitation of specific energy levels of atoms and molecules, and that forms the basis for selective detection and selective separation of elements and isotopes of interest [1-40]. This principle underlies the phenomenal growth of detection techniques for trace and ultra-trace elements and isotope in the nuclear fuel cycle [1-24]. More importantly, it paves a way to develop laser-based technologies for isotope separation and laser ultra-purification [25-40]. Other involvements, many of which fall in low power end of the first group, include laser-based diagnostics and measurement techniques/devices [11-20] and specialized sensors required in the various activities of a nuclear plant

[21-24]. Lasers are also indispensable in precision measurement of atomic and molecular data, which is central to the development of isotopic or elemental selective processes or techniques [25-28, 31-35]. Typical laser systems used in these applications are tunable dye and solid state lasers pumped by a variety of continuous wave and pulsed lasers (e.g., copper vapour lasers, diode pumped solid state lasers, Nd:Yag lasers, excimer lasers etc.), semiconductor diode lasers, gas lasers (e.g. CO₂ laser) together with nonlinear optical devices.

Lasers provide a source with high energy packing per unit area and this particular feature has been exploited for quite some time now in the industrial material processing, i.e., drilling, cutting, welding, surface modifications, micro-machining, rapid quenching etc. Several of these tasks assume special importance in nuclear energy programme [41-48] and they constitute the applications in the second group of Fig.1. The use of optical fibers to transport and deliver high power laser beams in remote radioactive areas multiplies the advantages many fold. Some of the straightforward applications include high quality and high efficiency welding of precision parts such as core internals of a nuclear reactor or welding of stainless steel tanks for nuclear fuel reprocessing plants [42-44]. For

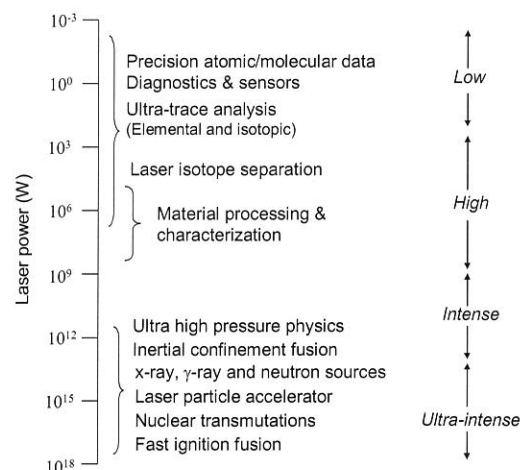


Fig. 1 Impact of lasers in nuclear energy programme described in terms of laser power. For the purpose of discussion various applications are categorized in three major groups. Frequently used terminology for laser power is depicted on the right

in-service-maintenance of nuclear plants, lasers provide a variety of technologies, which include laser-ultrasonic testing for non-destructing testing, laser peening for surface stress improvement and laser welding as a repair technology [45,46]. Also important in this context is the prospective use of lasers to cut and dismantle the dense piping structures, thick tank walls, flanges etc. while decommissioning of nuclear reactors [42-44]. Recent interest in the use of laser ablation to decontaminate radioactive surfaces [47] also forms a part of the applications in the second group. In addition to material processing, characterization of materials at high temperatures (2000-5000 K) is an important involvement in the nuclear energy programme [41,48]. High temperatures afforded by lasers provide extremely useful techniques to generate the high temperature thermodynamic, thermo-physical and thermo-chemical data of nuclear fuels and other nuclear materials. Typical laser systems used for the applications in the second group are CO₂ laser, Nd:Yag laser and fiber lasers.

In recent years the intense and ultra-intense lasers have emerged as a new tool for investigating advanced physics under extreme conditions and thereby providing several new opportunities in areas of nuclear energy programme, which are traditionally reserved for nuclear accelerators and reactors [49-64]. Very recent advances in laser physics and technology have led to the development of compact multi-terawatt (TW) to petawatt (PW) pulsed lasers. A laser of 100 TW peak power (10 fs pulse duration and 1 J pulse energy), when focused on a target, gives rise to intensity of 10²⁰ W/cm², electric field of 10¹¹ V/cm, magnetic field of 10⁹ G, temperature of 10¹⁰ K, pressure of 10⁹ bar and acceleration of 10²⁶ cm/s². Such extreme conditions are at the basis of applications in the third group in Fig.1. These include investigations of properties under ultra-high pressures such as equation of state, production of X-rays, production of γ rays (MeV to GeV), photonuclear reactions such as photo-fission and photonuclear transmutations, laser neutron sources and MeV to GeV range laser-plasma accelerators [49-57]. Finally the current research and development in the area of thermonuclear fusion and fast ignition fusion gives us a hope that soon the lasers will be able to find the 'holy grail' of nuclear energy, the fusion process [58-64], which is source of energy for the future.

Lasers, thus, have a decisive impact on the nuclear energy programme, its development and its future directions. In what follows, we provide a bird's eye view of some of the important issues concerning lasers in nuclear energy programme.

Laser-based Measurement Techniques and Devices

Monochromaticity of lasers results in a significant increase in resolution in atomic and molecular spectroscopy, and that makes it possible to unambiguously resolve spectral features of elements as well as their isotopes in a sample. Laser spectroscopy, therefore, is a method of choice for estimation of atoms, molecules, ions and their isotopes in diverse samples encountered in the nuclear energy

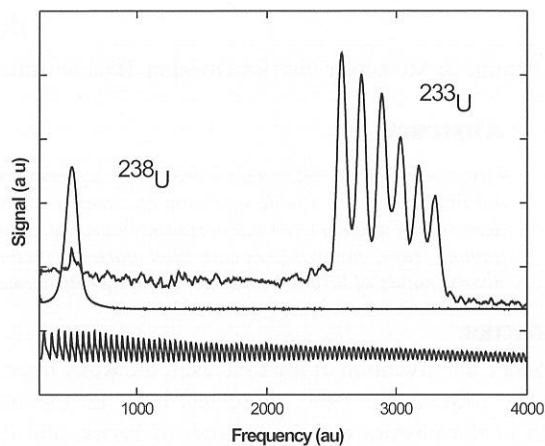


Fig. 2 High resolution OG spectrum of 682.69 nm line of ²³³U and ²³⁸U. The separation between the centers of gravities of spectral features of ²³³U and ²³⁸U is isotope shifts, which in the present case is ~ 8 GHz. Non-zero nuclear spin gives rise to the hyperfine structure in case of ²³³U. The frequency scale is calibrated with 300 MHz interferometer fringes (bottom).

programme [1-19]. A large variety of laser spectroscopic techniques are utilized to this end, the prominent amongst them are absorption, optogalvanic (OG), laser-induced fluorescence (LIF), photoacoustic and resonance ionization mass spectrometry (RIS and RIMS). These techniques provide elemental as well as isotopic composition of materials even at ultra-trace levels. As an illustration of the strength of laser spectroscopic techniques, we show in Fig. 2, the spectra of ²³³U and ²³⁸U obtained in our laboratory using scan averaged OG technique [1,2]. High resolution afforded by the laser technique makes it possible to unambiguously identify the spectral features belonging to ²³³U and ²³⁸U, which are separated by the so called isotope shift. Further it is also possible to resolve the hyperfine structure of ²³³U as may be seen in Fig. 2. Interestingly this relatively simple laser technique can also be used to identify spectral features of ²³⁵U even in natural uranium samples as may be seen from Fig. 3.

High resolution spectra such as those in Figs. 2 and 3 are essential in isotopic estimations since typical isotope shifts are in the range of a few MHz to a few GHz. For elemental analysis the demand on resolution is not that stringent. It is also important to stress here that the laser spectroscopic techniques offer very high detection sensitivities from trace to ultra-trace levels [3-8]. Specialized laser-based techniques such as atom trap trace analysis (ATTA) provide capability of even single atom detection [9]. While the range of applicability of laser spectroscopic techniques in the nuclear energy programme is exhaustive, we discuss a few representative examples in what follows.

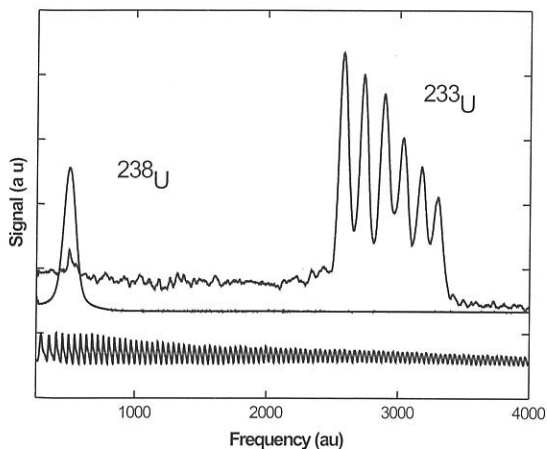


Fig. 3 High resolution OG spectrum of 860.8 nm line of uranium. Sample is natural uranium (0.72% ^{235}U). Hyperfine structure of ^{235}U and isotope shift (^{235}U , ^{238}U) is clearly seen. The frequency scale may be calibrated with 300 MHz interferometer fringes (top).

Elemental Analysis

Quantitative and reliable estimation of U is indispensable in practically all activities of nuclear energy programme from exploration and mining to waste management and storage. Laser-induced fluorescence (LIF) spectroscopy provides a very powerful technique for this [5,6]. The standard technique, used in laboratory as well as in fields, is based on the measurement of laser-induced fluorescence of aqueous uranyl ion (UO_2^{+2}) in phosphoric acid medium. UO_2^{+2} has strong absorption features in 300 nm region, which can be efficiently excited using a low cost nitrogen laser (337.7 nm) or a XeCl excimer laser (308 nm). Fluorescence spectrum of UO_2^{+2} has a characteristic structure consisting of 6-8 bands in 470-630 nm range with most intense bands in 470-530 nm region. Fluorescence lifetime of uranyl ion in aqueous solution is as high as 10^{-6} - 10^{-5} s, whereas that of organic or inorganic impurities is typically less than 10^{-8} s. Consequently, recording the LIF spectrum of UO_2^{+2} after a delay of 1-2 μs (delayed LIF technique) makes it possible to estimate uranium with very high reliability. The technique provides detection limit in the range of a few parts per billion (ppb).

Estimation of trace amounts of Pu in nuclear waste solution, which are produced in the PUREX processing of spent nuclear waste, is important task in the nuclear materials management programme. Standard technique used here is the isotope dilution mass spectrometry, which is tedious and effort intensive. Laser-induced photo-acoustic spectroscopy provides a simple but highly sensitive technique for analytical estimation of Pu [7]. In this technique, Pu^{+4} in aqueous solution is excited by Nd:Yag pumped dye laser operating at 830.5 nm (peak of the Pu^{+4} absorption band) and

the pressure wave caused by the heat energy released by the molecule through non-radiative decay processes is measured as the photo-acoustic signal. The technique is reported to provide the detection limit of 0.5 $\mu\text{g/ml}$.

Laser-induced breakdown spectroscopy (LIBS) is relatively new version of atomic emission spectroscopy [8,9]. Here, a high power laser is focused on a target of gas, liquid or solid surface, creating a dielectric breakdown. The high temperature plasma generated in this process creates atoms in highly excited electronic levels. Characteristic line emission from these atoms is detected to estimate their concentration in the target. LIBS is similar to other analytical spectroscopic techniques such as atomic absorption and inductively coupled plasma spectrometry which are routinely used in the quality control of nuclear materials. The advantage of LIBS is that it is simple, portable and rapid technique, which can be employed for online as well as offline applications in the nuclear fuel cycle.

On-line Monitoring and Diagnostics

Laser spectroscopy is a useful tool for on-line diagnostics of various complex processes encountered in the nuclear fuel cycle [11-18]. A straightforward application is in electron beam melting and evaporation of refractory metals, e.g. Zr, used in metallurgical processes. In these applications, the important requirement is to optimize and control the process of evaporation by on-line monitoring of metal vapour properties, i.e. number density, flux, temperature etc. This calls for a technique, which is non-invasive, reliable and fast. Importantly the method must allow remote operation since evaporation is carried in a hostile environment of high temperature, high vacuum, high voltage and in presence of corrosive metal vapour. Diode laser based absorption spectroscopy provides a useful technique in this context [11]. In case of Zr, a low power single mode tunable diode laser tuned to 676.24 nm transition is used to measure absorption of electron beam generated vapour. The technique can be remotized by use of optical fibers for coupling the diode laser output to the electron beam evaporator.

Laser spectroscopy has very recently been used to develop a laser-based sensor for detection of a coolant leak in nuclear reactors [12]. The device utilizes a tunable diode laser of 3 mW power, 5 MHz bandwidth and operating at 1392 nm to obtain high resolution spectrum of HDO and detect it at trace levels in the reactor neighborhood. Presence of HDO is a signature of leak since HDO is generated from the leaked D_2O by an isotopic exchange reaction with H_2O in the atmosphere, typically in 50 ms time scale after the leak occurs. The technique has been found to be superior to the currently used techniques, which include for example, radiation detection, humidity detection and acoustic emission detection. The laser-based technique provides a fast and reliable detection system for continuous monitoring of coolant leak during normal operation of the reactor. This is extremely important considering the disastrous

consequences of coolant leakage, i.e., sudden shutdown of the reactor and radioactive contamination of the environment.

Laser spectroscopy is increasingly finding applications in monitoring releases from plants in the nuclear fuel cycle [6,13]. Importance of these efforts lies in high speed monitoring of the contamination of atmosphere and water bodies surrounding the plants. One of the most dangerous components of accidental releases in nuclear fuel cycle is volatile UF₆. Release of UF₆ is accompanied by a rapid increase in atmospheric concentration of HF and UO₂F₂. Other important releases are HDO, HTO and ¹²⁹I from nuclear power stations. Tunable diode laser based absorption spectroscopy provides a convenient way of detecting all these molecules unambiguously in the atmosphere, i.e., HF is detected at 1.283 μm (2-0 R0 line of HF), UF₆ is detected at 7.68 μm (ν₃+ν₄ combination band) and HDO and HTO are simultaneously detected near 1.39 μm (harmonics and combination bands). The laser diagnostic techniques are of great interest since they can operate at a distance (several km) with high sensitivity (ppb range) and give information in real time (fraction of a second). Since these techniques are non-invasive and provide in-situ analysis with real time data, IAEA has advocated their use in detection of clandestine nuclear activities [13].

Laser-based diagnostics systems are becoming popular in the diagnostics of accelerators and related systems [14-18]. For example, Rayleigh scattering of the second harmonics of iodine laser (657.5 nm) and Nd:Yag laser (1064 nm) has been used as a diagnostic tool for measurement of electron temperature and its spatial variation in ITER tokamak system [18]. Another interesting application in the accelerator area is the on-line diagnostics of radiation enhanced aqueous corrosion of solid neutron targets and structural materials, achieved by laser Raman spectroscopy [16,17].

Another interesting application of laser spectroscopy is in the maintenance of nuclear weapons [19]. A nuclear weapon is hard to maintain since it requires continuous monitoring of the state of the components, corrosion, cracks and composition changing properties. Usual practice is to dismantle the weapon and assess the changes/damage. LLNL has developed a tiny sensor, which consists of an IR laser with fiber optical devices to continuously monitor gases. This sensor embedded in every weapon provides continuous monitoring of the state of health of every weapon and instantaneous detection of anomalies.

Ultra-trace Detection

RIS and RIMS techniques [3,4] are based on selective multi-step laser photoionization of elements and isotopes, and they are useful for ultra-trace elemental and isotopic analysis in the nuclear energy programme. Analysis of Pu at 10⁸ atom level and of ⁹⁰Sr at ~ 100 atom level are some of the examples of this kind. Analysis of ⁹⁰Sr in environmental samples assumed significance after the Chernobyl accident.

RIMS technique has been shown to be useful for trace detection of ⁴¹Ca (T_{1/2}=1.04 x 10⁵ y) in nuclear reactor concrete while decommissioning of a nuclear reactor [3]. The concrete (the biological shield of the reactor) contains ~ 10% Ca, which when exposed to a flux of neutrons produces ⁴¹Ca, i.e., ⁴⁰Ca (n,γ) ⁴¹Ca. Because of long half life ⁴¹Ca accumulates in the concrete during the life of the reactor. Radiometric estimation of ⁴¹Ca is difficult since it decays exclusively by electron capture to the nuclear ground state of ⁴¹K which subsequently emits only x-rays and Auger electrons with energies below 3.6 keV. This is where RIMS comes handy to estimate ⁴¹Ca.

Tracking Fission Events

Laser-based atom counting techniques provide a capability to detect and measure a few tens or hundreds of atoms of a specific isotope in environmental samples. Interest in this area has grown enormously in recent years, particularly in the context of ultra-ultra-trace detection of fissiogenic radio-nuclides [10]. An example is ⁸⁵Kr, which is an unambiguous tracer and ideal remote indicator for fission reaction. Measurement of ⁸⁵Kr in the atmospheric samples is of strategic importance in the nuclear energy programme for analysis of the performance of nuclear reactors, reprocessing facilities, nuclear explosions and also in detection of clandestine nuclear activities by rogue countries. This task, however, requires a measurement technique capable of analyzing ⁸⁵Kr at a few thousand atoms/l concentration level in ambient air at a selectivity level (⁸⁵Kr/Kr) of ~ 10⁻¹³. This is achieved by a very recently developed laser-based technique of atom trap trace analysis (ATTA). The technique is based on the concept of laser cooling and trapping of atoms and utilizes single mode tunable diode laser operating at 810 nm. A brief description of the technique is given in Fig. 4. The technique has been shown to be superior to the currently used techniques of low level counting and accelerator mass spectrometry, so much so that the International Network of Engineers and Scientists Against Proliferation (INESAP) has strongly advocated the use of ATTA technique for detecting clandestine production of fissile material [20].

Laser- and Fiber-Optical Based Sensors

We now discuss some of the representative applications of laser-based diagnostics techniques that are not based on the selectivity of excitation of specific atom, molecule or isotope. These techniques are based on light scattering and fiber optical systems, and are finding applications in nuclear reactors and accelerators [21-24].

In recent years interest in the on-line optical measurement of temperature in nuclear power plants is growing significantly. Use of optical fiber distributed sensors for temperature sensing is a powerful way of monitoring temperature at several locations simultaneously. Several methods have been discussed in the literature [21-23] for extracting temperature information from optical fibers and these include techniques based on Raman, Brillouin and Raleigh scattering, so also sensors based on

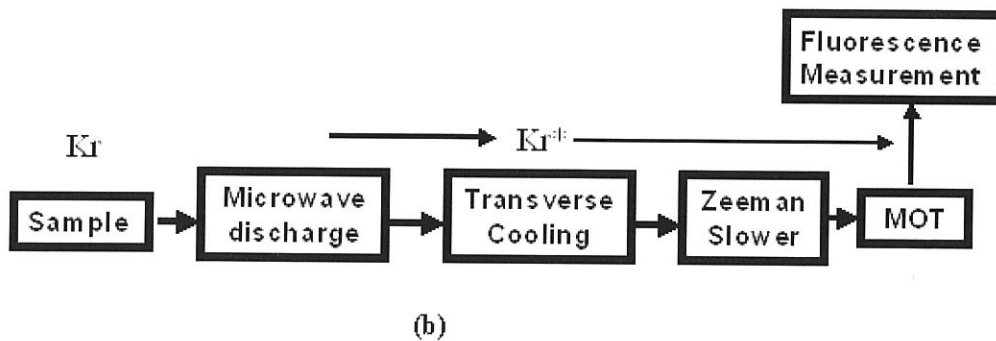
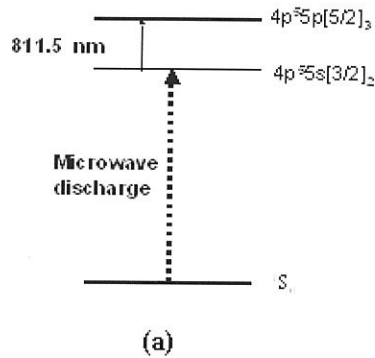


Fig. 4 (a) Energy level diagram of Kr showing relevant levels used for laser cooling and trapping. First excited level, which is a metastable level with lifetime of 40 s, is populated using microwave discharge. The transition 811.5 nm is used for cooling and trapping. (b) Schematic representation of ATTA technique [10]. An effusive atomic beam is generated from the gas in the sample chamber. Krypton isotopes are excited to the metastable level (Kr^*) by microwave discharge. The beam of Kr^* atoms is transversely cooled by lasers. The atomic beam then passes through a Zeeman slower, which makes it cold and mono-energetic. The output of the Zeeman slower is fed to a magneto-optical trap consisting of six laser beams and a spherical quadrupolar magnetic field. The balance coil is used to compensate for the earth's magnetic field. The atoms trapped at the center of the MOT are detected using fluorescence detection technique. By tuning the frequencies of the lasers used in this apparatus, various isotopes in the sample are concentrated at the center of the MOT at various times and their fluorescence measured. The fluorescence intensity is directly proportional to the concentration of the specific isotope trapped

Fabry Perot cavity and fluorescence. These fiber optical devices are useful for temperature measurements in the core, coolant loop systems, turbo-generator and also in nuclear waste management. In-situ measurement of dimensional changes is an important issue in testing of materials under irradiation in test reactors. For example, it is important to monitor the changes in the dimensions of the nuclear fuel assemblies as well as those of mechanically stressed structural material samples during irradiation. Fiber optical sensors based on the interference with light are exploited in these applications. A major problem in application of optical fibers in nuclear environment is the presence of ionizing radiations, which deteriorate the performance of the sensors. Considerable progress has been made in the search of radiation resistant optical fibers in very recent years.

There is yet another important application of laser-based diagnostics in nuclear industry, which is concerned with 3-D optical measuring technologies for dimensional inspection of nuclear plants. Increasing safety of nuclear reactors require a near total non-contact precise inspection of geometric parameters of the components,

which can be best achieved by laser-based imaging techniques [24].

Laser Isotope Separation

Isotope Separation in Nuclear Fuel Cycle

Isotope separation is a crucial process in nuclear technology for production of enriched uranium fuel and heavy water. Apart from these obvious involvements, isotope separation finds a large number of other applications in nuclear fuel cycle [25-37]. In thorium fuel cycle, removal of ^{232}U from ^{233}U (bred from thorium) is desirable since the daughter products of ^{232}U are hard γ emitter and consequently ^{233}U fuel, free of ^{232}U is expected to improve the economic gains of thorium utilization many fold [32,33]. A closely related isotope separation process is removal of ^{238}Pu , ^{242}Pu , ^{244}Pu from Pu chemically separated from the spent fuel. Gadolinium, enriched in ^{155}Gd and ^{157}Gd isotopes, is useful as burnable neutron poison [34,35]. Similar application exists for erbium enriched in ^{167}Er [4]. There has been much talk of isotope separation of ^{91}Zr from Zr used for cladding, since ^{91}Zr has relatively large neutron absorption cross-section and its removal is expected to

improve the neutron economy in a PHWR [34,35]. Another interesting application is the use of Zn, free of ^{64}Zn , in the primary coolant of a nuclear reactor [36]. Note that addition of Zn in the coolant suppresses ^{60}Co build up, but the presence of ^{64}Zn in natural Zn gives rise to the formation of ^{65}Zn ($t_{1/2}=245$ days). The obvious solution is to separate ^{64}Zn from natural Zn.

Isotope Separation in Nuclear Waste

Apart from the separation of naturally occurring isotopes listed as above, there has been a considerable interest in recent years to separate useful isotopes from nuclear waste [37]. Fission reaction generates a wide range of elements including precious elements belonging to the platinum group, i.e., Pd, Pt, Rh, Ru. In commercial light water reactors, at a burn up of ~ 33 GWd/te, the amount of platinum group elements generated is ~ 4 kg per ton of fuel, whereas in fast breeder reactor the amount estimated is ~ 19 kg per ton at a burn up of ~ 100 GWd/te. The nuclear waste, thus in principle constitutes a valuable source of these precious elements. This, however, cannot be done owing to the presence of radioactive isotopes in the nuclear waste. For example, Ru in nuclear waste contains two radioactive isotopes of mass 103 ($t_{1/2} = 39$ days) and 106 ($t_{1/2}=368$ days), while the other isotopes of mass number 99, 100, 101, 102 and 104 are stable. Similarly, the Pd in the nuclear waste contains stable isotopes of mass 104, 105, 106, 108, 110 and radioactive isotope of mass 107 ($t_{1/2}=6.5 \times 10^5$ days). If these radioactive isotopes can be removed by employing an efficient isotope separation process, the nuclear waste can become a rich source of valuable materials. In addition, the process can help to minimize the nuclear waste, thereby simplifying the task of waste management.

The capability to separate radioactive isotopes underlies the novel concept of self-consistent nuclear energy system [38]. This concept envisages on-line isotope separation of fission products so as to decrease the parasitic capture of neutrons and to keep the neutron balance in an operating nuclear reactor. An efficient and versatile isotope separation technology is key to achieving such advanced nuclear systems.

Isotope Separation Technologies

While isotope separation provides enormous opportunities in the nuclear fuel cycle, it must be known that the development of an effective and efficient isotope separation technology is one of the toughest scientific and technological challenges. The only known technology, which can cater to such diverse applications as discussed above, is the laser isotope separation (LIS) process. In what follows, we discuss the isotope separation technologies for enrichment of uranium, which occupies the major space in the nuclear fuel cycle, and then go on to discuss the merits of LIS.

Efficiency of an isotope separation technology is measured in terms of separative work unit (SWU) per

megawatt hour electricity consumed by the plant [25-30]. The first uranium enrichment method developed in 1940's was Calutron, which in essence was a mass spectrometer and provided extremely low efficiency (< 1 SWU/MWh). In 1950's came into existence the gaseous diffusion (GD) process, which relies on mass dependent diffusion of UF_6 gas through semi-permeable membranes and offered an improved efficiency (~ 2 SWU/MWh). This was followed by the development of gaseous centrifuge process in 1960's; the technology brought in a dramatic decrease in the energy required for the enrichment process. Starting from ~ 5 SWU/MWh in 1960's, the GC process today provides an efficiency of ~ 20 SWU/MWh. LIS technology, the development of which began in 1970's, is poised to compete with GC technology in terms of its efficiency. Further, unlike GD or GC technologies, LIS is a general and generic technology, which can be used for separation of isotopes of most of the elements in the periodic table, irrespective whether they are stable or radioactive. This later aspect is important in the context of isotope separation tasks involved in thorium fuel cycle as well as recovery of precious elements from nuclear waste. Further LIS is viewed as a promising technology for achieving self-consistent nuclear energy systems [38].

LIS is an industrial process, which is based on quantum mechanics and whose design is shaped by atomic, molecular and optical physics. While the traditional methods of isotope separation, i.e. GD and GC, make use of the small mass difference between isotopes, LIS exploits the minute difference in the energy levels of isotopes, popularly known as isotope shift (IS), which originates from the differences in the nuclear mass, volume and spin of isotopes under consideration. Monochromaticity of laser helps to excite a specific isotope of interest thereby making the laser-atom/molecule interaction process isotope selective. This results in a physico-chemical transformation, i.e. ionization (for atoms) or dissociation (for molecules), of one of the isotopic species in a mixture. The transformed species are then removed from the bulk by application of suitable techniques such as extraction by electric fields (in case of ions) or chemical separation (in case of molecules). Thus, LIS processes and related systems fall into two broad categories, namely atomic vapour LIS (AVLIS) [25-36] and Molecular LIS (MLIS) [25,39,40], depending on whether the process medium is an atomic or molecular beam. The atomic/molecular beam, rather than vapour, is used to avoid unwanted collision processes that can lead to the loss of selectivity and degradation of the product.

Atomic vapour Laser Isotope Separation

A schematic representation of AVLIS is displayed in Fig.5. Here the process medium is an atomic vapour, which is usually generated by electron beam evaporation of a metal substrate. The desired isotopic atoms (e.g. ^{235}U) in the vapour are selectively excited and ionized by using a set of precisely tuned narrow bandwidth lasers.

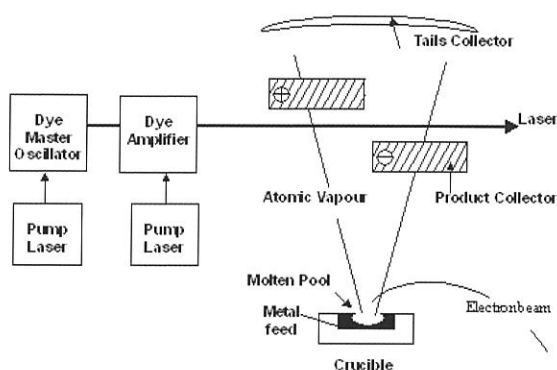


Fig. 5 Schematic representation of AVLIS process. Here atomic beam is generated by an electron gun impinging on the metal feed kept in a water-cooled crucible. Vapour is then illuminated with tunable lasers, which consist of dye amplifier, dye master oscillator and pump lasers, to drive isotope selective photoionization process. Photo-ions of target isotope are collected on product collector, whereas the waste is collected on tails collector.

The lasers used in this process are tunable dye or solid state lasers, which in turn are pumped by copper vapour lasers or diode pumped solid state lasers. Typical photon energy of the tunable output is ~ 2 eV. Since the ionization potential of most of the atoms of interest lies in the range 6-7 eV, a three step photoionization process, wherein the atoms are ionized with three independently tunable lasers, is used. Usually the first step is kept isotope selective, but if the demand on the selectivity is large the second step can also be made selective. The intensities and pulse repetition rates of the lasers must be kept high to ensure $> 90\%$ photoionization efficiency for the desired isotope. At the end of the selective excitation and ionization, the atomic vapour is converted into a photo-plasma which is a mixture of ions of desired isotope (e.g. $^{235}\text{U}^+$) and neutrals of the unwanted isotope (e.g. ^{238}U). The task then is to separate ions from the neutrals before scrambling reactions such as charge exchange, i.e., $^{235}\text{U}^+ + ^{238}\text{U} \rightarrow ^{235}\text{U} + ^{238}\text{U}^+$, take place. Ion extraction is the process by which the ions are extracted from the photoplasma by application of appropriate electric/magnetic fields to the structures placed near the atomic beam. There are a variety of ion extraction schemes based on DC and pulsed electric fields, ambipolar diffusion, magneto-hydrodynamics etc, and the choice is determined by the plasma density and the speed of extraction, which is governed by the rate of the scrambling processes. Finally the ions are collected on extractor structure (product collector) and the neutral vapour is collected on the roof of the separator (tails collector). This is an essence of AVLIS, which can be employed for practically all tasks of laser isotope separation. However, developing this simple idea into an industrial process requires putting together a number of disciplines, which include for example quantum electronics, spectroscopy, collision physics, gas dynamics, thermal physics, plasma

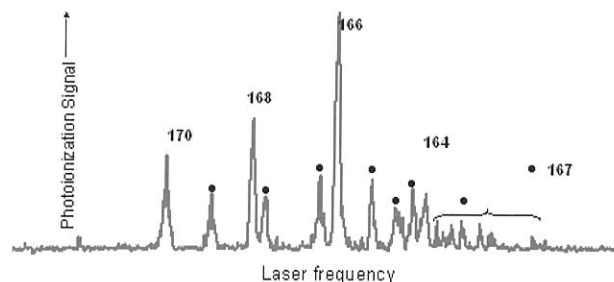


Fig. 6 Isotope selective photoionization of natural erbium sample consisting of isotopes of mass numbers 170 (14.9%), 168 (27.1%), 167 (22.9%), 166 (33.4%), 164 (1.56%) and 162 (0.14%) by three-step photoionization ($\lambda_1=582.7$ nm, $\lambda_2=559.7$ nm, $\lambda_3=621.6$ nm). Signals corresponding to the even mass isotopes appropriately marked. Hyperfine splitting is clearly seen for the odd mass isotope.

physics and optics, and meeting of several engineering and material handling challenges [25-37].

As an example of the strength of AVLIS, we show in Fig.6, our work on isotope selective three step photoionization of natural erbium vapour [4].

Natural erbium contains 5 even mass isotopes (162, 164, 166, 168, 170) and one odd mass isotope (167). Typical isotope shift between adjacent even mass isotopes is ~ 1 GHz while the hyperfine structure of the odd isotope is so widespread that it overlaps with the spectra of essentially all even isotopes. Isotopic discrimination is however possible in a photoionization process using narrow band tunable dye lasers.

Molecular Laser Isotope Separation

In MLIS, the process medium is a molecular gas that is irradiated with an IR laser to bring in chemical change in the molecules containing desired isotope [25,39,40]. For example, in MLIS for uranium enrichment, UF_6 gas is illuminated with an IR laser operating near $16 \mu\text{m}$ to excite selectively $^{235}\text{UF}_6$ molecules. There exist a variety of ways to deal with this vibrationally excited molecule. One way is to use a UV laser or a high power IR laser to dissociate the molecule to form $^{235}\text{UF}_5$ and free fluorine atom. The $^{235}\text{UF}_5$ formed in this process separates from the gas as a solid precipitate. Another way is to react the vibrationally excited molecule with a suitable reactant gas to form a product, which can be easily removed from the mixture. In very recent years a new MLIS process, called SILEX, is under development [30]. The physics and technology of this process is however classified, but the reported literature suggests that the process can provide efficiency in excess of 20 SWU/MWh. The process is probably based on selective excitation of $^{235}\text{UF}_6$ by $16 \mu\text{m}$ laser in a feed stream consisting of UF_6 and an unidentified diluting gas in a nozzle. The crucial ingredient for the development of MLIS is an efficient scheme for generating $16 \mu\text{m}$ laser with high

enough pulse repetition rate. Raman shifting of CO₂ laser in para-H₂ and CF₄ media has long been attempted as possible solutions.

Comparative View

The strength of LIS lies in the large single stage separation factor, which is defined in terms of the ratio of the mole fractions in the product and the tails, and further is related to the SWU/MWh [25-31]. In case of uranium enrichment, typical single stage separation factors achievable with AVLIS and MLIS are ~ 100 and ~ 1.2 respectively. These may be compared with the values 1.0036, and 1.2 for GD and GC respectively. Finally we may add here that for MLIS, GD and GC technologies, the necessary pre-requisite is a molecule with sufficiently high vapour pressure. This is, however, difficult to meet for all isotope separation tasks of interest in the nuclear fuel cycle. AVLIS technology, which works with metal feed and provide large single stage separation factor stands out in these regards.

High SWU/ MWh achievable by LIS has important consequences in uranium fuel cycle. Note here that SWU depends on mole fraction of ²³⁵U in the feed, product and tails. In a scenario where uranium feed stock is cheap and SWU is expensive, the fuel of given mole fraction can be obtained in a cost effective manner by using more feed and throwing tails at relatively higher mole fraction. This scenario applies to GD and GC processes. On the other hand the comparatively cheaper SWU in LIS technology makes it possible to separate much of ²³⁵U from the feedstock and throw tails at a very low moles fraction. This has considerable advantage in conserving uranium resources.

Lasers for Material Processing

Nuclear Material Processing

The scope of laser applications in material processing has become widespread in recent years in industry and in various technologies, including nuclear. These applications include laser drilling and cutting, surface modifications including surface melting, hardening, quenching and alloying [41]. The unique advantage of laser material processing are, localized heat zone, ability to weld dissimilar materials and complex geometries and ability to transport laser beam to difficult areas using optical fibers. Some of the applications of material processing in nuclear energy programme have been mentioned earlier, e.g., welding of precision parts such as core internals of a nuclear reactor or welding of stainless steel tanks for nuclear fuel reprocessing plants, laser cutting of burnt fuel assemblies and finally cutting operations involved during the decommissioning of a nuclear reactor [42-44].

Maintenance of in Service Reactors

Laser techniques are useful for maintenance of in service reactors [45-46]. In this context we may refer to a laser-based maintenance system, which has been developed

for in-service maintenance of nuclear power plants in Japan [45]. This system addresses to the initiation of stress corrosion cracks (SCC), which is a principle mechanism of deterioration in aged nuclear reactors. The maintenance system includes laser ultra-sonic testing as a non-destructive testing technology, laser peening as a surface stress improvement technology and laser welding as repair technology. Laser-based techniques are very useful in this context since they are non-contact and remote, and further are applicable to narrow and congested space of the reactor internals. Detection of cracks is done by the technique of laser ultrasonic testing. Here, a laser incident on a surface induces ablation plasma, which in turn gives rise to surface acoustic waves (SAW) on the inspection surface. SAW travel through the surface layer, which is as thin as one wavelength. SAW of higher frequencies are reflected according to the geometry of the crack, and that provides a way to detect micro surface breaking cracks. Actual measurement is performed using interferometric measurements. The method allows detection of small cracks having depth less than 0.1 mm. Once the cracks are detected, laser-welding technique is used to repair them. If no cracks are detected, laser-peening [46] is activated to improve the surface stress to prevent SCC initiation in future.

Decontamination in Nuclear Fuel Cycle

In very recent years, laser-based decontamination techniques are becoming increasingly popular in nuclear industry [47]. Decontamination is an important step in several activities associated with the nuclear technology including the decommissioning of aged reactors. Needless to say that decontamination reduces the occupational exposure and allows safe management of radioactive waste. Most of the radioactive contaminants are usually deposited on base metal surfaces as oxide layers. The conventional decontamination techniques include mechanical, chemical and electrochemical removal of the contaminants from the surface. A superior decontamination technique is that which is 'dry', efficient, does not allow recontamination and produces negligible radioactive waste. Most of these attributes are met by laser decontamination technique. Here, a high power laser is focused on the contaminated surface and the process of ablation is used to make the surface clean. A typical set up consists of a laser, an optical fiber for transportation of laser beam, a condenser lens for focusing and a nozzle to provide a shielding gas and to collect the particulate generated by laser irradiation.

Properties of Nuclear Materials at High Temperatures

Ability of high power lasers to generate high temperatures is useful in studies of nuclear materials at elevated temperatures [41,48]. Nuclear technology requires reliable thermodynamic, thermo-physical and thermo-chemical data in various temperature ranges, i.e., up to 2000 K for fuel fabrication, up to 2500 K to predict fuel behaviour under normal operating conditions and up to 5000 K for safety risk assessments. In particular, the fast breeder

reactors require the experimental equation of state input data for safety risk analysis. Note here that measurement of the properties at temperatures up to 5000 K is a severe problem since this is beyond the melting point of the refractory materials, which may be used as containers in the measurement studies. Laser pulse heating technique [41] is ideally suited for all these studies. For example, a pulsed Nd:Yag laser focused on a target at the intensity level of $\sim 10^7$ W/cm² can conveniently provide temperature range of 3000-5000 K. Further the entire heating process is 'container free', which helps in retaining the purity of the sample during measurement process. An advanced version of the pulsed laser heating for property measurements is 'laser autoclave technique' [41] wherein a sample is heated to very high temperature by a set of laser beams, e.g., four beams in tetrahedral geometry or six beams in three-axis geometry, under pressurized inert gas atmosphere. Pulse laser heating or laser autoclave set up combined with diagnostic equipments, e.g., mass spectrometers, pyrometers, x-ray diffraction set-up etc., provides very useful high temperature data for nuclear fuels including vapour pressure, thermal conductivity, chemical reactivity, compositional changes, loss of material strength, heat transfer etc.

Ultra-intense Lasers and their Applications

The advent of ultra-high peak power ultra-short pulse duration (10^{-15} s) lasers has ushered in a new class of physics, i.e., physics under extreme conditions, and technology applications [49-57]. The rapid progress in the peak power of the lasers is primarily due to the technique of 'chirped pulse amplification' (CPA) [49-51] introduced in mid '80s. In this technique a laser pulse of femto- or pico-second duration is temporally stretched by 3-4 orders of magnitude using dispersive grating thereby preventing damage to the laser amplifying medium at high intensities. The stretched pulse, after amplifying is recompressed to deliver a pulse with ultra-high peak power. Ultra-high intensity laser pulses interact with the electrons in high-density plasma through ponderomotive forces leading to relativistic velocities [52-54]. The laser accelerated high-energy electrons and the secondary bremsstrahlung gamma photons participate in a whole range of nuclear processes including nuclear fission and fusion [55-57]. All these areas of science and technology till recently were exclusively reserved for nuclear accelerators and reactors. In what follows we discuss some of the leading issues that are impacting the nuclear energy programme and its future directions.

Laser Fusion

Lasers have long been considered as promising tools to achieve the holy grail of nuclear energy, the inertial confinement fusion (ICF) [58,59]. Work in this direction began soon after the invention of lasers and much is known about it today. ICF is a process where nuclear fusion reactions are initiated by heating and compressing a fuel target containing a mixture of deuterium (D) and tritium (T). Here the high intensity laser beams delivered on the target

(~a few mg of D/T mixture) to provide energy for heating and compression. The outer layer of the target explodes outwards thereby producing a shock wave travelling towards the centre. The powerful shock wave compresses the inner core of the fuel at extremely high densities ($>10^3$ g/cm³) and temperatures (tens of millions °K), sufficient to satisfy the well known Lawson's criterion, i.e., $n\tau > 2 \times 10^{14}$ cm⁻³s, $nT\tau > 3 \times 10^{15}$ cm⁻³ keVs, $P\tau > 10$ atm.s, where n is the density, τ is the energy confinement time, and T and P are respectively the plasma temperature and pressure. The name 'inertial confinement' derives from the fact that the process is accomplished in a time interval $< 10^{-9}$ s which does not allow the nuclei to move appreciably due to their own inertia. The term 'ignition' is used when the energy released further heats the surrounding fuel to continue the fusion chain reaction.

The first evidence for ICF was obtained in late '60s with a high power pulsed Nd:glass laser focused on a LiD target to detect fusion neutrons. Shiva laser was the first generation of high power lasers developed for ICF at Lawrence Livermore National Laboratory (LLNL) in '70s [60]. This was followed by more powerful laser system called Nova, which consists of ten lasers focused to 1 mm diameter on a D-T target and dumping $\sim 10^5$ J energy in 10^{-9} s time scale, which achieved fusion 'breakeven' point in 1994. Rapid advances in ICF have taken place at National Ignition Facility (NIF) in USA [61] and Laser Megajoule (LMJ) facility at France [62], and the 'ignition' looks to be around the corner.

In recent years, LLNL has developed the concept of fast ignition fusion (FIF), a revolutionary concept which promises a less energy intensive route for harvesting fusion energy [57]. This concept relies on two different sets of lasers, long- and short- pulse durations for two stages, i.e., compression and heating. Fast fusion is mediated by the nuclei accelerated by short pulse (10^{-15} s) petawatt lasers. The role of the ultra-intense short pulse laser is to accelerate the nuclei to extremely high kinetic energies by the laser-induced ponderomotive forces (wakefield acceleration) to overcome the Coulomb barrier. Typically for deuterium target the collision energy is $E_{\text{col}} \sim 8$ KeV at 10^{21} Wcm⁻² which corresponds to fusion cross-section of $\sigma \sim 10^{-4}$ b, while at 10^{22} Wcm⁻², $E_{\text{col}} \sim 80$ KeV and $\sigma \sim 5$ b. Fast fusion was demonstrated at GEKKO XII laser at Osaka University in Japan in collaboration with UK researchers in 2001 [63]. Current work in FIF is focused in upgrading the laser systems to reach the 'breakeven' point and further improvements to reach the ignition stage. The European proposal HiPER (High Power laser Energy Research facility) [64] is based on the FIF concept. The facility will consist of 200 kJ long pulse laser (for compression) and 70 kJ short pulse laser (for heating) and it is designed to provide critical intermediate step between ignition and a demonstration fusion reactor.

Laser Plasma Accelerators

Nearly seventy years after the first accelerator by Lawrence, the accelerator technology has grown in a spectacular manner. The major problem in the conventional accelerator technology arises due to the limiting electric field strength of 10^6 Vm^{-1} that the accelerator structure can stand without electric breakdown. This can be improved to 10^7 Vm^{-1} by use of superconducting cavities; the technology however is complex and expensive [51]. It is here that the laser particle accelerators based on table-top ultra-intense lasers score. In fact, the laser-plasma accelerators have the potential to deliver accelerating gradients more than 10^3 times the conventional accelerator technology [49-51].

Research in laser-plasma accelerators began in late '70s with a path-breaking paper by Tajima and Dawson [52], who proposed a construction of laser-electron accelerator, based on an intense laser pulse, producing a wake of plasma oscillations. They showed that a laser of 10^{18} Wcm^{-2} illuminating a plasma of density 10^{18} cm^{-3} can produce electrons of GeV/cm of the acceleration length. Apart from wake field acceleration, a number of other mechanisms to accelerate electrons in plasma to several times the value of the pondermotive potential have been proposed and these include plasma wave breaking, $V \times B$ acceleration in presence of an azimuthal magnetic field and resonance absorption. The mechanism responsible for ion acceleration is related to the electron acceleration. The laser pondermotive force pushes the electrons in the forward direction leaving the ions behind. The charge separation creates large electrostatic fields, which in turn accelerate ions. At current stage of technology, laser driven particle accelerators providing mono-energetic particle beams with 10^{8-12} particles in ~ 1 ps pulse at 1-200 Hz rep rate are realizable [53,54]. However, laser accelerated particle beams have yet to achieve the quality of conventional accelerator beams, but that situation is certainly to improve as the technology matures in future.

The progress of conventional accelerator technology is usually discussed in terms of Livingston Chart, according to which the electron beam energies of conventional accelerators have increased by a factor 10 every six years over the last 70 years [49-51]. Compare this with the peak power of the lasers, which has increased on an average by one order of magnitude every three years in recent times. Moreover there is a widely held view [49-51] that the Livingston chart for conventional accelerators will flatten at 1 TeV, whereas there is no apparent limitation for laser accelerators. At present, most of the conventional accelerators planned in the world are likely to be completed by 2020-30. The laser accelerator technology is expected to mature by that time to take over from the conventional technology [49-51].

Laser Neutron Source and Laser Induced Nuclear Transmutations

Ultra-intense lasers are now increasingly viewed as a tool for neutron generation. The mechanisms used for

neutron production by lasers are laser-driven fast fusion in D-T targets and also the secondary reactions, i.e., photonuclear reactions (γ, n), photo-fission reaction (γ, f) and spallation by laser-accelerated proton beam (p, n). Other secondary reactions of interest are $d(d,n)^3\text{He}$ and $d(t,n)^4\text{He}$. Typical neutron production rates demonstrated are $\sim 3 \times 10^{10} \text{ s}^{-1}$ by spallation by laser-accelerated proton beam and $\sim 3 \times 10^8$ by laser-driven fast fusion in D-T. These laser-neutron sources offer efficiency of $\sim 10^8$ neutrons/J, which compares favourably with accelerator-driven spallation sources [55].

Another important direction in the ultra-intense laser-matter interaction is laser-induced nuclear transmutation [56], particularly in long-lived fission products ^{137}Cs ($T_{1/2} = 30 \text{ y}$) and ^{129}I ($15.7 \times 10^6 \text{ y}$). For example, (γ, n) reaction transmutes ^{137}Cs to ^{136}Cs ($T_{1/2} = 12.6 \text{ d}$), which decays to stable ^{136}Ba by β decay. In a similar manner, ^{129}I is transmuted to ^{128}I ($T_{1/2} = 25 \text{ m}$), which undergoes β decay to form stable ^{128}Xe .

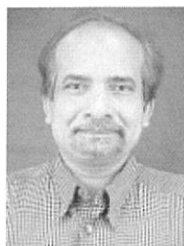
Conclusions

In this article we have reviewed the applications of lasers in nuclear energy programme. We have covered here wide ranging issues encompassing practically every aspect of nuclear power production — uranium prospecting, nuclear material characterization, laser isotope separation, on-line monitoring and diagnostics of nuclear facilities, monitoring of nuclear events, decommissioning of nuclear power plants etc. With the growth of ultra-intense lasers, the use of lasers in nuclear energy programme is expected to grow phenomenally. Applications in this class include x-rays, γ -rays, neutron generation, laser-particle accelerators and nuclear transmutations to take care of nuclear waste. The progress in the field of laser fusion gives us a hope that the holy grail of nuclear energy will soon be found. It is also possible now to think of laser-driven sub-critical systems (LDSS) in contrast to the much discussed accelerator drive sub-critical systems (ADSS). These issues will continue to keep the researchers busy for several years to come.

References

1. K.G. Manohar, A.P. Marathe, S. Pradhan and B.N. Jagatap, Indian Nuclear Society's conference on Nuclear Fuel Cycle technologies: Closing the Fuel Cycle, IGCAR, Kalpakkam, December 17-19, 2003.
2. Asawari P. Marathe, K.G. Manohar and B.N. Jagatap, National Laser Symposium, IIT Kharagpur, Dec. 22-24, 2003
3. P. Muller, K. Blaum, B.A. Bushaw, S. Diel, Ch. Geppert, A. Nahler, W. Nortershauser, N. Trautmann and K. Wendt, *Radiochim. Acta* 88, 487 (2000).
4. A.P. Marathe, S. Pradhan, A. Ray, K.G. Manohar, A. Venugopalan and B.N. Jagatap, Proceedings of the 9th International Workshop on Separation Phenomena in Liquids and Gases, Tsingua University, Beijing, China, Sept. 18-21, 2006, Tsingua University Press (2007) pp.64-67.
5. S. Kher in Recent Developments in Spectroscopy of Lanthanides and Actinides, Ed. B.N. Jagatap and A. Venugopalan, Ebenezer, Mumbai (2006) pp.181-184.
6. G. Yu Grigorev et al, *Atomic Energy* 105, 280 (2008).

7. N. Surugaya, S. Sato, S. Jitsukata, M. Watahiki, *Anal. Sci.* 24, 527 (2008).
8. M. J. Myers, J.D. Myers and A. G. Myers in *Lasers in Chemistry*, Vol.1, Ed. M. Lackner, Wiley (2006).
9. K. Stelmaszczyk et al, *Appl. Phys. Lett.* 85, 3977 (2004).
10. P. Collon, W. Kutschera, Z.-T Lu, *Ann. Rev. Nucl. Part. Sci.* 54, 39 (2004).
11. K.B. Thakur, G.K. Sahu, S.J. Gaur, R.C. Das, A.K. Tak, R.A. Patankar, G.K. Bhowmick, K.G. Manohar, B.N. Jagatap and N. Venkatramani, *Vacuum*, 77, 443 (2005).
12. T.S. Kim et al, *Appl. Phys. B*, DOI 10.1007/s00340-010-3947-A (2010).
13. Technical Meeting on Applications of Laser Spectrometry Technique in IAEA Safeguards, STR-352, 28, August-September 2006, Vienna.
14. A.G. Miller, *Anal. Chem.* 49, 2044 (1977).
15. K. Ishida et al, *Proc. Int. Conf. on Water Chemistry of Nuclear Reactor System*, Vol.1, British Nuclear Energy Society (2000).
16. R.S. Lillard and D.P. Butt, LANL Report, LAUR 96-1011 (1996).
17. H. Koziol, CERN/PS 2001-012 (DR), 2001.
18. V.A. Belykov et al, *Plasma Devices and Operations*, 1, 227 (1991).
19. *Science & Technology Review*, July-August 2008.
20. M.B. Kalinowski, H. Daerr and M. Kohler, *INESAP Information Bulletin No. 27*, December 2006.
21. F. Berghmans, E. Vos and M. Decreton, *IEEE Trans. Nucl. Sci.* 45, 1537 (1998).
22. S.O. Keeffe and E. Lewis, *Int. J. Smart Sensing and Intelligent Systems*, 2, 490 (2009).
23. Y. Zhang, G.R. Pickrell, B. Qi, A.S. Jazi and A. Wang, *Sensors* 6, 823 (2006).
24. Yu V. Chugui, *J. Phys. Conference Series*, 13, 366 (2005).
25. V.S. Letokhov, *Ann. Rev. Phys. Chem.* 28, 133 (1977).
26. J.A. Paisner, *Appl. Phys. B* 46, 253 (1988).
27. P.T. Greenland, *Cont. Phys.* 31, 405 (1990).
28. P.A. Bokhan et al, in *Laser Isotope Separation in Atomic Vapour*, Wiley-VCH Verlag (2006).
29. J.W. Erkens, J.F. Kunze and L. Bond, 14th Int. Conf. Nucl. Eng., July 17-20, 2006, Miami, Florida.
30. F. Slakey and L.R. Cohen, *Nature* 464, 32 (2010).
31. B.N. Jagatap, Proceedings of INSAC-2005, 'Science behind Nuclear Energy', Dec.14-16, 2005, BARC, Mumbai, Part I, p. 63.
32. L.M. Gantayet, B.N. Jagatap, K.G. Manohar and K.C. Sahoo, in Proceedings of INSAC-2000 on "Power from Thorium: Status, Strategies and Directions", June 1-2, 2000, Mumbai, Part I, p.123.
33. A.P. Marathe, A. Venugopalan, K.G. Manohar and B.N. Jagatap, *BARC News Lett.* 273, 145 (2006).
34. Y. Izawa et al, *J. Nucl. Sci. and Tech.* 39, 426 (2002).
35. S. Tokita et al, *J. Nucl. Sci. and Tech.* 40, 1014 (2002).
36. A.N. Tcheltson et al, *Nucl. Instr. Methods in Phys. Res. A* 561, 52 (2006).
37. R.P. Bush, *Platinum Metals Rev.* 35, 202 (1991).
38. A.N. Ezoubtchenko, H. Akatsuka and M. Suzuki, *Prog. Nucl. Energy*, 32, 729 (1998); M. Saito, *Prog. Nucl. Energy* 40, 365 (2002).
39. V. Parthasarathy, S.K. Sarkar, K.K. Pushpa, K.A. Rao, K.V.S. Rama Rao and J.P. Mittal, *Appl. Phys. B* 56, 101 (1993).
40. V. Parthasarathy, A.K. Nayak and S.K. Sarkar, *J. Chem. Sci.* 114, 639 (2002).
41. R.W. Ohse, *Pure & Appl. Chem.* 60, 309 (1988).
42. Y. Shimokusu et al, Mitsubishi Heavy Industries Ltd. *Techn. Rev.* 38, 1 (2001).
43. D.L. Carroll et al, *IEEE J. Quant. Electr.* 36, 40 (2000).
44. E.J. Menehara, *Proc. FEL08*, Gyeongju, Korea (2008) pp.525-528.
45. M. Ochiai, 1st Int. Symp. On Laser Ultrasonics: Science, technology and Applications, July 16-18, 2008. Montreal, Canada.
46. K. Okimura et al, Mitsubishi Heavy Industries Ltd. *Techn. Rev.* 47, 30 (2010).
47. Y. Kameo et al, *J. Nucl. Sci. Tech.* 41, 919 (2004).
48. D.P. Butt, P.J. Wantuk and A.D. Sappey, *J. Am. Ceramic Soc.* 77, 6 (1994).
49. C. Yamanaka and S. Sakabe, *Rev. Laser Eng.* 30, 185 (2002).
50. Y. Izawa et al, *J. Opt. Soc. Korea*, 12, 178 (2008).
51. K.W.D. Ledingham and W. Galster, *New J. Phys.* 12, 045005 (2010).
52. T. Tajima and J. M. Dawson, *Phys. Rev. Lett.*, 43, 267 (1979)
53. K. Krushelnick et al, *Phys. Rev. Lett.*, 83, 737 (1999).
54. V. Malka et al, *Nature Physics* 4, 447 (2008).
55. L. J. Perkins et al, *Nuclear Fusion*, 40, 1 (2000).
56. K.W.D. Ledingham et al, *J. Phys. D* 36, L79 (2003).
57. M. Tabak et al, *Phys. Plasmas* 1, 1626 (1994).
58. J. Nuckolls, L. Wood, A. Thiessen and G. Zimmerman, *Nature* 239, 139 (1972).
59. J.A. Maniscalco, *Ann. Rev. Energy* 5, 33 (1980).
60. Laser Program Annual Report, Lawrence Livermore Lab. UCRL-50021-77, UCRL-50021-78
61. <http://www.lasers.llnl.gov/about/nif/>
62. <http://www-llm.jcea.fr/>, <http://www.cilas.com/megajoule-laser/htm>
63. <http://www.ile.osaka-u.ac.jp/>
64. <http://www.hiper-lasr.org/>



Dr. B.N. Jagatap, Outstanding Scientist, heads the Atomic & Molecular Physics Division of Bhabha Atomic Research Centre, Mumbai. He is a Senior Professor in Homi Bhabha National Institute and Distinguished Professor (Adjunct) in the Department of Physics, Indian Institute of Technology, Mumbai. He is associated with the laser programme of BARC for over 30 years. His research interests are laser physics, laser spectroscopy, applications of lasers in nuclear fuel cycle, ultra-cold atoms, quantum optics and accelerator-based atomic and molecular physics. He is a recipient of Homi Bhabha Award for Science & Technology in the year 1999.

Plasma Physics and Technologies in DAE

A.K. Das

Laser & Plasma Technology Division, Bhabha Atomic Research Centre, Trombay, Mumbai 400 085, E-mail: akdas@barc.gov.in

Abstract

The uniqueness of the plasma state lies in the rich diversity of physical parameter space accessible to this medium. While the collective non-linear interactions of charged particles and fields, pave way for many new and interesting physics, the extremely high energy flux, high temperatures, abundance of activated species, steep gradients of plasma fields, high heating rates etc. have continuously driven plasmas towards realization of a number of new, efficient and environment friendly technologies for large-scale energy generation and materials processing. In India, The Department of Atomic Energy (DAE) adapted plasma science as one of the components for building a sustainable base for research and technology demonstration towards sustainable and self-sufficient nuclear power program. The major plasma programs, with significant scientific foundation and technology development achieved, include thermonuclear fusion grade plasmas, laser produced plasmas, low temperature processing plasmas and charged particle beams. The major thrust in demonstrable applications include energy generation, advanced materials processing, compact accelerators and light sources and waste beneficiation. The article focuses on the physics of some of these areas and the road-map of their development in DAE.

Introduction

The genesis of the plasma state goes back to earliest universe following the big bang. Chronologically, the very first state of matter that was created was quark gluon plasma. Subsequently, as the matter cooled, the universe, as we know today with its galaxies, stars, planets etc. was formed, with 99.9% being in the plasma state. Plasma can be thought of as an interacting aggregate of atoms, ions, electrons, molecules, free radicals, excited species and photons. In a large majority of cases, dispersed phases of tiny solid particles and liquid droplets could also be present. The temperature, pressure and particle number densities define the thermodynamic state, whereas the dynamic state is defined by the collective interaction of moving particles with the plasma fields. The uniqueness of plasma state lies in the astronomically large range of scale of physical parameters that they encompass. These vary from microscopic to cosmic i.e. 10^{-10} to 10^{+23} m in spatial dimension; from pico seconds to hours/days of life-times, 10^{-27} to 10^{+10} in Mass density (gms/cm³); $< 10^{-4}$ to $> 10^{+30}$ cm⁻³ in number densities; from near absolute zero (crystalline states in recent non-neutral laboratory plasmas) to more than 10 keV (10^7 K) in particle temperatures; less than 10^{-6} to more than 10^{+6} Gauss of magnetic fields and from micro volts to million volts in internal electric fields. The near-equal values of positive- and negative-charge-carriers manifest in large electrostatic fields with the aggregate of charged particles behaving collectively like a fluid, and exhibiting characteristic oscillations/instabilities. A length-scale called the Debye length ($\sim T/n$) and a time-scale called the plasma frequency ($\sim n$), decide the relative dominance of plasma behavior, as compared to neutral gas-like behavior. The wide variety of species, each with different atomic/molecular structure, opens up the possibility of multiple reaction channels and non-equilibrium states. Plasmas normally have different temperatures, corresponding to the various species and various degrees of freedom in the same species. In magnetized plasmas, physics gets more complex due to the infinitely large number of new modes or degrees of freedom

introduced due to the presence of magnetic field and its peculiar way of interaction with the charged particles.

While the collective non-linear interactions of charged particles and fields pave way for many new and interesting physics, the extremely high energy flux, high temperatures, abundance of activated species, steep gradients of plasma fields, high heating rates etc. have opened up possibilities of a number of new, efficient and environment-friendly technologies for large-scale energy generation and materials processing. India has a long history of Plasma Physics and technologies, starting from the famous ionization relation of Prof. Meghnad Saha, and many Indian scientists have made significant contributions to plasma science and technology.

Plasma Science in Atomic Energy Programs: Historical Perspective

Historically, plasma science made its first appearance in DAE's program, through the speech of Dr. H. J Bhabha, wherein he expressed his faith in plasma fusion's viability for future energy scenario in the first Geneva conference on peaceful uses of Atomic Energy. Immediately in 1957, a group was constituted by him in the Tata Institute of Fundamental Research (TIFR) to study theoretical plasma physics [1] and the next year, Dr. Bhabha invited Prof Alfvén to visit TIFR to give a series of lectures on "Magnetohydrodynamics and cosmic rays". The first experiment on toroidal plasma was also initiated at TIFR at the same time. However, the effort towards building a sustainable activity towards achieving plasma fusion did not take shape at that time. A decade later, the year 1970 saw resurgence in plasma science and technology when fresh efforts were initiated towards using plasmas as a technological tool for various applications. Development of underwater- and air-plasma-cutting-systems were initiated at the Bhabha Atomic Research Centre (BARC), primarily driven by the urgent requirement of cutting of thick stainless steel plates for the variable energy cyclotron project. The Technical Physics Division at BARC was entrusted with this task, and as in all DAE technologies, work was initiated at ab-initio level for designing and building an air- as well as

underwater-plasma-cutting-system. In fact the technology of the 100 kW plasma-cutting-torch was subsequently transferred to M/s Kirloskar Industries. As the plasma MHD generator program took shape, the plasma technology activities also included development of plasma-spray-coating of ceramic on metals. Plasma spray, as an important surface modification technology, has had a sustainable growth in DAE, and has been serving many user groups since then.

A few of the major programs in plasma science and technology that were taken up during the early seventies, also included plasma- and electron-beam furnaces, development of plasma MHD generator with specific emphasis on coal-based systems [2], and generation and transport of relativistic electron beam for plasma fusion technology. Since then, the BARC program on plasma science and technology has evolved to developing of high power plasma sources, process development on reactive spraying, metallurgical applications like melting, mineral dissociation and materials synthesis, with particular emphasis on rare earth minerals, low-pressure-plasma physical and chemical vapor deposition, plasma nano synthesis etc. BARC had also started working on high-temperature plasma physics research, which included laser produced plasmas, inertial confinement fusion, dense plasma focus devices and pinch systems. With the induction of the Institute of Plasma Research (IPR) in to the DAE fold, research on science and technology of magnetized plasma fusion and Tokamak research became part of major thrust areas of DAE. As the Department of Atomic energy completes the first decade of the new millennium, plasma science has grown to maturity as a thrust area of research in various units of DAE, like BARC, Raja Ramanna Centre for Advanced Technology (RRCAT), Indira Gandhi Centre for Atomic Research (IGCAR), IPR and Saha Institute of Nuclear Physics (SINP), both in terms of fundamental understanding of the plasma medium, as well as using plasmas as a technological tool. In the following sections, an attempt is made to briefly summarize the achievements as well as the progress in some of the exciting fields of plasma science and technology in DAE.

Basic Plasma Physics Research in DAE) Precursor for Technology Development

As a rule, DAE programs are planned and evolved through a synergistic route where the two major aspects, namely, basic physics research and technology development activities are implemented together, in a self-consistent manner. In other words, the knowledge derived from basic physics research, supports the various technology components of the self-sustained nuclear fuel cycle; and the needs of upgrading the technology, drives further research on scientific issues. Development of various plasma physics programs in DAE have been no exception to this fact. The program on controlled thermonuclear plasma fusion reactors is a case in point. The basic physics activities on both inertial and magnetic fusion plasmas, involving lasers, magneto

plasmas and relativistic electron beams, were initiated in early seventies, where the basic physics of particle-beam-generated-plasmas was studied through relativistic electron beam (REB) generation, transport of beam energy, understanding of energy exchange between beam/ gas/ and plasma, and issues in beam-focusing etc at BARC. Interesting experiments using REB on collective ion acceleration were carried out for acceleration of H, O, C and F ions to fractions of MeV. Similarly, at IPR, intense research activities were initiated on physics of hot magneto-plasmas, Tokamak configurations, excitation, propagation and non-linear interaction of waves and instabilities and plasma heating processes. Since non-linear phenomena and turbulence are extremely important to the understanding of plasmas, the activities were also focused on understanding intermittency in Tokamak edge turbulence, coherent structures, anomalous transport, equilibrium and stability of toroidal plasmas with RF waves. In fact, a large number of physics experiments like Thomson scattering for electron temperature measurement, ECE diagnostic for temperature profile measurement, soft X-ray camera etc. have been conducted on BETA device as well as Aditya, to generate a database on plasma phenomena and supported by computer simulation. As will be described later, establishment of a sound scientific knowledge-base in fusion science, helped in charting a fusion energy program in India.

Another area where plasma physics research in DAE has been of international standards, is the field of laser-produced plasmas and laser plasma interaction, where scientists at BARC, RRCAT and TIFR have improved the basic understanding of laser-plasma coupling, energy transport, relativistic self-focusing, wake field acceleration, x-ray conversion, laser induced ablation of various targets, x-ray enhancement in laser produced plasma expanding in a background gas, shock-wave propagation in thin foils, EOS measurements of variety of materials at high pressures, and generation of quasi-Planckian thermal x-ray radiation from laser heated gold hohlraum targets, growth and control of RT instabilities etc. Recently, experiments have been performed on absorption and scattering in plasmas, produced from gas cluster targets.

Ion sources and ion beam research is one of the major research areas in DAE, due to the emphasis on development of accelerators. The physics of resonance energy transfer between a microwave source and a low-pressure gas under a confining magnetic field, has been utilized for development of ECR ion-sources for accelerators and ion-beam production. Some of the other areas in hot plasmas, where a large amount of scientific research base has been created, include studies on inertial confinement fusion (RRCAT, BARC), studies on imploding snowplow shocks, dense plasma focus experiments (BARC), large volume plasma device studies (IPR), Free-Electron Laser (FEL) experiments (IPR), non-neutral toroidal plasma studies (IPR), dusty plasma experiments (IPR), dynamics of coherent structures (solitons, double layers, shocks etc.), magnetic reconnection, parametric instabilities,

wave-induced particle acceleration (IPR), Coulomb explosion and physics of highly charged states (BARC, TIFR), physics of transient photo-plasmas (BARC), where DAE scientists have contributed towards improved understanding, generation of new data and setting up of innovative experiments.

Though, in the area of low temperature processing plasmas, the physics research is driven by the need of the technology to become sustainable in terms of robustness, long-life, energy efficiency and environment friendliness, DAE has made significant contributions towards understanding of glow- and arc-discharge fluctuations (BARC, SINP), mechanism of arc connection at the electrodes (BARC), non-equilibrium phenomena in high-pressure plasma jets (BARC), plasma nano-synthesis (BARC), understanding of MHD generator flows, physics of combustion plasmas (BARC) etc.

In the computational plasma physics, notable advancements have been made in all the DAE institutes in developing and using 3D "Particle In Cell" (PIC) codes, radiation hydrodynamic codes, molecular dynamic codes, Monte Carlo based algorithms, computational fluid dynamics programs, including shock-wave propagation, multi-phase thermo-physical and non-linear dynamic codes, to analyze data and predict system behavior.

Controlled Thermonuclear Fusion

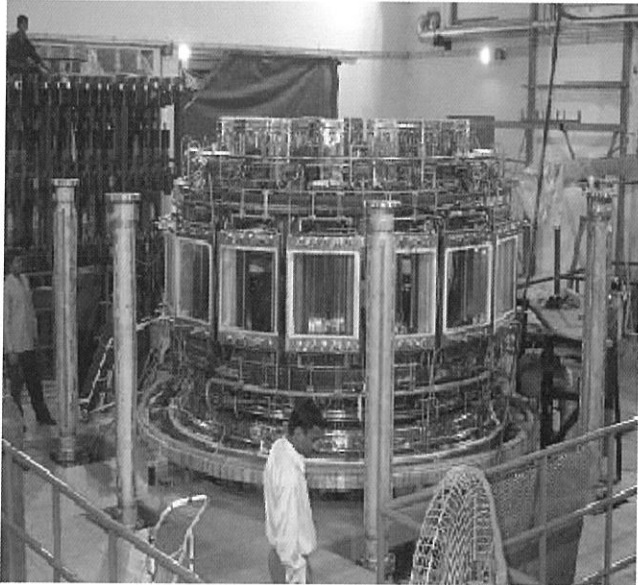
Controlled thermonuclear fusion reactor technology still remains the most important and cherished application of plasma technology, leading to hopes for achieving safe and unlimited electrical energy for the future. Therefore, research on hot magnetically confined fusion plasma and development of controlled thermonuclear fusion reactors is one of the emerging areas of long-term energy securities in Indian Atomic Energy Program. In a thermonuclear fusion reactor, nuclei of deuterium and tritium are confined in an extremely high temperature plasma medium. The plasma provides: (i) the requisite energy/ temperature to overcome the Coulomb barrier, (ii) the requisite number densities for sufficient number of fusion reactions to occur and, (iii) the requisite stability in time and space for achieving net energy production from the reactor. The two most often investigated thermonuclear plasma systems include the toroidal magnetic confinement system called the Tokamak or the inertial confined system, produced using high power lasers. One needs to achieve about 100 to 200 million degree Kelvin of ion temperatures, densities of 10^{20} ions per m^3 and confinement times of few seconds so that the famous Lawson criterion ($n \cdot T \cdot \tau > 5 \times 10^{21} m^{-3} keV sec$) is satisfied, leading to net energy production in Tokamak systems. For inertial confinement using laser produced plasmas, the number density increases ten-fold, with the confinement times of fraction of a nanosecond. Though both the approaches have been attempted, the former is now being accepted in the Department of Atomic Energy as the nearest to achievement of a demonstration-scale fusion reactor.

The various challenges faced by Tokamak plasma fusion systems, involve achievement of plasma heating, where processes other than Joule heating are needed to be employed and various turbulent processes as well as micro instabilities control the energy and particle transport. In recent years, RF wave, as well as neutral beam heating, is able to produce temperatures up to 400 million degrees. New and larger devices like PLT, ALCATOR, TFTR, D-III D, JET, ASDEX, TORE SUPRA, JT-60U have been built elsewhere in the world and experimented upon. With use of a number of new auxiliary-heating and current-drive methods and new regimes of Tokamak operation, progress in terms of the $nT\tau$ criterion has been increased by about 5 orders of magnitude. Scientific break-even point has been crossed, and one is within a factor of 3 – 5 from the final ignition criterion.

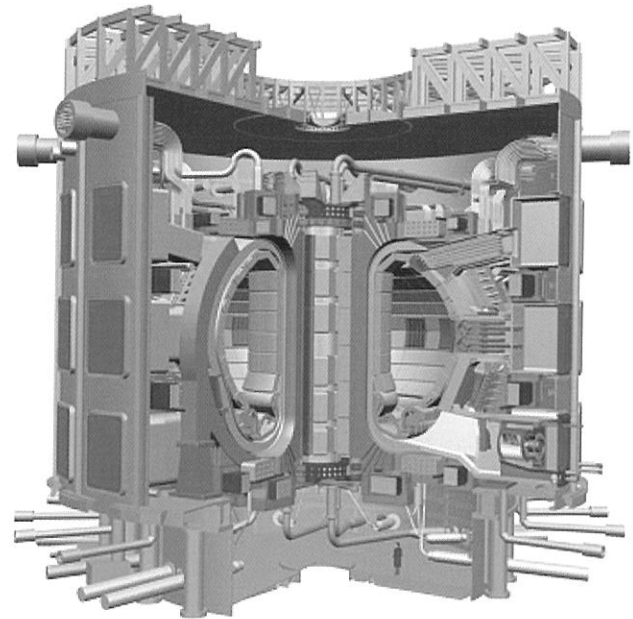
The Indian plasma fusion program in the Department of Atomic energy, started in the backdrop of expertise developed through the indigenously designed and fabricated ADITYA Tokamak at IPR, Gandhinagar as well as experience gathered with the SINP Tokamak imported from Japan [3]. ADITYA was the first indigenously designed and built medium size Tokamak of the country, operating for over a decade. Plasma discharges ~100 msec and 80-100 kA, toroidal field of 8.0 kG were studied for better understanding of energy transport in Tokamak plasmas due to edge plasma fluctuations, turbulence etc. Many plasma diagnostics have been employed during these measurements. Figure below gives a view of ADITYA with the auxiliary heating systems attached to it.

As reported, over the years [4], ADITYA has been upgraded with vacuum system having more cleaning facilities, incorporation of a radial magnetic field through four fast-feedback-coils for compensation of the error magnetic fields as well as plasma current feedback on the loop voltage and vertical field. To increase the plasma energy content during the discharge, auxiliary heating systems have been integrated. A 20-40 MHz, 200 KW Ion Cyclotron Resonance Heating (ICRH) system has been integrated to ADITYA vacuum vessel and successfully operated in the last campaign. A 28 GHz, 200 KW gyatron-based electron cyclotron resonance heating (ECRH) system has also been successfully commissioned.

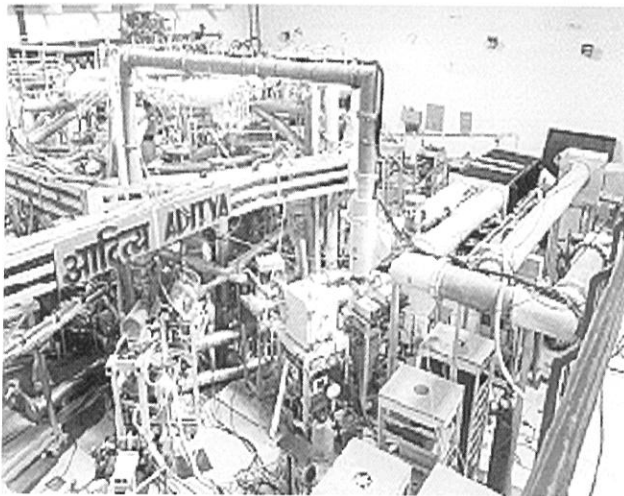
The development of Aditya was soon followed by a second generation Tokamak, the superconducting steady state Tokamak, SST-1[4]. This was designed to be a large aspect ratio Tokamak, configured to run double null diverted plasmas with significant elongation and triangularity, aiming at: (i) generation and maintaining shaped, double/single null plasmas with non-inductive current-drive & auxiliary-heating, (ii) steady-state operation with controlled particle and power exhaust, (iii) advanced Tokamak configurations with bootstrap current. Several new technologies relevant to steady-state Tokamak operation i.e. superconducting magnets, large-scale cryogenic system (He and LN₂), high-power RF systems, energetic neutral particle



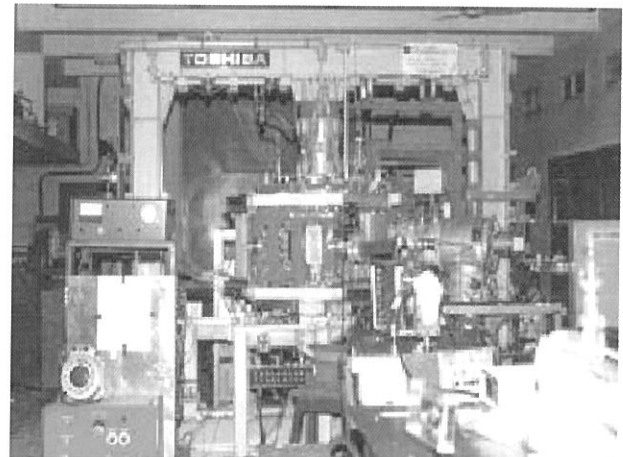
SST-1 Tokamak Assembly



Schematic of ITER



A View of Aditya Tokamak



A view of SINP Tokamak

beams and high heat flux handling, have been developed. The Indian fusion road-map also envisions a machine SST-2 beyond SST-1, resembling the Joint European Torus followed by a DEMO machine by 2037, and a plasma fusion power reactor by the year 2050.

A significant transition, in the DAE road-map for fusion, occurred in 2006 when India became a full partner in the international thermonuclear experimental reactor (ITER) program[5]. In ITER, India has been allotted half a port for placing its lead lithium ceramic-breeder-based test blanket module (TBM) to test its capability to: (i) breed tritium with Tritium Breeding Ratio (TBR) >1 , and (ii) extract the high grade heat from the Tokamak with acceptable thermal efficiency. It is also committed to deliver a number of sub-systems in which the Indian group has developed sufficient expertise. To achieve the goals set in the road-map, DAE now has initiated a national fusion programme which encompasses the plasma and other allied scientists and engineers working in related fields to contribute to the

various aspects of this multi-disciplinary effort. While ITER India program looks at the deliverable components and the test blanket module, the national fusion program envisages development of indigenous fusion reactor by 2050 and includes many other fields, like fusion materials, fusion neutronics, RF & microwave power systems, power engineering, plasma diagnostics, cryogenic technology, super conducting magnets, robotics, data acquisition and controls etc. BARC and IGCAR are major partners in many of these programs. Justifiably, a large number of universities and institutions in India are also participating.

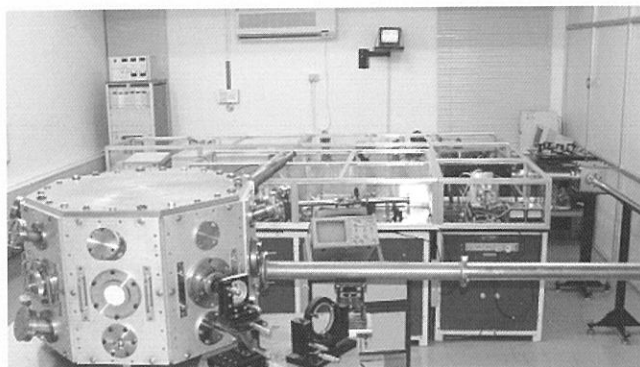
The Saha Institute of Nuclear Physics, another unit in DAE, has also been working on understanding fusion plasma science through Tokamak experiments. The SINP Tokamak is a small iron-core-device with major radius (R) 530 cm, minor radius (a) 57.5 cm, maximum toroidal field (B_w) 52 T, and maximum plasma current (I_p) 575 kA with a duration of about 10–20 ms. The major emphasis has been in developing plasma diagnostics, plasma heating and edge effects [6].

Laser-produced Plasmas

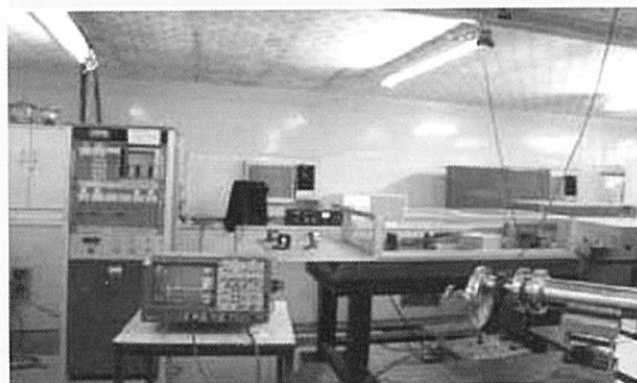
The interaction of intense laser beam with matter, in nano second to femto seconds, at energies of few milli-joules to joules, creates a high-density high-temperature plasma, consisting of fast electrons and ions. Apart from being a candidate for inertial confinement fusion, it is possible to induce many nuclear excitations and reactions. Proton beams of energy greater than 50 MeV, heavy ions of several hundred MeV energies and copious quantities of neutrons have also been observed. The particle accelerations in laser-produced plasma are among the highest that have been obtained. The light pressures on the target can simulate the pressures near a black hole. Since such devices can generate giga bar pressures and giga gauss magnetic fields, they are extremely handy to study astrophysical environments. Laser-produced plasmas have direct applications in compact particle accelerators, nuclear waste transmutation, fast ignition research, sub-picosecond radiography, etc. The laser wake field technology is evolving fast where nearly mono energetic electrons of up to 1 GeV have been measured. The availability of ultra-short-pulse and hence extremely high intensity of lasers and subsequent laser-produced plasmas have made possible, study of new regimes of the properties of matter, at extremely high energy densities. This has opened up numerous and diverse research fields, ranging from practical applications in integrated optics, to laboratory simulation of astrophysical phenomena; development of intense sources of extreme ultraviolet (EUV) to hard x-ray emission etc. This is an emerging area of frontline physics where considerable activity is being pursued at the laboratories of RRCAT, BARC, TIFR and IPR. A brief account of focus of activities in each of the DAE centres is given below.

The RRCAT program [7] in laser plasmas include building of high-power short-pulse lasers, development of X-ray-based and other plasma diagnostics techniques and laser plasma simulation studies. The laser plasma group has constructed a few Nd-glass nanosecond lasers in energy of few joules as well as a 1 TW table-top Nd-glass laser, based on chirped pulse amplification, for their research activities. In addition, a 10 TW Ti:Sa laser is being used at ultrahigh intensities, to study laser wake field acceleration of electrons, high energy X-ray generation, generation of highly charged ions, laser cluster interaction etc. In addition, the laser plasma group has set up many innovative diagnostic experiments on measurement of energy transport, X-ray conversion, shock-wave propagation, equation-of-state measurements, characteristics of laser-ablated plasma-plume, absorption and scattering in laser-produced plasmas etc.

At BARC, the laser plasma activities have focused on setting up of a Nd-Glass laser (1 joule 100 ps), for applications related to generation of neutrons, generation of high-density high-temperature plasma, multi-mega bar shock pressure in materials, and measurement of equation-of-state as well as opacities of materials of DAE



Nd Glass Table Top Terawatt laser at RRCAT[7]



30 Gigawatt Nd:Glass laser at BARC

interest. A one Terawatt/ 100 femtosecond pulse Nd-glass laser is being developed for generating a laser-based neutron source and for studies related to ultra-fast phase transitions in materials subjected to laser driven shock waves. Development of ultra-fast diagnostics for lasers, laser-plasmas and laser driven shocks, is also an important part of BARC activity. Studies related to resonance ionization due to interaction of low intensity lasers with atomic vapors, is another area of plasma physics activities at BARC, which is motivated towards fundamental studies in determination of resonance excitation and ionization cross sections as well as identification of auto ionization levels in lanthanides and actinide group of elements. The laser resonance photo ionization method, of photo plasma generation, has high ionization yield and high selectivity. Study of the transient photo plasma has generated basic data on sheath dynamics and ion diffusion coefficients [8].

At the Institute of Plasma research at Gandhinagar, laser plasma activities are mainly concentrated on theoretical studies, both in terms of analytical modeling and PIC simulations to understand basic physics of laser plasma interaction, soliton propagation, energy transport and instabilities arising due to the interaction.

The TIFR, an autonomous institute of DAE, has been highly active in the field of laser-produced plasmas. The laser plasma experiments were initiated in the 1990s with studies on molecules and clusters. However, with the 20 Terawatt 30 femto second, 600 mJ table-top laser

installation, a large amount of work on understanding basic physics [9] of light coupling to the plasma, energy sharing, particle acceleration and energy transport, temporal evolution of giant magnetic fields and transport of fast electrons, creation of hot nano plasma through coupling of laser energy to rare gas clusters, production of energetic highly charged ions etc have been published.

Basic and computational Plasma Physics Research

Though the research and development in plasma science in DAE has primarily been application-driven, a number of basic plasma theory and innovative experiments have been carried out to understand various aspects of plasma physics. The work on diagnostics in laser-produced plasmas (RRCAT), studies on inertial confinement fusion (RRCAT, BARC), studies on imploding snowplow shocks, dense plasma focus experiments (BARC), glow- and arc-discharge fluctuations (BARC, SINP), large volume plasma device studies (IPR), Free-Electron Laser (FEL) experiments (IPR), non-neutral toroidal plasma studies (IPR), dusty plasma experiments (IPR), dynamics of coherent structures (solitons, double layers, shocks etc.), magnetic reconnection, parametric instabilities, wave-induced particle acceleration, turbulent transport phenomena (IPR), Coulomb explosion and physics of highly charged states (BARC, TIFR), physics of transient photoplasmas (BARC), magnetohydrodynamic flows (BARC), and physics of combustion plasmas (BARC), are some of the areas where DAE scientists have contributed towards improved understanding, generation of new data and setting up of innovative experiments. In the computational plasma physics, notable advancements have been made in all the DAE institutes, in developing and using "Particle in Cell" (PIC), molecular dynamics, Monte Carlo, computational fluid dynamics, multi-phase thermo-physical and non-linear dynamic codes, to analyze data and predict system behavior.

Physics and Technology of Low temperature processing plasmas:

While high temperature and magnetized fusion plasmas have been the focus of attention and major funding for many years, the non-fusion low-temperature plasmas, otherwise known as processing plasmas or industrial plasmas, have been gradually making inroads due to their immense value addition to advanced materials processing and energy generation. These plasmas are now being used in industrial applications, related to advanced surface engineering, materials processing, metallurgy, chemical synthesis, waste remediation and nano material generation. In fact, a survey published a few years back, put the annual value of products that owe their existence to plasma technology, to be well beyond the 500 billion dollar mark.

The processing plasmas are endowed with highly concentrated energy flux (CEF) (density = 10^{10} W/m²), high temperatures, velocity, electromagnetic fields, currents, steep gradients resulting in ultra rapid heating/cooling (10^{7-8} K/sec), exotic reactive species, precursors for new synthesis

routes and extremely broad ranges of space and time resolutions. It is therefore, possible to have: (i) access to non-equilibrium operating regime, (ii) achieve submicron scale in temporal and spatial resolutions, (iii) obtain large throughputs with high efficiency, ultrahigh purity and specificity and above all (iv) conform to eco-friendly technology. One of the major advantage of the low temperature plasma beams, lies in their versatility to perform in any of the three material processing regimes; be it physical modification, chemical reaction or thermal processing. In the Department of Atomic Energy, the research and development program on low temperature plasmas are being carried out mainly at BARC and Facilitation Centre for Plasma Technologies (FCIPT, IPR). In the following, a few of the major technological applications that have found use in DAE or other strategic sectors are described briefly.

Magneto-hydrodynamic Power Generation and MHD Phenomena

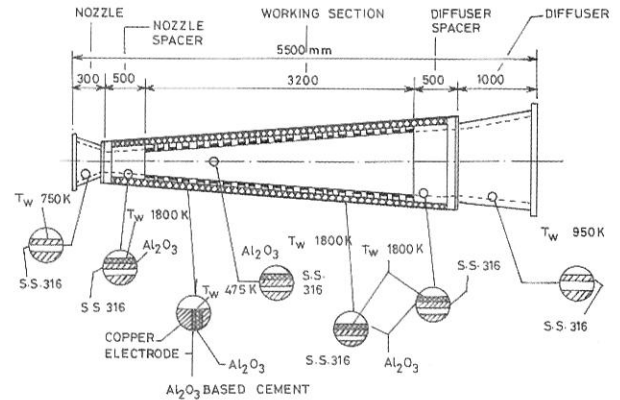
When a fast moving plasma interacts with a magnetic field, an emf is induced, and with appropriate configuration of electrodes, electrical power can be extracted from the high velocity plasma. This concept was utilized to develop a gasified coal-based MHD power generator in India, under a DST-DAE joint effort, executed by BARC and BHEL, with Russian collaboration. The idea was to use MHD as the topping cycle, and the conventional thermal plant as the bottoming cycle, leading to an improvement of about 10% in efficiency. In this context, an open cycle MHD experimental plant was commissioned at BHEL, Thiruchirapalli, and proof of the concept was established [10] with a large number of accessory technologies, including large electromagnet, combustor and air pre-heater technologies, material development for electrodes and insulators, comprehensive codes for multiphase plasma properties and MHD flow/heat transfer characteristics and various MHD plasma diagnostics. The high points of the program included the joint test of Indian channel at IVTAN, Moscow and the plasma run at BHEL. The figure below, shows the horizontal section of a long duration channel design for Indian MHD plant to operate with seeded combustion product of blue water gas. This design used hybrid structure of water-cooled copper and high-density controlled-porosity alumina, in contact with plasma. The basic design features and fabrication technology was validated through the joint Indo-USSR experiment on Indian-built channel at UO₂ installation in Moscow in 1980. The electrode current density of 0.8–1.0 A/cm² and heat fluxes of the order of 100 W/cm², simulating commercial generator conditions, were recorded during experiment. The test channel performed satisfactorily for test duration of 64 hours [10, 11].

BARC developed a large number of spin-off technologies that are being used in nuclear fuel cycle programs even today. The plasma spray technology, initiated then for insulation coatings, is one of the most used technologies for thermal barrier and corrosion resistance coatings for various programs. The liquid metal MHD

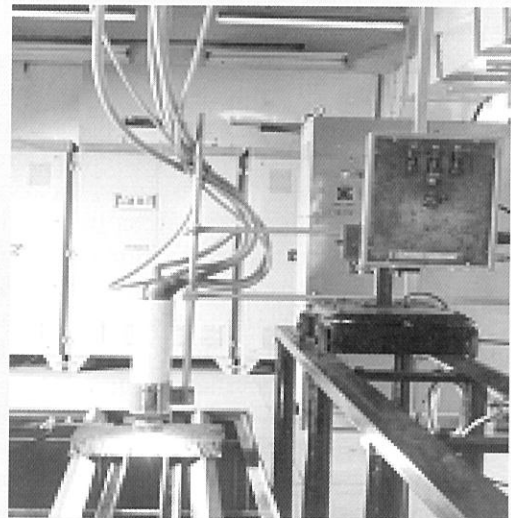
expertise developed then, is now fully utilised in the ADS and ITER programs.

Development of High Power Plasma Torches

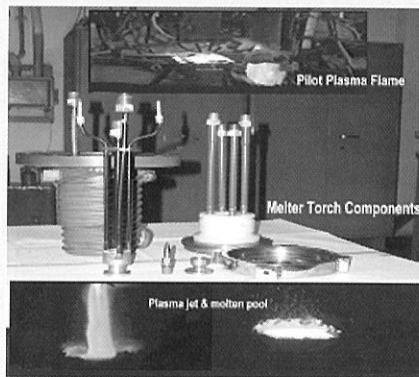
High power plasma torches are designed to efficiently convert electrical energy to thermal energies in the form of a well stabilized plasma column in an efficient manner. Normally the non-transferred arc plasma torches are aimed to operate >70% and the transferred arc torches above 90% efficiency. They are routinely exposed to high electric fields, currents and heat fluxes. Design development of a robust plasma torch is an exercise in computational simulation and experiments. BARC has been developing high power plasma torches from few kW to hundreds of kW ratings for spray, melting, gas heating and space re-entry applications. It has, over the years, built high power test stands (few kW to 1 MW) equipped to test and characterize these torches. The high power plasma torch program, in particular, has been instrumental in actively helping Indian Space Research Organization (ISRO), Defense Research and Development Organization (DRDO) etc. in setting up High Enthalpy Facilities and plasma probes for space reentry applications.



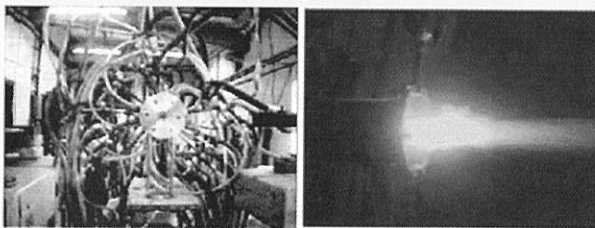
Horizontal Section of MHD Channel Designed at BARC



Air Plasma Cutting machine at BARC



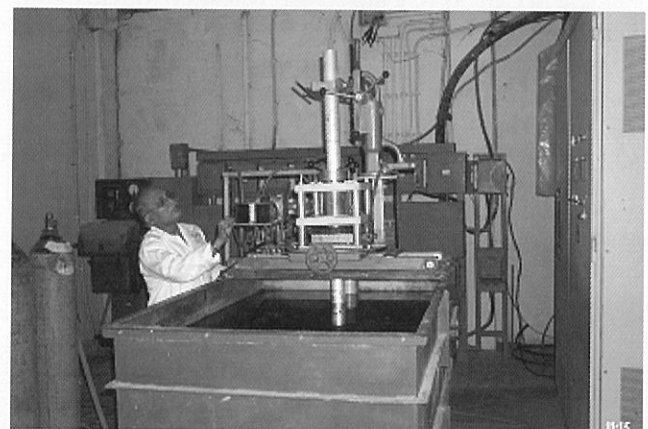
300 kW Plasma Melter Developed at BARC



(a) plasma tube (14 ring) The Constrictor Arc Plasma Jet Plasma

Plasma Cutting of Thick Metal Plates

Plasma cutting of metal plates of ms, ss, Al as well as many other metals is today a matter of routine. As mentioned earlier, during very early seventies, BARC undertook development of transferred-arc-plasma-cutting-torches and both under-water- as well as air-cutting-systems for in-house needs. Apart from metal plates, under-water cutting of alpha-active piping and aluminum jacket of burnt-fuel-bundles have also been demonstrated.



Under-Water Plasma Cutting system at BARC

Plasma Spray Processing and Deposition

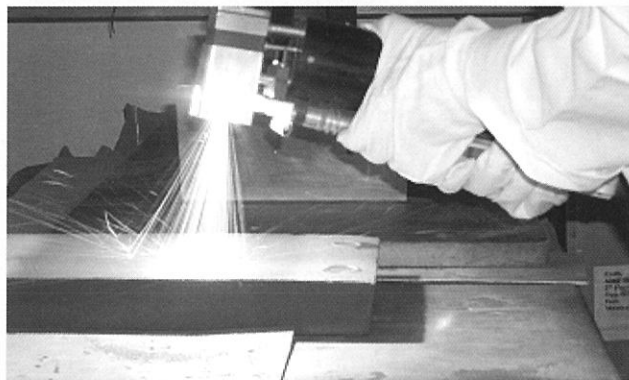
Plasma spray deposited coatings of metals, alloys, ceramics and composites, to meet the specialized requirements of the department of atomic energy in general, and BARC in particular, was developed in the seventies for MHD generators and is one of the most utilized plasma processes today. Besides development of ceramic-alloy

duplex coatings for handling corrosive melt and ceramic-alloy composite coatings for strategic and specialized nuclear applications, research on advanced thermal barrier coating (TBC) systems has been a major R&D area. A TBC system usually consists of two layers- a metallic bond coat and a top ceramic coat. The function of the bond coat is to protect the substrate from oxidation and provide sufficient bonding of the top ceramic coat to the substrate. The insulating ceramic layer provides a reduction of the temperature of the metallic substrate, which leads to improved component durability. Thermal barrier coating system currently employs a duplex design, consisting of a bond-coat and top ceramic layer. Some of the state-of-the-art TBC material developed at BARC are yttria-stabilized zirconia (YSZ), containing 7-8 wt % of yttrium oxide, which is deposited over MCrAlY (M = Co, Ni) or Pt-modified aluminide. For use above 1200°C, R&D efforts are presently directed towards development of new class of ceramic materials for the top layer of TBC, with improved thermal and chemical stability and lower thermal expansion coefficient. The rare earth phosphates, lanthanum zirconium oxide and yttrium oxide have many desirable features, which are not exhibited by the other materials. These materials have high melting points (>2400 K), thermal stability, and do not react with many molten metals, including molten uranium and molten lead. Lanthanum phosphate has excellent thermal stability and corrosion resistance against many molten metal and other chemically corrosive environments. Plasma spheroidization and melting studies on Lanthanum phosphate, and its compatibility with molten uranium have established [12] that these phosphate coatings are effective in high temperature containment of molten uranium. The rare earth phosphates are resistant to corrosion by molten slag, glass and are ideally suited coatings for containment of radioactive waste. In addition, yttrium oxide and lanthanum phosphate are not wetted by molten lead and bismuth and are therefore ideal candidate materials for ADS applications. The plasma group at BARC has also developed an arc-wire-spray technique for preparing metallic nickel coating on carbon electrodes [13].

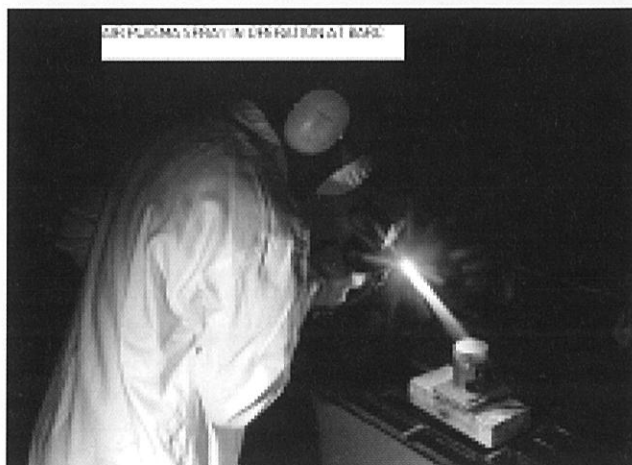
Reactive Plasma Spray Processing and Plasma Chemistry

Reactive plasma spraying is a relatively recent development, which takes advantage of the high temperature and high enthalpy of the plasma jet, to effect 'in-flight' chemical reactions, in the presence of a reactive gas. The unique feature of reactive thermal plasma synthesis is independent control of plasma power and the reactive environment. The high temperature gas phase chemistry, and temperature of the plasma medium, can be customized to promote the desired chemical reaction. Some of the promising opportunities that reactive plasma synthesis offers, include development of novel coatings, processing of advanced ceramics and conversion of industrial wastes to value-added materials. This technology can also be extended for synthesizing nano-sized powders of advanced ceramics.

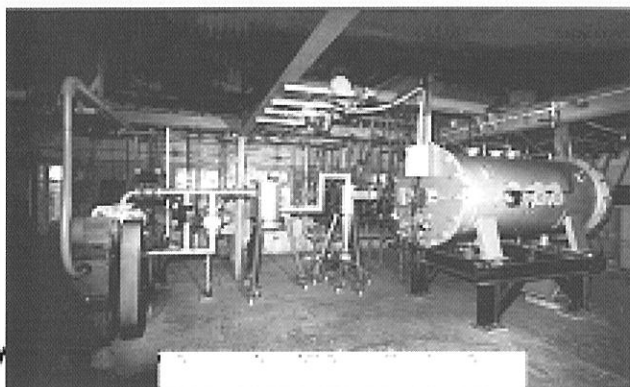
Reactive plasma processing has been successfully applied to synthesize nano-crystalline titanium oxide by 'in flight' oxidation of micro-sized TiH₂ powder in a DC non-transferred arc thermal plasma reactor, designed and developed at BARC. Complete conversion of the injected TiH₂ powder to nano-sized TiO₂ that is functionally as effective as commercially available photocatalytically active titania powder, could be accomplished. The same technique has been applied to synthesize Nickel aluminide, an excellent bond-coat material in a plasma torch, operating in a non transferred arc mode, using premixed powders with excess aluminum as precursor material, argon as carrier gas and argon and nitrogen as plasma gas. The reactive plasma processing technique has also been extended to generate metallic and ceramic aerosols of importance in nuclear industry. A 20 kW plasma-torch-based aerosol generator has been integrated with the nuclear aerosol test facility (NATF) and is being used for the study of aerosol generation and settling behavior. Reactive plasma synthesis can be most gainfully employed for processing of minerals. Plasma dissociation of zircon (zirconium silicate mineral), conversion of ilmenite to titanium oxide, titanium carbide and titanium nitride, plasma conversion of fly-ash to value-added materials, are some of the interesting applications. The principal advantage of this direct method is that it uses cheap raw material. At BARC, DC



Arc wire Spray at BARC



Plasma Spray System in operation



Vacuum Plasma Spray Equipment

plasma-torch-based reactors have been developed for dissociation of zircon to zirconium oxide and silica. The process consists in feeding zircon particles into the thermal plasma jet, where they undergo thermal dissociation to zirconium oxide and silicon dioxide and the high quench rate associated with the process prevents recombination of the oxides, leading to the formation of a product that consists of the individual oxides. Zirconium oxide is suitably extracted from this oxide-mixture by acid or alkali treatment. Recent innovations, that include the addition of carbon and use of air as the plasmagen gas, have resulted in one-step process, eliminating the down-stream wet chemical operation and thus, leading to improved process economics.

The technique can also be extended to convert industrial waste, such as fly-ash into value-added materials. Fly-ash is a waste product from coal-based thermal power plants. The major chemical constituents of fly-ash are silica and alumina and its disposal is a matter of great ecological concern. Only a very small percentage (5-7 %) of fly-ash is utilized for gainful application. By proper control of the flame chemistry and plasma power, fly-ash can be converted to silicon carbide- and nitride-based composites.

Low-pressure Plasma Surface Modification and Deposition

Low-pressure plasmas are characterized by high reactivity due to the presence of highly energetic electrons, free ions and excited species. Due to high internal energy of low-pressure plasma, processes which are thermodynamically allowed but kinetically hindered in a conventional process, proceed with a high rate under plasma conditions. In low-pressure plasmas it is possible to effect the deposition at low deposition temperature, low ion temperature (less bombardment), which results in small grain size.

There are two general classifications of how low-pressure plasmas are applied in surface modification. The first involves the use of the ions from the plasma, which can be accelerated from the edge of the plasma by an electric field. The kinetic energy of these accelerated ions can be used to physically erode a surface or to implant the ion below the bombarded surface. The second general use of plasma is



Plasma Chemical Reactor at BARC

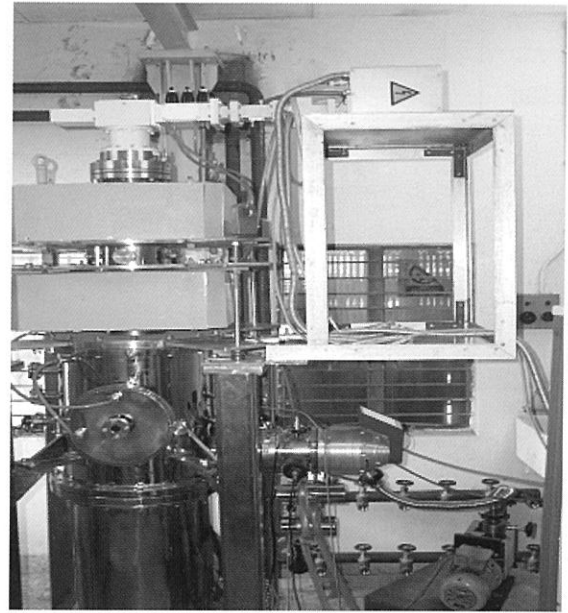
to generate energetic or metastable species from the gas, such as excited states of atoms and ions, active chemical species from molecules and photons. The presence of these energetic metastable species will cause various surface phenomena, such as reactive etching or deposition that would not have occurred thermally, in the absence of the plasma medium. In DAE, low-pressure plasma deposition activities are mainly being carried out at BARC, IGCAR and IPR. The work at BARC and IPR are more holistic, as they range from device to process to characterization activities. At the IGCAR, work is more focused on the use of plasma devices for coating development.

At the Laser and Plasma Technology Division of BARC, a 2 kW, 2.245 GHz large volume microwave electron cyclotron resonance (ECR) system has been developed for large area deposition of highly adherent non-porous coatings of diamond, diamond-like carbon (DLC), cubic boron nitride and super-hard nano-composite coatings. The system has been used to deposit diamond-like carbon (DLC) films on silicon (111) substrates, using methane and argon gas plasma. The energy of the ions impinging on the substrate during deposition, is varied by changing the rf self bias voltage developed on the substrate, to get highly adherent films. This microwave ECR plasma CVD system has been adapted to grow thin films of yttrium oxide on Si (111) and s.s. substrates by metal organic chemical vapour deposition (MOCVD), using a $Y(thd)_3$ ($thd = 2,2,6,6$ -tetramethyl-3,5-heptanedionate) precursor. The technique has been optimised to deposit yttrium oxide and yttria-stabilized-zirconia coatings on various substrates including stainless steel and tantalum [14]. In addition, R&D efforts on in-situ plasma diagnostics, carbon nanostructures for electron emitter applications and oriented diamond films, are reported.

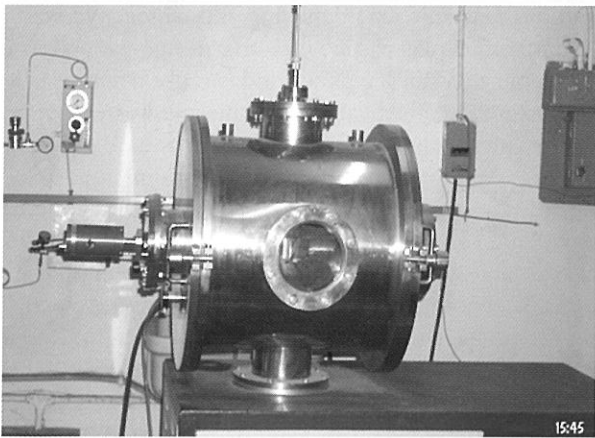
At IPR, a large amount of work has been carried out at the Facilitation Centre for Plasma Technologies (FCIPT), aiming at achieving commercialization of plasma technologies. Though low-pressure plasma processing has been their forte, they have been working on a broad spectrum of plasma technology activities. Some of the notable achievements of FCIPT include plasma nitriding of industrial components to increase wear-resistance and



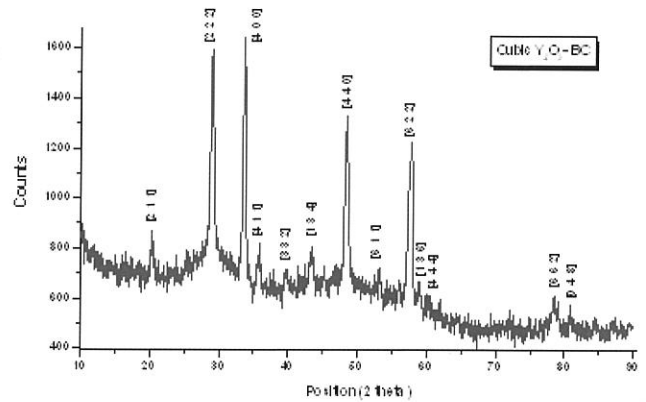
Microwave Plasma CVD Reactor (2.45 GHz, 2 kW) for Oriented Diamond Thin Film Deposition



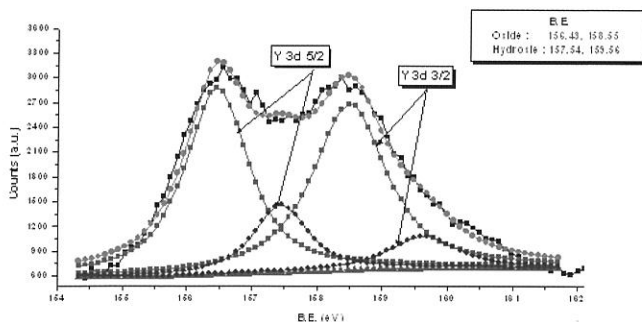
Low pressure large volume plasma source – Microwave – ECR Plasma



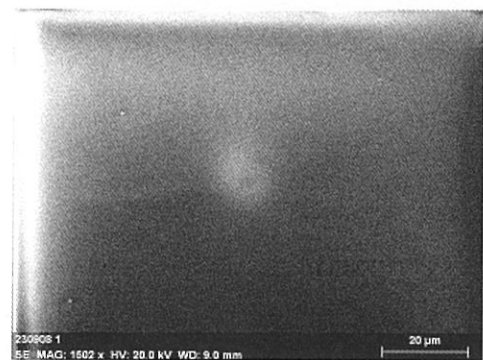
Radio Frequency Plasma CVD Reactor (13.56 MHz, 250 kW) for Deposition of DLC-SiO_x Thin Films



X-Ray diffraction pattern taken on Y₂O₃ deposited on Si (111).



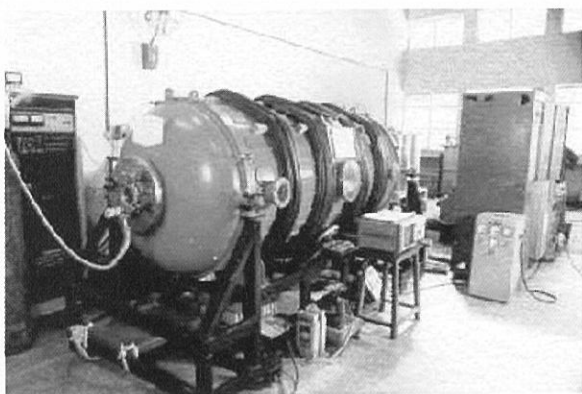
XPS spectra of Y₂O₃ deposited on Si (111)



SEM Image on Y₂O₃ on Tantalum (Annealed sample)

hardness, coating of quartz-like films on brassware to inhibit oxidation and tarnishing, thermal plasma technologies for waste treatment, plasma processing for textile industries, deposition of TiN coatings to increase abrasion resistance, deposition of amorphous silicon coatings for anti-reflection properties, etc. [15]. Plasma Ion Implantation is one of the

oldest activities at IPR-FCIPT, where, not only considerable research on ion implantation has been carried out but also commercialization of materials modification at normal or elevated temperature, by doping with atoms, through pulsed ion acceleration from a conformal sheath, with both gaseous and metallic ions. The surfaces can be metallic or dielectric.



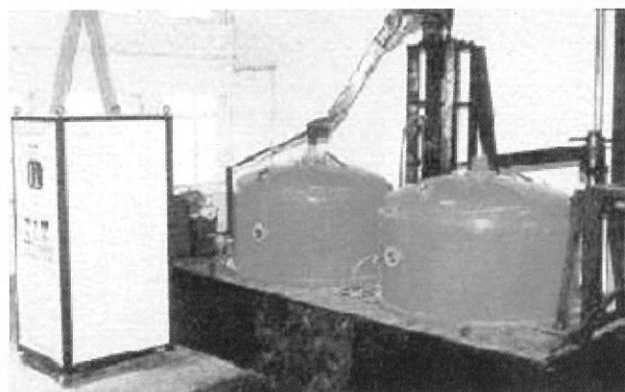
FCIPT PIII Machine

Apart from installing a PIII system at IIT Kharagpur, the machine at FCIPT is also used by Universities, ISRO, NML etc. [16].

Plasma Nitriding has been another of the flagship programs of FCIPT, where nitriding systems with FCIPT technology are installed at M/s Metal Treat, Ahmedabad, NAL, Bangalore, BIT Jaipur and IGCAR, Kalpakkam [17].

Plasma Nanosynthesis

Plasma assisted synthesis of nanoscale structures is known to offer opportunities in terms of bulk production, purity and good alignment. The thermal plasma techniques offer high yield, with prospects of production of both particles as well as rods/tubes/wires, but with lesser degree of control on shapes and sizes. The low pressure, low temperature non-equilibrium plasmas on the other hand, have the capability to effect controlled growth and alignment in nano tubes and rods. This is the other emerging application of plasma-materials technology. The Laser & Plasma Technology Division in collaboration with University of Pune, Centre of Plasma Physics Guwahati and Bharathiyar University, Coimbatore has designed and developed transferred-arc nanogenerators, to synthesize nanostructures of AlN nano-wires, Al₂O₃, TiO₂, ZrO₂, ZnO, γ -Fe₂O₃, Fe₃O₄ particles and single elemental materials, like carbon nano-tubes and nano-sheets. Significantly, a plasma parameter control regime, in terms of plasma gas, flow pattern, pressure, local temperature and the plasma fields have been established to obtain the desired nano-phase structures. Use of simple in-situ measurements, like heat fluxes, emission spectra, electron densities, arc voltage, pressure and temperature and an array of particle characterization techniques have indicated possibility of definite correlation between plasma parameters and characteristics of the nano-materials generated. While pressure and arc current have shown definite controlling effect on phase structure and size, the magnitude of fluctuations have shown to affect the size of nano-particles. In the case of arc synthesis of carbon nano structures, it has been demonstrated for the first time, that high purity MWCNT and graphene can be synthesized with proper optimization of electric and magnetic fields [18, 19, 20].



Plasma Nitriding Equipment at FCIPT

Plasma-Assisted Waste Remediation and Pollution Control

Waste remediation and pollution control is one of the emerging and exciting large-scale application of plasma technology, where the thermal plasmas have been used as a single-step solution for treatment of biomedical, municipal, hazardous plastic, ozone depleting and radioactive wastes, the non-thermal plasmas are effective in flue-gas and water purification. Plasma lamps are industrially being used for large-scale water purification. The plasma waste treatment also provides value-added material and fuel gas as by products. Applications of non-equilibrium atmospheric pressure plasma, for gas-phase-scrubbing of volatile and non-volatile contaminants and environmental remediation, is also a viable process. The Facilitation Centre for Industrial Plasma Technologies has developed Pyrolysis System for disposal of medical waste. The unit is operating at the Gujarat Cancer Research Institute at Ahmedabad and the technology has been transferred to a private entrepreneur M/s Bhagwati Pyrotech Pvt. Ltd., Ahmedabad, Gujarat.

Concluding Remarks

It is apparent that over the last five decades, plasma science and technology has formed a part of many DAE Programs across units. It is significant to note that in most of these programs, the thrust has been in capacity-building, wherein the devices and the process equipment are indigenously developed. Simultaneously, a large number of innovative and path-breaking, theoretical as well as diagnostics experimental work has been carried out, that has opened of new directions of research. This approach has provided a certain expertise and technological competence essential in these advanced areas. In future, fusion energy, plasma surface engineering applications in nuclear fuel cycle, laser plasma accelerators, plasma nanosynthesis and plasma waste beneficiation might be the emerging technologies, due to the increasing needs from energy, materials and environment sectors. On the basic plasma physics and chemistry aspects, (i) understanding and control of non-linear waves and instabilities in all types of plasma systems, (ii) high temperature chemistry of plasma-assisted reactions, (iii) understanding and controlling plasma nano

synthesis, (iv) understanding intense laser plasma interaction, are a few problems that will continue to be investigated in DAE. Considering the ITER Collaboration and the fusion energy program, it is absolutely essential that the science and technology of plasmas be nurtured and supported.

Acknowledgements

The author wishes to acknowledge grateful thanks to all his colleagues working on plasma science and technology at various units of DAE like BARC, TIFR, IGCAR, RRCAT, IPR, SINP etc. The information presented has been drawn from most of their work. This is only a brief perception and by no means a representation of the entire gamut of plasma activities in DAE.

References

1. Plasma Physics and controlled thermonuclear fusion, a brief historical account, R. K. Verma, Physics news, 28, 1&2, 20, 1997.
2. Plasma programme at BARC, Some recollections of the past, V. K. Rohatgi, Physics news, 28, 1&2, 29, 1997.
3. Excitement and Challenge of Plasma Science, P. K. Kaw, Physics news, 28, 1&2, 4, 1997.
4. IPR, Annual Report 2003-04, 9, 2004.
5. Materials issues in fusion reactors; A. K. Suri et. al, IOP Publishing Journal of Physics: Conference Series 208 012001, 2010.
6. Status of SST-1 Project and Fusion Research in India, Yogesh C. Saxena, www.ipr.res.in
7. www.cat.gov.in/technology/ laser/lpd/lpl/prlpic.html
8. Two dimensional expansion of finite size barium photoplasma in an electrostatic field, A. Majumder et al, Phys. Plasmas 15,123508 (2008).
9. Intense, ultrashort light and dense, hot matter; G. Ravindrakumar; PRAMANA, Journal of Physics, Vol. 73, No. 1 July 2009, 113- 155, 2009.
10. An Indo-Soviet experiment on an MHD generator test section at the Soviet U-02 facility; P.V. Ananthapadmanabhan, A.V. Bapat, A.K. Das et al., Sadhana, 5, 169-195,1982
11. Recent Advances in MHD Electrical Power Generation, V.K. Rohatgi, N. Venkatramani, Sadhana, 7, 1, 1984.
12. P.V.A. Padmanabhan, L & PT Division, BARC; Personal Communication, 2010.
13. BARC Progress Report 2002, BARC/2003/P/001
14. D. S. Patil, L & PT Division, BARC; Personal Communication, 2010.
15. www.plasmaindia.com/update56.pdf
16. www.ipr.res.in/talksarchive/S-Mukherjee.pdf
17. www.plasmaindia.com/plasmanitriding.html
18. Effect of focusing electric field on the formation of arc generated carbon nanotubes' Soumen Karmakar , A. K. Das et al, Nanotechnology, 17, 23, 5895-590, 2006.
19. Synthesis of nanowires and nanoparticles of cubic aluminium nitride; C. Balasubramanian, V.P. Godbole, V.K. Rohatgi, A.K. Das and S.V. Bhoraskar ; Nanotechnology 15 370, 2004
20. A novel approach towards selective bulk synthesis of delaminated graphenes in an electric arc; Soumen Karmakar, A. K. Das et al. JI. hys D, Applied Physics, 2008.



Dr. A. K. Das is a scientist of repute in the field of plasma technology. During his career spanning more than 35 years in the Department of Atomic Energy, he has been instrumental in the indigenous development of major technology areas like Magneto plasma dynamic generator, High power innovative thermal plasma sources, plasma chemical reactors and plasma systems for nano materials generation. His work has significantly contributed to the understanding of thermal plasmas in general and arc plasmas in particular. He is a recognized Ph.D. Guide for both Mumbai and Pune Universities and Senior Professor with the Homi Bhabha National Institute. He is a recognized expert in plasma physics with the DST, Govt. of India and has served as Member, Program Advisory Committee of SERC, faculty for SERC schools as well as in ICTP workshops on industrial plasmas. He has also served as international steering committee member at ICTP Trieste for thermal plasma program. Currently, he heads the Laser & Plasma Technology Division at BARC.

DAE's Accelerator Physics Programme Relevant to Nuclear Energy

V.C. Sahni

Bhabha Atomic Research Centre, Trombay, Mumbai 400 085

Abstract

The article describes High Current Proton Accelerator R&D being pursued in DAE laboratories for nuclear energy applications. Current effort is focused on the design and prototype development of many subsystems at RRCAT, and injector accelerator system at BARC. This should be able to pave the way leading to the construction of a full system in future.

Introduction and Possible Role of Accelerators in Nuclear Energy

Currently, the world annually produces nearly 18 trillion units (1 kWh) of electricity, which is likely to double over the next decade. In this growth, nuclear energy could be an important player, if we can find a way to mitigate nuclear waste problem and also develop breeder reactors. In this context, a limitation of uranium-based reactors (in the form of long-lived minor actinides (MA) & long-lived fission products (LLFP)) can be traced to poor neutron yield of the fission process. So, a way forward is to integrate the fission process to the neutron-rich spallation process. This can be done using a high-energy proton beam falling on a high Z (like Pb, W, U, Th) material. An integrated system (ie a spallation neutron source coupled to a fission reactor) can most effectively tackle the radiotoxic waste [1] and also transform fertile material into fissile material. Indian interests in this scheme are compelling, because using indigenous sources, the nuclear power generation on a large and sustainable basis will crucially depend on two issues, viz. breeding fissile U-233 (from Th-232) and reducing the burden on geological repositories (for storage of high-level radioactive waste). Building high-current proton accelerators, can play the role of a game changer for both these goals. However, before we can turn this concept into a reality, a lot of R&D is needed, since for spallation process to be effective, typically one needs a proton beam of ~1 GeV, ~10 mA, which is way beyond the reach of current machines. So, in the last few years DAE labs have started serious developmental work on high-current proton accelerators (after a broad road-map was identified [2]) especially doing the required R&D for such accelerators. Present status of this effort is described in a later section.

Historical Remarks on Accelerator-Related Developments in DAE

Accelerator-related R&D has a long history in DAE. About six decades back, Saha Institute of Nuclear Physics pioneered these developments, by setting up a cyclotron and a 400 KeV Cockroft-Walton accelerator, and Tata Institute of Fundamental Research built a 1 MV Cascade Generator. In the early sixties, BARC set up a 5.5 MV Van de Graff accelerator. In the seventies, VEC Centre at Kolkata built and installed country's largest accelerator, viz, the 84" variable energy cyclotron. The other major developments involved the commissioning of 14 MV BARC-TIFR Pelletron in the eighties, and in the nineties BARC focused

effort on the design and construction of FOTIA (Folded Tandem Ion Accelerator) that eventually started functioning in 2000. In the last decade, DAE labs have also built 450 MeV storage ring Indus-1 & 2.5 GeV synchrotron radiation source Indus-2 at RRCAT, and k=500 superconducting cyclotron at VECC. In addition, superconducting linac boosters have been built and operated at Delhi and Mumbai pelletrons, with the machine at IUAC using solid niobium resonators, while that at TIFR employing lead-plated copper quarter wave resonators. All these activities have made Indian accelerator scientists and engineers in general, and those in DAE labs in particular, confident that they can take up major R&D on high-current proton accelerators. Over the past few years, they have made notable progress, as will be described below.

High-Current Accelerators: The Physics Challenges

To design a proton accelerator that can deliver up to ~10 mA beam-current and a energy of ~1 GeV, is an arduous task. In fact, it would be fair to say that such accelerators are machines of next generation! In principle, for reaching such high energies, one could think of both the options, viz, a linear accelerator or a circular machine, like, a cyclotron or a synchrotron. Indeed the Spallation Neutron Source at ORNL, USA and the cyclotron at PSI, Switzerland are good illustrations of both the options. DAE labs too have been studying both the options, with VECC concentrating on cyclotron route, and BARC/RRCAT working on linac and synchrotron arrangement. But it is now becoming increasingly clear that while cyclotron offers a nice route to do exploratory work, if one has to reach high power levels nearing ~10 MW (that may be needed for actual energy systems), linac route is preferable. Almost all designs that have been proposed so far, rely on a high-current ECR ion source, from where ions are extracted and fed into a low-energy-beam transport line that is attached to a radiofrequency quadrupole (RFQ) unit. After this stage, several options exist, that includes room temperature drift tube linac (DTL) structure (or variants, like CCDTL, SFDTL) or spoke resonators that help raise the beam-energy to several tens of MeV. Thereafter, all designs switch to superconducting cavities, to take the beam-energy to ~1 GeV. However, in all designs a number of physics issues need careful attention and deserve comments. These include material issues, space charge effects, right choice of radio frequency for operation of each accelerating structure (of the full machine), aperture available for the beam as it passes

through different stages, and, of course a detailed beam optics evaluation of the full system, based on the basic electrodynamics (involving Maxwell's equation) and motion of charged particles. In addition, when one deploys superconducting sections, one must examine other parameters that include choice of materials, temperature of operation etc.

In all the proposed schemes, ECR ion source is preferred because it offers the advantage of delivering high currents and, by adjusting plasma parameters, one can optimize delivery of positive or negative ions. The choice of RFQ (for the first stage of machine) is dictated by the fact that it combines three functions, namely, bunching, focusing and acceleration. In addition, as the focusing is done electrically (and not by magnetic field), it does not depend upon the ion speed. Since the aperture in a RFQ varies inversely with λ (the radiofrequency chosen for operation), lower λ is preferable, because it helps reduce beam-loss. Typically, radiofrequencies of ~ 100 MHz are used and energy of the beam emerging from RFQ is a few MeV. Next stage in the acceleration, involving DTL (or its variants) or superconducting spoke resonators have their own pros and cons. Both have their votaries, and at this time, one can say that the latter (superconducting spoke resonator) option is helpful if one wants to get high beam-currents. (IUAC is already engaged in developing superconducting spoke resonators.) Since most of the energy-gain of the beam occurs in the superconducting sections, a lot of attention has been devoted in recent years for understanding the factors that affect the performance of superconducting radiofrequency (SCRF) cavities, particularly those based on solid niobium. This aspect has been of personal interest to the author and is considered next.

Basics of rf Superconductivity and Choice of Superconductor

In accelerator applications, large-scale use of superconductivity enters either via superconducting magnets or through accelerating cavities. Of course, the primary advantage of using superconductors lies in that one is able to avoid energy losses that otherwise occur on account of dissipative (ohmic) heating effects. Superconducting magnets generally operate in a dc or a low-frequency (typically < 100 Hz) ac mode, where there is zero electrical resistance. So, one uses so-called "hard" superconductor (SC) having high upper critical magnetic fields (~ 10 – 20 T) and strong flux pinning, to get high critical current density; such features are only found in the alloys like niobium-titanium or niobium-tin. But, in accelerating cavity application, real gain lies in that, one is able to transfer nearly the entire RF power to the beam, with negligible losses being encountered in the cavity surface. In this context, limitation on the cavity performance is not due to upper critical field (as in the case of superconducting magnet application) but due to a "lower" field (H_p) at which flux lines can first penetrate and lead to dissipation. Its value is well below 1 T for all

known SCs. Also, strong flux-pinning is not advantage, as it can lead to hysteretic losses [3, 4].

In actual fabrication of SC cavities, two options exist. One is to make them from solid sheets of a superconductor; alternatively a thin layer of superconducting material can be sputtered onto inside of a copper cavity. Both approaches have been successfully applied, especially using niobium. A SC, like niobium, is still regarded as the best material although its T_c is only 9.2 K and it has a lower field H_p of ~ 200 mT, whereas Niobium-tin (Nb_3Sn), with a T_c of 18 K, and $H_p \sim 400$ mT may initially seem attractive. In reality, the gradients achieved in "Nb₃Sn coated on Cu cavities" have been < 15 MV/m, probably due to several materials issues connected with the Nb₃Sn layers. Performance of cavities made with High- T_c material, sputter-coated on Cu, is even poorer, as compared to those made from niobium. So, presently, it is fair to say that solid niobium cavities enjoy a pre-eminent position in this field.

Right Choice of Operating Parameters

For microwave fields (in contrast to dc fields), SC exhibit a non-zero energy dissipation. This is because at radiofrequency (rf), magnetic field penetrates a thin surface layer and induces oscillations of electrons, that are not bound in Cooper pairs, resulting in a dissipation of RF power in the (inner) surface of the cavity. This power dissipation is proportional to cavity's surface resistance R_s and an integral involving square of magnetic field $\approx \int H^2 dS$. To minimize power dissipation, lower operating temperature is preferable since number of such "free electrons" drops exponentially as one cools down; and as per Bardeen-Cooper-Schrieffer theory, in the range $T < T_c/2$, R_s is given by $(\omega^2/T) \exp(-1.76 T_c/T)$, where $\omega/2\pi$ is the microwave frequency. In the two-fluid model of SC, one can derive a refined expression for R_s , given by $(C/T)\omega^2 \sigma_n \Lambda^3 \exp(-1.76 T_c/T)$, where C is a constant, σ_n the normal-state conductivity of material and Λ an effective penetration depth, given by $\Lambda = \lambda_L \sqrt{1 + \xi_0/\ell}$, λ_L is the London penetration depth, ξ_0 is the coherence length and ℓ is the mean free path of the unpaired electrons [3]. The fact that σ_n is proportional to mean free path ℓ , leads to the surprising conclusion that surface resistance does not assume its minimum value, when the superconductor is as pure as possible ($\ell \gg \xi_0$), but rather in the range $\ell \approx \xi_0$. For Nb, BCS surface resistance at ~ 1 GHz amounts to ~ 800 n Ω at 4.2 K and drops to ~ 10 n Ω at 2 K. Note that this drop in surface resistance by five orders of magnitude, in going from copper to superconducting niobium, enables us to reach quality factor $\sim 10^9$ to 10^{10} in SC cavities. This is also the reason why operation at ~ 2 K is regarded essential for achieving high accelerating gradients in combination with very high quality factors.

Functioning of superconducting cavities also depends upon the choice of radiofrequency ν besides the temperature of operation. Since there is a quadratic increase in BCS surface resistance with frequency, a lower value of ν may

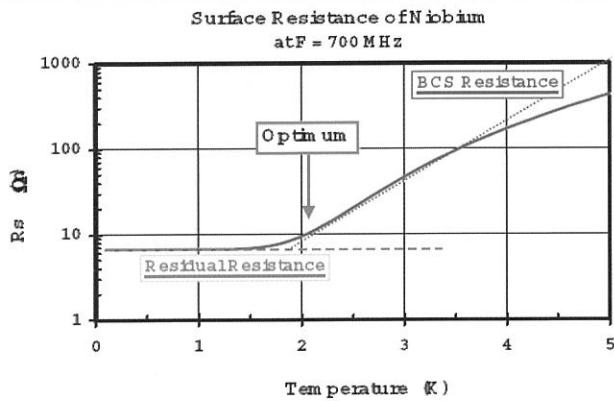


Fig. 1 The temperature variation of BCS surface resistance for niobium; It shows why optimum choice for operating the cavity is around 2K.

seem preferable. However, lower ν leads to an increase in cavity size that goes as $1/\nu$, which in turn increases the possibility of field emission. So, finally there is a trade off, and optimum ν lies in 0.5 to 1.5 GHz range. As noted above, optimum operating temperature for the superconducting cavities made out of niobium is ~ 2 K (Fig. 1). However, a lot of R&D is still being pursued to understand the root cause(s) of under-performance of niobium superconducting cavities, and several studies are on, to find the “right” processing conditions (from the point of achieving best superconducting properties) to repetitively realize highest gradients. In fact, through a number of studies, we had shown that the BCP (buffered chemical polishing) treatment (that is often used for processing niobium cavities) leads to a noticeable degradation in the superconducting properties and that electrochemical polishing is a better option for cavity processing. Some results are shown in Fig. 2 and details of these studies are contained in [4-6].

R&D Effort in DAE, Related to High Current Proton Accelerators

Some years ago, Indian DAE embarked upon the design and development of high current machines [7, 8]. Visualizing a plan for 1 GeV, 30 mA machine (Fig 3), detailed physics design was initiated, keeping in view that beam loss in the accelerator must be minimum, allowing a hands-on-maintenance of the entire linac. The design involves [7, 8] a 50 keV ECR ion source, 4 vane 3 MeV Radio Frequency Quadrupole (RFQ), Drift Tube Linac (DTL) up to 40 MeV, Cavity Coupled DTL (CCDTL) up to 100 MeV and elliptical 5 cell Superconducting (SC) cavities to get to 1 GeV beam energy. Initially SC sections were planned with gradient of 5 MV/m; but with improved SC technology ~ 25 -30 MV/m gradients seemed possible. Still, in the revised design only 15 MV/m gradient was used, that brought down the length of 1 GeV linac from ~ 880 m to 400 m. The SC cavities (designed to perform over the given velocity range) are identified by the so-called geometric velocity, β_G . The BARC design exploits the large velocity acceptance of superconducting cavities. Transverse and

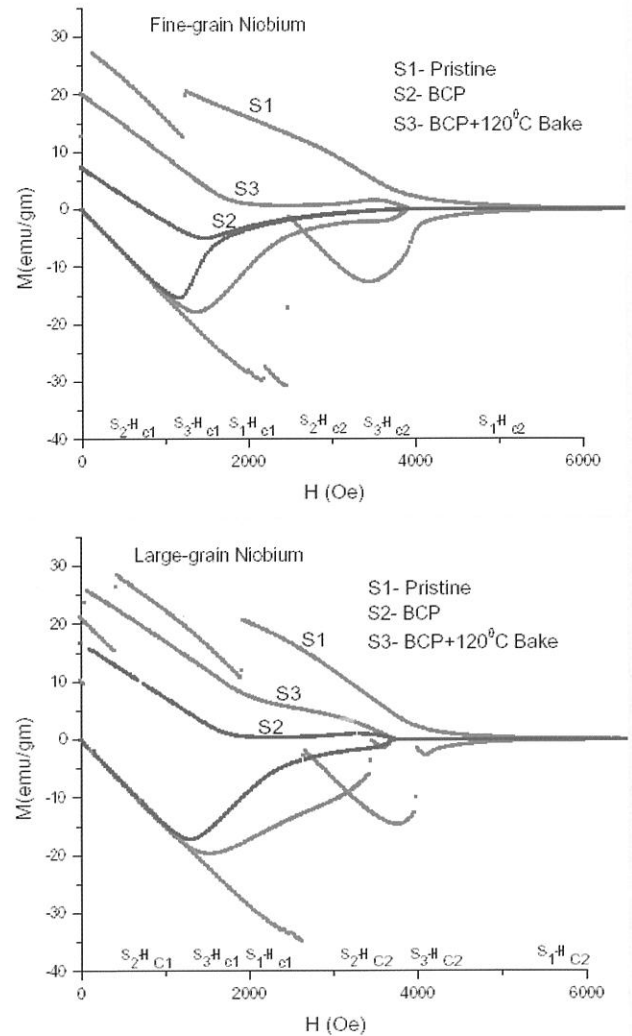


Fig. 2 Magnetization data (in the superconducting state) on fine grain and large grain Nb samples, obtained from the same batch, which were used for making SCRF cavities at JLab, USA. The samples were subjected to same BCP and annealing treatments as was given to the SC-RF cavities. Note large grain material is better. Estimated H_{C1} of the BCP-treated samples correlates well with the reported surface magnetic fields, above which a severe degradation of the Q -factor is observed in the BCP-treated Nb SC-RF cavities. Note the significant reduction on the lower critical field in the BCP-treated sample, and which partially improves when a mild bake is given to the sample.

longitudinal phase advances per unit length, are maintained constant at all transitions between the structures, to provide a current-independent match into the next structure. While the operating frequency for RFQ and DTL was chosen as 352.21 MHz, that for CCDTL and SC linac was chosen as 704.42 MHz. Simulation results revealed that over the full (400 m) accelerator-length, beam transmission is 98%, with 2% loss (confined to RFQ during the beam bunching), posing no

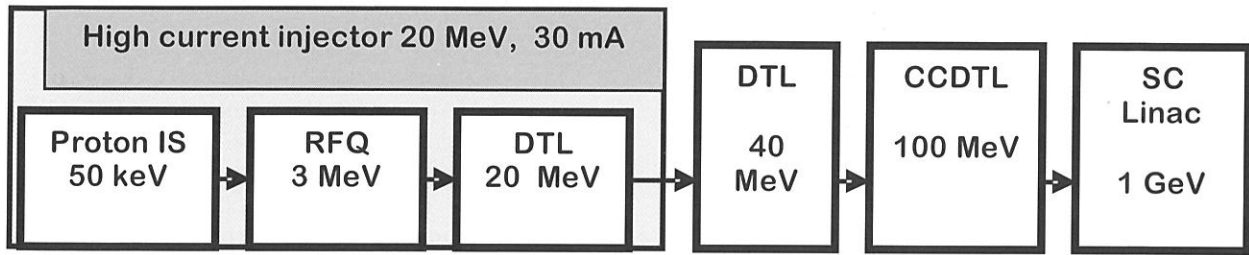


Fig. 3 Schematic arrangement of the 1 GeV linac designed for nuclear energy application

TABLE 1. Design parameters of various parts of the 1 GeV linac

Parameters		DTL	CCDTL	SC
Input Energy (MeV)		3.0	40.12	100.24
Output Energy (MeV)		40.12	100.24	1016.5
Frequency (MHz)		352.21	704.42	704.42
Synch. Phase (deg)		-30	-30	-30/-35
Accelerating field gradient (MV/m)		2.5	1.37	15.0
Total Power (MW)		3.0	6.4	26.9
Total Length (m)		22.7	69.6	306.2
Normalised rms transverse emittance (π cm-mrad)	In x	0.0233	0.0232	0.0351
	In y	0.0242	0.0236	0.0313
Longitudinal emittance (deg-MeV)		0.1150	0.2373	0.2549

serious radiation problem, as energies involved are low. Our design scheme is given in Fig.3 and the main design parameters are given in Table 1.

Most challenging part of a CW accelerator is the low-energy injector, usually in the 10-20 MeV range, where space-charge effects dominate. Hence a 3-phase program (with target energies of 20 MeV, 100 MeV and 1 GeV) was thought of and work was started at BARC on a low-energy (20 MeV) high-intensity (30 mA) proton accelerator (LEHIPA) to validate the design of front-end injector. The details of LEHIPA are described below [7-9] (Fig. 4).

Proton beam, extracted from the ECR ion source, is injected into RFQ, through a Low Energy Beam Transport (LEBT), containing two solenoids, meant to match the beam from the ion source to the RFQ and includes useful beam diagnostics and beam position monitors. Space charge expansion of a high current beam is one of the major processes responsible for increase in beam size and emittance. To facilitate transport of high current beam and to reduce emittance growth due to space charge forces, space charge compensation of the beam is done in LEBT. LEBT's solenoids have been designed, fabricated and also tested at RRCAT. RFQ design has been done using the equi-partitioning scheme, where longitudinal and transverse beam temperatures have to be equal. By this technique, the emittance growth could be brought down to less than 2%. In this design, the vane voltage has been kept constant, keeping the peak surface field, less than 1.8 times the Kilpatrick limit.

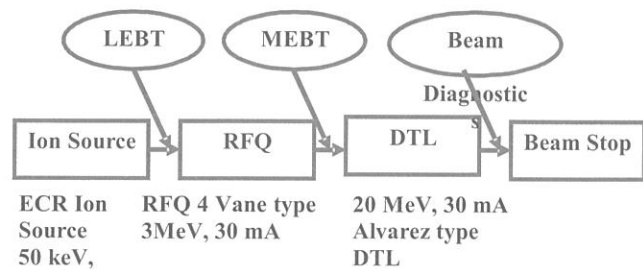


Fig. 4 Layout of LEHIPA

Table 2 shows the RFQ parameters. Full RFQ (4 m length) will be built in 4 segments, which will be coupled with coupling cells. The total RF power requirement is 500 kW that includes 88.5 kW of beam power. The cavity optimization of the RFQ has been done using superfish. In order to include 3D features, like end cells, coupling cells, tuners, vacuum and RF ports, mafia and CST Microwave Studio were used.

Current Status of Ongoing Activities and Plans for Future

The LEHIPA project involves handling of very large RF power and fabrication of complex structures. To learn such technologies, BARC first decided to build a 400 keV RFQ-based machine that will replace an existing dc accelerator (of a 14 MeV neutron source coupled to a sub-critical assembly). This machine consists of a 50 keV/1mA deuteron ion source, a LEBT and a RFQ. After the

TABLE 2. Parameters of the RFQ

Parameters	Value
Frequency	352.21 MHz
Input energy	50 keV
Output energy	3 MeV
Input current	30 mA
Transverse emittance	0.02/0.0204 π cm-mrad
Synchronous phase	-30 ⁰
Vane voltage	80 kV
Peak surface field	32.8 MV/m
Length	4 m
Total RF power	500 kW
Transmission	

design, a prototype of RFQ in ETP Cu was made (Fig.5 a&b), and another 600 mm RFQ has been made in OFHC copper, and tests on it are in progress. The RF group of Technical Physics Division of BARC has built many sub-systems for this RFQ-based 400 keV machine. Foremost amongst these is a tetrode-based RF source at 352 MHz, which is currently undergoing elaborate tests. A LEPT line along with 1 mA ion source and 2 solenoids for focusing the beam, are also being assembled for this program. An indigenous power coupler development has also been initiated. Two 50 kW CW coaxial couplers are under fabrication at BARC. The design incorporates disc type alumina windows with double barrier for better mechanical stability and reliability. A shorted stub provides RF matching along with providing support for central conductor and cooling channels. A prototype RF coupler has been fabricated at BARC. A 250 kW iris type coupler, with tapered transition to WR 2300 half-height wave-guide, is also being designed. Its thermal-loss estimation and

mechanical tolerance-level requirements, are being worked out.)

In parallel with 400 keV machine work, design of DTL is going on at BARC, to hike beam-energy in LEHIPA from 3 to 20 MeV. The 12.8 m long DTL will be built in 4 tanks. Its power requirement is 1.2 MW. Based on this design, a 1.2 m long prototype DTL has been fabricated (Fig. 5(c)). Frequency measurements on it have been done and found to be 349.5 MHz. For focusing the beam, permanent magnet-based quadrupoles, placed inside the drift tubes, will be used. Design of the quadrupoles has been done and a prototype has been built.

To reach an energy of ~ 1 GeV, one must also develop niobium-based Superconducting Radio Frequency (SCRF) cavities. Infrastructure is being built (mostly at RRCAT) for multi cell cavity fabrication, chemical processing and cleaning, materials characterization etc. Efforts have also begun towards design of cavity test set-up which will be later followed up with facilities to test the cryo-modules. In this regard, while the R&D to make and characterize $\beta=0.47$ SCRF cavities is in progress at BARC, RRCAT is rapidly making parallel progress. In partnership with Fermilab (FNAL), RRCAT scientists and engineers have learnt and started to contribute to the development of 1.3 GHz niobium SCRF cavities, needed for Project-X. Project-X is a major initiative launched by FNAL over the past 3 years and envisions construction of a high intensity proton accelerator (HIPA). It is meant to serve a dual purpose. Firstly, HIPA would open up new vistas to explore "Intensity Frontier" in High Energy Physics as well as address a number of cutting-edge problems in fundamental physics. It will also provide a strong foundation to develop superconducting RF technology that would come in handy, whenever the electron-positron International Linear Collider is built in future, or exotic new colliders, like muon colliders are considered. The focus of the first stage of Project-X also is to produce a high-current proton beam, up to 2-3 GeV energy and a few MW beam-power, with an adjustable time

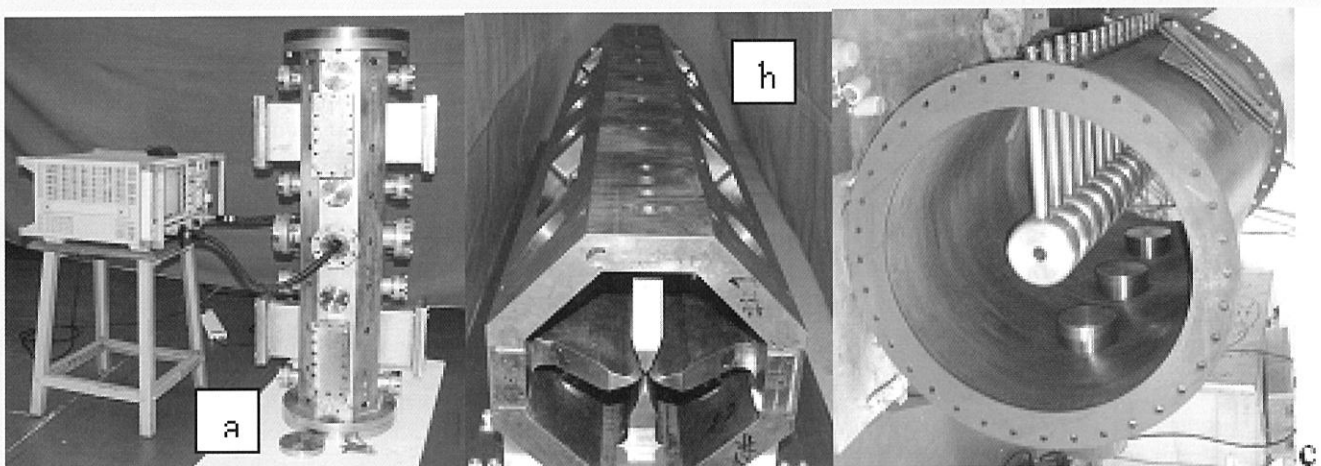


Fig. 5 (a) & (b) are photographs of the 1.02 m long RFQ made by Centre for Design & Manufacturing, BARC for 400 keV machine, while (c) shows picture of a prototype 1.2m long DTL under fabrication.

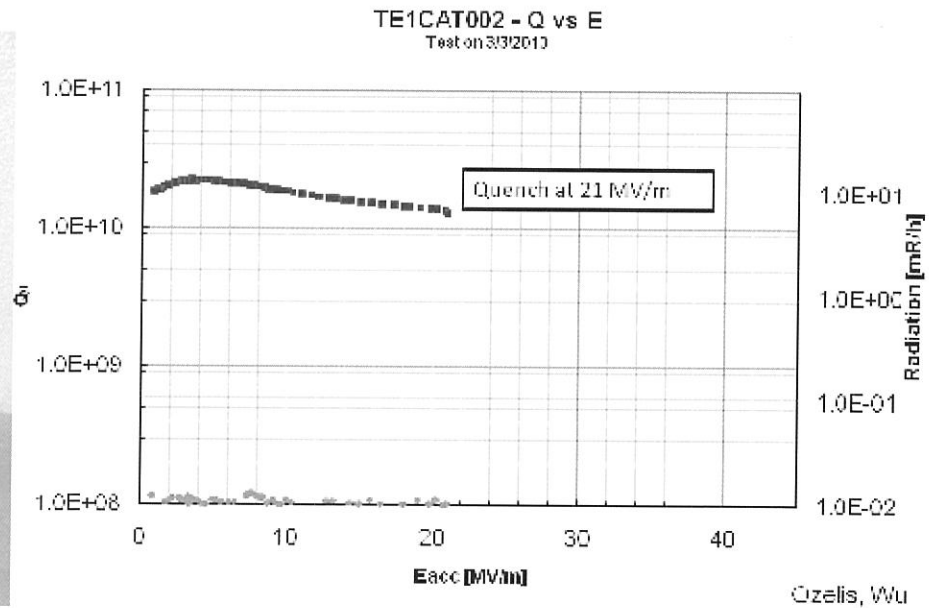


Fig. 6 First solid Nb single cell cavity (left) fabricated by a team from IUAC & RRCAT and first results (right) obtained with the Vertical Test Stand at Fermilab.

structure to suit specific experiments. In this sense, there is a strong synergy between the goals of Project-X and DAE's interest in HIPA, which has brought the two programs in excellent alignment.

In the light of above interests, the work on developing niobium cavities was begun at RRCAT in 2008. Using the e-beam welding facility at IUAC, New Delhi, a team lead by A. Puntambekar (RRCAT) & P. N. Prakash (IUAC) made two single-cell solid niobium cavities, which showed very credible performance, when these were recently tested at FNAL (see Fig. 6). Furthermore, working closely with FNAL scientists, a team of RRCAT engineers have also done value engineering on many system designs evolved elsewhere. Some of the items on which work has been done are: (a) A new way to make the elliptical cavity half-cells to ensure better parallelism between planes passing through the equator and iris. (b) A more economical way to make cavity end groups, wherein number of e-beam welding operations is greatly reduced to save many kilo dollars (c) A new way of mounting the cavities in a cryomodule that not only relaxes the stringent specifications on helium return gas pipe (thus reducing the cost) but also simplifies the procedure of aligning the cavities in the cryomodule. (d) An exhaustive analysis of beta=0.81 cavity that has brought out new options. (e) An improved design of cryomodule that will hold such cavities. (f) An improved design of a VTS (Vertical Test Stand) to test multi-cell niobium cavities etc. RRCAT has also built and delivered to FNAL, tools to make half-cells for the 1.3 GHz elliptical cavities. These will be used by PAVAC in Canada to make cavities and eventually also help in the development of electron linac that VECC plans to use for its RIB programme. In addition RRCAT and FNAL teams are closely working on many facets of R&D, related to Project-X. Overall, a strong collaboration between

Fermilab and Indian labs has emerged beneficial to both the sides. (To learn more details of how this partnership is progressing, please see reference 9 and site <http://iifc.fnal.gov/>).

Summary and Conclusions

Over the past two decades, major advances have been made internationally towards a deeper understanding of the physics of high intensity proton accelerators (HIPA). Looking at varied applications of HIPA, many groups have given great thrust to it the world over, and laudable technological developments have been realized. It is reassuring to see that the investments made by DAE in the past decades, and vigorous efforts put in the recent years, have brightened the prospects of using HIPA in DAE's three-stage nuclear program. From the account given in this paper, it will become clear that we can look forward to a challenging as well as rewarding future for us in this area.

Acknowledgement

Work reported here is an effort of many colleagues at RRCAT & BARC, whom I compliment for their excellent contributions.

References

1. B. R. Bergelson, A. S. Gerasimov, G. V. Kiselev & V. G. Tikhomirov, Nucl. Engg Int. March 1, 2002, p. 42. (Website: www.neimagazine.com).
2. S.S. Kapoor, "Roadmap for development of Accelerator Driven Sub-Critical Reactor Systems", BARC/2001/R/004.
3. B. Aune et al arXiv:physics/0003011v1 [physics.acc-ph] 4 March 2000.
4. S. B. Roy, G. R. Myneni and V. C. Sahni (Paper submitted to Supercond. Sci. & Technol, September 2010).
5. S. B. Roy, G. R. Myneni and V. C. Sahni, Supercond. Sci. & Technol 21, 65002 (2008).

6. V. C. Sahni, Invited talk delivered at the Particle Accelerator Conf PAC2009 at Triumf, Canada. Proceeding available at <http://jacow.org/>
7. Rajni Pande, Shweta Roy, T. Basak, S.V.L.S. Rao and P. Singh, Beam Dynamics for the 1 GeV Proton Linac for ADS, Proc. Indian Particle Accelerator Conference (InPAC-2006), BARC, Mumbai, Nov. 1-4, 2006, page 207.
8. P. Singh, S.V.L.S. Rao, Rajni Pande, T. Basak, Shweta Roy, M. Aslam, P. Jain, S.C.L. Srivastava, Rajesh Kumar, P.K. Nema, S. Kailas and V.C. Sahni, Accelerator Development in India for ADS Programme, *Pramana – J. Phys.* 68, 33 (2007).
9. V. C. Sahni and P. Singh, in Proc. of “Workshop on Applications of High Intensity Proton Accelerators” Fermilab, USA Oct 2009 published by World Scientific.



Dr. Vinod Chandra Sahni (born in 1945) obtained his B.Sc. Honours in Physics from Delhi University in 1964 and joined the 8th batch of BARC Training School. He topped his batch & during the period 1965-96 did his research work in condensed matter physics, earning a Ph.D. from Bombay University in 1973. From 1996-2001 he served as the Head, Technical Physics & Prototype Engineering Division and during 2000-2009 as Director, Physics Group, BARC. In the period 2003 -2009 he concurrently served as Director, RRCAT and was instrumental in setting up 2.5 GeV synchrotron ring Indus-2 at Indore. Presently he is a DAE Homi Bhabha Chair Professor at BARC. He is an INSA Young Scientist Awardee, a Fellow of National Academy of Sciences and a recipient of M. M. Chugani Award of Indian Physics

Association (IPA) for Excellence in Applied Physics. He continues to assist several organizations in the country as well as abroad and is a Member of the Scientific Council of JINR, Dubna & a past President of IPA. His research interests include synchrotron radiation sources & their use in condensed matter research, particle accelerators & their applications.

Modern Nuclear Instrumentation: Advances in Sensors and Electronics Development

V.B. Chandratre¹, Menka Sukhwani¹, R.S. Shastrakar¹, K.M Sudheer¹, V. Shedam¹, Sourav Mukhopadhyay¹, V.D. Srivastava¹, S. Khole¹, Shiv Kumar¹, Anubha Keni², Veena Salodia², Aditya Darad²

1. Electronics Division, Bhabha Atomic Research Centre, Mumbai 400 085, Email: vbc@barc.gov.in

2. Electronics Corporation of India Limited, Mumbai

Abstract

The radiation detection and nuclear instrumentation methods have undergone a paradigm shift due to rapid growth of semiconductor technology and up scaling of High Energy Physics Experiments. The radiation measurement systems are now based upon compact and fast detectors with high channel densities, operating at high count rates for imaging and tracking requirements. These advances in the detector development has put challenges for design and development of compact, multi-channel, low power and low noise detector mount read-out and pulse processing electronics. The modernization of radiation detection and measurement instrumentation has been met by indigenous design and development of Silicon sensors, Application Specific Integrated Circuits (ASICs) and Hybrid Microcircuits (HMC) in close collaboration with the semiconductor foundries. This paper discusses the evolution of detectors and corresponding electronics development along with various development activities of sensors, ASICs and HMCs at Electronics Division, Bhabha Atomic Research Centre.

Preamble

Nuclear and High Energy Physics Experiments are set up to study, analyze and determine characteristic parameters of various nuclear and particle physics phenomenon respectively. The radiations originated in various nuclear and subatomic processes may be categorized in two general types: charged particles radiation (e^- , e^+ , protons, K^+ , α^+ , F^+), neutral particles (X-ray, Gamma ray, neutron, and neutrino). These radiations interact differently with the matter. The experimental set ups for their detection thus generally comprise a combination of different radiation detectors designed for specific measurements.

The rapid advances in the field of nuclear and high energy physics requires setting up large scale experiments with excellent energy, time and spatial resolution specifications. The advances in semiconductor technology has supported these high performance detection and measurement requirements with design and development of compact, low power and low noise semiconductor detectors having high channel densities and excellent response time.

The detector read out and data processing electronics are also required to be designed to match the modern detector performance as conventional instrumentation approaches of using off-the-shelf components, which are subject to rapid obsolescence, no longer serve the contemporary instrumentation requirements. With use of the sensors of higher granularity, higher event rate coupled with complex trigger mechanism, the approach has changed to low power, compact, multi-channel, and low noise detector mount electronics or monolithic sensor with electronics, along with Application Specific Integrated Circuits (ASICs) and Hybrid Micro Circuits (HMCs) solutions.

The semiconductor detectors, particularly silicon based detectors and corresponding low power, compact electronics are also extensively being used in modern sophisticated nuclear instrumentation, personal dosimeter

and medical imaging applications, military or strategic applications besides other commercial applications like aviation, non destructive testing, mineral exploration, security surveillance.

This paper describes the evolution of contemporary radiation detection and measurements techniques with emphasis on the initiative taken at Electronics Division, Bhabha Atomic Research Centre to cope up with the technological advances in radiation detection and measurement methods with design, development and characterization of various semiconductor sensors, ASICs, Hybrid HMCs and System on Chip (SOC) solutions.

Introduction

Rapid growth of semiconductor technology and up scaling of high energy physics experiments (HEP) have led to the design and development of compact high performance semiconductor detectors with related read out and pulse processing electronics. These detectors exhibit excellent spatial resolution due to high density of semiconductor materials and good energy resolution owing to the lower energy threshold (~ 3.6 eV) for creation of the charge pair as compared to the ionization energy in a gas (30 eV) or the approximately 300 eV necessary to extract an electron from a photocathode coupled to a plastic scintillator. The semiconductor detectors are therefore generally configured as one or two dimensional arrays of small radiation detection elements for tracking and imaging applications.

Semiconductor detectors usually comprise a reverse biased p-n junction as its active volume with large electric field applied across it. The incident radiation interacts with the detector material in its active volume, losing its energy completely or partially in generation of electron-hole pairs. These charge carriers are then collected at the electrodes under the influence of large electric field providing a measure of the energy deposited by the incident radiation. Design and characterization of a semiconductor detector

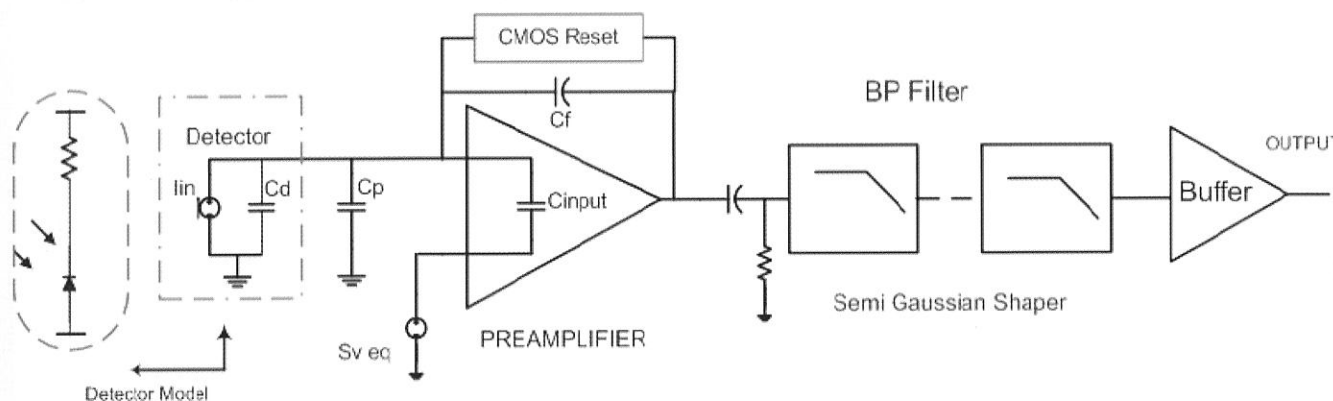


Fig. 1 Simplified block diagram of a typical detector system with its associated readout electronics

therefore requires a good insight into fabrication process steps along with device mask preparation techniques. Fabrication process parameters such as type and density of substrate doping, number and type of surface traps, affect the electrical and optical characteristics of the detector strongly. Effective use of CAD tools with 2-D and 3-D process and device design capabilities are therefore essential requirement of sensor design as they minimize the fabrication risk, cost and design time considerably.

The simplified block diagram of a typical radiation detector system along with the associated readout instrumentation is shown in the figure 1 below. The typical configuration of readout instrumentation for a radiation sensor comprises charge or current preamps, pulse shapers (filters), peak detectors and data conversion and acquisition functional blocks. The primary goal of the readout and data acquisition electronics varies with the application. The entire chain of detector and readout electronics has to be carefully chosen keeping in mind the primary goal of the application (e.g. tracking, calorimetry, energy spectroscopy, etc).

The nuclear detectors have undergone tremendous changes over the past few decades. Solid state detectors have now become the backbone of majority of high energy physics experiments. The stage is dominated by Silicon based detectors, with other semiconductor materials such as Germanium, Gallium Arsenide, Boron Carbide, Silicon Carbide, Diamond, Cadmium Zinc Telluride etc. also playing an important role. Advances in VLSI technology has greatly aided the development of planar Silicon detectors and a large variety of detector types such as strip, micro-strip detectors, pixel detectors, drift detectors, photo diodes, avalanche photo diodes coupled to scintillator directly or through wavelength shifting fibres have become available now.

In nuclear spectroscopy applications, the readout electronics is designed to measure accurately the small charge impulse generated by the incident radiation. Hence it should exhibit low noise and good linearity. Further, now low operating power is a prime criterion for multi-channel detector readout electronics. The modern detectors for

tracking or imaging applications require a higher granularity that constrains the use of discrete electronics. Thus, low power, low noise solutions to cater to higher channel density detector electronics with reduced readout latency is the driving force behind integration of the detector with pulse processing and data conversion electronics. This domain has also undergone a paradigm shift with the CMOS technology based monolithic solutions dominating the readout instrumentation scene.

The CMOS technology is preferred choice for designing signal processing and readout integrated circuits in view of its low power, high density, higher impedance for handling small charge, ease of implementing high gain amplifiers, availability of passive components (i.e. capacitors resistors) along with bipolar transistor. Further, this technology features engineering support for low power digital and analog standard cells tightly coupled to modern IC design CAD tools. Nowadays, it is possible to implement photo detectors like photodiode, Avalanche photo detectors, DP-FET, Silicon photomultipliers in conventional CMOS technology.

Evolution of Nuclear Instrumentation

Nuclear instrumentation methods have evolved phenomenally over the years from large size, vacuum tube circuit based systems to international nuclear standards based modular electronics bins to present days compact solid state detector with integrated circuit based readout or monolithic sensors with electronics followed by computer algorithms based data processing and analysis techniques.

Nuclear instrumentation standards were introduced in 1960's to provide flexibility, interchangeability, reduced design efforts and ease of up gradation. These standards defined the electrical and mechanical specifications for electronics modules used in experimental particle and nuclear physics. Nuclear Instrumentation Module (NIM) standard is suitable for small scale linear processing requirements, whereas Computer Aided Automated Measurement and Control (CAMAC) standard is defined mainly to deal with multi-detector systems involving large digital data processing. The development was concurrently

followed by VME (Versa Modulo Europe) and Fast-Bus. However, the Fast-Bus did not survive due its odd form factor and ECL logic adaptation.

It would not be an overstatement, if we say that the driving force for modern electronics fueled by the high-energy physics requirements. It is at this time when large HEP were planned and the manner in which the electronics was designed and developed changed. New challenges of power, radiation hardness, speed and high density was imposed along with the never seen data bandwidth requirement.

The bus based system utility survived on the data acquisition and trigger generation. The detector, the readout electronics and signal processing has to be located near the detector. The era of "Detector Mount Electronics" was born. Initially, two approaches were chosen the development of hybrid microcircuits (HMC) and the bipolar ASIC in mid 1980. This approach was not power economical and did not provide the requisite electronics density. The Hybrid microcircuit advanced into thin film and multichip modules were the passive elements fabricate or integrated on alumina substrate with active components use at die level. These developments were just advance packaging technologies that used the conventional of the shelf components. These technologies matured into 3D hybrid microcircuits using the LTCC (Low Temperature Co-fired Ceramic) technology. Despite the advancement of vertical bipolar device technology, the ASIC development using this technology lacked scaling with little relief for power consumption. This technology did not become commercially viable as the major foundries migrated to CMOS technology.

Initially, efforts were made at CERN and other places to explore the possibility of using CMOS technology for high density HEP instrumentation. The high performance analog design and radiation hardness was a challenge. In later years, with the development of submicron CMOS technology, the radiation hardness issues were mitigated to an extent. This lead to a new field of CMOS ASIC design for HEP leading to new generation of signal processing techniques in nuclear instrumentation.

Above developments made it possible to utilize the novel detectors for tracking and imaging application with advantage of cost, density, lower power and synergy of analog and digital elements together. The outcome of these efforts was extensive use and development of multi-wire proportional chamber, Gas electron multiplier chamber, single/ double side silicon micro strip detector, pixel and strip detectors, PN-CCD etc. It was now possible to integrate detector, signal processing, and readout on a single chip. The fallout of these developments not only enabled the HEP experiments but also grossly enhanced the medical imaging technologies.

Consequently, in such instrumentation the trigger generation techniques have also become immensely complicated because of highly dense detector modules

operating at high event rates. Mixed approaches of trigger generation using hardware logics and software algorithms have become mainstay.

Evolution of Semiconductor Detectors

Previously semiconductor detectors were bulk-type detectors viz. Lithium drifted Germanium detector (GeLi), Lithium drifted Silicon detector (SiLi), High Purity Germanium (HPGe) etc. they are the golden standards for fine nuclear spectroscopy. However, post 1980's there has been a phenomenal development in the field of semiconductor detector fabrication technology using planar VLSI technology. These developments lead to the invention of planar detectors [1]. Since then, silicon detectors have been continuously improved and several novel detector types have been evolved to meet challenging requirements of tracking, energy measurements and imaging applications.

The present generation of detector applications can be broadly classified under two categories viz. tracking and calorimetric. Majority of present generation of detectors fall under these two categories. The tracking detector require low power, large active area and volume, multi-channel detection imposed by HEP experiments has lead to development of novel detector types such as micro or macro strip, pixel detectors, silicon drift detector (SDD), DPFET, photodiodes, Avalanche photodiodes, Hybrid Photon Detectors, Silicon Photo multipliers, Multi Pixel Photon Counters etc. The tracking detectors are complimented by non-silicon solution such as proportional pad, resistive plate chambers and GEM (Gas electron Multiplication) detectors.

The new planer technology of detectors have enhanced the performance in terms of achievable position resolution (~few microns), temporal resolution (~ few picoseconds) and energy resolution (~ 140 eV). A majority of these detectors are operated at room temperature or at the most cooled to -20°C which can be achieved using peltier cooler, thus eliminating the need for bulky liquid nitrogen dewars. Some of these can be integrated along with their front end readout electronics, thereby making it possible to develop a single chip solution for the given application.

Semiconductor technology development Activities at BARC: Processes and Sensors.

Since mid-90s under the initiatives of Late Dr S K Kataria, Electronics Division has been pursuing R&D activities for the development of planar silicon detectors required for BARC / DAE as well as for catering to India's commitments to high energy physics experiments at CERN for the Compact Muon Solenoid detector. As a spin-off of this technology development activity 32 channel macro strip detector was designed in Passivated Implanted Planar Silicon (PIPS) technology. These detectors have been successfully deployed for charge particle detection in silicon based tracking detector at CMS CERN. Subsequently, design and development of silicon drift detectors, avalanche photo diodes, UV enhanced photo diodes, silicon photo multipliers and multi pixel photon counters was taken up

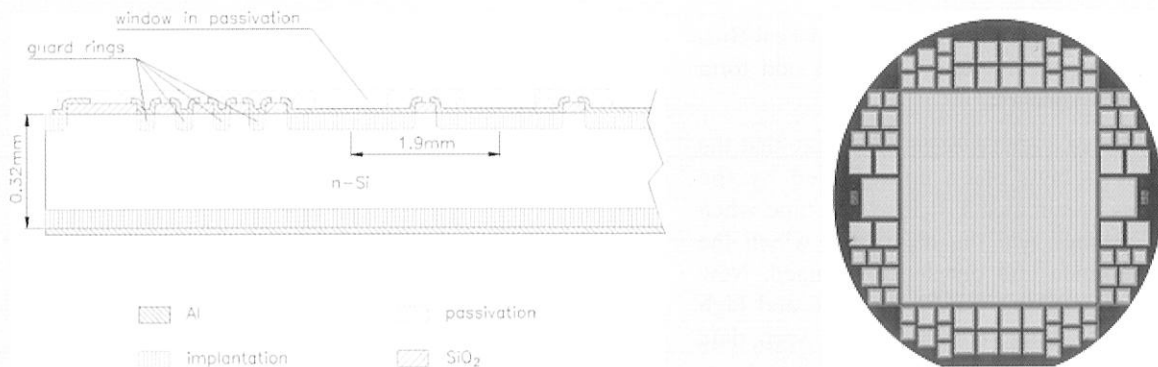


Fig. 2 (a) Schematic cross section of strip detector (b) 32 channel strip detector along with PIPS detectors at periphery

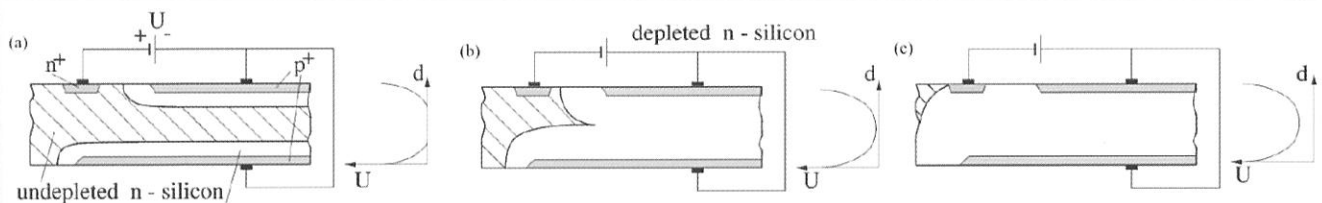


Fig. 3 The principle of sideways depletion. In (a) no reverse voltage is applied, only the intrinsic depletion zones are depicted. (b) Shows the full depletion, starting from the rectifying junctions on both wafer surfaces. (c) Shows the configuration of over depletion

keeping in mind the national and international scenarios. The R&D activities are summarized in the following sections.

Development of Silicon Strip Detectors

Silicon strip detectors are large area 32-channel detectors targeted for position sensing applications. It was designed specifically for meeting the requirements of pre-shower detectors of the CMS experiment at CERN. The detector consists of 32 strips, each being 60 mm long and at a pitch of 1.8mm. Thus an entire 4" wafer consists of just one 32-channel strip detector. The starting wafer used for fabrication of strip detectors were high resistivity (5 - 10 $\text{k}\Omega\text{-cm}$), n-type double-side polished wafers.

To meet the stringent specifications set by CERN (leakage current of individual strips to be less than 10nA, breakdown voltage of individual strips to be in excess of 250V) each aspect of the fabrication technology was carefully optimized in collaboration with semiconductor foundry at BEL Bangalore [2]. The critical design element in the detectors that of electricfield termination aspects was addressed by carefully in design using well spaced of guard-rings for the entire detector. The leakage currents were reduced to acceptable levels by incorporating extrinsic gettering technique during fabrication of the detectors.

Passivated Implanted Planar Silicon (PIPS) Detectors

A large number of PIPS detectors with areas from $3 \times 3 \text{ mm}^2$ to $1 \times 1 \text{ cm}^2$ have been designed and fabricated along with the silicon strip detectors. These detectors have a P-I-N structure with P+ region on the top forming a p-n junction with the high resistivity n-type bulk and N+ region at the backside for taking out an ohmic contact. Each detector has 3 to 7 guard-rings for reducing the dark-current and for

achieving high breakdown voltage. Detail technology CAD process and device simulation studies were carried out for optimization of the detectors performance [3]. A phosphor-silicate glass layer is deposited on the front side that serves as a protective layer. The thickness of these detectors is approximately 300 microns. These detectors are much superior to traditional SSB (Silicon Surface Barrier) and DJ (Diffused Junction) detectors in terms of ruggedness and operational stability. The PIN detectors have been successfully used for room temperature low-energy x-ray / gamma ray spectroscopy applications. Shallow junction variant of PIN detectors has also been fabricated and used for alpha and charge particle spectroscopy applications. These detectors have also been deployed for personal dosimetry applications.

Development of Silicon Drift Detectors

Silicon drift detector (SDD) is based on the principle of sideways depletion and a novel charge transport scheme proposed by Gatti and Rehak in 1984 [4]. Here, a large active area fabricated on a high resistivity n-type silicon can be fully depleted from a small n+ type ohmic anode contact positively biased with respect to the p+ contacts covering both surfaces of the silicon wafer (see Fig. 3). Additionally a sideways drift field is also applied by biasing the p+ strips at progressively higher voltages with respect to the anode.

A major advantage of the SDD is that whereas in the conventional structures the detector capacitance is always proportional to the active area, in an SDD the detector capacitance is independent of the active area of the detector. This decoupling of the detector capacitance with the active area of the detector allows the use of large area SDDs for a

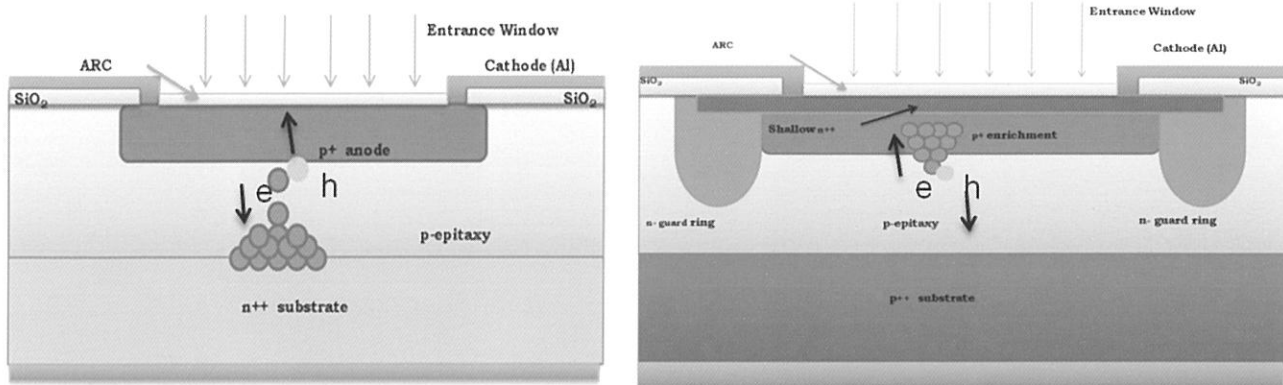


Fig. 4 (a) A typical MPPC (b) A typical SiPM

given application, without worrying about the detector capacitance. The low values of anode capacitance leads to better energy resolution even at higher count-rates. Various types of prototype SDDs with on-chip JFET and poly-silicon bias resistors have been fabricated in collaboration with BEL Bangalore foundry. Process technology development and optimization is presently underway, for achieving the target performance. These detectors can offer 100 eV energy resolutions with dynamic range of 100 keV. They are not replacements of bulk high-resolution semiconductor detectors but they are preferred where portability is required.

Development of Avalanche Photo Diode, Silicon Photomultiplier and Multi Pixel Photon Counter

Avalanche Photo Diode (APD) with finite internal gain has been used for detection of low level light since early 1960s [5]. An alternative method was operating the APD in Geiger Mode (GM-APD) wherein the APD is biased above the breakdown voltage. This ensures that any photoelectron generated by incident light or thermally generated electron triggers an avalanche breakdown which results in a pulse in the external circuit. The breakdown is then quenched using an external passive or active quenching circuit. Based on the above concept and technological advances in Silicon VLSI technology novel family of multi pixel photon detectors have been developed viz. Silicon Photomultiplier (SiPM) and Multi Pixel Photon Counter (MPPC). Both the varieties consist of an array of large number of APD micro-pixels operated in the G-M mode. Both SiPM and MPPC are an array of APD micro-pixels, each with a typical size of 20–100 μm . But whereas the SiPM has a junction very close to the surface the MPPC has a deeper junction and hence a larger breakdown voltage. The MPPC devices have higher enhanced blue responsivity. These pixels (in both SiPM as well as MPPC devices) are finally connected to a common load resistor for summing the output of all these pixels. Although individual pixels act as binary device, for low incident photon flux the output signal is proportional to the number of pixels fired. Thus a SiPM / MPPC device can be considered to be analogous to an “analog” detector that can measure the incident light intensity. These detectors are rapidly evolving as an alternative to conventional photomultiplier tubes (PMT) because of their fast response,

low voltage operation along with insensitivity to magnetic field and photon counting capability [6,7].

SiPM and MPPC family of detectors are fabricated on different substrates using entirely different process technology. But there exist a lot of geometrical similarities between these detectors (Fig. 4). Taking the advantage of their similarities a common mask set was designed for both the SiPM and MPPC detectors so as to reduce the NRE charges for mask-set fabrication. Process technology was optimized individually for both these detectors. A large variety of SiPM and MPPC prototype devices have been designed and fabricated in collaboration with BEL Bangalore foundry. This work has been reported in [8,9] and the R&D for performance enhancement of these detectors is an ongoing activity.

Readout Electronics: ASICs and HMCs

As a consequence to the successful development of in-house silicon detectors [11] and participation in HEP collaborations in house ASIC development activity was actively pursued. The indigenous foundries have played a crucial role in successful development of semiconductor devices [12,13]. The following read-out electronics evolved in response to successful indigenous detector development.

In the whole process the development of readout electronics was driven by the indigenous requirements and need to modernize the nuclear instrumentation and mitigating technological denial. The development has to be carried out with available resources within the country and mix and approach was selected that best suited the requirements. As a result, the ASIC and the Hybrid development activities are carried out using the industrial facilities that enable manufacturability. The reactor instrumentation has its unique problems of qualification and component obsolescence. The signal swing, drives and safety related issues along with component qualification does require bipolar devices. Therefore, Electronics Division along with BEL, IITK developed fast bipolar process for catering to development of integrated circuits for high bandwidth. The indigenous development of ASIC and HMC is developed keeping in focus the requirements of low power portable instruments for radiation monitoring.

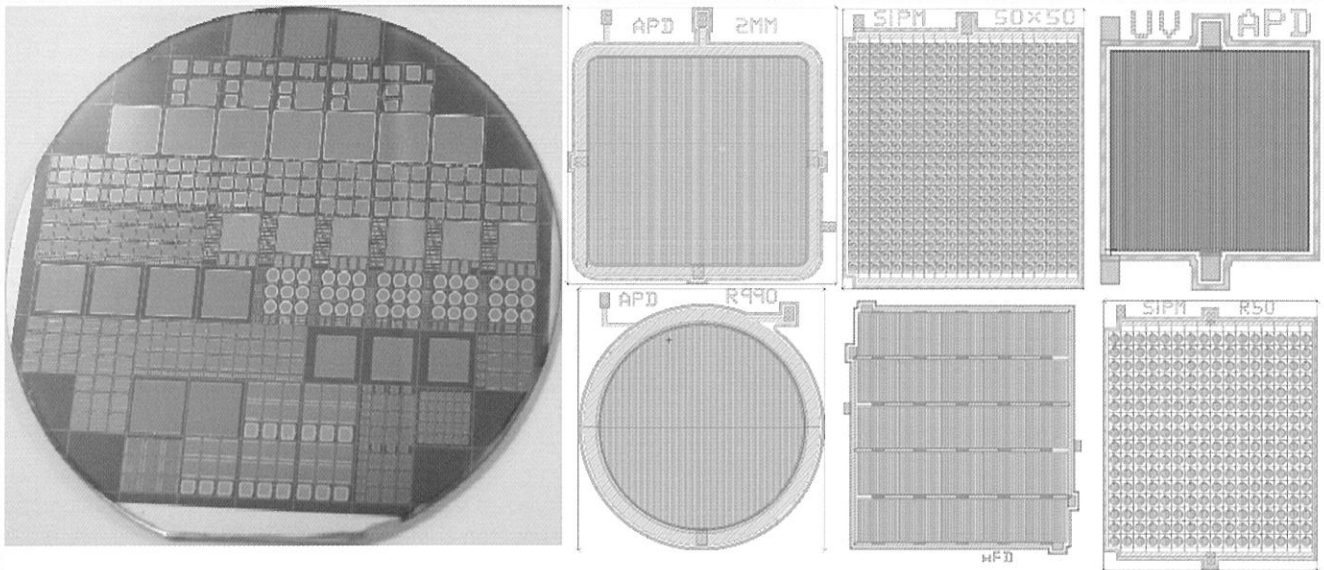


Fig. 5 (a) Processed 4" wafer consisting of various designs of photo detectors (b) Layout of photo detectors

The approaches to development of readout electronics in elaborated below.

Detector Signal Processing Solutions

The ASIC development activity was initially started using 1.2 micrometer technology at Semiconductor Complex Ltd., Chandigarh and ASICs CODA, MICON and OCTPREM were developed for read-out electronics of silicon detectors catering to various energy ranges with detector capacitance up to 50pF.

OCTPREM ASIC is an eight channel low-noise charge sensitive amplifier (CSA) in a modified folded cascode topology capable of driving 50 ohm load with charge gain of 2V/pC and is packaged in two versions, Ceramic DIP and Chip on board.

CODA (CO-chip for Dosimeter Application) is a pulse processing ASIC with low-noise charge-sensitive amplifier, semi-Gaussian shapers followed by a general-purpose comparator best suited for input dynamic range of 120 KeV to 8 MeV, targeted both for counting (e.g. dosimeter) and low energy spectroscopy applications.

SPAIR (Silicon-strip Pulse Analog Integrated Readout) ASIC is an 8-channel pulse processing ASIC with each channel comprising charge amplifier, shaper, track & hold followed by an analog multiplexer for multiplexed output best suited input dynamic range of 660 KeV to 10 MeV, targeted for spectroscopy applications in multi-channel environment e.g. Si-stripes detectors. Both CODA and SPAIR ASICs have additional trigger channel for generating trigger input for track and hold in spectroscopy applications. Further both of these ASICs have external controls for gain, peaking time, input/output polarity and output fall time.

MICON (Modified Current Conveyer) is an 8 channel pulse-processing ASIC with each channel comprising of a

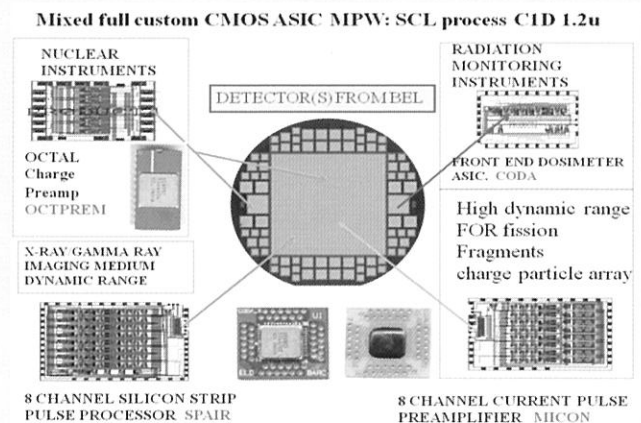


Fig. 6 ASICs for different applications

current pulse amplifier, shaper, track & hold and an analog multiplexer best suited for very large input dynamic range of 10 MeV to 150 MeV, targeted for both counting (with high counting rates) and spectroscopy applications in multi-channel environment e.g. fission detectors, electron shower. It can take either polarity inputs and output polarity can be fixed using polarity control. ASIC can be DC connected with the detector and can handle detector leakage current of the order of 100 micro Ampere.

These ASIC provided the crucial knowhow and enabled the understanding, expertise to handle the nitty-gritty in development of ASIC required. Besides the development of CMOS ASIC the approach to development of bipolar ASIC was also perused in view of critical requirements in reactor instrumentation.

INDIPLEX and SINGLEPLEX ASIC were designed following, using 0.7u CMOS process for CERN ALICE experiment pad detectors for VECC, Kolkata. SINGLEPLEX [14,15] is single channel (Fig 7(a)) and INDIPLEX is 16 channel pulse processing ASIC. The

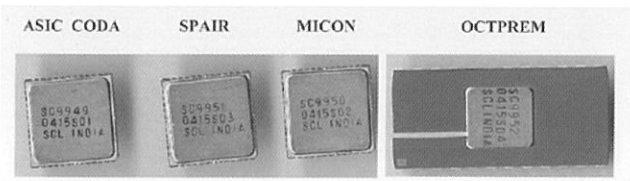


Fig. 7 Packaged ASICs

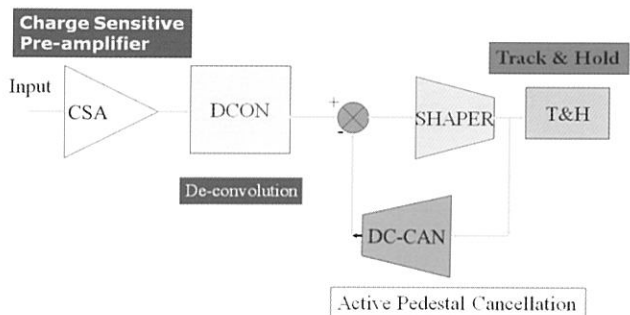


Fig. 8 Channel architecture of SINGLEPLEX & INDIPLEX ASIC

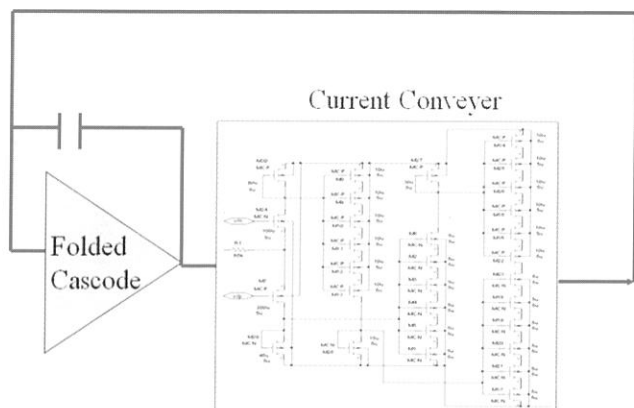


Fig. 9 Architecture of the CSA

ASICs are targeted for gas proportional counters / Si strip detectors.

The ASIC comprises three stages. The first stage is the Charge Sensitive Amplifier (CSA) based on the folded cascode architecture which is followed by the Deconvolution filter based on the Gm-C filter architecture as the second stage. The final stage is the 4th order Semi Gaussian shaper (CR-RC⁴) based on sallen-key filter.

The CSA is divided into two parts i.e. folded cascode stage and an active feedback resistor stage. The input device is pmos with large W/L so as to match the detector capacitance ($C_{gs} \sim Cd/3$ for optimum ENC) and also to reduce flicker noise contribution (large area pmos). The device is biased in weak inversion with a current of 500 μA to give high transconductance $-g_m$ which also helps in achieving low-noise performance. The feedback resistor of the order of 12 Meg-ohm is implemented with a poly resistor of 5.8 kilo ohm followed by a current conveyor. Since current conveyor has low input impedance (common-gate stages on either rails followed by mirror additions), folded

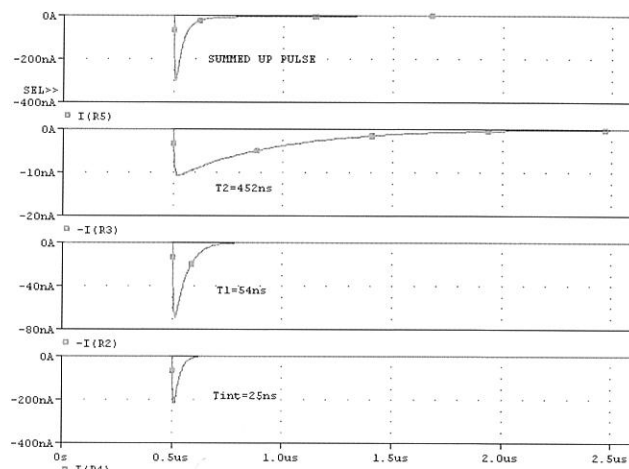
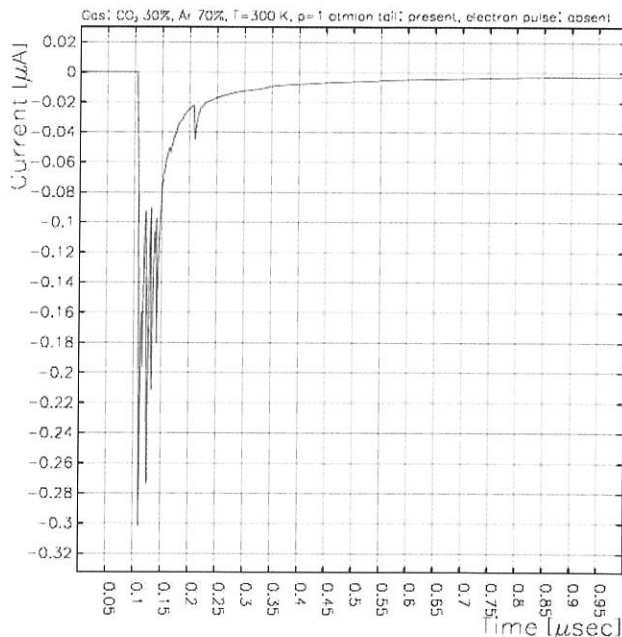


Fig. 10 (a) A typical detector pulse (b) the approximate exponents extrapolated

cascode stage of the CSA is followed by a source follower. The mirror divides the signal current to the ratio of 185 which along with feedback capacitor of 0.7 pF effectively gives a CSA decay time constant of $\sim 10 \mu s$.

A dedicated filter, based on the de-convolution principle, is used for cancellation of the long hyperbolic signal tail, produced by the slow drift of ions, typical in gas proportional with the filter time constants, derived from the actual detector input signal shape. The transfer function of the de-convolution filter has to be the exact inverse of the transfer function of the detector so as to recreate a Dirac pulse. In Singleplex and Indiplex ASIC this filter is designed based on the Gm-C filter topology.

The hyperbolic detector signal current can be represented by the sum of three exponents as shown above. Each exponent can be modeled by placing a pole in the feedback of a summing amplifier to implement the inverse transformation as shown below.

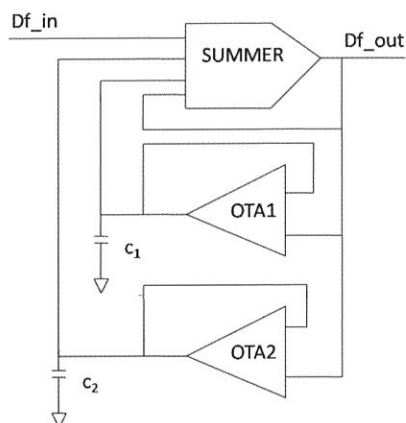


Fig. 11 Architecture of Gm-C filter topology based Deconvolution filter

The Sallen-key shaper based Semi Gaussian shaper is built around an op-amp designed with rail to rail capability. The rail to rail capability is achieved by input nmos-pmos pairs with push-pull output stage. The shaper is built in two stages to give a semi-Gaussian shape with a peaking time of 1.2us.

Due to the pole given by the time constant of the CSA, it is necessary to introduce a zero in the transfer function of the shaper for a perfect recovery to the base line. Placing an active resistor across the differentiation capacitor does this. The 'zero' can be tailored by adjusting the gate voltage of the active resistor externally. This stage serves to tie down the dc pedestal output voltage to zero volts actively so as to eliminate the channel to channel dc pedestal offset voltage variations. This is done with an error amplifier with moderate gain and with unity gain bandwidth of the order of 1 kHz so that the block will not have any detrimental effect on genuine signal but will effectively track the dc pedestal.

The design is optimized for the dynamic range of +500 fC to -500 fC, with provision for externally adjusted pole-zero cancellation. The pole-zero adjustment and DC pedestal can be adjusted by external DC voltage to achieve perfect base-line recovery to 1% after 5 microseconds and equal DC pedestal in all the channels. The ASIC's 0 pF noise is 500 electrons (e^-) r.m.s for the peaking time of 1.2 micro-second with noise slope of $7e^-/pF$. The gain is 3.4 mV/fC over the entire linear dynamic range with power dissipation of 14 mW per channel. The ASIC has feature of equal gain on both polarities and swing is $\pm 2V$ with supply of $\pm 2.5V$.

The SINGLEPLEX ASIC serves as diagnostic chip for INDIPLEX. The design contains many unique circuit concepts. The feedback resistor greater than 100 M Ω is implemented by using current conveyer. In this ASIC an analog multiplexer is implemented to provide multiplexed output. Being a low power, low noise ASIC it has been integrated in the front end modules of radiation monitoring instruments.

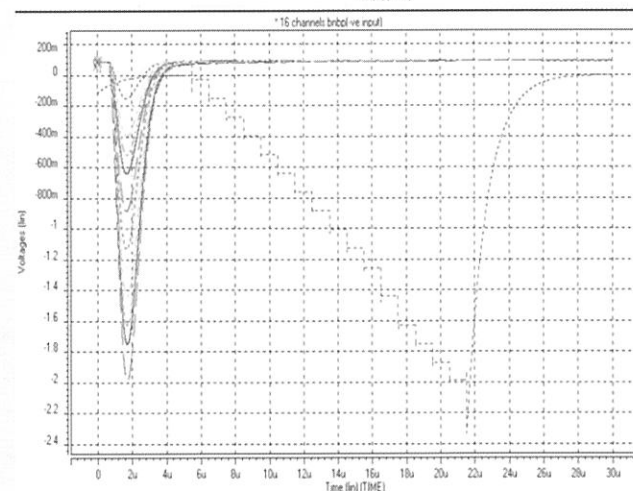
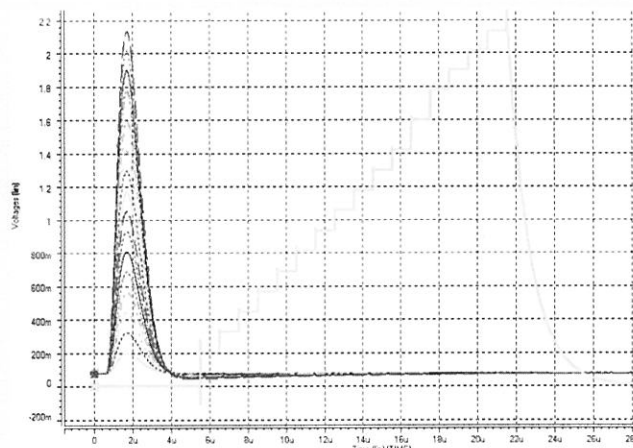


Fig. 12 (a) 8 Channel Outputs with Serial Read out for -ve charge input (b) 8 Channel Outputs with Serial Read out for +ve charge input

Further, an ASIC ANUPRAVAH is developed in 0.7u mixed CMOS process specifically with ultra-low noise specifications to match the excellent energy resolution of Silicon drift detectors. This pulse processing ASIC employs a novel concept to achieve active mega-ohm feedback resistor leading to low noise specifications of 100-250 e^- at room temperature [16,17].

ASIC ANUSPARSH is also developed in 0.35 micrometer mixed CMOS technology as a low power, fast front-end for the glass Resistive Plate Chamber (RPC) detector of Indian Neutrino Observatory (INO) ICAL experiment (Fig. 14). The ASIC comprises eight read out channels, each having regulated cascode [18] trans-impedance preamplifier, differential amplifier, and discriminator and LVDS driver [19]. The ASIC has been optimized for sub nanosecond rise time and lower power consumption to meet the timing and power requirements of the RPC detector readout having 3.6 million pick-up channels.

ASIC Anusuchak is a three channel low power (5 mw / channel) single supply front end signal processing ASIC prototype for personal dosimeter with charge gain of 3 V/pC, shaping time of 1.2 μs and noise slope of $8 e^-/pF$, designed in

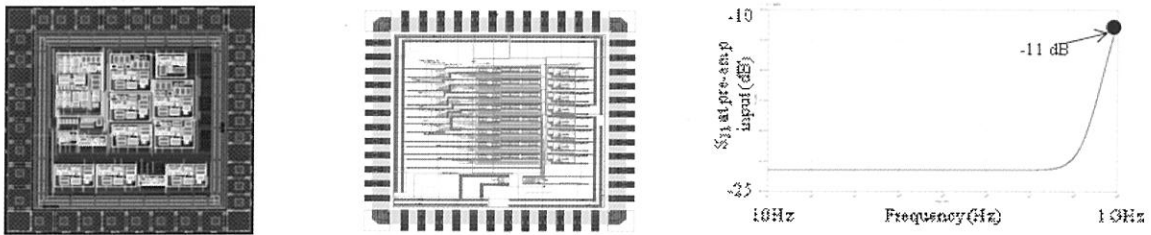


Fig. 13 (a) Anupravah ASIC Layout; (b) Anusparsh ASIC Layout; (c) S11 plot for RGC input

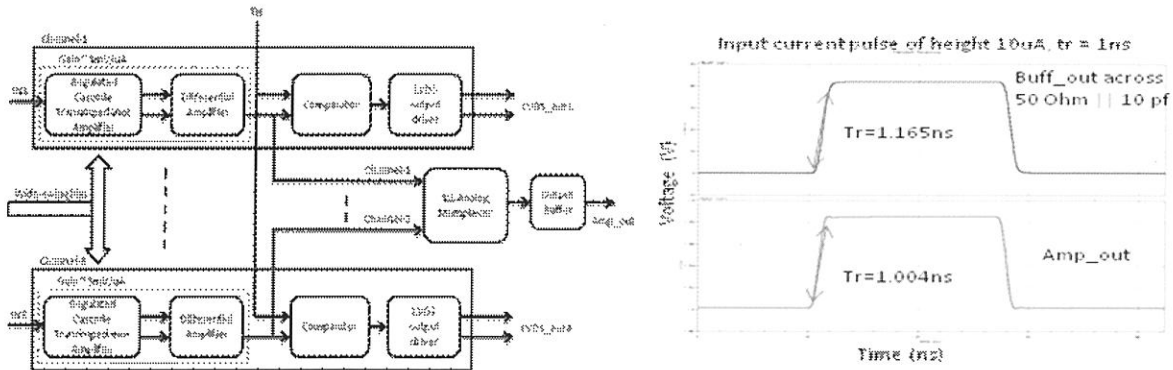


Fig. 14 (a) Architecture of 8-channel Anusparsh ASIC; (b) Amplifier and buffer transient outputs

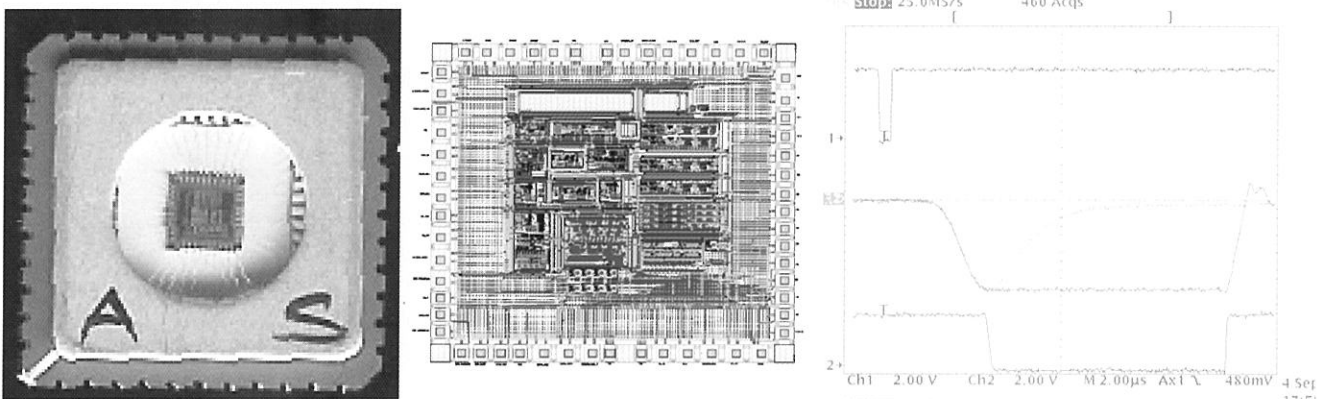


Fig. 15 (a) ANUSHIKHAR ASIC; (b) ANUROOP ASIC Layout; (c) ANUSHIKHAR output on oscilloscope

0.35 μm CMOS process. The ASIC is specifically designed for PIN diodes sensors.

Data Conversion Solutions

The detector signal processing ASICs would require compatible signal conversion solutions for spectrum building and data acquisition.

ANUSHIKHAR ASIC (peak detect and hold circuit) and Anuroop ASIC (Wilkinson ADC) were developed in 0.7 μm Mixed-CMOS technology as a part of the chipset being designed for low power portable nuclear spectroscopy application. ANUSHIKHAR ASIC comprises of a peak detect and hold circuit, linear gate, window comparator and Start of Convert (SOC) interface logic to interface an ADC [22]. The ASIC has unique concept to bias dynamically the Peak detect and hold circuit so as to ensure good linearity and lower ballistic deficit.

ANUROOP ASIC is a low power 10-bit Wilkinson ADC with conversion time of 42 μs [23]. The ASIC architecture is built around the ANUSHIKHAR ASIC, linear discharge current source and a gray counter thereby inheriting the merits of low ballistic deficit and pulse pile-up rejection of the ANUSHIKHAR ASIC. The Gray counter is designed to count at both the clock edges thereby reducing the conversion time by a factor of two. It also minimizes the digital switching noise as in a Gray code only one bit changes per count (Figure 15 and 16). This ASIC with SINGLEPLEX ASIC enables two chip solution for 1K channel portable Multi-Channel Analyzer (MCA).

An ASIC ANUSMRITI is designed to cater to the ultra high speed data conversion requirements in transient digitization in various applications like beam line instrumentation, gamma ray telescope, ultrasound based NDT (non destructive testing). An elegant solution is to use a

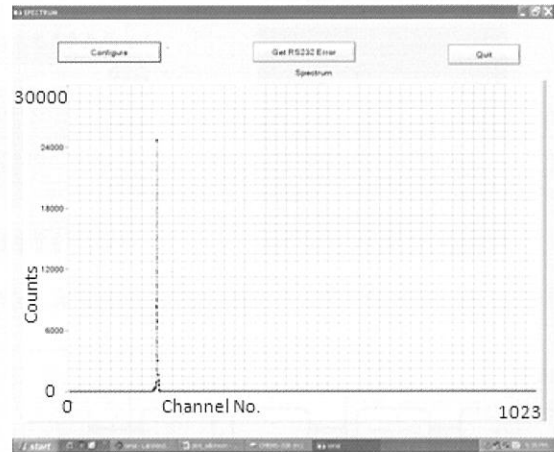
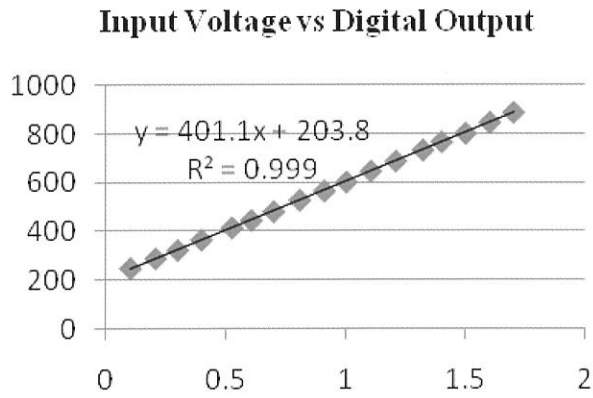


Fig. 16 (a) Measured Linearity plot; (b) Single point response of the ANUROOP ASIC

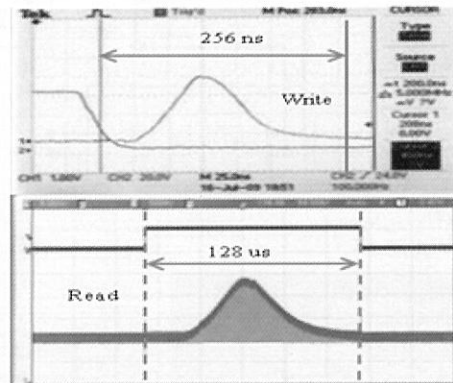
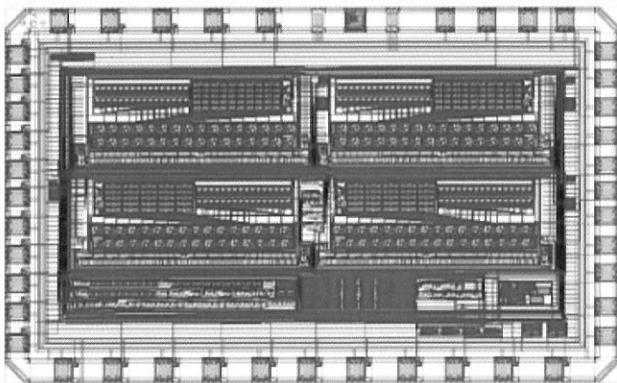
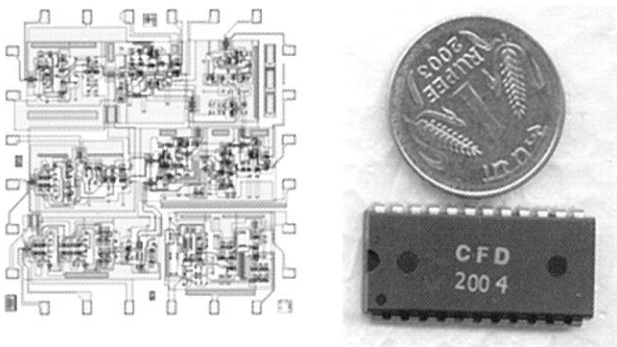


Fig. 17 (a) ANUSMRITI ASIC Layout; (b) ANUSMRITI ASIC test results on Oscilloscope



Mask Layout

CFD ASIC

Fig. 18 (a) Layout of CFD ASIC, (b) CFD ASIC in 24 pin DIP package

high speed analog memory to capture the required event as snap shot with slow readout by an ADC facilitating high resolution digitization at high sampling rate with lower overall power dissipation and cost. A 128-cell Delay Lock Loop (DLL) based switched capacitor analog memory ASIC (ANUSMRITI) with sampling rate of 500 MSPS (Mega samples per second) was developed successfully for transient waveform digitization [24].

A Constant Fraction Discriminator (CFD) ASIC was successfully developed as fallout of development of junction

isolated bipolar process technology at the BEL foundry. The ASIC is designed to mitigate the unacceptable effects of time walk in leading edge discrimination in physics experiments involving multiple detectors configured for coincidence / timing application. The CFD ASIC was developed in technical collaboration with I.I.T Kharagpur, fabricated using 4µm fast, junction isolated bipolar process developed at BEL foundry. The ASIC comprises of ECL D-Flip-flop, RS-Flip-flop and four comparators with ECL to TTL level translator driver. The ASIC achieved rise time of ECL ~ 4 ns, TTL ~ 5 ns, time walk less than 1ns over the signal range of -2.5V to -100 mV. A NIM module was developed for eight channel CFD discrimination.

Monolithic sensor with readout electronics (Anudrishti ASIC)

Anudrishti ASIC is an integrated photodiode and readout electronics ASIC designed in commercial 0.35 µm CMOS process [20,21], (Fig 19). The ASIC comprises three different structures of CMOS photodiode with peak responsivity at different wavelength region of visible light spectrum. The designed area of each of the photodiodes is 1 mm² each. The ASIC also contains two different kinds of signal processing channels. One is slow pulse processing channel and the second one is the fast counting channel. Brief specifications of the ASIC are as follows

Slow channel		Fast channel		Type of photodiode	Sensitivity
Channel Gain	30 mV/fC	Channel Gain	8 mV/ μ A	N-well/p-substrate	Green light
Peaking time	2 μ s	Rise time	<1 ns	P+/N-well/p-substrate	Whole visible range of light
Power	8 mW	Power	40 mW	P+/N+ lateral photo diode	Ultraviolet ray
Technology				0.35 μ m CMOS process	
Die area				11 mm ²	
Package				44 pin CLCC	
Total power				50 mW	

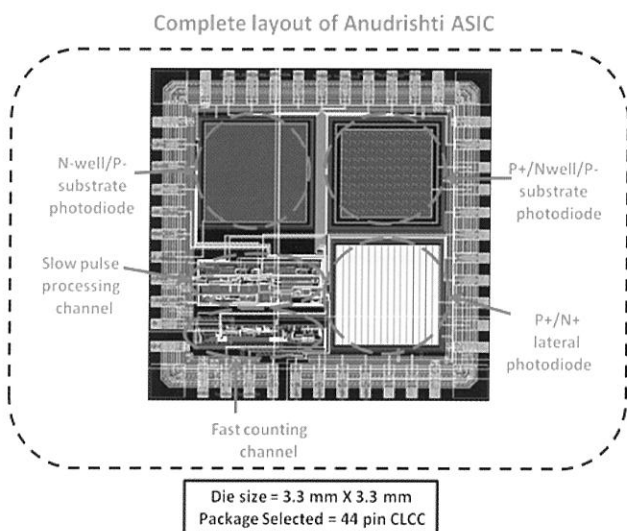


Fig. 19 Anudrishti ASIC layout

Development of Hybrid Microcircuits (HMCs)

The ASIC development was complimented with the development of thick film hybrid micro circuit (HMC) enabling system on chip solution that incorporated the ASIC die form and providing compact solution for portable instrumentation.

Detector Signal Processing Family HMC

Indian Neutrino Observatory (INO) required large number of fast (rise time ~1 nano second) amplifiers for prototype detector. A family of fast voltage amplifier HMCs containing four HMCs namely BMC 1595, BMC 1596, BMC 1597 and BMC 1598 was designed using HMC facilities of BEL ltd, Bangalore and supplied in quantity. These four HMCs exhibit rise time of < 2 ns, gain of 10, input/output impedance of 50 ohm, power consumption of 120mW and input dynamic range of 200mV with dual power supply of +/- 6V. They differ in the polarities of the input and output voltage signals.

Low power, low noise HMCs (BMC 1599 and BMC 1576) integrating charge amplifier and pulse shaper were developed for portable radiation monitoring instruments. A

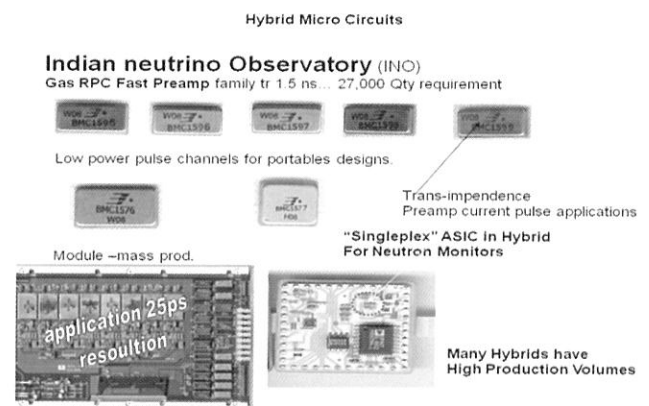


Fig. 20 Hybrid Microcircuits developed by BARC in collaboration with BEL, Bangalore

SOC solution for detector front end signal processing was further developed in BMC 1600 HMC (Fig 20) using Singleplex ASIC to get TTL output from charge input [13]. The HMC gives shaped pulse out of 3 μ s width and TTL output of 2 μ s width.

Signal Conversion HMCs

An HMC solution for time interval measurement better than 25 ps resolution was developed for high density Time to Digital Converter (TDC). Further, a peak stretcher was also developed for high resolution nuclear ADCs [13]. These HMCs are being used by large number of users across the country to build their own instrumentation in high-energy physics experiments [25,26].

Applications of ASIC and Critical Advanced Instruments

Neutron monitor using Singleplex ASIC

A prototype neutron REM monitor has been developed using Singleplex ASIC as the nuclear pulse processing channel. The REM monitor also has an HTTP interface via 10/100 Mbps Ethernet port for centralized logging and dose monitoring in the field.

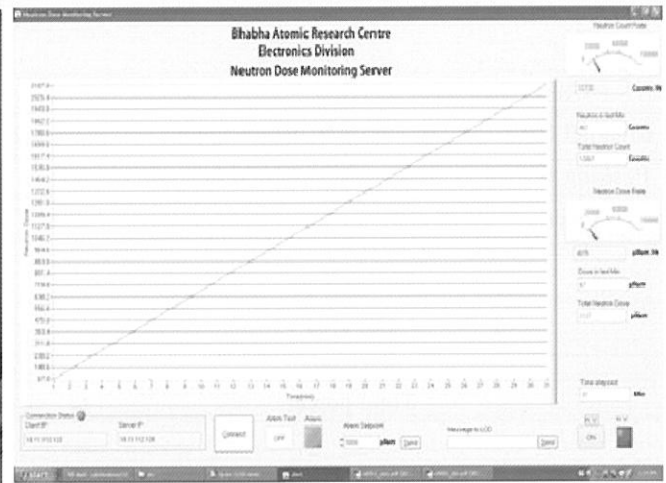
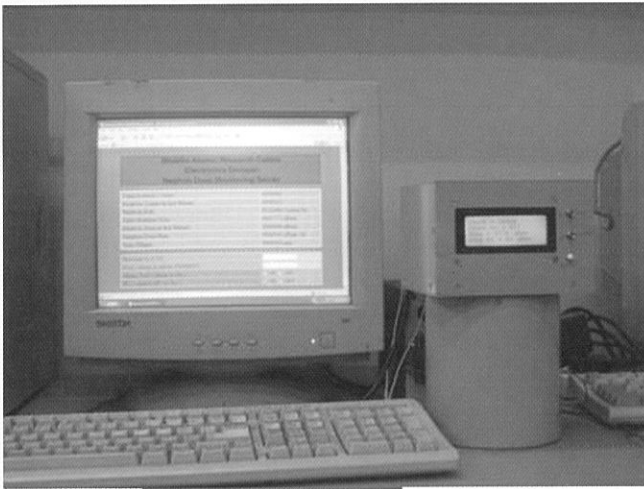


Fig. 21 (a) Neutron monitor using Singleplex ASIC (b) Graphical user interface for neutron monitor

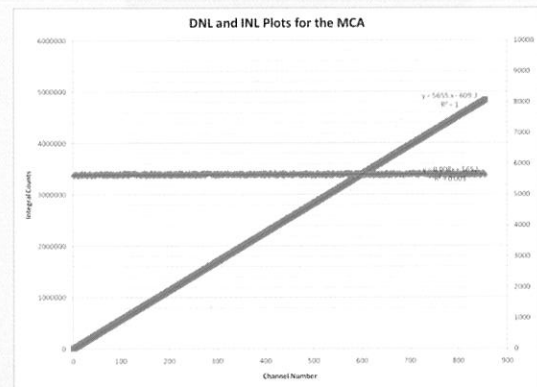
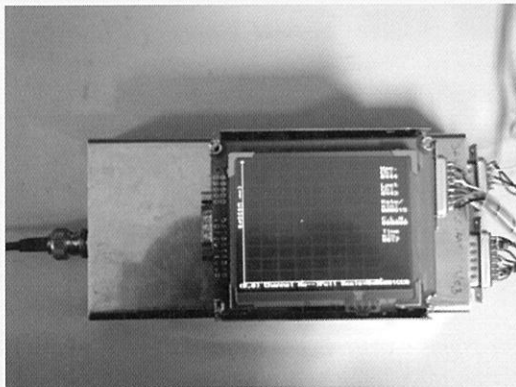


Fig. 22 Prototype handheld MCA using Singleplex and Anushikhar ASICs

Prototype handheld MCA using Anushikhar and Singleplex ASICs

A prototype 1K channel MCA has been developed using Singleplex and Anushikhar ASICs. This system is targeted for hand-held radio-nuclide identification applications.

The HMCs used to build Indian Neutrino Observatory prototype detector at TIFR.

A family of HMC solution was developed for the front end glass RPC for the prototype detector developed at TIFR [27].

Summary

A VLSI R&D facility “Centre for Microelectronics” for design, development, modeling and packaging of ASICs, HMCs, sensors and detectors, is built in Prabhadevi, Mumbai in collaboration with ECIL (Electronics Corporation of India ltd). The Centre is capable of highly complex design activities in IC design, Technology CAD, Embedded design, Semiconductor device characterization, Spice modeling, Packaging and Wafer level IC testing. It has state-of-the-art CAD tools on multi-node networked computing platforms, characterization and test-equipments housed in class 10k clean room.

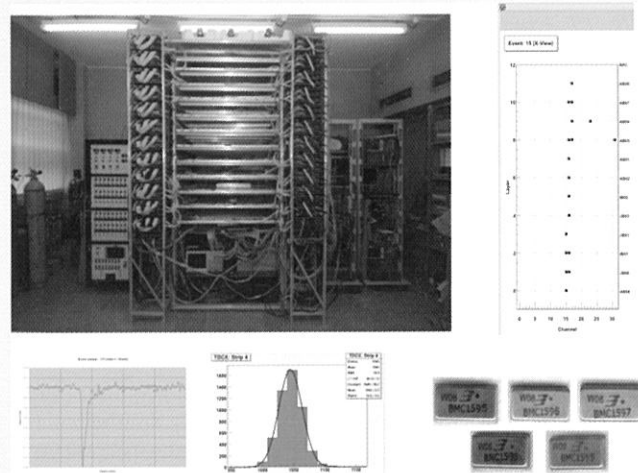


Fig. 23 (a) Prototype INO electronics rack at TIFR (b) HMCs used as readout frontend

References

1. “Fabrication of low noise silicon radiation detectors by the planar process”, J. Kemmer, Nucl. Instr. Meth, Vol. 169 (1980), pp-499.
2. “Studies on reducing leakage current and improving breakdown voltage of large-area silicon detectors: technology and results”, V. Mishra, V.B. Chandratre, M.Y. Dixit, V.D. Shrivastava, A. Topkar, S.K. Kataria, Y.P.

- Prabhakar Rao, N.P. Shankarnarayana, Nuclear Instruments and Methods in Physics Research Section A, Vol 527, Issue 3, (2004), pp 308.
3. "Role of guard rings in improving the performance of silicon detectors", Vijay Mishra, V D Srivastava and S.K. Kataria, Pramana Journal of Physics, Vol. 65, No. 2, (2005), pp. 259.
 4. "Semiconductor drift chamber — An application of a novel charge transport scheme", Emilio Gatti and Pavel Rehak, Nuclear Instruments and Methods in Physics Research, Volume 225, Issue 3, (1984), pp 608.
 5. "Theory of microplasma instability in silicon", R.J. McIntyre, Journal of Applied Physics Vol. 32, Issue 6, (1961), pp 983.
 6. "Silicon photomultiplier and its possible applications", P. Buzhan, B. Dolgoshein, L. Filatov, A. Ilyin, V. Kantzerov, V. Kaplin, A. Karakash, F. Kayumov, S. Klemin, E. Popova, S. Smirnov, Nuclear Instruments and Methods in Physics Research Section A, Volume 504, Issues 1-3, (2003), pp 48.
 7. "Comparison of a silicon photomultiplier to a traditional vacuum photomultiplier", V.D. Kovaltchouk, G.J. Lolos, Z. Papandreou, K. Wolbaum, Nuclear Instruments and Methods in Physics Research Section A, Vol 538, Issues 1-3, (2005), pp 408
 8. "Design and Development of Multi Pixel Photon Counter Having Enhanced Response for Blue and UV Light" V.B. Chandratre, V.D. Srivastava, Sudheer K. M., Y. P. Prabhakara Rao and Rejeena Rani Y., Centre for Microelectronics, ECIL, Mumbai DAE-BRNS National Symposium on Nuclear Instrumentation, (2010), pp- 284.
 9. "Design and Development of Avalanche Photo Diodes and Silicon Photo Multiplier" V.B. Chandratre, V.D. Srivastava, Sudheer K. M.1, Y. P. Prabhakara Rao2 and Rejeena Rani Centre for Microelectronics, ECIL, Mumbai DAE-BRNS National Symposium on Nuclear Instrumentation, (2010), pp- 290.
 10. "Design and Fabrication of a Monolithic Constant Fraction Discriminator" V.D. Srivastava, P.K. Mukhopadhyay, S.K. Kataria, Y.P. Prabhakara Rao, Rejeena Rani and S. Kal, International Microelectronics & Packaging Society (IMAPS) Indian National Conference (IINC) on Microelectronics & VLSI IEEE Components, Packaging and Manufacturing Technology (CPMT) India Council Chapter, IIT Bombay, Mumbai-400076, DEC 19, 2005.
 11. "Silicon Strip Detector Development under India CMS collaboration", S K Kataria, M D Ghodgaonkar, M Y Dixit, V B Chandratre, Proceedings of the Intelligent Nuclear Instrumentation symposium INIT-2001, pp 153.
 12. "Design & development of low noise Octal CMOS Charge Amplifier", V B Chandratre, S V Sardesai and S K Kataria, Proceedings of the National Symposium on Nuclear Instrumentation, NSNI 2004, pp 261.
 13. "ASIC & HMC designs for portable nuclear instruments", V B Chandratre, invited talk in Compact Nuclear Instruments and Radiation Detectors symposium, CNIRD – 2005.
 14. "Single Channel Analog Pulse Processor ASIC for Gas Proportional Counters and Si Detector", V. B. Chandratre, Soumen Sarkar, S. K. Kataria & Y. P. Viyogi, Proceedings of the Compact Nuclear Instruments and Radiation Detectors symposium, CNIRD – 2005.
 15. "Prospects for charge sensitive amplifiers in scaled CMOS", Paul O'Connor, Gianluigi De Geronimo, Nuclear Instruments and Methods in physics Research Section A, Vol. 480 (2002), pp 713.
 16. "A low-power, low-noise front-end for multianode silicon drift detectors", L. Caponetto, D. Lo Prestib, N. Randazzo, G.V. Russob, E. Leonorab, L. Lo Nigroa, C. Pettab, S. Reitoa, V. Sipalaba Sezione, Nuclear Instruments and Methods in Physics Research Section A, Vol. 552, (2005), pp 489.
 17. "CMOS preamplifier for low-capacitance detectors", G. Gramegna A, P. O'Connor B, P. Rehak B, S. Hart C, Nuclear Instruments and Methods in Physics Research Section A, Vol. 390, (1997), pp 241.
 18. "A packaged low-noise high-speed regulated cascode transimpedance amplifier using 0.6um N-well CMOS technology", S. M. Park and C. Toumazou, Proc. European Solid-State Circuit Conference, Stockholm, Sweden, (2000), pp 432.
 19. "A Power-Efficient LVDS Driver Circuit in 0.18um CMOS Technology", A. Tajalli, Y. Leblebici, IEEE 3rd Conf. on Ph.D. Research in Microelectronics and Electronics (PRIME), Bordeaux, (2007).
 20. "GASIPLEX, A low noise analog signal processor for readout of gaseous detectors", W. Beusch, S. Buytaert, J C Santiard, CERN-ECP/94-17.
 21. "Which Photodiode to Use: A Comparison of CMOS-Compatible Structures", Kartikeya Murari, Ralph Etienne-Cummings, IEEE Sensors journal, Vol. 9, Issue. 7, July 2009.
 22. "A low-power, CMOS peak detect and hold circuit for nuclear pulse spectroscopy", Ericson M.N., Simpson M. L., Britton C.L., Allen M.D., Kroeger R.A., Inderhees S.E., IEEE transactions on Nuclear Science, Vol. 42 (1), No.4, Aug 1995, pp.724.
 23. "Design of CMOS Wilkinson ADC", V.B. Chandratre, Asif Iqbal, Menka Tewani and S.K. Kataria, Proceedings of the Compact Nuclear Instruments and Radiation Detectors symposium, CNIRD – 2005.
 24. "A 700-MHz switched capacitor analog waveform sampling circuit", Haller, G.M., Wooley, B.A, Nuclear Instruments and Methods in Physics Research Section, A458 (2001), pp 729.
 25. Technical Report on Quad Timing Filter Amplifier Module, S.Venkataramanan, Arti Gupta, S.Muralithar, IUAC/TR/SV/2007-2008/01.
 26. "Technical Report on Time To Analogue Converter for Neutron Array at IUAC", S.Venkataramanan, Arti Gupta, K.S.Golda, IUAC/TR/SV/2006-2007.
 27. "INO prototype detector and data acquisition system" Anita Behere, M.S. Bhatia, V.B. Chandratre, V.M. Datar, P.K. Mukhopadhyay, Satyajit Jena, Y.P. Viyogi, Sudeb Bhattacharyad, Satyajit Sahad, Sarika Bhide, S.D. Kalmanie, N.K. Mondale, P. Nagaraje, B.K. Nageshe, Shobha K. Rao, L.V. Reddy, M. Saraf, B. Satyanarayan, R.R. Shinde, S.S. Upadhyaya, P. Verma, Saikat Biswas, Subhasish Chattopadhyay and P.R. Sarma Nuclear Instruments and Methods in Physics Research Section A, Vol 602, Issue 3, (2009), pp784



Mr. V.B. Chandratre did his M.Sc (Physics) from University of Poona 1988, joined the 31st batch of BARC training school. His areas of expertise are Nuclear Instrumentation, Hybrid Microcircuits and ASICs. His fields of interest include nuclear pulse processing, data conversion, analysis, design of CMOS integrated circuits and TCAD. Currently he is involved in the development of ASICs and HMC design. He has made significant contributions to various DAE/ E&I programs and is recipient of DAE's technical excellence award in 2005.

Imaging Techniques using X-rays, Gamma and Neutron

Amar Sinha, Yogesh Kashyap, P.S. Sarkar, Tushar Roy

Neutron and X-ray Physics Facilities, Bhabha Atomic Research Centre, Trombay, Mumbai 400 085,
E-mail: imasge@basrc.gov.in

Abstract

Since the discovery of X-rays, they have been used extensively for imaging of internal structure solely based on their inhomogeneous attenuation properties. However, this approach ignores the wave aspect of X-rays i.e. like visible light they can also undergo scattering, phase shift etc. as they travel through matter. The wave-matter interaction and its understanding have opened a completely new field in the area of X-ray imaging. This paper presents development of new imaging techniques based on conventional absorption mechanism and recently developed phase contrast mechanism and their applications using X-rays, gamma and neutrons. We report our work on Phase-contrast X-ray Imaging, X-ray Microtomography, Digital Medical Imaging System (DMIS) and Single Photon Emission Computed Tomography for nuclear applications.

Introduction

It has been a dream of scientists to understand the behaviour of materials based on their microscopic and macroscopic properties and visualize the underlying processes. Today a host of methods exist to achieve this objective. Among these, X-rays, gammas and neutrons have the ability to penetrate bulk of the material and have been used to visualize and characterize materials. Most of these techniques do not exploit the coherence properties of the sources. Over the years, there have been new developments in sources of these radiations and in particular, synchrotrons can provide highly coherent X-rays like lasers. The coherence properties of the radiations have resulted in new approaches to imaging which are based on the coherent scattering of radiation from the materials. Thus, with this new approach, new imaging techniques like coherent X-ray diffraction, X-ray holography, non-interferometric neutron phase imaging etc have become feasible.

New techniques have also emerged due to development in detection technology as well as faster computing techniques. We describe some of these new developments in imaging using these radiations. In particular, we shall describe phase contrast imaging technique which has overcome the imaging limitations of conventional absorption-based imaging technique, microtomography for imaging on micron scale, advancement in digital medical imaging and single photon emission computed tomography, as applied to position-sensitive imaging of gamma-emitting nuclides for nuclear applications.

Phase Contrast Imaging

A paradigm shift in X-ray Imaging have taken place with advent of new X-ray sources such as synchrotron source or microfocus or nano-focus sources etc. The conventional approach of X-ray imaging relies on X-ray absorption as the sole source of contrast and draws exclusively on ray or geometrical optics to describe and interpret image formation. The contrast in conventional absorption-based X-ray imaging techniques depends upon the object thickness and its atomic number. Hence the contrast of the absorption-based X-ray images decreases when either atomic number of the object or object thickness decreases. The conventional absorption

X-ray imaging is able to distinguish between hard (high Z) and soft (low Z) materials but it fails to image soft materials like polymers, carbon-composites and soft tissues, as the absorption is very less for such materials. This approach ignores another, potentially more useful source of contrast, the phase information. Phase-sensitive techniques, which can be understood using wave optics rather than ray optics, offer ways to augment or complement standard absorption contrast by incorporating phase information. In the last few years, this new imaging technique named Phase Contrast Imaging [1] is being developed to remove the limitations of conventional X-ray imaging. This has happened due to advent of coherent source of X-ray which is a primary requisite for formation of image using phase information of X-ray as explained below. The development of this new technique was well appreciated particularly in medical and biological studies. In medical field, conventional absorption contrast works well on bones and teeth having high Z elements like calcium, however, in many clinical applications, such as mammography, where there is a need to be able to distinguish between different kinds of soft tissues, for example between a tumor and healthy tissues, conventional absorption-based technique fails, as there is very little absorption from these soft tissues.

Mechanism of phase-sensitive imaging

The behavior of X-rays as they travel through a sample can be described using a complex index of refraction, just as in conventional optics. In the X-ray region, the index of refraction, n , deviates only slightly from unity and it can be written as $n = 1 - \delta - i\beta$, where β describes the absorption of X-rays and the phase-shift term δ incorporates refractive effects. At typical X-ray energies of interest for soft material studies 15-40 keV, the phase-shift term can be up to 1000 times greater than the absorption term. Thus, it may be possible to observe phase contrast when absorption contrast is undetectable. Another factor which favours phase contrast over absorption-based imaging is the fact that phase term falls off less quickly; $\delta \propto E^{-2}$ whereas $\beta \propto E^{-4}$. The refractive decrement (δ) and (β) both depend on frequency or photon energy. These two quantities can be expressed as:

$$\delta = [r_e h^2 c^2 / 2\pi E^2] N_0 f_R \quad (1)$$

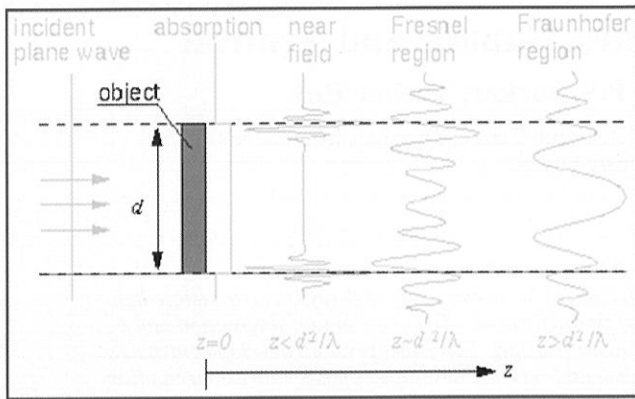


Fig. 1 Classifications of different regimes as a function of distance from the object.

$$\beta = [hc / 4\pi E] \mu(E) \quad (2)$$

in which, N_0 is the number of atoms per unit volume, r_e is the classical electron radius, λ is the wavelength of X-rays, $f_R \propto Z$ is the real part of atomic scattering factor and $\mu \propto Z^n/E^3$ (where n lies between 4 and 5) linear attenuation coefficient. In phase imaging technique, one can record the variation of the phase of the passing X-ray beams rather than amplitudes in order to enhance the obtained image. There are several ways of obtaining images out of these phase information. In one such method called phase contrast imaging, the X-rays transmitted through the object at various angles will propagate over the distance between the object and the detector. For the situation of the detector being located directly behind the sample, a conventional absorption image is obtained, while at greater distances from the object, a phase-contrast image will be formed due to interference between waves coming out after phase shift from the object and those propagated directly. This is explained in Fig. 1. The radiation sources that can be used must have spatial coherence as well as temporal coherence, though temporal coherence is not a stringent requirement. Thus, synchrotron sources, where both spatial and temporal coherence is obtainable, are ideal choice for conducting phase imaging. However, as stated, condition of spatial coherence is more important than temporal coherence for phase imaging. For this reason, X-ray sources with a very small focal spot of the size of a few micron (microfocus) or nano focus sources can also be used for obtaining phase images, though due to their polychromatic nature of X-ray, the quality of images will not be as good as those due to synchrotron. Figure 2 shows intensity profile due to step change in object density for the case of conventional absorption-based image and phase contrast image.

Work at BARC on Phase contrast imaging

Experimental setup

A facility was set-up using a combination of 160 kV (max) 1 mA X-ray microfocus source and a high resolution CCD camera for carrying out phase-contrast X-ray imaging experiments. Fig. 3 shows photograph of the experimental

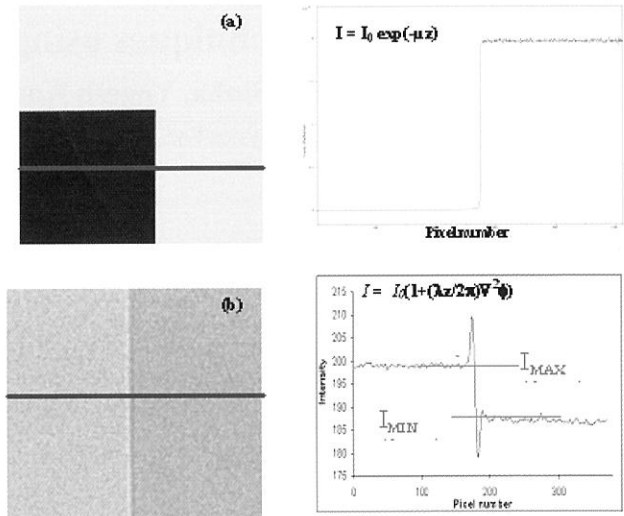


Fig. 2 Radiograph and Intensity profile of a step change in density (a) Absorption radiograph (b) Phase contrast radiograph (Note that the step position in (b) is different from that in (a) i.e. its mirror image)

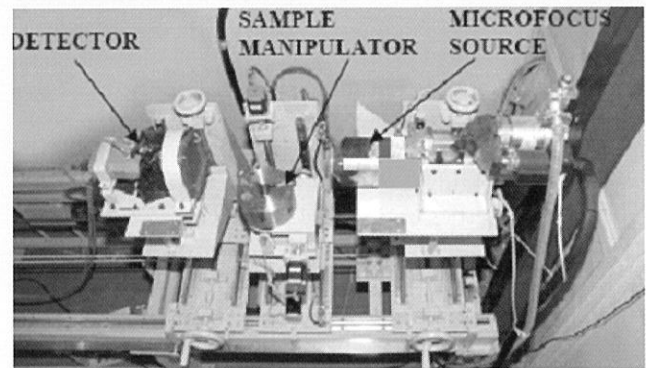


Fig. 3 Experimental setup at BARC for phase contrast using microfocus source

set-up. The detector consists of a cooled CCD (1024 X 1024) coupled to $Gd_2O_3:S:Tb$ phosphor layer deposited on an entrance window of 4:1 glass fibre-optic taper. The pixel pitch of the CCD is $13.5\mu m \times 13.5\mu m$. The microfocus X-ray source with focal spot as small as $5\mu m$ ensures that the system has high degree of spatial coherence so that the edge enhancements can be made to manifest.

Experimental Results using Microfocus Source

Phase Imaging of Material Science Samples

TRISO Particles

We have carried out a set of experiments on carbon coated zirconia microspheres to study the feasibility of this imaging system for phase imaging of coated materials. These kind of coated materials (also called as TRISO particles) are potential candidates for future generation of high temperature nuclear reactors. The fuel particles consist of fuel kernel (here zirconia is used as a dummy kernel) surrounded by four coatings (Fig. 4): from inside to outside a porous pyrolytic carbon coating, a high density carbon

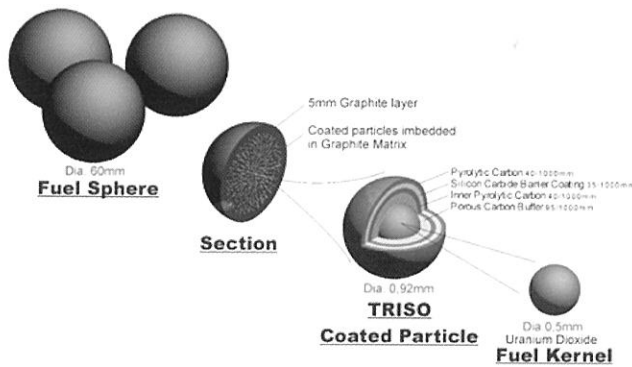


Fig. 4 Illustration of a typical High temperature reactor TRISO particles

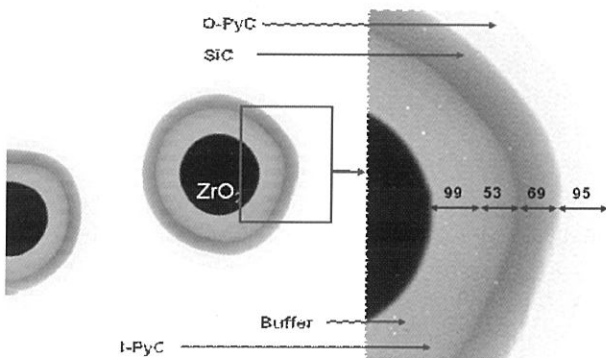


Fig. 5 Zirconia microsphere coated with 4 layers of different materials. A magnified view is shown on the right (All units are in μm)

coating, a silicon carbide coating and an outer pyrolytic high density carbon coating. Development of these particles having different layers with controlled thickness is in itself an engineering challenge. Moreover once these fuel particles are fabricated, parameters such as coating thickness and its uniformity need calibration by suitable method. This is an important step towards the optimization of various parameters in the fabrication of these particles.

Zirconia microspheres of approximately 500 μm diameter [2,3] were deposited with different materials in an electrically heated graphite vessel under different conditions so as to make an equivalent fuel particle. In fact, we are the first group internationally to apply phase imaging for such simulated TRISO samples. Fig.5 shows zirconia microspheres coated with 4 layers – (starting from the innermost layer) low-dense pyrocarbon, high-dense pyrocarbon, SiC and high-dense pyrocarbon – which have average coating thickness of 99 μm , 53 μm , 69 μm and 95 μm respectively. The image was acquired at 30 keV energy, 250 μA current with an exposure time of 360 sec and a magnification of 12X. Hence, it can be inferred that X-ray based phase contrast technique offers attractive possibilities for non-destructive characterization of these advanced reactor fuel particles.

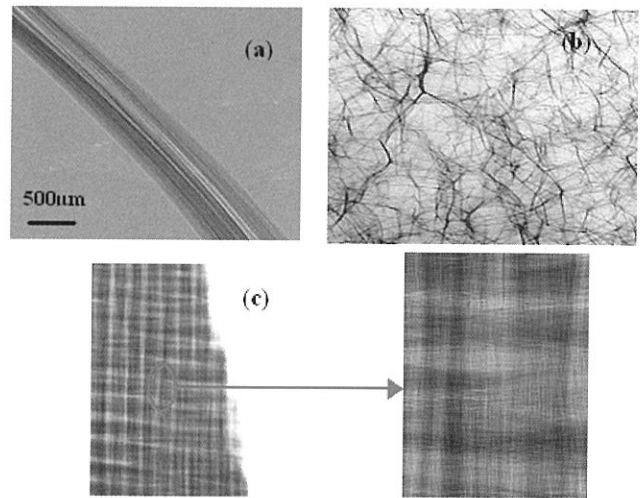


Fig. 6 Phase Radiographs of (a) Carbon fibre with multiple layers (b) Foam used in packaging industry (c) Carbon composite fibre used in aircraft industry; a magnified part is shown on the right

Phase Imaging of Carbon Composites, Carbon Fibre, Foam etc.

The phase contrast technique is suitable for visualizing the internal details of carbon based materials like carbon fibre [4], carbon composites, foam, etc. Fig.6 shows the phase contrast images of multilayered carbon fibre, foam used in packaging industry and carbon composite. The phase images of carbon fibre have been collected at energy $E = 30$ keV, current $I = 250$ μA and time $t = 120$ sec. The strength and stiffness of the fiber may change due the presence of micro-defects or porosity in the bulk of the material. This technique when used in combination with tomography technique can give detailed information about the distribution of the micro-defects or porosity. Thus, this technique can be a valuable tool in characterization of these composite fibers. The carbon composite fiber material (Fig.6(c)) which is used in design of wings & braking system of the aircrafts was also imaged. The image has been recorded at $E = 30$ keV, current $I = 250$ μA and time $t = 120$ sec. For the phase contrast image of foam, the parameters are energy $E = 30$ keV, current $I = 250$ μA and time $t = 180$ sec.

Phase Imaging of Biological Samples

We have used phase contrast technique for imaging some biological samples such as honey bee, mosquito, cockroach etc (see Fig.7 & Fig.8). Fig.7. shows the conventional radiograph as compared to the phase radiograph of a honey bee. The image was acquired at 30 keV energy, 200 μA current with an exposure time of 120 sec and a magnification of 4.4X. It can be seen that the weakly absorbing anatomic features of the bee is observed in much detail in the phase image than that obtained from radiography experiment.

Figure 8(a) shows the X-ray phase contrast image of the top portion of a cockroach [5]. The image was acquired at

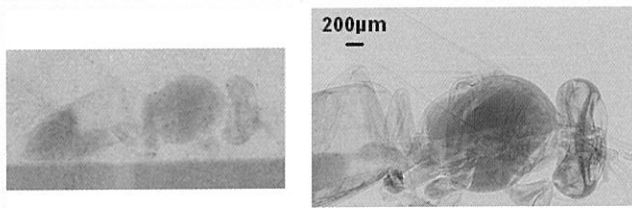


Fig. 7 Image of a honey bee (a) Absorption Radiograph (b) Phase Radiograph

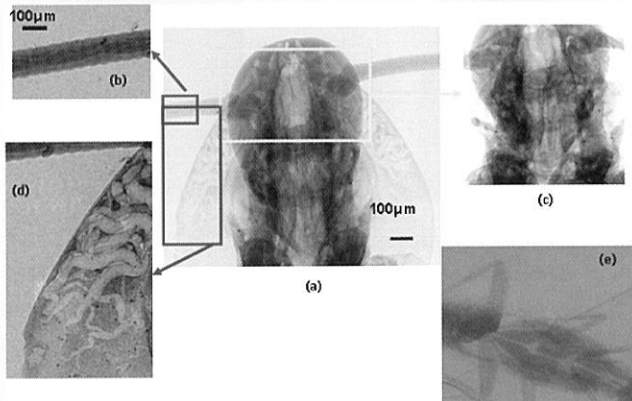


Fig. 8 (a) Phase radiograph of a cockroach. Magnified parts showing (b) antenna (c) head (d) wings (e) Absorption radiograph of cockroach

30 keV energy, 200 μ A current with an exposure time of 120 sec and a magnification of 11X. Figure 8(b-d) shows the magnified images of the antenna, head and wing of the cockroach. The detailed structures inside the antenna and the wings are clearly visible due to edge-enhancement effects. In contrast, the absorption image shown in Fig. 9(e) does not reveal any internal details. Hence this technique can be suitably modified to suit the clinical application, such as mammography, for improving the feature sensitivity in the conventional X-ray imaging process.

Experiments on Phase Contrast Using Synchrotron Source

The experiment was carried out at the SYRMEP beamline at the ELETTRA synchrotron radiation facility in Trieste, Italy. ELETTRA, a third generation synchrotron facility, can run at 2.0 or 2.4 GeV with a maximum ring current of 320 or 140 mA, respectively, which can deliver X-rays ranging from the soft X-ray region to the hard X-ray region. The radiation source results from a bending magnet of the storage ring. A monolithic channel-cut Si (111) crystal is used to narrow the energy bandwidth of the incoming white beam. A monochromatic beam, with energy tunable within the range 8–35 keV and an energy resolution of about 0.2%, is thus available in the experimental area. The beamline is characterized by a large source-to-sample distance of 22 m and the object-to-detector distance can be varied up to 1.87 m. A CCD detector and fibre-optic combination having an effective pixel pitch of 4.5 μ m was used for collecting high-resolution images.

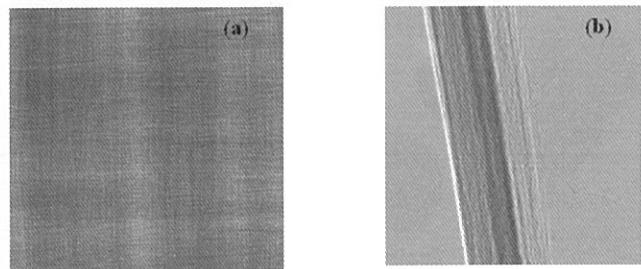


Fig. 9 Phase Images of (a) Carbon composite (b) Carbon fibre

Figure 9 shows phase images of carbon composite and carbon fibre, recorded using synchrotron source. The observed contrast enhancement in the images due to the phase effect is clearly visible in these images. Both the images were recorded at energy of 17.5 keV with an exposure time of 2.3 sec and object-to-detector distance of 50 cm.

We have also compared some of the images [6] acquired at synchrotron source with those acquired with our laboratory-based microfocus source in terms of contrast and signal-to-noise ratio. As synchrotron sources provide X-rays with high flux and a high coherence, it results in improved signal-to-noise ratio and better edge enhancement. Moreover, monochromatic nature of X-rays helps in avoiding beam hardening effect hence it is advantageous to do phase contrast studies at synchrotron sources. Figure 10(a) and 11(b) shows phase contrast images of PyC-coated alumina microspheres acquired using microfocus X-ray source and Synchrotron X-ray source and from these images the image contrast was calculated. The contrast with microfocus source at alumina-to-PyC & PyC-to-air interfaces are 0.0689 & 0.0577 respectively and with synchrotron source the contrast are 0.2066 & 0.1732 respectively. A comparison of the edge enhancement effect on pyrocarbon coated alumina microspheres shows that there is remarkable increase in edge contrast with synchrotron X-ray source as compared to the Laboratory-based source.

We are also building a phase contrast imaging beamline at INDUS-II synchrotron at RRCAT, Indore. It is proposed to develop it as a national facility for microimaging having provision to conduct experiments with phase contrast and diffraction enhanced technique and microtomography, with both monochromatic and white beam.

Neutron based Phase Imaging and experimental setup at CIRUS

Most coherent scattering techniques at present are being implemented using X-rays due to the availability of high flux coherent radiations sources such as Synchrotron. As neutrons can provide complementary information about the object to that of X-rays, there is great potential to these techniques of phase imaging, if these can be implemented using neutrons. The relative transparency of many high Z

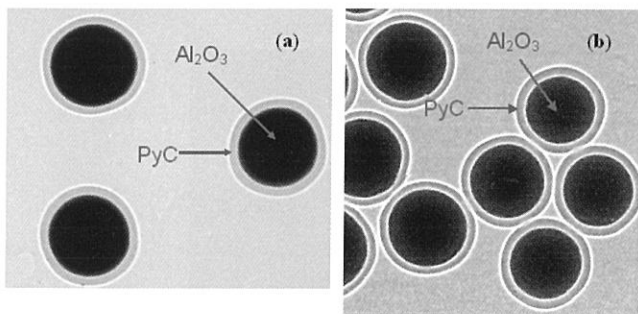


Fig. 10 Comparison of phase images of pyrocarbon-coated alumina microspheres recorded using (a) Microfocus source ($E = 30 \text{ keV}$, $I = 250 \mu\text{A}$, $t = 120 \text{ sec}$, Magnification $M = 10$) (b) Synchrotron source ($E = 17.5 \text{ keV}$, $t = 1.6 \text{ sec}$, $z_{OD} = 50 \text{ cm}$)

elements to the neutrons essentially allow us to obtain an inside look into bulk of objects which are opaque to X-ray and to make 3D reconstructions of their internal structure. Similarly, materials like Pb, Be, C, Al, Si are more easily probed using neutrons than X-rays. Moreover, the phase sensitive measurements in combination with neutron imaging can also provide 3D spatially resolved information on the scattering length density distribution.

For neutrons the refractive index is described by

$$n = 1 - \frac{\lambda^2 n}{2\pi} \sqrt{b_c^2 - \left(\frac{\sigma_r}{2\lambda}\right)^2} + i \frac{\sigma_r N \lambda}{4\pi} \quad (3)$$

Here, σ_r is the sum of absorption and incoherent scattering cross-section, b_c is coherent scattering length.

The shift in phase ϕ of coherent field after passing through a given medium is given by

$$\phi = -\frac{2\pi}{\lambda} \int_s \frac{\lambda^2}{2\pi} b_c \rho ds \quad (4)$$

For a large class of materials phase shift dominates over the absorption (see Table 1). Moreover some of these materials can be studied only using neutrons, as X-rays can not penetrate through them. This is particularly true of nuclear materials, as they are mostly made up of high atomic number. Hence neutron phase contrast imaging technique provides a valuable tool for the investigation of these materials. Alternatively, one can also use this technique to retrieve the coherent scattering length density of a material.

We have simulated phase-contrast imaging conditions for sphere of Fe embedded in a matrix of Th. We have used Fresnel-Kirchhoff integral formula of parallel wave for simulation, to calculate the amplitude of the wave function. The absorption and phase contrast images are displayed in Fig 11. The phase contrast image clearly brings out the structural details which is not possible using conventional neutron radiography mode.

In order to test these effects and use it for nuclear applications, we have setup at CIRUS a neutron imaging beamline which will have a provision for phase contrast

TABLE 1. Comparison of neutron (thermal) phase shift and attenuation values

Materials	Phase shift (cm^{-1})	Attenuation (cm^{-1})
Be	1.79×10^3	1.3×10^{-3}
C	1.4×10^3	4.1×10^{-4}
Si	3.8×10^2	8.0×10^{-3}
Al	3.8×10^2	1.4×10^{-2}
Zr	5.7×10^2	8.2×10^{-3}
Fe	1.5×10^3	0.25
Pb	5.8×10^2	6.0×10^{-3}
Th	5.8×10^2	0.2

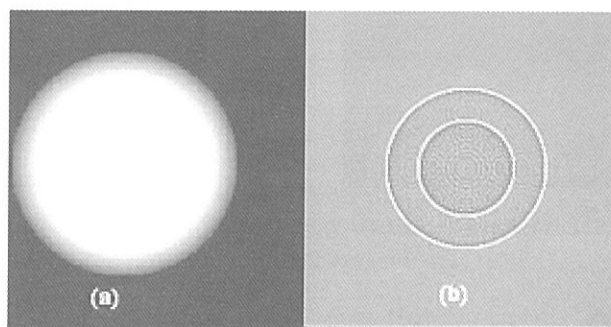


Fig. 11 (a) absorption & (b) Phase image of phantom consisting of Fe & Th spheres

imaging using neutrons. This will be achieved by using a special pin hole type collimator. At present the testing of beamline is in progress.

Microtomography set-up at BARC

Microtomography [7, 8], like tomography, uses X-rays to create cross-sections of a 3D-object that is used to reconstruct a virtual model without destroying the original model. The term micro is used to indicate that the resolution of the reconstructed 3D volume is in micron range. The experimental facility used for microtomography was same as the one used for phase imaging, that is, a combination of 160 kV (max) 1 mA (max) X-ray microfocus source with a $5 \mu\text{m}$ focal spot and a high resolution CCD camera.

Experimental Results

A lot of samples of interest to material science and medical science were investigated using this X-ray microtomography facility. These include raw diamonds, Aluminum foam, carbon-carbon reinforced composites, coated CC composites, carbon-coated graphite samples etc. Some of them are discussed here.

Rough Diamonds

Three dimensional internal details regarding optically opaque rough (uncut and unpolished) diamonds are of immense help to locate defects, inclusions, impurities etc and minimize the loss while cutting and maximizing the diamond output. A prior knowledge about cracks, deformities,

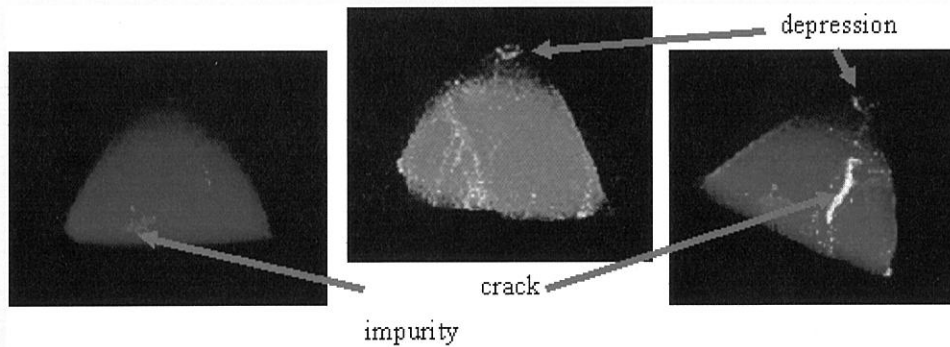


Fig. 12 3D images of rough diamonds showing depression, impurity and crack

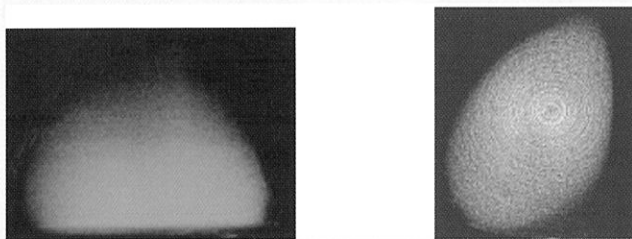


Fig. 13 3D reconstructed image of a defect-free rough diamond in different orientations

inclusions inside the rough diamond, their position and size helps in finding out the maximum size and numbers of good quality defect-free diamond while cutting. Three dimensional microtomography studies can be used to characterize rough diamond. We have carried out initial 3D X-ray μ CT experiments on a number of optically opaque rough diamonds. The tube parameters were 50 kV and 400 A with acquisition time for each projection varying from 45 seconds to 60 seconds. Fig. 12 shows a 3D reconstructed image of a rough diamond with a notch at the top marked as “depression”. Contrast stretching and pseudo-coloring of the 3D image clearly shows the defects (inclusions) (marked as “impurity”) and a large crack (marked as “Crack”) as depicted in the figure. A defect-free rough diamond

tomograph with two different views is also shown in fig.13 to highlight the difference.

Aluminum Foam

Aluminum foam (AIF) is made up of porous aluminum material with a cellular structure having isotropic distribution. This material exhibits extraordinary mechanical as well as physical properties at a very low density. Some of the important features of this material are high stiffness though very less weight, good absorber of impact and hence shockproof, completely recyclable etc. The importance of AIF thus demands a high degree of quality assurance while preparing them. They can be formed using either pre-aluminum or in alloy form. They are manufactured through sintering technique, electroless process or pyrolysis method in closed cell or open cell structure. The closed cell foam looks more like the kitchen sponge. To have the internal details of an Al Foam in its three dimensional perspective, we have performed X-ray μ CT studies. Fig. 14 shows the 3D reconstructed image of Al Foam. The closed cell structure is clearly visible. The cell to cell interconnections are seen to coalesce and reappear as we go from one plane to the other.

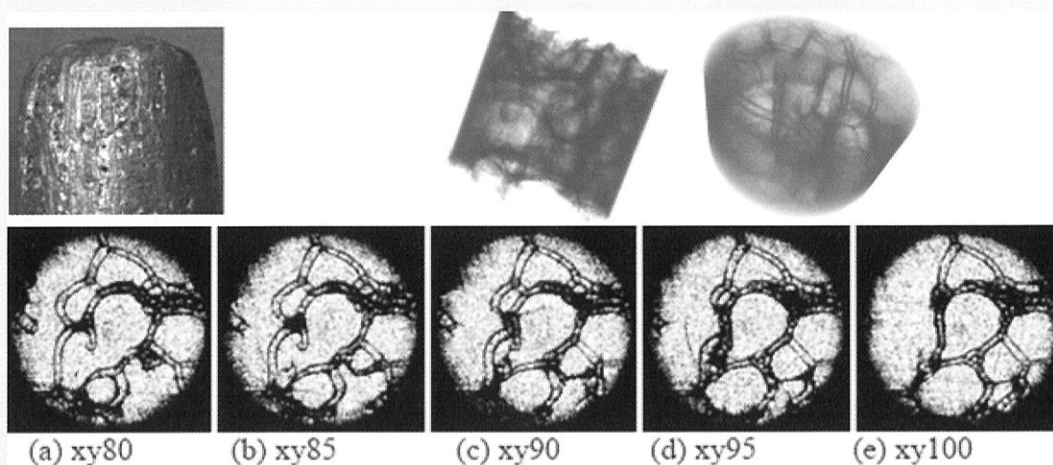


Fig. 14 (clockwise from top) Optical Photograph, Reconstructed 3D volumes and 2D slices of aluminum foam (experimentation performed at 40 kV and 400 μ A with each exposure of 40 seconds)

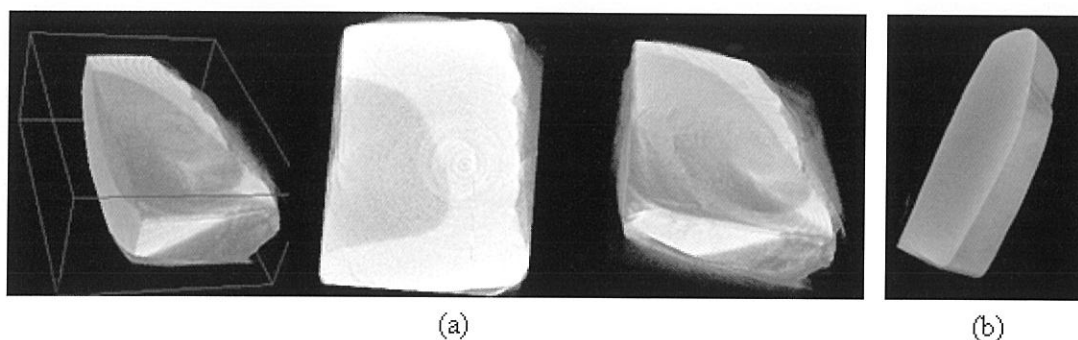


Fig. 15 Reconstructed images of (a) De-mineralized samples (b) Re-mineralized sample

Mineralization of Human Dental Samples

Mineralization of human dental samples was investigated in in-vitro conditions using 3D microtomography technique. These samples were provided by a dental college at Mangalore. Samples were prepared by treating enamel samples using demineralizing and remineralizing solutions prepared using phosphates, fluorides to simulate the factors affecting enamels in humans. These samples were subjected to microtomography to understand the effect of the solutions and its effect on the enamels. Figure 15(a) shows 3D reconstructed images of one of the demineralised sample (the darker shade is the demineralised portion) and Fig. 15(b) that of a remineralized sample (uniform shade suggesting proper mineralization). These studies helped us in standardizing the solutions and understanding their effect on enamels.

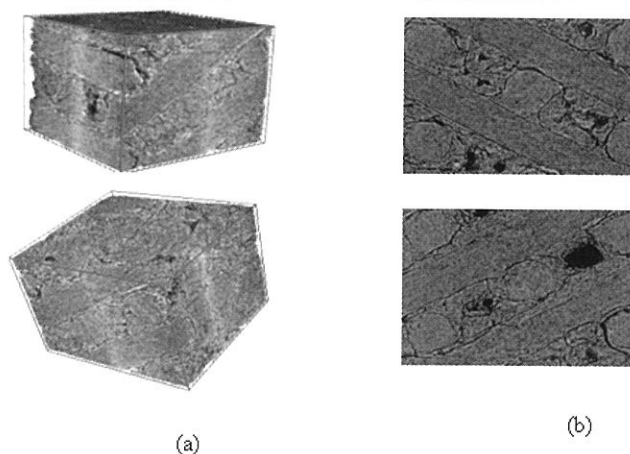


Fig. 16 (a) Reconstructed 3D volume (b) Reconstructed slices

Carbon-carbon Reinforced Fibre

Carbon-carbon fibre reinforced composites are of great interest to material scientists due to their special properties such as retaining their mechanical properties at higher temperatures, high specific strength, excellent resistance to abrasion and thermal shock etc. These find huge application in different sectors such as aviation, industry, nuclear etc. A number of CC composite samples of interest to materials used in reactor technology have been investigated. Fig. 16 shows the reconstructed 3D image and cross-sectional image of a 4D CC composite sample. The internal details provide information related to the fibre orientations, presence of defects, voids, cracks etc and also helps in standardizing the manufacturing process parameters.

Brachytherapy Catheter

Brachytherapy equipment is used extensively all over the world for the intracavitary/ interstitial radiation therapy of cancer. Bhabha Atomic Research Centre (BARC), Mumbai with help of Raja Ramanna Centre for Advanced Technology (RRCAT), Indore is developing indigenous HDR source-assembly for Board of Radiation and Isotope Technology (BRIT), Mumbai. A typical HDR source-assembly, which has four miniature stainless steel micro-machined components viz.; machine end terminal, rope joining sleeve, source retaining capsule and cover and two stainless steel wire ropes. The welding between wire

rope and the miniature components plays an important role in the overall assembly strength and rigidity. The laser welding spots are very fine and have to be perfect, devoid of any imperfections such as micro crack, air-bubble void etc. Generally, the welding point is characterized by load testing mechanism which is a destructive process. Non-destructive process like the 3D X-ray micro-tomography has provided useful insight into its three dimensional spatial distribution without destroying it. Figure 17 shows a typical wire to metal microweld photograph on the left, and reconstructed slice images at the bottom.

Development of Indigenous Digital Medical Imaging at BARC

Medical imaging is an advancing and growing industry and it has evolved rapidly in last one decade. Several such systems have evolved during this period using technologies from CCD, imaging plate to flat panel. However the fruits of digital imaging technology have been very limited in developing countries primarily because such systems are being marketed at huge cost which is beyond the reach of most of the hospitals with the exception of a few large ones. Moreover, to implement such a technology on large scale in large country like India, it requires customization of such systems to suit to the local conditions which vary widely between different regions of the country. Also, it is required that such systems have either low maintenance or have local

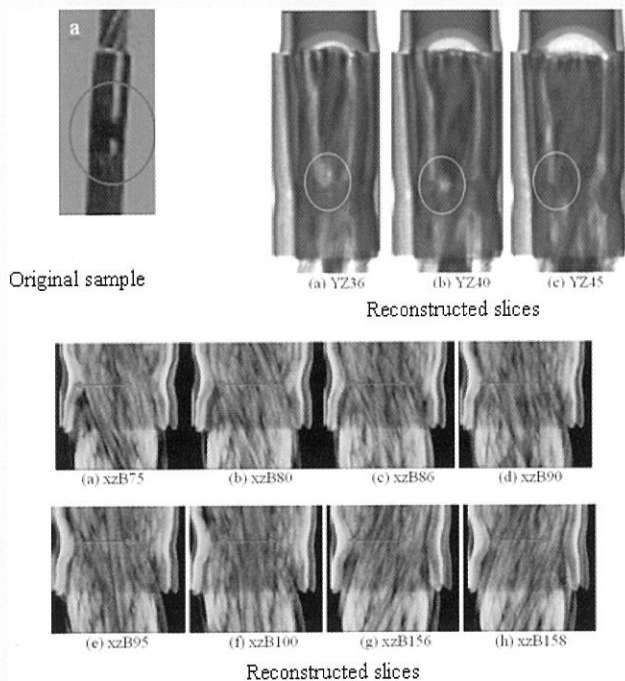


Fig. 17 Brachytherapy catheter

solutions to maintenance problem. It is thus imperative that technologies for low-cost digital medical imaging system be developed within the country which can take care of both large and small hospitals, urban and rural population etc. This requires careful selection of technology and its components so that it is reliable, affordable and easily available. Digital medical imaging is not only about assembling hardware component but software plays an important role to all these developments. Since such instruments have to be operated by technicians, care has to be taken to make the system as much user friendly as possible. It has to be packaged with data base management procedure for easy archival of images, proper tagging of images, coupling with hospital database management system, networking, teleradiology, advanced image processing software etc. Keeping this in mind, few years ago (2002-2003), a program was initiated on development of digital medical imaging system (DMIS) within the country. Such a system was developed which was designed to be a multipurpose digital medical imaging system using both indigenous and imported components, incorporating several advanced features and in-house developed software for control, graphic user interface, image management, networking, database management and integration with hospital information system. We used a state of art digital CCD and high dynamic range intensifier along with locally available X-ray generator which was made computer-controlled to suit the needs of digital system, in-house developed control system, advanced software. This system was tested with international quality anthropomorphic phantoms and scientific phantoms to assess its imaging characteristics. The system was designed to serve as multipurpose unit combining digital fluoroscopy, radiography and digital subtraction angiography. It had an offline study mode for



Fig. 18 DMIS installed at BARC Hospital (left- imaging unit and right – controls)



Fig. 19 Images of patients acquired using DMIS (Courtesy: BARC, HOSPITAL)

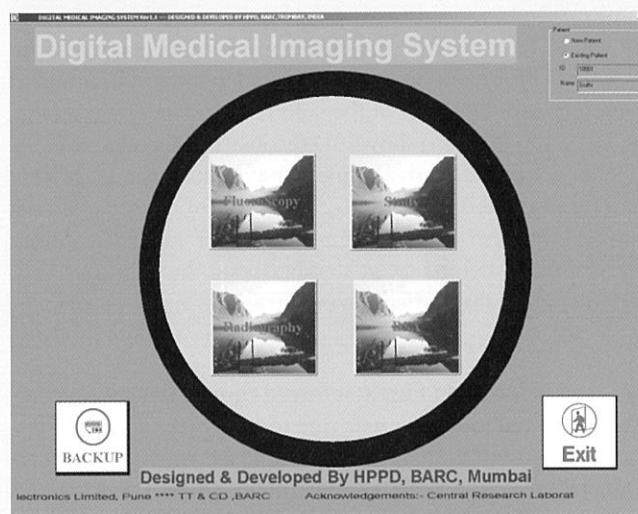


Fig. 20 Front end GUI of DMIS

examining the images by specialist besides advanced Data Management and Networking, Dicom 3.0 Compatibility, microradiography and measurement tools. This system developed in 2003, has been used at BARC hospital since 2004. Based on the feedback from radiologist, a new version of the system using flat panel detector is under development.

Figure 18 depicts the installed system and its control units at BARC Hospital and fig. 19 shows some images of investigations performed using this system

Figure 20 shows the front end graphical user interface (GUI) of the DMIS software. Figure 21 displays a high resolution image taken from a set of images of barium enema examination.

Imaging Gamma Sources – Emission Tomography

SPECT (Single Photon Emission Computed Tomography) [9,10] provides for an invaluable non-invasive technique for the characterization and activity distribution of the gamma-emitting source and generally

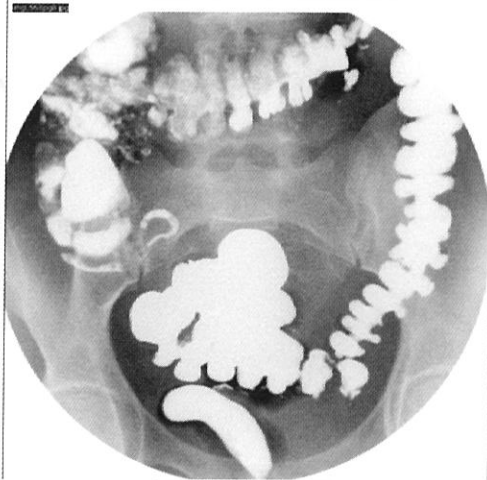


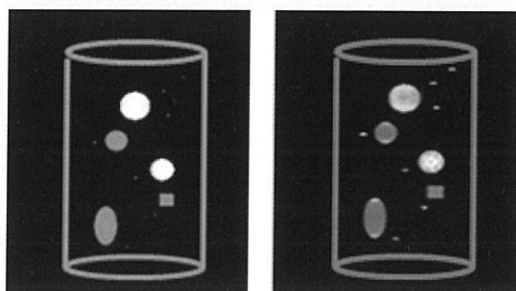
Fig. 21 X-ray image of Barium Enema

they have been used for medical purpose. We have adapted it for nuclear applications. SPECT involves the measurement of gamma rays emitted by a radionuclide. The intensities of the radiation measured are directly related to the radionuclide distribution inside the object. These intensities are used as input to the different types of reconstruction techniques for identification of emissions from the given volume. SPECT can be used in combination with transmission CT for getting complete information about the position and strength of radioisotopes. In such cases, emission tomography combined with transmission tomography is ideally suited. For a faster examination, not only 2D information is needed but also 3D information of the constituent of the object is required. This has got applications in non destructive examination of burnup distribution of nuclear fuel bundle or visualization inside a waste drum as shown in Fig. 22, which shows a representative result from LLNL, USA to illustrate the potential of this technique.

One of the main tasks in developing such a system is development of algorithm and its testing. We have developed algorithm for SPECT in parallel beam geometry, fan beam geometry and cone beam geometry. This has been tested on simulated phantoms.

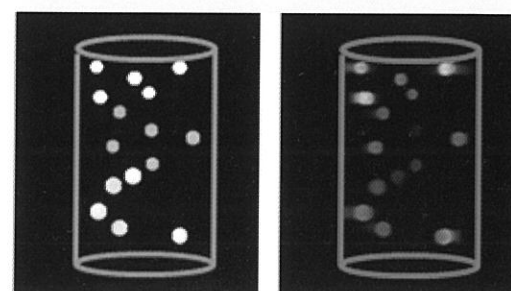
Simulations

A cylindrical waste drum containing radioisotopes has been modeled for SPECT imaging. The cylinder has a



Phantom D1

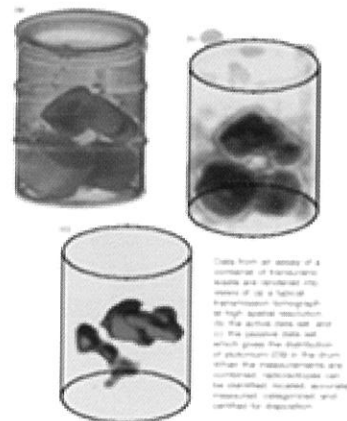
Reconstructed activity- D1



Phantom D2

Reconstructed activity- D2

Fig. 23 3D reconstructed activity for simulated waste drums



Ref: Science & Technology, LLNL

Fig. 22 Emission tomography of waste drum showing source locations

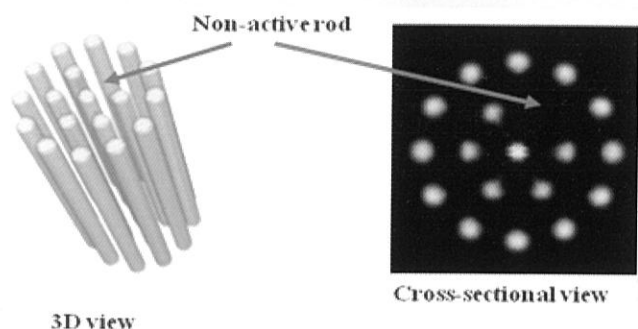


Fig. 24 3D reconstructed activity for Cs-137 at 200 MWD/T burnup for PHWR fuel (simulated)

diameter of 55 cm and a height of 87 cm with 2 mm thick lead-lining. Two phantoms [11] D1 and D2 have been modeled with different source positions and attenuation matrix. A fuel bundle model has also been simulated with Cs-137 as the gamma source inside the fuel pins. For numerical simulation purpose, the phantoms were discretized on a regular grid of 101 X 101 X 161 units. The physical dimension of each voxel is 5.5 mm X 5.5 mm X 5.5 mm. The noise-free projections were generated for 300 views/rotations with angular step of 1.2° on 101 X 101 X 161 equally spaced detector points. The reconstructed images are shown in Figs. 23 & 24. It can be seen that the activity

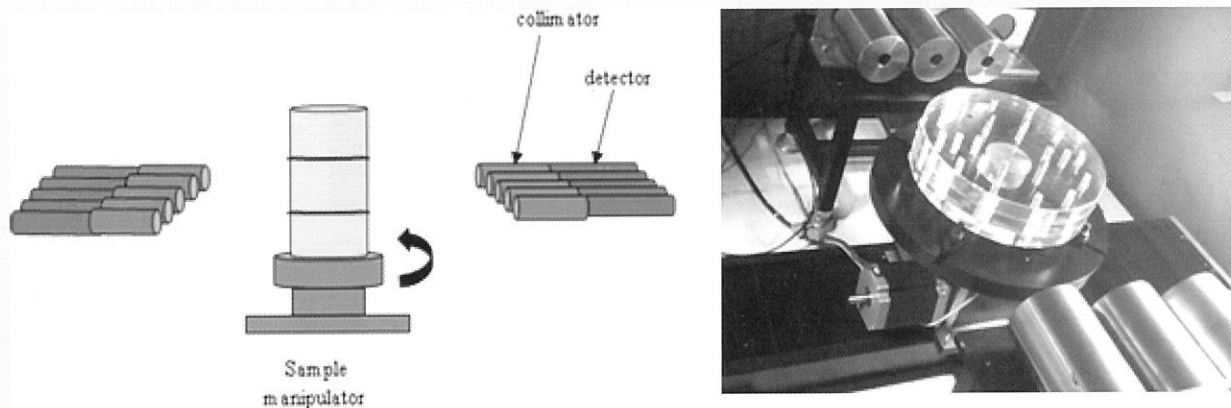


Fig. 25 Schematic and actual Experimental-set up

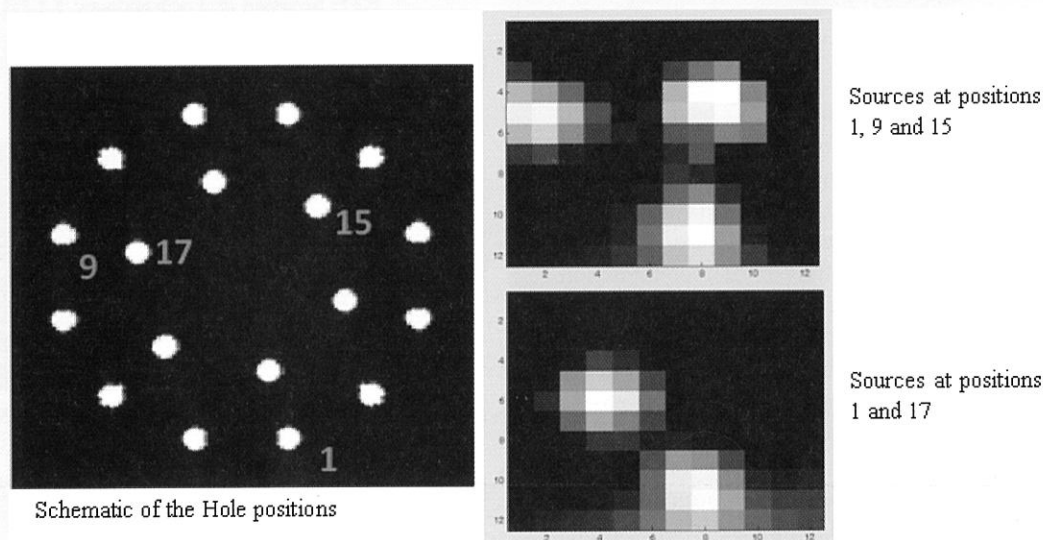


Fig. 26 2D reconstruction of Cs-137 sources

distribution is well reproduced in the reconstructed images. In Fig.24, the absence of activity in the non-active rod is clearly evident.

Experiments

In order to validate the theory, several feasibility experiments were conducted. A fuel bundle model was used for the initial experiment (Fig. 25). The sample used is 300 mm diameter Perspex disc with indexed holes – 6 holes at 60 mm radial distance and 12 holes at 120 mm radial distance from the centre. Cs-137 sources were placed in some of the holes. The detector used is 1” X 3” NaI(Tl). The spatial resolution is limited to 25 mm with the help of collimator assembly as seen in Fig. Initially, data was collected for 12 lateral positions and 72 angular positions in a single plane. The 2D reconstruction is shown in Fig. 26. It is evident from the reconstructed images that the spatial position and the source strength (relative in this case) can be accurately determined.

These feasibility experiments validate the algorithm and technique for determining position and source strength for spatially distributed gamma emitting radionuclide. This has got several applications in non destructive determination

of pin dependent burnup in a nuclear fuel bundle or visualization inside waste drum. We plan to take up to next step of designing a prototype system for this purpose.

Conclusions

We have described several new techniques on X-ray and neutron imaging which are being developed at BARC. These techniques have become possible due to advancement of new types of radiation sources, detectors and fast computing power. In particular with the development of more powerful X-ray sources such as synchrotron, several new areas of research will open up in material, medical and in NDT.

Acknowledgements

We are highly grateful to Dr. S. Kailas, Director, Physics Group BARC for his constant encouragements and support for undertaking these activities. We are also highly indebted to Dr. S.K. Sikka and Dr R. Chidambaram for assigning us the work on phase contrast imaging and supporting the research activities.

References

1. A. Pogany, D. Gao and S.W. Wilkins; "Contrast and resolution in imaging with a microfocus X-ray source", Rev. Sci. Instrum. 68 (1997), p. 2774
2. Y.S. Kashyap, P.S. Yadav, P.S. Sarkar, A. Agrawal, T. Roy, Amar Sinha, K. Dasgupta, D. Sathiyamoorthy; "Application of X-ray Phase-contrast Imaging Technique in the Study of Pyrocarbon-coated Zirconia Kernels", NDT&E International, 42(2009), 384-388.
3. Y.S. Kashyap, Tushar Roy, P.S. Sarkar, P.S. Yadav*, Mayank Shukla, A. Sinha, K. Dasgupta and D. Sathiyamoorthy; "Characterization of pyrocarbon coated materials using laboratory based Phase-Contrast Imaging technique", Rev. Sci. Instr. 78, 083703 (2007)
4. Amar Sinha, Y. Kashyap, Tushar Roy and P.S. Sarkar; "Phase Contrast Imaging and its applications in Materials Science", Journal of Non destructive Testing & Evaluation, Vol. 8, Issue 1 March 2009.
5. Y.S. Kashyap, P.S. Yadav, Tushar Roy, P.S. Sarkar, M. Shukla, Amar Sinha; "Laboratory based X-ray phase-contrast imaging technique for material and medical science application", Appl. Radiation Isotopes, 66(8), Pg 1083-1090 (2008)
6. P.S. Yadav, Y.S. Kashyap, Tushar Roy, P.S. Sarkar and A. Sinha; "Quantitative studies of pyrocarbon-coated materials using synchrotron radiation", J. Synchrotron Rad. 15 100-105 (2008)
7. Natterer F: "The Mathematics of Computerized Tomography", New York, Wiley, 1986
8. Kak, A.C. and Slaney, M.: "Principles of Computerized Tomography" IEEE Press 1987
9. Novikov R G: "An inversion formula for the attenuated x-ray transformation" Ark. Math. 40 (2002) 145-67
10. Huang Q, Zeng G.L., You J. and Gullberg G.T.: "An FDK-like cone-beam SPECT reconstruction algorithm for non-uniform attenuated projections acquired using a circular trajectory" Phys. Med. Biol. 50 (2005) 2329-2339
11. Tushar Roy, P.S. Sarkar and A. Sinha; "Simulation Study of Single Photon Emission Computed Tomography for Industrial Applications", AIP Conf. Proc. (2008) Volume 1050, pp. 79-90



Dr. Amar Sinha, presently Project Manager, Neutron and X-ray Physics facilities, graduated from the 20th Batch of BARC training school. He has worked extensively on the neutron physics and x-ray imaging research in particular on the commissioning of D-D and D-T neutron generator and their applications, development of neutron tagging technique, feasibility studies on coupling of neutron generator to subcritical assembly, neutron imaging techniques with reactor- and non-reactor sources, development of x-ray phase imaging, imaging beamline at INDUS-II synchrotron, 3D x-ray and neutron tomography, real time and high-speed imaging systems for basic and applied research etc. He and his team have been responsible for designing a digital medical imaging system and a Microtron based photoneutron source at Mangalore University. He was a Visiting Scientist (1986-87) at the Joint Research Centre of European

Communities, Ispra, Italy. He was principal investigator of several of IAEA coordinated research programs on advanced neutron sources and neutron-based explosive and fissile material detection. He was awarded the DAE-Technical Excellence Award -2005 for his work on X-ray and neutron imaging.



Mr. Y.S. Kashyap obtained M.Sc. Degree in Physics from I.I.T. Kanpur. He graduated from 44th batch of training school. He is presently working in Neutron and X-ray Physics Facilities, BARC. He is involved on the projects for the development of X-ray and neutron imaging techniques such as X-ray holography, tomography, phase-contrast imaging etc. He has worked on the setting up of laboratory-based phase contrast technique at Purnima Labs, BARC. He is also involved on design and development of imaging beamline at the Indus-II and neutron imaging beamline at CIRUS.



Mr. P.S. Sarkar obtained M.Sc. Degree in Physics from I.I.T. Kharagpur. After graduating from 43rd batch of training school, he is presently working in Neutron and X-ray Physics Facilities, BARC. He has performed two phase flow visualization experiments through neutron radiography at APSARA reactor. He has also performed X-ray radiography based experiments for visualization of fluidized bed for void fraction determination in collaboration with BHEL and NTPC for their coal gasification project. He has also been involved in the development of 3D X-ray Cone Beam tomography system for industrial purpose and reverse engineering and Digital Medical Imaging System which is already installed at BARC hospital and Battery based X-ray portable baggage inspection unit for checking of any unattended object. He is at present working on experimentation on phase contrast imaging, development of portable imaging units,

X-ray microtomography, real time imaging of two phase flow in micro-channel reactors and neutron radiography and tomography.



Mr. Tushar Roy obtained M.Sc. Degree in Physics from University of Allahabad. After graduating from 48th batch of training school, he is presently working in Neutron and X-ray Physics Facilities, BARC. He is involved in developing gamma imaging technique for emission tomography. He is also involved in experiments on X-ray imaging techniques like phase contrast imaging and microtomography. He is presently working on experimentation on emission tomography, neutron radiography and tomography and other neutron-based techniques like neutron backscattering and associated particle imaging.

Nuclear Reaction Analysis: Principles and Applications

V.S. Raju and Sanjiv Kumar

National Centre for Compositional Characterisation of Materials, Bhabha Atomic Research Centre, Hyderabad 500 062;
E-mail: rajucccm@rediffmail.com

Abstract

Characterisation of surfaces specifically for low Z elements has been a challenging problem in materials science and other fields. In this regard, among the available surface analytical tools, the nuclear reaction analysis, a powerful tool of Ion beam analysis, has been very useful and has many advantages of quantification, lateral and depth distribution and isotopic ratio determination, in addition to being nondestructive. In this article, besides explaining the basics, determination of hydrogen, boron, nitrogen, oxygen, fluorine in a wide range of materials using nuclear resonance reactions is described. The complexity and nature of the materials science problems related to these and other elemental characterization is also described in a limited perspective while explaining the results.

Introduction

Nuclear reaction analysis (NRA) is a prominent ion beam analysis (IBA) technique for probing elemental composition and depth distribution on surface and near surface regions of materials. Sensitivity to light elements and non-destructive depth profiling capability are the two most attractive features of NRA which make it a powerful surface technique, particularly in the area of thin film technology. As the name suggests, the technique utilises a known nuclear reaction, preferably with a high Q-value and involves prompt measurement of one of the reaction products. The projectiles often used in the nuclear reactions are protons, deuterons, α -particles or heavy ions like ^{15}N , ^{19}F etc. The energy of a projectile may vary depending on the nature of the reaction, from ~ 100 keV to several MeV. The reaction products can be a charged particle, γ -rays or their combinations as in $[^{11}\text{B}(p,\alpha)2\alpha]$, $[^{27}\text{Al}(p,\gamma)^{28}\text{Si}]$ and $[^1\text{H}(^{19}\text{F},\alpha\gamma)^{16}\text{O}]$ respectively. As NRA is isotope specific it usually enables interference-free determination of that isotope. The detection sensitivity of NRA varies from percentage level, down to trace levels. It is worthwhile mentioning that such surface analytical techniques as X-ray photoelectron spectroscopy (XPS), Auger electron spectroscopy (AES) or secondary ionization mass spectrometry (SIMS) also provide the detection of light elements but depth profiling by these techniques is destructive as these utilize sputtering for progressive surface removal.

Concepts Essential to NRA

Energetics

The utilization of NRA requires a comprehensive understanding of kinematics and energetics of a nuclear reaction. A nuclear reaction, depicted pictorially in Fig.1, is characterized by its Q-value as given by equation 1. The reaction is exoergic if the Q value is +ve and endoergic if it is -ve. For all endoergic reactions there is a threshold energy for the incident particles, below which reaction cannot occur. This threshold is always greater than the absolute value of Q and is given by equation 2.

$$Q = (m_B + m_b - m_A - m_a) c^2 \text{ MeV} \quad (1)$$

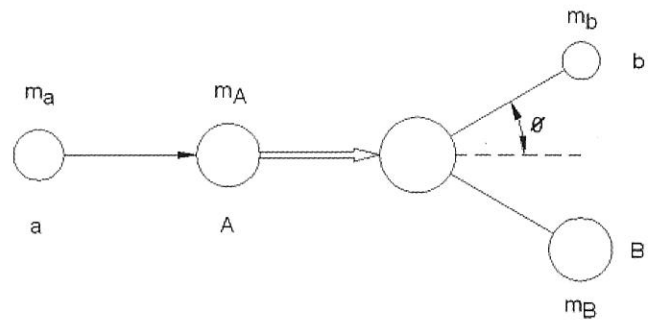


Fig. 1 A schematic of a nuclear reaction ('m' represents the mass of ions)

$$E_{th} = -Q \cdot \frac{m_B + m_b}{m_B + m_b - m_a} \text{ MeV} \quad (2)$$

The energy of ejectile depends on Q value and the angle of emission. The reactions with high +Q values are preferred for analysis as the ejectiles would have higher energies to facilitate better discrimination against other charged particles, e.g. backscattered ions. An extensive description of kinematics of a nuclear reaction is presented in ref.[1]. A list of nuclear reactions generally used for analysis with their Q values is given in Table 1.

Stopping Power and Quantification

In addition to kinematics, stopping power or stopping cross-section is an essential factor for NRA. In fact, it is the quantity which lends non-destructive depth profiling capability to NRA or other IBA techniques. A physical treatment of stopping power is given in ref.[1]. Briefly, it provides the energy loss suffered by an energetic ion beam in traversing unit distance in a medium and is expressed in the units of keV/micron or $\text{eV}/10^{15} \text{ atoms/cm}^2$.

Nuclear Reaction Cross Section

All nuclear reactions have a finite probability of occurrence which is denoted by reaction cross section measured in barns ($1 \text{ barn} = 10^{-24} \text{ cm}^2$). A plot of the incident particle energy on X-axis vs the yield of the reaction on Y-axis is termed excitation function of the reaction. The excitation function in some cases can show elevation or dips in yield or resonant behavior, either sharp or broad at specific

TABLE 1. List of nuclear reactions and their Q-values

Proton induced reactions	Q [MeV]	Deuteron induced reactions	Q [MeV]	³ He induced reactions	Q [MeV]	⁴ He induced reactions	Q [MeV]
⁶ Li(p,α) ³ He	4.02	² H(d,p) ³ He	4.03	² H(³ He,p) ⁴ He	18.3	¹⁰ B(α,p) ¹³ C	4.06
⁷ Li(p,α) ⁴ He	17.35	³ He(d,α) ¹ H	18.3	⁶ Li(³ He,p) ⁸ Be	6.79	¹¹ B(α,p) ¹⁴ C	0.78
⁹ Be(p, γ) ¹⁰ B	6.58	¹² C(d,p) ¹³ C	2.72	⁹ Be(³ He,p) ¹¹ B	0.32	¹⁴ N(α,p) ¹⁷ O	1.19
¹¹ B(p,α)2α	8.58	¹³ C(d,p) ¹⁴ C	5.95	⁹ Be(³ He,α) ⁸ Be	18.9	¹⁹ F(α,p) ²² Ne	1.67
¹⁵ N(p,αγ) ¹² C	4.97	¹⁴ N(d,p) ¹⁵ N	8.61	¹² C(³ He,p) ¹⁴ N	4.78	³¹ P(α,p) ³⁴ S	0.63
¹⁸ O(p,αγ) ¹⁵ N	3.98	¹⁴ N(d, α) ¹² C	13.57	¹² C(³ He,α) ¹¹ C	1.86		
¹⁹ F(p,αγ) ¹⁶ O	8.11	¹⁶ O(d,p) ¹⁷ O	1.92	¹⁸ O(³ He,p) ²⁰ F	6.87		
²³ Na(p,αγ) ²⁴ Mg	11.7	¹⁶ O(d,a) ¹⁴ N	3.11	¹⁸ O(³ He,d) ¹⁹ F	2.50		
²⁷ Al(p,γ) ²⁸ Si	11.6	¹⁹ F(d,α) ¹⁷ O	10.03	¹⁸ O(³ He,α) ¹⁹ O	12.51		

energies of projectiles. Some times they can be a mixture of all these features. Hence the nuclear reaction is chosen by taking the objectives of analysis in consideration.

Different type of Nuclear Reaction Analysis Practices

Though a large number of nuclear reactions have been studied in great length and documented, only a few have been utilized to their full capacity for analytical applications. There is scope for exploring more reactions, for specific applications in providing better answers.

Offline NRA

The nuclear reaction generates the proposed radioactive nuclei and they are studied after irradiation off-line using the relevant detection setup and processing if any, in the laboratory. This is mostly referred to as charged particle activation analysis CPAA.

Online NRA

The nuclear reaction is initiated with projectile ions and all the products are detected and analysed in prompt mode, if the product nuclei are not long-lived beyond irradiation times. In this paper we limit to the online NRA techniques.

The sensitivity of a nuclear reaction is essentially governed by its cross section. It is a function of beam energy and may also show angular dependence. Some of the reactions exhibit resonance structures in their excitation functions. Such reactions are very useful for depth profiling applications. This NRA group is often referred to as nuclear resonance reaction analysis (NRRA). The resonances should be preferably strong, narrow and isolated for sensitive and high-depth resolved measurements. The width of a

resonance can be in the range of 50 eV to several keV. Depth profiling using resonances having widths ≤ 500 eV is known as narrow resonance profiling (NRP).

The yield formula given by equation (3) serves as a primary method to determine the depth profile of an element

$$Y(E_b) = C \int_0^\infty dx \int_0^\infty dE' \int_0^\infty dE N(x) g(E_b, E) F(E, E', x) \sigma(E') \quad (3)$$

where Y is the yield of one of the reaction products, N(x) is the concentration profile, $\sigma(E)$ is shape of resonance cross-section, $g(E_b, E)$ is the energy distribution of beam, (E, E') is the energy straggling of the particles and C is function of detection geometry and charge. It can be easily seen that the extraction of depth-profile from the yield formula is difficult and prone to errors as well. In many instances, reference targets are used for better quantification wherein they are examined under identical conditions as those of samples. However, the reference targets should meet certain criteria; these should preferably be conducting, these should have lateral as well as depth uniformity, and must be stable in vacuum and under ion bombardment. Even as a reference target is used, accurate charge (current) measurement and reproducible energy calibration are essential for precise quantitative analysis. The stopping powers for beams required for quantification and construction of depth scales can be calculated using a software program, Stopping and Range of Ions in Matter (SRIM). This program can be downloaded from web freely.

Experimental

The energetic ion beams used as projectiles are produced by a particle accelerator, usually a DC machine, based on Van de Graaff or Cockroft-Walton principles.

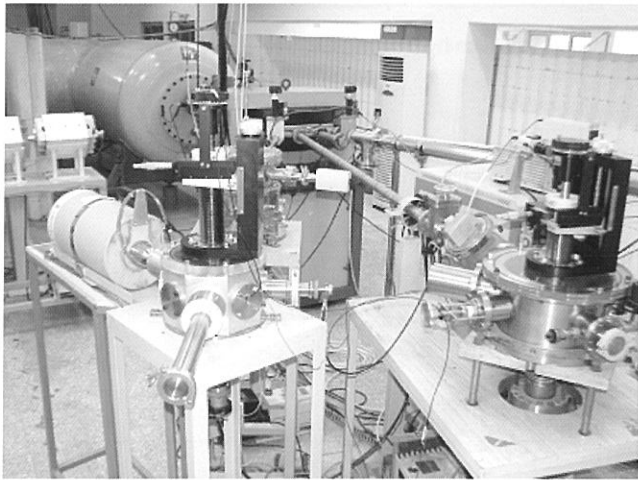


Fig. 2 A view of 3 MV Tandatron and its beam lines at CCCM

These machines can be single-ended or tandem in nature. Currently most of the commercial accelerators are tandem type which produce +ve ion beams of energies $(n+1)V$ keV where n is charge state of the beam and V the terminal voltage with -ve ion beam injected into the accelerator from ground potential. The terminal voltage of the machines range from a few hundred kilovolt to several million volts with a stability around 0.1%. High stability of terminal voltage is required to perform high-depth resolution measurements using NRA. A pictorial view of the 3 MV Tandatron (HVEE, Europa) at NCCCM is presented in Fig. 2.

The beam is collimated to ~ 1 mm sized spot before it impinges on a sample fixed onto a target manipulator, which in turn, is mounted on a scattering chamber consisting of gadgetries as detectors, electron suppressor etc. A Si-surface barrier detector is employed to detect charged particles, whereas scintillation detector viz., NaI(Tl), bismuth germanate (BGO, $\text{Bi}_4\text{Ge}_3\text{O}_{12}$) or a high purity Ge detector is used for γ -rays detection. NRA measurements are performed in high or ultra high vacuum. All through the accelerator and beams lines where ion beam are handled, a vacuum better than 10^{-6} mbar is maintained by turbo-molecular pumps. The signals of radiations produced in the detector are processed using a combination of preamplifier and amplifier and acquired on a PC-based multichannel analyzer (MCA). A

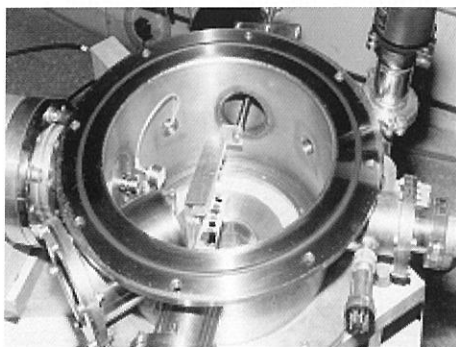
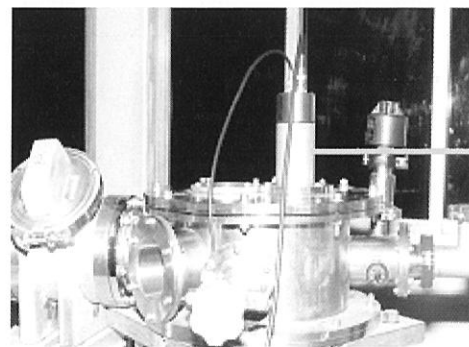


Fig. 3 Scattering chamber



NaI detector

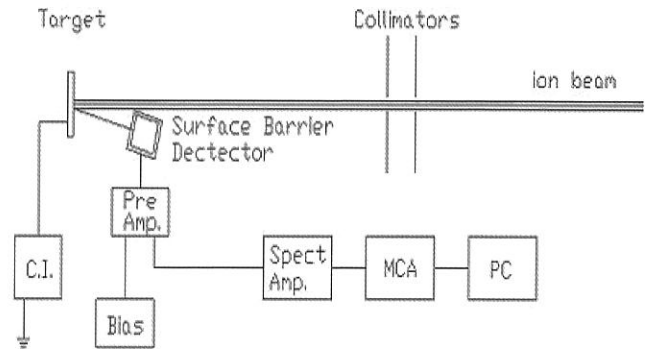


Fig. 4 Signal processing

typical scattering chamber and a schematic of signal processing are shown in Fig.3 and Fig.4.

Applications

Determination of Hydrogen and Depth Profiling

Hydrogen is probably the most common elemental contaminant in materials, especially in thin films. Its presence can have dramatic effects on the electrical, mechanical and chemical properties of materials. Hydrogen diffuses rapidly, being the smallest and lightest atom. It severely deteriorates the mechanical properties of structural materials such as Zr and Zr-based alloys by way of hydrogen embrittlement or delayed hydrogen cracking (DHC). In electronic materials it displays a range of complex behavior by acting as an amphoteric impurity. It is an indispensable ingredient in the fabrication of integrated circuits as it passivates the defects at Si/SiO₂ interface. But in many cases it causes erratic performance of devices by inducing electrically active states. Similarly, the presence of hydrogen is known to decrease the superconducting transition temperature (T_c) of intermetallic (Nb_3Ge) compounds. Due to these reasons the detection of hydrogen and its depth profiling is of immense interest.

NRA involving $^1\text{H}(^{15}\text{N},\alpha\gamma)^{12}\text{C}$ or $^1\text{H}(^{19}\text{F},\alpha\gamma)^{16}\text{O}$ reaction is a very good method for depth profiling hydrogen on materials surfaces [4,5]. $^1\text{H}(^{15}\text{N},\alpha\gamma)^{12}\text{C}$ reactions exhibits a strong and sharp (fwhm = ~ 1 keV) resonance at 6.38 MeV and emits 4.4 MeV γ -rays. Similarly $^1\text{H}(^{19}\text{F},\alpha\gamma)^{16}\text{O}$ reaction exhibits a comparatively wide (fwhm = 45 keV) resonance at

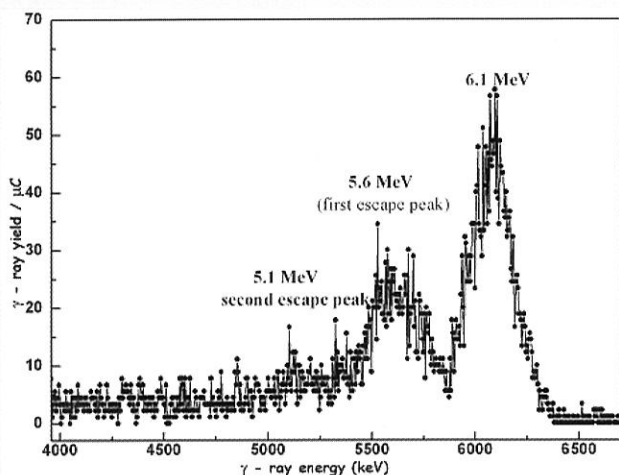


Fig. 5 γ -ray spectrum from ${}^1\text{H}({}^{19}\text{F},\alpha\gamma){}^{16}\text{O}$ resonance reaction

6.44 MeV. 6.1, 6.9 and 7.1 MeV γ -rays are characteristic of this reaction. It can be easily observed that ${}^1\text{H}({}^{15}\text{N},\alpha\gamma){}^{12}\text{C}$ offers highly depth resolved (<10 nm) measurements. Though α -particle is also a product in both reactions, measurements often involve the detection of 4.4 MeV or 6-7 MeV γ -rays primarily because of the absence of any interference.

Depth profiling is accomplished by increasing the beam energy beyond the resonance energy in steps. When the beam energy is equal to the resonance energy, the reaction takes place at the surface, while at higher beam energies, the reaction occurs inside the material. The depth scale is obtained by invoking the concept of stopping power. 4.4 MeV or 6-7 MeV γ -rays are usually measured by a scintillation detector. The experimental conditions in terms of beam current, position of the detector etc. need to be optimized so as to estimate hydrogen with good sensitivity. A sensitivity of about 0.1 at.% can be obtained with an optimised detection system. Some of the materials undergo loss of hydrogen under the influence of the bombarding beam. Care must be exercised while analyzing such materials. Low beam current and target cooling are useful in alleviating such problems.

Figure 5 shows a typical γ -ray spectrum from a hydrogen-containing material, as a result of ${}^1\text{H}({}^{19}\text{F},\alpha\gamma){}^{16}\text{O}$ resonance reaction. In addition to the main photo peak at 6.1 MeV, the associated first and second escape peaks are also seen in the spectrum. The peaks of 7.1 MeV and 6.9 MeV are broad and comparatively much less intense. As a result, these are not clearly discernible in the spectrum. However, the area integrated between 7.1 MeV to 4.8 MeV serves as total hydrogen signal. Figure 6 shows the depth profile of hydrogen in H-implanted (implantation energy = 19 keV) Si specimen. As mentioned earlier, hydrogen is ubiquitously present on the surface of a material as a contaminant. It is referred to as surface hydrogen and is clearly discriminated against the implanted hydrogen. Fig.7 shows the depth

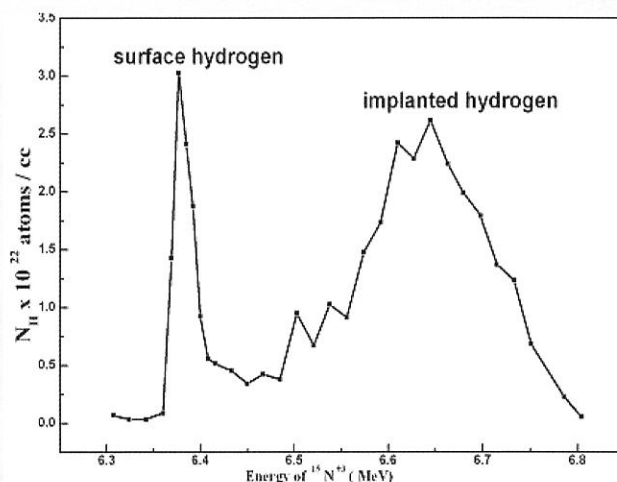


Fig. 6 Depth profile of hydrogen in H implanted Si

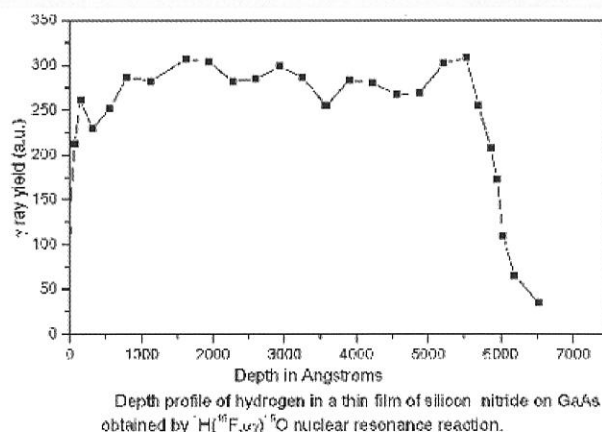


Fig. 7 Depth profile of hydrogen in SiN film on GaAs sample

profile of hydrogen in silicon nitride film deposited by plasma enhanced chemical vapor deposition (PECVD) on gallium arsenide. The content of hydrogen in the film is about 20 at.% and is found to be distributed uniformly across the film. The presence of such a large amount of hydrogen results from the use of silane (SiH_4) gas during deposition.

Further, Figure 8 shows change (gradual decrease) in hydrogen content in a diamond like carbon film as a function of beam fluence during the course of hydrogen measurement by ${}^1\text{H}({}^{19}\text{F},\alpha\gamma){}^{16}\text{O}$ resonance reaction. This serves as a typical example of problems encountered in depth profiling hydrogen in materials wherein it is weakly bonded and undergo desorption. It is to be noted that no loss of hydrogen is observed during depth profiling in silicon nitride film (Fig.7), as hydrogen is bonded strongly to Si and N in the film. Special experimental arrangements like target cooling or rotation are required for an accurate analysis of materials which undergo deterioration under the influence of the beam.

Determination of hydrogen is also required in hydrogen storage materials. Storage of hydrogen, preferably in solid-state, is crucial for the realization of hydrogen

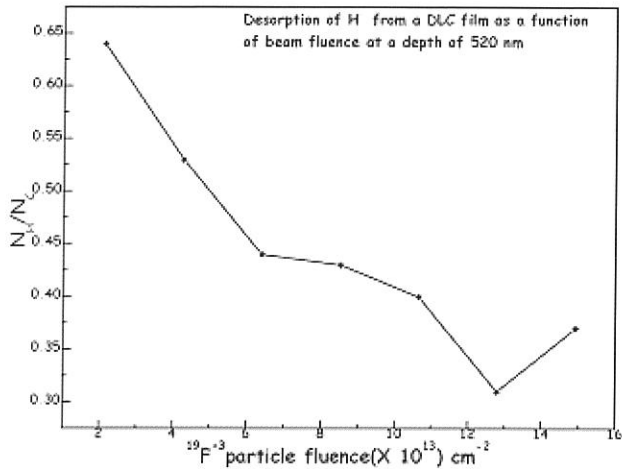


Fig. 8 Change in hydrogen content in a DLC film as a function of beam fluence

economy, the energy source of the future. The content of hydrogen in such materials should be very large. Figure 9 shows the depth profiles of hydrogen in a Pd-capped Mg film, which has been developed in our laboratory to store hydrogen. Profile (a) pertains to the hydrogenation step of first cycle of hydrogenation-dehydrogenation.

The film contains about 7.0 wt% (~60 at.%) hydrogen which is amongst the highest achieved so far. Profile pertaining to dehydrogenation step is not included due to the complete desorption of hydrogen (no 6-7 MeV γ -rays were detected). Profile (b) represents the hydrogenation step of second cycle of hydrogenation-dehydrogenation. The nondestructive nature of the technique facilitates repetitive examination of a specimen during the cycles of hydrogenation-dehydrogenation. Cyclic stability is one of the major requirements of a hydrogen storage material. These profiles also provide an insight into the mechanism of hydrogen incorporation in Mg crystallites which is governed by grain boundary-mediated diffusion.

Hydrogen determination and depth profiling is also achieved through Energetic Recoil Detection Analysis ERDA, using a heavier ion like He to impinge on target containing hydrogen to be estimated. The heavier projectile knocks out the lighter atoms from the target which in turn can be collected in the forward angles using relevant filters for incoming beam scatter. The kinetic energy of the knocked out atoms of hydrogen is a measure of the quantity and depth of interaction. Though this is a rapid and easy method with good kinematics, the quantification is complicated and depth resolution achievable using NRP is not matched.

Determination of Boron

Sensitive Determination of B

Boron is a technologically important element. It is a prominent dopant in semiconductor (Si) and a major constituent of boride hard coatings. As a result, depending on application, the determination of boron from percentage to trace levels may be required. $^{11}\text{B}(p,\alpha)^8\text{Be}$ reaction satisfies

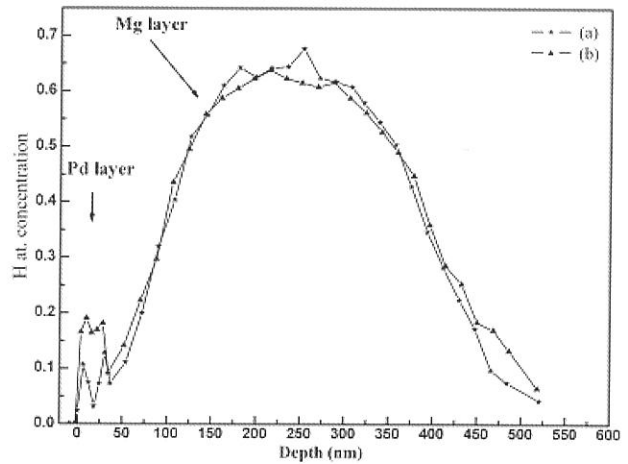
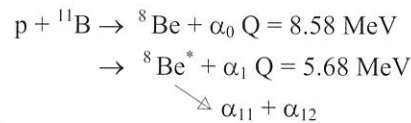


Fig. 9 profiles of hydrogen in Pd capped Mg films

such analytical requirement [2,3]. This reaction is a typical example of particle-particle reaction. It exhibits a strong and broad resonance [cross section = 600 mb, FWHM = 300 keV] at 660 keV. The reaction formula of $^{11}\text{B}(p,\alpha)^8\text{Be}$ is as follows:



The energies of the α -ejectiles for a projectile energy of about 700 keV are in a continuum, extending from 5.5 MeV down to 5 keV. The α -particles are detected by a Si-surface detector positioned at about 150° relative to the beam direction. The different groups of α -ejectiles overlap one another and are not distinguishable. Low energy protons backscattered from the target are the major source of interference in the detection of boron by this method. Therefore a 7.5-12 micron mylar foil is placed in front of the detector to prevent the backscattered protons from being detected.

The detection sensitivity of the method depends strongly on the composition and nature of the matrix. In the case of light elements such as Si, the detection sensitivity is about 0.5 ppm. However, the pile up of backscattered protons from high Z matrices (SS, zircaloy) limits the sensitivity of this technique to about 10 ppm. It is to be noted that the intensity of backscattered protons exhibits Z^2 dependence. The precision of the method in the measurement of boron is <0.5%. A typical α -spectrum from this reaction for a Si specimen containing about 1 ppm of B is shown in the fig.10(a) while that from a thick elemental B target in Fig.10(b).

Determination of ^{10}B : ^{11}B Isotopic Ratio

NRA also facilitates a quantitative estimation of the isotopic ratio of ^{10}B and ^{11}B in different matrices. Compounds of boron enriched in ^{10}B to $\geq 65\%$ (ca. its natural abundance of ~ 19.8%) find important applications in nuclear reactors. While enriched boron carbide is utilized in

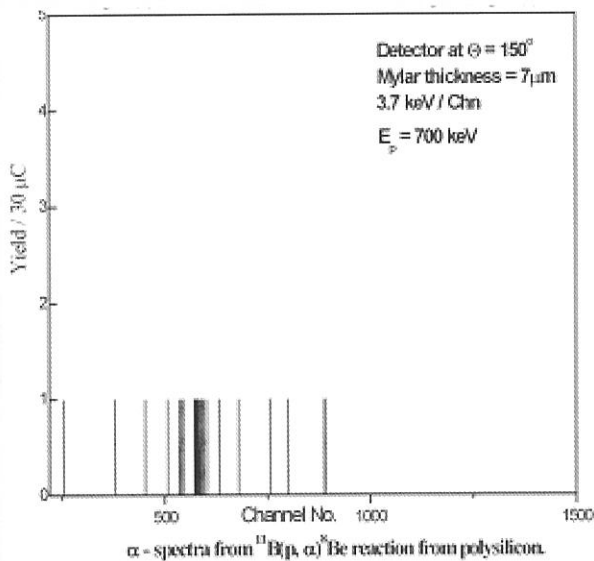


Fig. 10a ~1ppm of Boron on Si

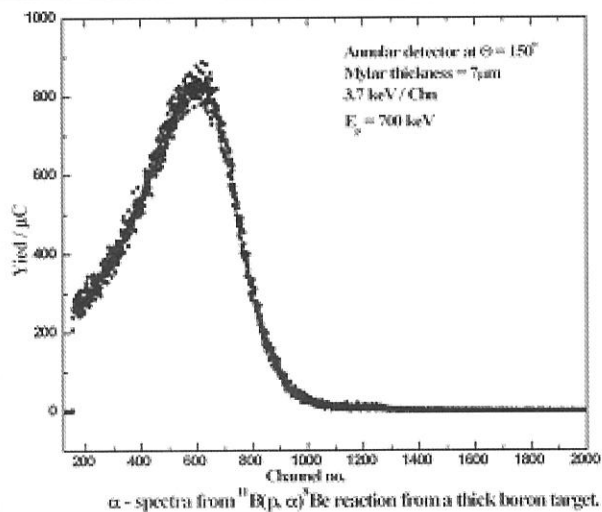


Fig. 10b Thick elemental Boron

control rods in a fast reactor which is the mainstay of third stage of the nuclear energy programme of the country, enriched boric acid is useful in controlling Axial power Offset Anomaly and excess reactivity in PWR. The methodology of determination utilizes $^{10}\text{B}(p,\alpha)^7\text{Be}$ and $^{10}\text{B}(p,\gamma)^{10}\text{B}$ nuclear reactions involving ^{10}B isotope and $^{11}\text{B}(p,\gamma)^{11}\text{B}$ involving ^{11}B isotope, which occur simultaneously following the bombardment of 3-4 MeV protons. 429, 718 and 2124 keV prompt γ -rays are emanated from these reactions respectively. The measurement of these γ -rays by a high purity germanium (HPGe) detector facilitates the quantitative estimation of the isotopic ratio of ^{10}B and ^{11}B . A typical prompt γ -ray spectrum obtained by bombarding 3.0 MeV proton beam on a target consisting of elemental boron with natural isotopic abundance is shown in Fig. 11 for illustration wherein 429, 718 and 2124 keV γ -rays are conspicuously observed.

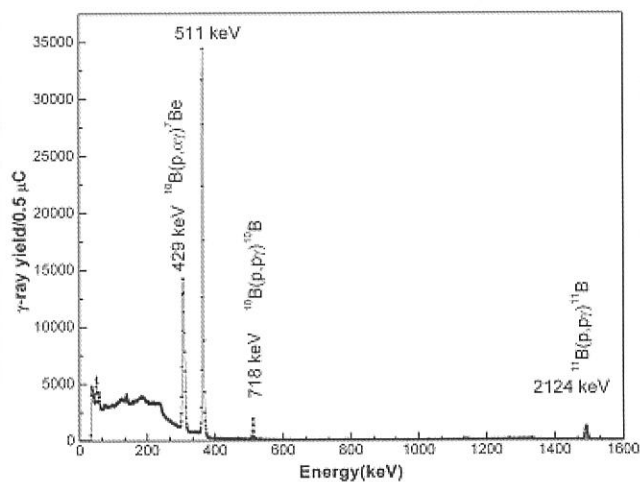


Fig. 11 γ -ray spectrum recorded on bombarding a boron target of natural isotopic abundance with 3.0 MeV proton beam

Depth Profiling of Nitrogen

The reaction $^{15}\text{N}(^1\text{H},\alpha\gamma)^{12}\text{C}$ is used extensively for depth profiling nitrogen. It is actually the inverse of the reaction $^1\text{H}(^{15}\text{N},\alpha\gamma)^{12}\text{C}$ in centre of mass units. This reaction has strong resonances at 429 keV and 897 keV. The resonance at 429 keV is very narrow and therefore offers nanometric depth resolution. It is to be noted that these reactions are based on ^{15}N isotope that has a natural isotopic abundance of only 0.39%. As a result measurements are performed using 200 nA or more beam current. Figure 12 shows the depth profile of nitrogen in a zirconium nitride film measured using the resonance at 429 keV. Nitrogen isotopes in the film are present as per their natural abundances [6,7]. This reaction can be very effectively utilized to study the oxidation kinetics of nitride films and, incorporation and diffusion of nitrogen in construction materials in reactive environments. Depth profiles in Fig. 12 depict the oxidation of a zirconium nitride film as a function of duration of annealing in air at 475°C.

Depth Profiling of Oxygen by $^{18}\text{O}(p,\alpha)^{15}\text{N}$ Nuclear Reaction

Oxygen non-stoichiometry has a profound effect on the electrical and magnetic properties of oxygen bearing films as well as bulk materials. A vacancy of oxygen releases two electrons in the system for charge compensation which causes an increase in the electrical conductivity of the material. Similarly oxygen present as a contaminant which is ubiquitous as hydrogen also modifies the properties of materials. Thus it is desirable to depth profile oxygen in films and surface regions of bulk materials. $^{16}\text{O}(\alpha,\alpha)^{16}\text{O}$ resonant scattering, a variant of Backscattering Spectrometry (BS), at 3.05 MeV α -particle energy, is used for probing oxygen depth profiles in compound films due to high scattering cross-section of the resonance and multielement capability of the technique. These features of the technique are very

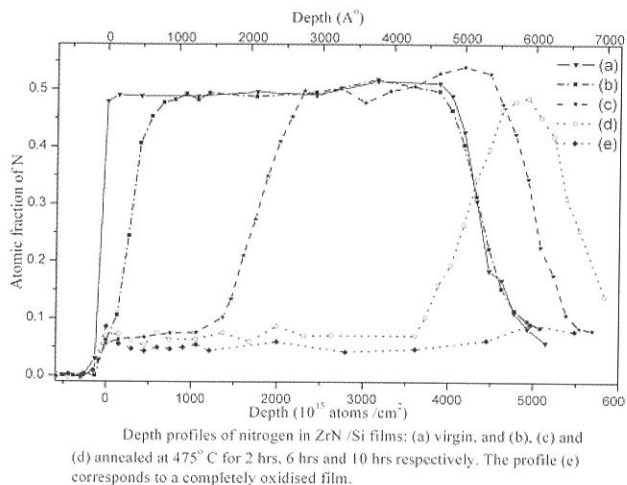


Fig. 12 Depth profiles of nitrogen in ZrN/Si films

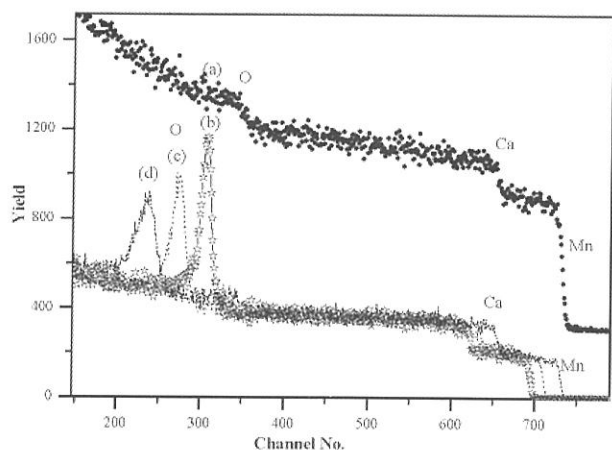


Fig. 13 (a) 2.4 MeV α -RBS spectrum from CaMnO_3 and (b), (c) and (d) are the backscattered spectra obtained with 3.07, 3.13 and 3.23 MeV α -particles involving 3.05 MeV $^{16}\text{O}(\alpha, \alpha)^{16}\text{O}$ resonant scattering

well illustrated by Fig. 13 which shows 3.05 MeV $^{16}\text{O}(\alpha, \alpha)^{16}\text{O}$ resonant scattering spectrum of CaMnO_3 . In addition to a strong signal of oxygen, the signals of Ca and Mn are also discernible in the spectrum.

$^{18}\text{O}(p, \alpha)^{15}\text{N}$ nuclear reaction that exhibits resonances at 157 keV and 629 keV can be utilized to depth profile ^{18}O in films. The resonance at 157 keV is sharp and narrow and therefore is useful for high-depth resolved measurements. The resonance at 629 keV, on the other hand, is comparatively wide (width = 2.1 keV) and has a depth resolution of about 30 nm in SiO_2 films. The measurement is based on the detection of α -particles. Hence the experimental set-up is identical to that for boron determination by $^{11}\text{B}(p, \alpha)^8\text{Be}$ reaction. In the analysis of specimens containing oxygen in natural isotopic abundance, high proton beam currents (~ 300 nA) are used in view of low abundance (0.2%) of ^{18}O . The depth profile of oxygen in a

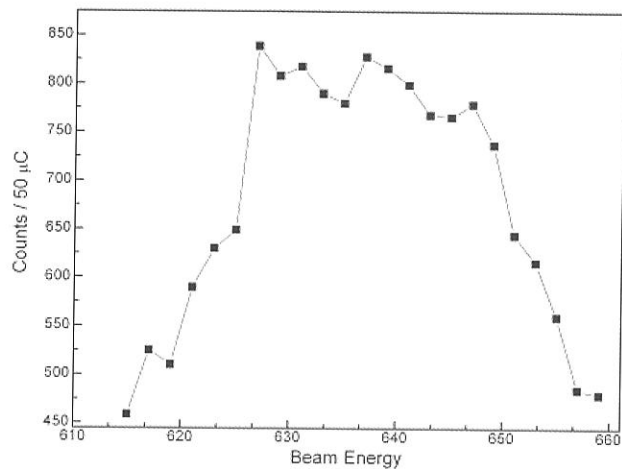


Fig. 14 Depth profile oxygen in a thin film of SiO_2 by $^{18}\text{O}(p, \alpha)^{15}\text{N}$ nuclear resonance reaction

thermally grown SiO_2 film obtained by 629 keV resonance is shown in Fig. 14.

Depth Profiling of Fluorine

$^{19}\text{F}(^1\text{H}, \alpha\gamma)^{16}\text{O}$ nuclear reaction has been widely used for depth profiling fluorine on materials surfaces. The reaction exhibits several strong and narrow resonances below $E_p < 2000$ keV, however, those at 875 keV and 1375 keV are most frequently used. The detection usually involves the measurement of 6.1, 6.9 and 7.5 MeV γ -rays using, depending on requirement, either NaI(Tl) or high purity Ge detector. This reaction is also utilised for the sensitive determination of fluorine in materials, finding applications in fields ranging from semiconductor technology and nuclear industry to biological and environmental sciences. Low levels of fluorine is usually determined using $E_p > 3$ MeV and detection of γ -rays by NaI(Tl) or BGO detector. Though there are no major interfering nuclear reactions, care must be exercised while analyzing the element in certain materials such as Al or Ti which also emit high energy γ -rays.

Depth Profiling of Magnesium

Mg-based thin films are promising materials for hydrogen storage [6]. These find applications in optical devices and superconductors as well [7, 8]. Depth profiling of Mg in such films is desirable to study interfacial reactions or any compositional variation that may arise during processing or usage. $^{26}\text{Mg}(p, \gamma)^{27}\text{Al}$ and $^{24}\text{Mg}(p, p\gamma)^{24}\text{Mg}$ reactions that exhibit resonances at 1548 keV and 2010 keV respectively are the two potentially well-suited reactions for this purpose. The latter reaction has a width of 350 eV. This reaction falls under the category of narrow resonance profiling (NRP). SPACES, a program to a computer code to calculate the energy straggling distributions and excitation functions of narrow nuclear reactions, can be utilized to discern the depth distributions.

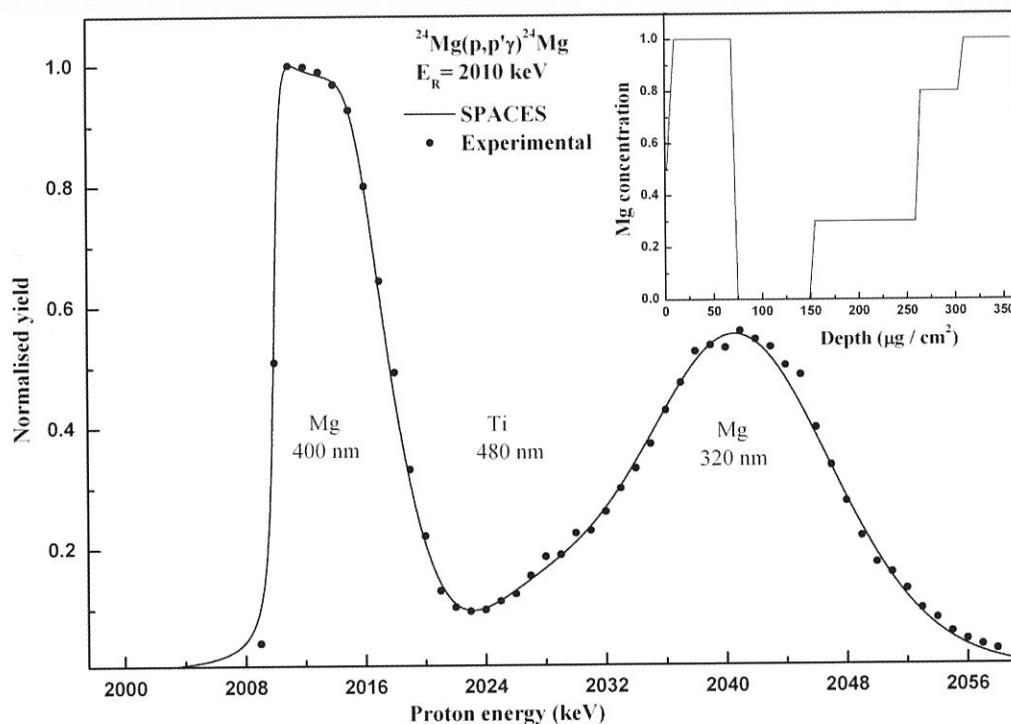


Fig. 15 Experimental and simulated (SPACES) excitation curves of Mg / Ti / Mg / Si film. Inset shows the Mg concentration profile used in SPACES for fitting the experimental data

For example, Fig.15 shows the excitation curve of trilayered Mg(400nm)/Ti (480nm)/Mg(320nm)/Si film recorded for 2010 keV resonance of $^{24}\text{Mg}(p,\gamma)^{24}\text{Mg}$ reaction. The examination of the curves reveals that the coating has, in fact, the following layer structure (arising due to interfacial reaction between Mg and Ti): MgO(4.2nm)/Mg(388 nm)/Ti(177nm)/Ti_{0.7}Mg_{0.3}(244nm)/Ti_{0.2}Mg_{0.8}(100nm)/Mg(310nm).

TABLE 2. List of nuclear reactions used for Narrow Resonance Profiling (NRP)

Reaction	Resonance energy(keV)	Resonance width (eV)
$^{18}\text{O}(p,\alpha)^{15}\text{N}$	152	100
$^{29}\text{Si}(p,\gamma)^{30}\text{P}$	413.9	—
$^{15}\text{N}(p,\alpha\gamma)^{12}\text{C}$	429	120
$^{30}\text{Si}(p,\gamma)^{31}\text{P}$	620.4	68
$^{18}\text{O}(p,\alpha)^{15}\text{N}$	629	2200
$^{27}\text{Al}(p,\gamma)^{28}\text{Si}$	632.23	6.7
$^{23}\text{Na}(p,\gamma)^{24}\text{Mg}$	676.7	<70
$^{27}\text{Al}(p,\gamma)^{28}\text{Si}$	991.86	70
$^{52}\text{Cr}(p,\gamma)^{53}\text{Mn}$	1005	50
$^{19}\text{F}(p, p'\gamma)^{19}\text{F}$	1088	400
$^{13}\text{C}(p,\gamma)^{13}\text{N}$	1748	135
$^{24}\text{Mg}(p, p'\gamma)^{24}\text{Mg}$	2010	350

Conclusion

Nuclear reaction analysis is an eminently suitable technique for analyzing elemental profile in the surface regions of the materials. Its sensitivity to light elements is complementary to other ion beam techniques. Therefore, in combination with Rutherford backscattering spectrometry (RBS) which is more sensitive for mid or high Z elements, NRA can be effectively utilized for complete compositional analysis.

References

1. G. Deconnick, Introduction to Radioanalytical Physics, Elsevier, 1978.
2. E. Ligeon and A. Bontemps, J. Radioanal. Chem. 12(1972) 335.
3. Sanjiv Kumar, G.L.N. Reddy, J.V. Ramana, S. Vikram Kumar and V.S. Raju, Int Symposium on Materials Chemistry, 4-8 December 2006, BARC, Mumbai
4. W.A. Lanford, Nucl. Instr. Meth. in Phy. Res. B66(1992) 65.
5. Sanjiv Kumar, J.V. Ramana, C.David, V.S. Raju, S. Gangadharan, Nucl. Instr. Meth. in Phy. Res. B142(1998) 549.
6. Sanjiv Kumar, S.V. Kumar, G.L.N. Reddy, V. Kain, J.V. Ramana, V.S. Raju, Nuclear Instruments and Methods B, 240 (2005)704.
7. G.L.N. Reddy, J.V. Ramana, Sanjiv Kumar, S. Vikram Kumar and V.S. Raju, Applied Surface Science 253 (2007) 7230.
8. I. Vickridge, G. Amsel, Nucl. Instr. and Meth. B 45 (1990) 6.
9. Sanjiv Kumar, G.L.N. Reddy, V.S. Raju; J.Alloys and Compounds 476(2009) 500.



Dr. V.S. Raju had his M.Sc. in Nuclear Physics from Andhra University and joined 18th batch of BARC training school in physics. He was awarded Ph.D in surface science studies from Mumbai University in 1994. He had worked extensively on surface analytical techniques like Ion Beam Analysis, X-Ray photoelectron spectroscopy and had established the Surface and Profile Measurement laboratory at CCCM, Hyderabad with leading analytical expertise in thin film characterization. Along with his team of scientists he has developed the competence in providing solutions to several difficult problems in surface characterization of samples for departmental and other research establishments. He has about 35 international journal publications. He is presently head of the Surface and Profile Measurement Section, CCCM and an authorized research guide for Osmania University and HBNI.



Dr. Sanjiv Kumar had his M.Sc. from Patna University in Chemistry and joined 30th batch of BARC training school. He obtained his Ph.D from Indian Institute of Science, Bangalore, in material science. He has expertise in surface analysis, particularly in using multiple ion beam analytical techniques and X-ray photoelectron spectrometry. He developed the surface and profile measurement laboratory at CCCM with state of art technologies and analytical competence. He was awarded DAE scientific and technical excellence award for the year 2008 for his remarkable contributions in synthesis and characterisation of energy related materials. He is presently the group leader for Ion Beam Analysis at CCCM.

An Overview of Radiological Safety in Nuclear Installations

P.K. Sarkar

Health Physics Division, Bhabha Atomic Research Centre, Mumbai 400085, E-mail: pksasrkar@basrc.gov.in

Abstract

Radiological safety is an integral and essential part of nuclear installations, like nuclear reactors, accelerators and nuclear fuel fabrication or reprocessing facilities. The main aim of radiological safety programme adopted in India is to establish an appropriate level of protection for people and the environment against the harmful effects of radiation exposure, without unnecessarily restricting the desirable human actions that may be the cause of such exposure. The ongoing radiological safety programme of the Department of Atomic Energy, India, is discussed along with the scope and objective of radiological safety in general and specifically for each different types of nuclear installations, taking into consideration the support needed from all branches of physical sciences. The recent recommendations of the International commission on Radiological Protection, are reviewed.

Introduction

With many nuclear and other radiation generating facilities in operation and being commissioned in various units of the Department of Atomic Energy, a full-fledged and robust radiation protection programme has been formulated, as a mandate, to protect the radiation workers, the public and the environment, from harmful effects of radiation. Physics underpins the discipline of radiation protection. Knowledge of physics is used to describe the production and behavior of radiation and radioactivity and interactions that determine the energy deposited in media (dose), and allow its detection and modification (shielding). It is standard practice, which is perhaps unique for radiation protection, to optimize protection, as far below established safe levels, as reasonably achievable, and an understanding of the physics of the various elements is fundamental to its accomplishment.

The nuclear and radiation generating facilities for which radiological safety programmes are formulated, are broadly categorized in three different groups: Nuclear power and research reactors, nuclear fuel cycles and other radiation generating facilities like accelerators, irradiators etc. The basic philosophy of radiation protection remains the same for all of them, though there are certain important differences, based on their operating parameters. For nuclear power plants the main safety concern has always been the possibility of an uncontrolled release of radioactive material, leading to contamination and consequent radiation exposure off-site. It has long been asserted that nuclear reactor accidents are the epitome of low-probability but high-consequence risks. Understandably, with this in mind, some people were disinclined to accept the risk, however low the probability. The nuclear fuel cycle consists of a broad range of installations, including mining and milling, conversion, enrichment, fuel fabrication (including mixed oxide fuel), reactor, interim spent fuel storage, reprocessing, vitrification and waste disposal facilities. Although some similar safety hazards may be posed at reactor and non-reactor fuel cycle facilities, the differences between them give rise to specific safety concerns at the non-reactor fuel cycle facilities that must be especially taken into consideration in the design and operation of these facilities. Radiological safety aspects in general, and neutron dosimetry in particular, around medium- and high-energy

particle accelerators, pose some unique challenges to the practitioners of radiation protection. This is mainly because the source of radiations are directional, dynamic, pulsed and a mixture of different types. In conventional dosimetry, measurements are done in the units of the quantities in which the radiological protection limits are expressed. In the accelerator environment, measurement or computation of energy and angular distribution of radiations is preferred instead. Wherever measurements are difficult or at times impossible to carry out, the radiation protection activities puts a high premium on computational dosimetry.

Computational radiation dosimetry involves the calculation of the energy imparted by radiation per unit mass and the relation of this parameter to biological effects, such as the risk of cancer induction or cell death, or damage to materials in intensive radiation fields. Such computations are necessary for radiation protection purposes in practically all uses of ionizing radiation. To be effective, a computational dosimetry system has to comprise three key elements: an accurate computer model of the human body, a robust numerical technique and appropriate testing protocols. Viewed as the sub-discipline of computational physics, computational dosimetry is devoted to radiation metrology. Computational simulations directed at basic understanding and modeling are important tools, provided by computational dosimetry, while another very important application is the support that it can give to the design, optimization, and analysis of experiments.

For more than four decades, the Department of Atomic Energy in India has ensured that nuclear facilities are designed and operated safely. As a result, a sound regulatory system has evolved through a series of government acts and rules. The Atomic Energy Regulatory Board (AERB) is mandated to review and authorize the safety of nuclear power plants, fuel cycle facilities and particle accelerators for their siting, construction, and operation. Authorization at each stage is preceded by a detailed review from three different levels. The AERB has put in place, a three-tier review system to provide a comprehensive review of the safety status of nuclear installations and enforcement of safety regulations during the operational phase of nuclear installations.

This article describes the scope and objective of radiation protection programme in general, with special emphasis on DAE installations. Then it will briefly review the concept of dose in connection with radiological safety and the recent recommendations of the International Commission on Radiological Protection (ICRP). It will also brief the salient features of radiological safety in each of the different types of nuclear installations. Finally, our stand on the protection of the environment and non-human biota, will be reviewed.

The Philosophy of Radiation Protection

The primary aim of the radiation protection discipline is to establish an appropriate level of protection for people and the environment against the detrimental effects of radiation exposure, without unduly restricting the desirable human actions that may be associated with such exposure. This aim cannot be achieved solely on the basis of scientific knowledge on radiation exposure and its health effects. It requires a model for protecting humans and the environment against radiation. Such models are formulated, based on scientific knowledge and on expert judgment [1]. Scientific data, such as those concerning health risks attributable to radiation exposure, are a necessary pre-requisite, but societal and economic aspects of protection have also to be considered. All of those concerned with radiological protection, have to make value judgments about the relative importance of different kinds of risk and about the balancing of risks and benefits. In this, radiological protection is not different from other fields concerned with the control of hazards. In this context it is imperative that the basis for, and distinction between, scientific estimations and value judgments should be made clear, whenever possible, so as to increase the transparency, and thus the understanding, of how decisions have been reached.

Radiological protection deals with two types of harmful effect, namely, deterministic and stochastic. High doses will cause deterministic effects, often of an acute nature, which only appear if the dose exceeds a threshold value. Both high and low doses may cause stochastic effects (cancer or heritable effects), which may be observed as a statistically detectable increase in the incidences of these effects occurring long after exposure. For stochastic effects a Linear-Non-Threshold (LNT) model is adopted [1], which is a dose-response model based on the assumption that, in the low dose range, radiation doses greater than zero will increase the risk of excess cancer and/or heritable disease in a simple proportionate manner. The probabilistic nature of stochastic effects and the properties of the LNT model make it impossible to derive a clear distinction between 'safe' and 'dangerous', and this creates some difficulties in explaining the control of radiation risks. The major policy implication of the LNT model is that some finite risk, however small, must be assumed and a level of protection established based on what is deemed acceptable. In protecting individuals from the harmful effects of ionising radiation, it is the control (in

the sense of restriction) of radiation doses that is important irrespective of the type of source.

The system of radiological protection aims primarily to protect human health. Its health objectives are relatively straightforward: to manage and control exposures to ionising radiation so that deterministic effects are prevented and the risks of stochastic effects are reduced to the extent reasonably achievable. In contrast, there is no simple or single universal definition of 'environmental protection' and the concept differs from country to country and from one circumstance to another.

In India, our aim is to adopt a policy of preventing or reducing the frequency of deleterious radiation effects to a level where they would have a negligible impact on the maintenance of biological diversity, the conservation of species, or the health and status of natural habitats, communities and ecosystems. In achieving this aim, it may be noted that exposure to radiation is but one factor to consider, and is often likely to be a minor one.

Because of the variety of radiation exposure situations and of the need to achieve a consistency across a wide range of applications, DAE has established a formal system of radiological protection aimed at encouraging a feasible and structured approach to protection. The system has to deal with a number of sources of exposure, some already being in place, and others that may be introduced as a matter of choice by society, technology or as a result of emergencies. These sources are linked by a variety of interconnected events and situations leading to exposure of individuals, groups, or entire populations, both in the present and in the future. The system of protection has been developed to allow this complex network to be treated by a logical structure.

The system of protection of humans is based on the use of a) reference anatomical and physiological models of the human being for the assessment of radiation doses, b) studies at the molecular and cellular level, c) experimental animal studies, and d) epidemiological studies.

Epidemiological and experimental studies have resulted in the estimation of risks associated with the external and internal radiation exposure. For biological effects, the data come from human experience, supported by experimental biology. With neutrons, the difference between the external and the internal field can be substantial for a large receptor, such as the human body. One reason is degradation of the neutron energy within the body. Another, even more important reason, is that thermal neutron capture generates a substantial component of gamma rays in the body. The resulting large difference between the external and the internal radiation field implies a considerable numerical difference between radiation weighting factors that are related to the external field and radiation weighting factors for the internal field. If a small specimen of tissue is irradiated by neutrons, the absorbed dose is mostly due to recoil protons or heavier recoils from neutron collisions, or neutron induced nuclear reactions. For fast neutron radiation

fields, the neutron moderation in a small specimen will be minor: hence, only very few photons from thermal neutron capture are generated and absorbed in the specimen. The absorbed dose in the tissue, due to the external neutron field, is therefore nearly equal to the absorbed dose from the charged neutron recoil particles. When larger tissue volumes, e.g. mice, rats, or humans, are irradiated, the situation becomes increasingly more complex because of the mixed radiation field in the body.

Concept of Dose as an Operational and as a Protection Quantity

Dose, in the field of radiation protection and dosimetry, is conventionally understood as energy transfer from ionising radiation into substantial volumes of body tissue, expressed as Joules per kilogram, revealing the pivotal role of physics in this area. Absorbed Dose is the amount of energy transferred into body tissue. This energy transfer is averaged over large volumes of tissue, for example, whole organs, the whole body, or even entire populations - as in the case of the collective doses. However, it is well known that the vital target for radiation damage is not the whole body but individual cells, or the DNA to be more specific. So, the important effects are happening at the level of the individual cell, and we should remember that cancers are "monoclonal" - that is, DNA analysis of cancerous tissue indicates that all the cells are descended from a single mutated cell.

Defining quantities like the dose equivalent or equivalent dose is an attempt to consider the biological effects of radiation and to solve the problem that has been created by concentrating on the physical (and perhaps the only measurable) quantity, the absorbed dose. Dose equivalent is obtained using a factor by which Absorbed Dose is multiplied to allow for differences in biological effectiveness of different types of radiation. This gives rise to the concept of Relative Biological Effectiveness (RBE) and the radiation weighting factor, for the type and energy of radiation, incident on the body. The resulted weighted dose is designated as the organ- or tissue-equivalent dose. The sum of the organ-equivalent doses weighted by the ICRP organ-weighting factors, is termed the effective dose. None of these quantities are measurable, nor are derivable using the laws of physics. Measurements can be performed in terms of the operational quantities, ambient dose equivalent, and personal dose equivalent. These quantities continue to be defined in terms of the absorbed dose at the reference point weighted by the quality factor, which is a quantity dependent on the Linear Energy Transfer (LET) of the radiation. The ambient dose equivalent is of great utility in some aspects of dosimetry but there are significant problems with its application to neutron dosimetry, particularly at high energies.

Radiation damage is caused by discrete events - single particles passing through tissue. Cells are either hit or they are missed. If they are hit, the energy transfer (dose) can be high; if not, then the dose is zero. Cells that are hit may be damaged; the damage may or may not be repairable. If it is

not repairable then the cell dies and causes no further problems, but if the damage is repaired it may be improperly repaired, passing defects on to daughter cells. There are newly discovered field effects, which mean that cells, near a cell that is hit, may get the same symptoms as if they themselves had been hit (the bystander effect), and genomic instability which shows up many cell generations after the exposure. These amplify the error in the conventional view, since there are even more effects at low dose.

Every single radiation track may cause a mutation, which may turn out to be deleterious or fatal to the individual person or to his/her descendants. Until one gets into the realm where the exposure is so high (acute) that the results can be predicted with fair certainty (deterministic effects), every exposure is associated with chance - harm may or may not happen, and those that do happen, may not be detectable. These are known as stochastic effects. Some people and some cell types are more susceptible, and some stages of development (e.g. fetus) are more sensitive. In other words, it's a matter of possibilities. Such effects do not vary in severity, but they do vary in frequency in proportion to dose. The shape of the dose-response curve is, however, disputed - it's unlikely that effects are strictly proportional to dose.

Recommended Values of Radiation Weighting Factor

The report ICRP-92 [2] accepts that change is necessary in the radiation-weighting system. In ICRP-92, a major effort is directed towards the development of an average radiation-weighting factor applicable to the whole body. Even if this goal is achieved, the practical utility of this factor at high energies is not at all clear. The radiation weighting factor is not comparable with the LET-dependent quality factor, but may correctly be compared with other average factors, such as the mean or effective quality factor for the whole body. In turn, the radiation weighting factor must therefore be regarded as a member of the family of average quality factors. There is, already then, an existing indirect and complicated link between the two quantities but that cannot be simply expressed in a functional form. Furthermore, it is clear that no simple or self-evident relationship exists between any member of the family of average radiation-weighting factors and some weighted average linear energy transfer (LET) of the incident radiation. In any event, such a relationship will generally be complex, particularly for neutrons and all high-energy radiations. There also remains the added complication of, to which measure of absorbed dose the approximate radiation weighting factors are to be applied. At high energies, particularly when radiation equilibrium has not been established, both the absorbed dose and LET-spectrum vary within the body.

Recent Recommendations of the ICRP and its Implications

Following an intense debate for about a decade, involving scientists, regulators and users, the ICRP in 2007 has published its general recommendations in ICRP

publication 103 [3], replacing the previous 1990 recommendations [1]. In this recent report ICRP has retained the concept of the tissue weighting factor (w_T) and the radiation weighting factor (w_R) but with modified values. The w_R value for protons has been reduced from 5 to 2, while for neutrons; a new continuous function has been defined. For neutrons, the w_R values have been reduced mainly in two energy regions; below 1 MeV and above 50 MeV. Compared to ICRP-60 [1] the number of specified organs and tissues has been increased and tissue weighting factors (w_T) have been changed in ICRP-103 [3]. The w_T values have been lowered for the gonads from 0.2 to 0.08 and increased for the breast and the remaining organs, from 0.05 to 0.12. Using a single set of tissue weighting factors for all human, ignoring the effect of sex, age and other individual properties, is considered to be an acceptable simplification by the ICRP. The definition of operational quantities like the ambient dose equivalent has not been changed in ICRP-103, and hence with the lower estimated effective dose in the case of neutrons (due to lowering of w_R), the ambient dose equivalent now gives a more conservative estimate of the effective dose. According to ICRP-103, the effective dose is to be used for prospective dose assessment for planning and optimization in radiological protection, and is not recommended for epidemiological evaluations. In ICRP-103, it is also stated that the values of w_T are finally selected by “judgment”, based on experimental radiobiological data. In fact, it appears that such a judicious choice has been based more on practicability, rather than on firm radiobiological knowledge, since data for high energy neutrons are scanty.

ICRP-103 has recommended introducing sex-specific voxel phantoms, to represent the reference male and the reference female, for future update of organ dose as well as effective dose conversion coefficients, for both internal and external radiation sources. Technical descriptions of the voxel phantom are released as a common ICRP/ICRU publication ICRP-110 (ICRP, 2009). The report ICRP-110

[4] describes, along with the development and intended use of the computational voxel phantom, graphical illustrations of conversion coefficients for some external and internal exposures, computed using several Monte Carlo simulation codes. From the recent calculated results following the new recommendations, it is apparent that the change in w_T or incorporation of the voxel geometry does not have any significant effect on the calculated effective dose. For neutrons, the only noticeable change is because of change in w_R values below 1 MeV.

Calculation of organ dose from internal or external exposure involves complex simulation process, where detailed interactions of radiations of different types with different elements in the human body, and all the physical processes involved, need be considered. In Table 1, we give an illustrative example of such calculated organ doses, where high energy neutrons produced due to nuclear interaction of 144 MeV ^{12}C ions with thick Ti and Ag targets are incident on the front face of the human body (antero-posterior), and when the person is standing at different angles with respect to the projectile (^{12}C ions) direction. In the simulation production of secondary charged and uncharged particles, their interactions and transport through human tissue are considered in detail. As we can see, the absorbed dose is dependent on the organ type, its location inside the human body, the angle with respect to the projectile direction, and on the mass number of the target element.

ICRP recommends a model for the assessment of detriment. Because of intrinsic uncertainties in the fundamental science, the model is somewhat approximate. The model has two components: physical and biological. Dosimetrists determine the physical components of this model with high precision and good absolute accuracy. The biological components of the model necessarily have poor absolute accuracy, mainly because of the absence of experimental data.

TABLE 1: Absorbed dose D (with errors in parentheses) due to antero-posterior exposure to neutrons from the two reactions $^{12}\text{C}^{+5} + ^{\text{nat}}\text{Ti}$ and $^{12}\text{C}^{+5} + ^{\text{nat}}\text{Ag}$ at 12 MeV/amu.

Organ	Reaction	Absorbed dose D (error) ($\times 10^5$ fGy ion $^{-1}$) for the angle			
		0°	30°	60°	90°
Bladder	$^{12}\text{C} + \text{Ti}$	1.7E+2(3.1)	3.1E+1(0.5)	1.2E+1(0.4)	2.0E+0(0.1)
	$^{12}\text{C} + \text{Ag}$	8.5E+1(1.3)	2.2E+1(0.4)	1.1E+1(0.3)	3.7E+0(0.1)
Bone marrow	$^{12}\text{C} + \text{Ti}$	1.4E+2(2.2)	2.5E+1(0.3)	1.0E+1(0.3)	1.6E+0(0.1)
	$^{12}\text{C} + \text{Ag}$	5.5E+1(0.85)	1.4E+1(0.3)	6.6E+0(0.2)	2.3E+0(0.1)
Breast	$^{12}\text{C} + \text{Ti}$	1.7E+2(3.0)	3.1E+1(0.5)	1.3E+1(0.4)	2.1E+0(0.1)
	$^{12}\text{C} + \text{Ag}$	8.6E+1(1.3)	2.2E+1(0.4)	1.1E+1(0.3)	3.1E+0(0.2)
Gonads	$^{12}\text{C} + \text{Ti}$	1.6E+2(2.9)	3.0E+1(0.5)	1.2E+1(0.4)	1.9E+0(0.1)
	$^{12}\text{C} + \text{Ag}$	8.1E+1(1.2)	2.0E+1(0.4)	10.0E+0(0.3)	3.5E+0(0.2)
Liver	$^{12}\text{C} + \text{Ti}$	1.5E+2(2.8)	2.8E+1(0.5)	1.1E+1(0.4)	1.8E+0(0.1)
	$^{12}\text{C} + \text{Ag}$	7.6E+1(1.13)	1.9E+1(0.4)	9.3E+0(0.3)	3.2E+0(0.2)
Lung	$^{12}\text{C} + \text{Ti}$	1.5E+2(2.8)	2.7E+1(0.4)	1.1E+1(0.3)	1.7E+0(0.1)
	$^{12}\text{C} + \text{Ag}$	7.3E+1(1.1)	1.8E+1(0.4)	8.9E+0(0.2)	3.1E+0(0.2)

Radiation protection in Nuclear Reactors and fuel Cycle Facilities

Nuclear Reactors

The operation and periodic maintenance of nuclear reactors is always under strict radiological safety surveillance, and as such, do not pose any significant radiation hazard. However, accidental conditions in nuclear reactors have a high potential for release of radioactive materials in the environment. Such potentials may turn out to be notional, in view of passive natural attenuating mechanisms and comprehensive engineered safeguard provided in modern plants.

In a nuclear reactor, the bulk of the radioactivity normally resides in the fuel and is well contained, as long as the fuel sheath is adequately cooled and protected from mechanical damage. For any significant release of radioactivity from the fuel, it must be overheated and subsequently melt. Earlier assumptions were that this would be likely in the event of a major loss of coolant accident (LOCA) that resulted in a core melt. Experience has proved otherwise, in any circumstances related to modern reactor designs. In light of better understanding of the physics and chemistry of material in a reactor core under extreme conditions, it became evident that even a severe core melt, coupled with breach of containment, could not create a major radiological disaster from any recently developed reactor design. Studies of the post-accident situation at Three Mile Island (where there was no breach of containment) support this finding. The physics and chemistry of a reactor core, coupled with but not wholly dependent upon the engineering, mean that the consequences of an accident are likely to be much less severe than those from other industrial or energy sources.

Nuclear Fuel Cycle Facilities

Nuclear fuel cycle facilities, particularly the reprocessing part, pose a range of safety challenges, including criticality, radiation, chemical toxicity, fire and explosions. These challenges can pose hazards to workers, members of the public, and the environment, if they are not properly controlled. Taking these hazards into account, national regulatory authorities have established a variety of regulatory frameworks, including prescriptive- and performance-based standards, to reduce potential risks from the hazards.

The nuclear fuel cycle begins with mining of uranium. When an economically viable deposit is located, the mineral is mined and processed to yield nuclear grade uranium. The first phase generally ends with the production of chemical concentrates of uranium. The remaining waste that contains all decay products of uranium, is separated into coarse and fine particulates. While the coarser fraction is returned to the mine for filling up, the finer fraction is pumped to a "tailings pond". In the pond, the solids settle and the supernatant liquid is drained out. There is no significant radiological

hazard to the workers or the public, from this stage of the fuel cycle.

After being used in the nuclear reactor, the spent fuel is transported to a reprocessing plant to recover the remaining fissile materials: uranium-235 and various plutonium isotopes. The principle of operation for a reprocessing plant is to dissolve the irradiated reactor fuel elements to extract the useful isotopes of uranium and plutonium. This is typically accomplished by removing fuel elements from the fuel assembly components, using first a mechanical process and then a chemical dissolution process. The enriched chemical slurry, containing uranium and plutonium, is subjected to a solvent extraction process, where the desirable uranium and plutonium isotopes are removed and purified, to be reintroduced back into the fuel cycle.

In the nuclear fuel cycle, the reprocessing stage has the potential hazard of contamination and release of radioactive materials to the environment. Stripping and dissolving reactor fuel elements liberates large inventories of volatile and gaseous fission products, which need to be collected. As a consequence, the radioactive waste management system for reprocessing facilities, is made robust, to prevent the routine or accidental release of radioactive materials. Because of the high radiation levels, reprocessing plants are designed for remote, automated operations. Reprocessing stages, which involve uranium and plutonium concentrates, are also designed to prevent any possibility of a criticality occurrence.

The nuclear fuel cycle facilities differ from reactors in several important aspects. First, they employ a greater diversity of technologies and processes. Second, fissile material and wastes are handled, processed, treated, and stored throughout the nuclear installations. These treatment processes use large quantities of hazardous chemicals which can be toxic, corrosive or combustible. Consequently, the materials of interest to nuclear safety are more distributed throughout the nuclear installations, in contrast to reactors where the bulk of the nuclear material is located in the reactor core or fuel storage areas. For example, the nuclear materials in fuel cycle facilities are often present in solutions that are transferred between vessels used for different parts of the process, whereas at reactors the nuclear material is generally concentrated in the solid fuel. This greater distribution and transfer of material requires greater attention to account for the nuclear material throughout the installations, not just for safeguards purposes, but also to ensure nuclear safety. Third, the facilities are often characterized by more frequent changes in operations, equipment and processes, which are necessitated by treatment or production campaigns, new product development, research and development, and continuous improvement. Fourth, the fuel cycle facilities rely to a greater extent on operator and administrative controls to ensure safety, and less on active and passive engineered controls. Fifth, for these facilities, maintaining criticality is not a part of the operational process, thus usually there are systems designed to prevent the criticality

occurrence, but not designed for fast 'shutdown', as such systems exist at nuclear research and power reactors. Finally, fuel cycle facilities have a greater requirement, inherent in the process, for operator 'hands-on' involvement.

It is important to recognize that the hazards vary from facility to facility, depending upon the processes employed, age, throughput, inventory, and material condition. For example, the radiation hazards at a vitrification facility are generally greater than those at a uranium mill, although both types of facilities pose some risk to workers and members of the public. Hazards may also vary depending upon the specific conditions at the facilities. For example, processing and storage of UF₆ may pose criticality hazards if the uranium is enriched. However, if the uranium is natural, criticality is not credible. Similarly, criticality hazards may not be credible at a vitrification facility if the high activity waste-stream has been sufficiently processed to remove significant quantities of fissile materials. However, criticality hazards may exist under abnormal operating conditions (for example leading to greater amount of fissile material in waste streams) or if fissile materials are intentionally immobilized using vitrification. Although some similar safety hazards may be posed at reactor and fuel cycle facilities, such as radiation hazards, the differences between reactor and fuel cycle facilities spawn some different safety considerations at the fuel cycle facilities. These differences have been taken into consideration during design, construction, operation and decommissioning stages.

Criticality Safety Considerations

Criticality safety is one of the dominant safety issues for the fuel cycle facilities. These facilities employ a great diversity of technologies and processes; thus the materials of interest to nuclear safety are more distributed throughout these nuclear fuel cycle facilities. They may be used not only in a bulk form (fuel pellets, fuel elements, fuel rods, fuel assemblies, and so on), but in the distributed and mobile forms as well (different kinds of solutions, slurries, gases, powders, and so on). This is in contrast to reactors, where the bulk of the nuclear material is located in the reactor core or fuel storage areas. As a result, the fissile materials may accumulate in some parts of the equipment and may also escape from the facility, as a result of equipment leakage. The distribution and transfer of potentially critical nuclear material, requires operator attention, to account for this material, throughout the installation, and thus ensure that nuclear criticality safety is maintained, and to prevent the potentially lethal effects of gamma and neutron radiation doses to workers, and the subsequent release of fission products from an inadvertent nuclear criticality.

All areas of fuel cycle facilities, which process or contain fissile material, need to be evaluated for criticality hazards, and this is done in DAE. The evaluation must show whether the presence of nuclear materials, with greater than natural enrichment, presents a credible scenario for an

inadvertent criticality, during the processing being conducted at the facility. As regards nuclear criticality, fuel cycle facilities may be split into two groups: (1) facilities where a criticality hazard is not credible — mining, milling, and conversion of natural uranium facilities, and (2) those where the criticality hazards may be credible — enrichment, reprocessing, fuel fabrication, fresh fuel storage (and transportation), spent fuel storage (and transportation), waste treatment and waste disposal facilities. Those facilities in group (2) are designed and operated in a manner that provides a high level of assurance that critical parameters and controls are followed. Designs of such facilities ensure sub-criticality in all areas, first by engineering design, utilizing where possible, 'criticality safe designed equipment'. Similarly, for the operation of these facilities, critical parameters and controls are maintained. This includes assurance that excessive amounts of fissile material do not accumulate above the specified limits in vessels, transfer pipes and other parts of the facility. To prevent inadvertent nuclear criticality, the process safety limits must not be violated, and the safety limits must have enough margins to preclude criticality during the postulated abnormal operating conditions. Particular attention is paid to fissile material in waste streams; process changes or modifications which may be inadequate (from the point of view of criticality); nuclear materials accounting and control procedures which may lack the appropriate accuracy to ensure sub-criticality; and controls which are used to prevent the accumulation of nuclear materials in zones which are not included within the design parameters of the installations (or equipment). Fuel cycle facilities with credible criticality hazards have in place the programme to ensure sub-criticality. Provision has been made to cope with an accident and to alarm the facility personnel, should an inadvertent criticality occur.

There are various methods by which the criticality can be controlled. These are mass-, volume/geometry-, concentration- and poison-control, etc.

Mass Control

Mass handled at a given location or in a single operation is restricted. Minimum critical (bare and water reflected) and safe mass limits for various fissile materials, as metal and in aqueous solution, are presented in tables below. The critical mass under the worst foreseeable condition, and applying proper safety factor given in the last column, is allowed to handle. When large quantities of fissile materials are to be handled, mass control may be unnecessary restriction and it may be essential to use other methods of control. In Table 2 and Table 3 we show the Monte Carlo calculated results of safe mass limits for ²³⁵U and ²³⁹Pu.

Geometry control: Method to employ geometrically favorable containers, so that solutions of any concentrations or up to a certain concentrations can be easily handled. It is designed in such a way that the high leakage of neutrons, prevents criticality. e.g:

TABLE 2. Safe mass limits for individual units- ²³⁵U

System	Critical Mass(kg)		Safe mass (kg)
	Bare	Water reflected	
Metal	47.0	22.0	10.0
Solution	1.4	0.82	0.35
Solution (75%)	1.45	0.84	0.36
Solution (30%)	1.6	1.0	0.44
Solution (10%)	2.	1.4	0.6
Solution (5%)	3.1	1.9	0.8
Solution (4%)	3.6	2.3	0.94
Solution (3%)	4.7	3.0	1.2
Solution (2.5%)	5.8	3.95	1.47

TABLE 3. Safe mass limits for individual units- ²³⁹Pu

System	Critical Mass(kg)		Safe mass (kg)
	Bare	Water reflected	
Metal (α phase) (19.6 gm/cc)	10.2	5.6	2.6
Metal (β phase) (15.2 gm/cc)	16.28	7.6	3.5
PuO ₂ (11.46 gm/cc)	21.61	10.76	4.63
PuC (13.6 gm/cc)	17.07	8.64	3.72
Pu solution	0.91.	0.51	0.22
U-233 metal	17.0	7.5	3.2
U-233 solution	1.2	5.9	0.25

- (i) an infinitely long cylinders where diameter is less than a certain limiting value,
- (ii) an infinite slab, where thickness of the slab is less than a certain limiting value.

The main advantage of geometry control is that in addition to increasing throughputs it gives complete freedom to the operator and does not involve any risk to human error. Table 4 gives the calculated critical diameters of cylinders (bare and water reflected).

Radiation safety is an important consideration at nuclear fuel cycle facilities. Special attention is warranted to ensure worker safety, because of their intimate contact with nuclear material in the process, which may include open handling and transfer of nuclear material in routine processing. Potential intakes of radioactive material require careful control, to prevent and minimize contamination, and to adhere to operational dose limits. In addition, releases of radioactive material into the facilities and through monitored and unmonitored pathways, can result in significant exposures, particularly from long-lived radio-toxic isotopes.

TABLE 4. Safe cylindrical diameter for individual systems

System	Critical diameter (inches)		Safe diameter (inches)
	Bare	Water reflected	
Pu -239 Metal	2.4	1.7	1.4
PuO ₂		2.96	2.5
Pu solution	8.3	4.9	4.2
U-235 metal	4.5	3.1	2.7
U-235 solution	8.5	5.4	5.0
Solution (75%)			5.2
Solution (30%)			6.3
Solution (10%)			8.2
Solution (5%)			10.25
Solution (4%)			11.2
Solution (3%)			12.8
Solution (2.5%)			14.5

Some facilities, such as fuel fabrication, reprocessing, and vitrification facilities, require careful attention to shielding design, containment, ventilation and maintenance procedures, to reduce external exposures. All facilities have in place, a radiation protection programme that is adequate to protect the radiological health and safety of workers and the public. To accomplish this, facilities evaluate and characterize the radiological risk, and typically provide sufficient robust controls, to minimize the radiological risks at the facility. Potential accident sequences are considered in assessing the adequacy of the controls, which aim to minimize radiological risk and contamination. Some of the fuel cycle facilities may pose special safety hazards because they produce large quantities of effluents, or they have the potential to produce highly hazardous effluents, to the environment. For example, uranium milling and processing, generate large quantities of radioactive and chemically toxic effluents that must be stored or disposed close to the point of generation, to avoid large expenses. Similar effluents can be generated by fuel fabrication facilities. Other facilities, such as reactors, and vitrification facilities have the potential to produce effluents to air and water with high concentrations of fission products and transuranic radionuclides that might pose risks to members of the public and the environment.

Environmental Considerations

It is recognized that the siting, construction, operation, modification and decommissioning of nuclear facilities, has the potential to adversely affect the environment, either directly or indirectly. Direct effects can occur during the preparation or use of the site, as when existing features are altered to make the site suitable for the facility, e.g., vegetation is removed or wetlands are drained so that foundations can be installed or an uranium ore body can be accessed by open pit mining. Other direct effects include

damage to vegetation, resulting from the release of toxic substances from a nuclear facility, such as metals contained in effluents and tailings from uranium mining and nitrogen oxides and fluoride compounds from uranium processing. The effects may arise indirectly, for example, due to the construction of a new road to provide access to a facility or a dam to provide a source of water, or even by eliminating the habitat of some species which is important to the ecology of the region in which the facility is located. In certain cases, there is also the potential for significant socio-economic effects from the installation, operation or decommissioning of nuclear facilities, due to factors such as the influx of new populations or changes to employment patterns, which result from commissioning or closing down the nuclear facility.

DAE has a full-fledged programme for environmental impact Assessment around Power plant site and other nuclear installations. This involves a comprehensive study of radionuclide migration through aquatic environment and atmospheric environment, before it reaches human population as well as non-human biota. The environmental survey laboratories (ESL), commissioned near all nuclear power plants, carry out intense measurements and analyses of environmental (atmospheric, terrestrial and aquatic) data to look for any possible increase in radionuclide concentration, above natural background levels, up to a distance of about 30 km from the nuclear plant site. The activities can be broadly categorised as follows.

Atmospheric Dispersion of Radionuclides

ESLs are involved in understanding the effect of atmospheric parameters such as wind speed, wind direction, thermal induced convection, etc on the physical transport of radionuclides, consequent to release from stack of a plant. Micrometeorology labs of ESLs use sophisticated instruments, such as SODAR (Sound Detection And Ranging) system and Ultrasonic anemometers, for wind profiling and measuring the atmospheric parameters such as roughness length, mixing height, temperature lapse rate, etc. Efforts are in progress to parameterise the physical processes taking place in the atmosphere, especially in complex terrains such as Kaiga and in sea coast (Coastal fumigation). The application of dispersion models are being tried and are being validated at various power plant sites.

Studies on wet and dry deposition of radionuclides, from air to soil and air to vegetation, are undertaken by various ESLs. R&D program is planned for understanding the physical process (Sorption/desorption equilibrium between rain droplet and surrounding air) during the process of rain-wash-out of particulates (^{137}Cs) and vapours (^{131}I , HTO).

Radio-ecological Studies

Radio-ecological studies are undertaken to understand the migration of radionuclides in terrestrial environment and aquatic environment. The migration of radionuclides is very complicated and is influenced by many physico-chemical properties of soil, plant and atmospheric components.

Studies are in progress to understand the influence of physical, chemical and biological processes involved in migration of radionuclides.

The system Soil → Soil solution → Plant is driven by the processes such as diffusion and osmosis.

Migration in aquatic environment: The migration in aquatic environment depends upon the physico-chemical properties of water and sediment underneath the water. ESLs are generating water quality data such as pH, conductivity, temperature, salinity, alkalinity, etc and sedimentological parameters such as particle size, organic content, etc.

1. Ecological Modelling: ESLs are developing mathematical models to quantify the uptake of radionuclides by general public and subsequent impact assessment.
2. Validation of models: ESLs proposes to establish experimental facility to conduct experiments to understand the influence of these physicochemical processes on the uptake of radionuclides by the plants. These experimental facilities will be used for validating the ecological models.
3. ESLs are also involved in the analysis of radionuclides and trace elements using instruments such as HPGe-gamma spectrometry system, Liquid scintillation counting system, Atomic Absorption Spectrometry system and Neutron Activation analysis.

Radiation Protection in Particle Accelerators

Particle accelerators have evolved over the last decades from simple devices to powerful machines and are having an increasingly important impact on research, technology, medicine and lifestyle. Requirements from new technological and research applications have emerged and the number of accelerator facilities in operation, being commissioned, designed or planned has significantly increased. A number of high energy, high current accelerators primarily for the application of accelerator driven technologies [5] like the ADSS, RIB facilities are being commissioned. The operating parameters (such as the beam energy, beam currents and intensities, targets composition, etc.) of these different facilities vary widely giving rise to new radiation protection and neutron dosimetry problems.

Accelerated charged particles, except for the singular phenomenon of synchrotron radiation, do not produce radiation unless there is some interaction with matter. The charged particles directly accelerated, and otherwise manipulated by the electromagnetic fields within the accelerator, are referred to as the primary particles or beam. If one considers primary particles incident upon a physical object such as a target, the yield of secondary particles like neutrons is a crucial parameter in radiation protection. Such neutron yields, dependent upon target material, thickness and incident projectile energy, are reported in terms of energy, and angular distributions. Particle accelerators can

be categorized as two types based on the type of the primary beam: electron accelerators and positive ion accelerators. In electron accelerators high energy gammas dominate the radiation environment while in positive ion accelerators neutrons are the dominant component. The neutron production mechanism is different in these two types of accelerators.

In an accelerator facility the following situations can contribute as a source of ionizing radiation depending on various beam-material interactions:

- During the acceleration process, a small fraction of the partially stripped ions will loose electrons due to interaction with the rest gas. These ions leave the acceleration path and hit the accelerator structure, thus inducing radiation. During the extraction of the beam in cyclic accelerators, some beam is lost, which when hits the accelerator structure.
- With the help of collimators and scrapers, the extracted beams are sometimes shaped into special geometries. These are strong sources of radiation, which need to be shielded locally by thick iron and concrete walls.
- The target to be experimentally irradiated is an important source of radiation.
- Finally, the beam, which has not undergone any interaction, is dumped into the 'beam dump' where all the energy is lost in nuclear reactions and electromagnetic stopping.

In addition, worst-case scenarios of, e.g., lost beams due to the malfunction of beam optics elements, cause high radiation fields in unwanted locations.

The large dynamic range of neutron/gamma energies, strong interference from other radiations as well as radio frequency waves and pulsed nature of the radiation field makes neutron dosimetry in the accelerator environment significantly different from other well established, conventional techniques. In an accelerator environment neutron dosimetry is also done for purposes other than radiological protection, e.g., to protect (from radiation damage) certain delicate instruments that are required to be placed close to the beam line for experimental or operational purposes. For radiological safety, neutron dosimetry in accelerators is done mainly for accidental exposures and environmental monitoring apart from routine radiation protection surveys. In accelerator environment, neutron energy spectra and, therefore, the doses have directional dependence with respect to the particle beam direction. Hence, measurements have to be done at different angles.

This is the major issue where accelerator dosimetry differs from the conventional. In the later case, measurements are done in the units of the quantities in which the radiological protection limits are expressed. In publication 60 ICRP recommended the effective dose as the quantity in which the dosimetric measurements are finally to be expressed [1]. In the accelerator environment,

measurement of energy and angular distribution of radiations is preferred. This is because of several reasons. First, necessary and more reliable instruments are available for such measurements. Secondly, the results of physical (distributions in energy and angle) measurements of the radiation field may be applied to a variety of tasks such as the design of accelerator shielding, prediction of induced activity and radiation damage etc. The effective dose or equivalent dose can also be estimated from such data using appropriate conversion factors. It is not possible, on the other hand, to estimate the energy distribution from the measured dose. Furthermore, the physical characterization of radiation field has the stability yet to be achieved by dose-equivalent quantities.

To have knowledge of the radiation environment in accelerators, though measurement is the best choice, it is not feasible to do so for all target-projectile combinations. Therefore, one has to rely heavily on computational procedures. Such computational techniques can be classified in two categories: (i) calculation of the source term for emitted radiations: (ii) transport of the radiations through shield materials. While radiation transport is a subject more or less standardized, calculation of source terms involves computations using complex nuclear reaction model codes. There are different computational techniques for different types of projectiles (e.g. electrons, light ions and heavy ions) as well as for different projectile energy ranges. Extensive studies and validation of the models using feedbacks from experimental measurements are necessary before they can be employed to generate the required data.

Measurements of thick target neutron yield distributions from light or heavy ion induced nuclear reactions provide useful data for radiological safety and medical applications of particle accelerators. The neutron yield and energy distributions are important parameters in neutron dosimetry and shielding studies of heavy-ion accelerators. Data on the energy-angular distribution of secondary neutrons from targets thick enough to stop the accelerated ions completely, known as the thick target neutron yield (TTNY), are essential to estimate source terms of the accelerator shield design. Such data are also useful to calculate the dose delivered to the patient by secondary neutron interactions during therapy with light or heavy-ions. Furthermore, these data are expected to provide some insight into the nature of the neutron spectra produced by interactions of heavy ions present in galactic cosmic rays with shielding materials used to protect humans engaged in long-term missions outside the geo-magnetosphere. Additionally, an analysis of such data gives insights into the nuclear reaction mechanisms involved, even though the emitted energy spectrum from a thick target is a superposition of spectra from different stages of a continuously degrading projectile energy. For thick stopping targets it is possible to make measurements at extreme forward angles with respect to the incident projectile direction, which is important since emission in the forward

direction essentially carries information about initial stages of the nuclear reaction mechanism.

Measurements of TTNY for the purpose of neutron dosimetry can also give important physical insights of the nuclear reaction mechanisms as well as can help fixing important input parameters or incorporate modifications in the existing nuclear reaction model codes [4-11] that can subsequently be utilized for theoretically computing TTNY data where experimental measurements have not been performed.

Shielding of Accelerators

Modern accelerators are capable of producing extremely high intensity mixed radiation fields. The goal of efficient accelerator-shield design is to attenuate these high radiation intensities to acceptable levels outside the shield and to do so at reasonable cost and, insofar as is practical, without compromising the utility of the accelerator for its designed purpose.

At high energy particle accelerators the design of adequate shielding and techniques of safety assessment becomes complex with increasing beam energy due to cascade phenomena. A high-energy hadron interacting with a nucleus typically creates a rather large number of short-lived particles (pions, kaons, etc.), as well as protons, neutrons and nuclear fragments. Another important result of high-energy interactions is the production of muons, which can represent a significant shielding problem. The interactions of the high energy beams can also produce significant radioactivation of the beamline components and the surrounding environment.

There are three principal reasons why accelerator and beamline components are shielded for radiation protection purposes:

- to reduce the dose received by personnel during beam-on conditions;
- to reduce exposure to personnel from highly radioactive targets and beam absorbers, etc.; and
- to prevent contamination of the environment by creation of radioactivity in locations outside of areas controlled for personnel protection.

The major issues for the shielding design are bulk shielding, duct streaming, skyshine and activation. Because of the uncertainties in primary beam loss conditions except in beam dumps and targets, a serious problem in shield design arise and thus only semi-empirical formulas and simplified methods can practically be applied for most of the design study. The most important feature of neutron shielding at higher energy accelerators is the fact that the attenuation length becomes almost constant at high energy. As the energy increases, the neutron inelastic cross sections also increase rapidly until about 25 MeV. Then they level off and fall rapidly with energy in the region $25 < E_n < 100$ MeV to a value which becomes independent of energy. At high energies development of hadronic and electromagnetic

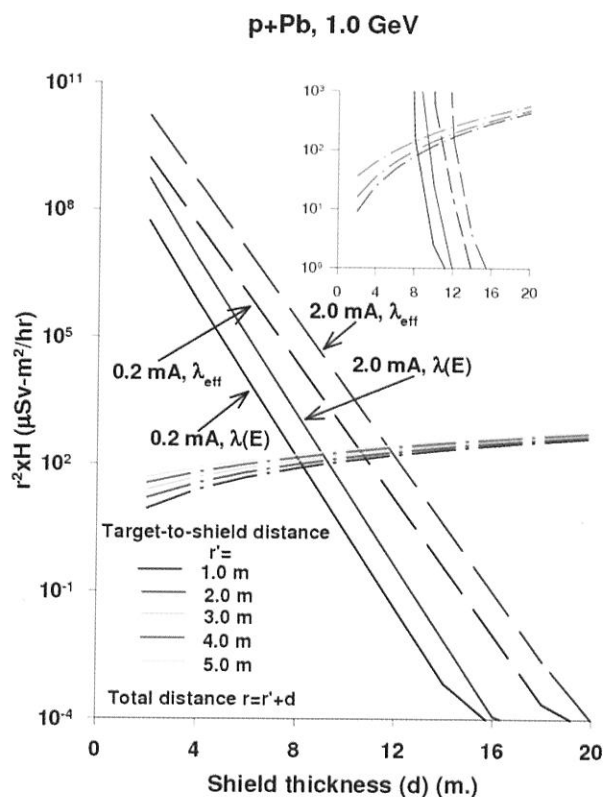


Fig. 1 Transmitted dose through different shield thicknesses and the regulatory limits (horizontal curves), both multiplied by r^2 (the square of the distance from the target).

casades complicate the calculations and detailed Monte Carlo simulations are required. Such simulations take into consideration all physical processes, reaction models and interaction models involved. Finally, the selected shield thickness should comply with the regulatory requirement of dose rate outside the shield. As an illustrative example, in Fig. 1, we plot the transmitted dose through concrete shields of different thicknesses and also the regulatory limits (horizontal curves) for different distances from the target for 0.2 mA and 2.0 mA proton beam current of 1 GeV. The thickness of concrete shield corresponding to the intersection point is the required shield thickness complying with the regulatory constraint [5].

All accelerators evidence the need to control the transmission of neutrons by penetrations since all have access-ways to permit entry of personnel and equipment as well as penetrations for cables and for radio-frequency (RF) waveguides. Personnel access penetrations will typically have cross-sectional dimensions of about 1 meter by 2 meters (door-sized) while utility ducts will generally be much smaller, typically no larger than 0.2 m by 0.2 m. Often the utility penetrations are partially filled with cables and other items and even cooling water in pipes.

Thin roof shielding represents a serious problem that has plagued a number of accelerators. The phenomenon, known as skyshine, is the situation in which the roof of some portion of the accelerator or an associated experimental facility is shielded more thinly than are the sides of the same enclosure that directly view the radiation source. The radiations get scattered by air molecules and come back to the ground level at a distance from the facility. Neutron skyshine, while it is usually "preventable" through the application of sufficient roof shielding, has been encountered at nearly all major accelerators. This has resulted either from lack of consideration of it at the design stage or from the need to accommodate other constraints such as the need to minimize the weight of shielding borne by the roofs of large experimental halls.

Based on several years of experience at accelerator laboratories and consequent to the research and development efforts the radiation safety programmes at particle accelerators are emerging with significant improvements. Operational flexibility, such as high beam current and multi-beam capability together with research-oriented requirements from Spallation Neutron Source (SNS), Accelerator Driven Systems (ADS) and Radioactive Ion Beam facilities (RIB) has placed new demands on radiation protection systems. Development of sophisticated computational techniques, particularly those based on Monte Carlo simulations, has made it possible to undertake otherwise intractable calculations. Results of these calculations do serve as necessary adjuncts to experiments where measurements are too difficult or not feasible. Even then, radiation dosimetry at particle accelerators particularly with emerging scenarios is facing problems yet to be resolved satisfactorily.

Summary

Radiological safety programmes for the nuclear and radiation generating facilities like nuclear power and research reactors, nuclear fuel cycles and other radiation generating facilities like accelerators, irradiators etc. have been reviewed. Though the basic philosophy of radiation protection remains the same for all of them, still there are certain important differences based on their different modes of operation. In nuclear fuel cycle facilities special attention is warranted to ensure worker safety because of their intimate contact with nuclear material in the process, which may include open handling and transfer of nuclear material in routine processing. Environmental impact of the releases from nuclear power plants and reprocessing facilities needs to be assessed carefully. High energy particle accelerators generate complex radiation fields and requires advanced

computational and measurement techniques for proper shield design and radiation dosimetry. The International Commission on Radiological Protection update from time to time their recommendations, which serve as useful guidelines for implementation of proper radiation protection programmes at nuclear installations with newer technologies and unconventional radiation environment.

References

1. ICRP Publication 60, "Recommendations of the International Commission on Radiological Protection", Ann. ICRP 21 (1-3), (1991). Elsevier Science, Oxford.
2. ICRP Publication 92, "Relative Biological Effectiveness (RBE), Quality Factor (Q), and Radiation Weighting Factor (W_R)", International Commission on Radiological Protection, (2003). Elsevier Science, Oxford.
3. ICRP Publication 103, "The 2007 Recommendations of the International Commission on Radiological Protection", International Commission on Radiological Protection, (2007). Elsevier Science, Oxford.
4. ICRP Publication 110, "Adult Reference Computational Phantom", International Commission on Radiological Protection, 2009. Elsevier Science, Oxford.
5. P.K. Sarkar and Maitreyee Nandy, "Accelerator Driven Systems from the Radiological Safety point of view", PRAMANA, 68(2) 225-234, (2007).
6. P.K. Sarkar, T. Bandyopadhyay, G. Muthukrishnan and S. Ghosh, "Neutron production from thick targets bombarded by alpha particles: Experiment and theoretical analysis of neutron energy spectra.", Physical Review C 43, (1991) 1855-1866.
7. N. Chakravarty, P.K. Sarkar, M. Nandy and S. Ghosh, "Excitation function measurement and reaction mechanism analysis for alpha induced reactions on 197-Au."- Journal of Physics G 24, (1998) 151-166.
8. M. Nandy, S. Ghosh and P.K. Sarkar, "Angular distribution of pre-equilibrium neutron emissions from heavy-ion reactions", Physical Review C 60, (1999) 044607.
9. M. Nandy, T. Bandyopadhyay and P.K. Sarkar, "Measurement and analysis of neutron spectra from a thick Ta target bombarded by 7.2A MeV 16-O beam" Physical Review C 63, (2001) 034610.
10. D. Dhar, S.N. Roy, M. Nandy and P.K. Sarkar, "Analysis of neutron emission spectra for 30-50 MeV alpha-particle induced reactions in thick targets", Physical Review C 67, (2003) 064611.
11. M. Maity, Maitreyee Nandy, S.N. Roy and P.K. Sarkar, "Systematics and empirical expressions for neutron emission from thick targets in α -induced reactions", Physical Review C 71, (2005) 034601.
12. C. Sunil, M. Nandy, P.K. Sarkar, "Measurement and analysis of energy and angular distributions of thick target neutron yields from 110 MeV ^{19}F on ^{27}Al ", Physical Review C 78, (2008) 064607.



Dr. P.K. Sarkar (1951 born) joined the Health Physics Division of BARC in 1970 and is presently heading that Division. He is a Professor of the Homi Bhabha National Institute. He is supervising environmental radioactivity surveillance at all nuclear power plants as well as in and around Trombay, radiological safety surveillance of fuel reprocessing plants in Tarapur and Kalpakkam. He has also been supervising internal dosimetry activities and the computational safety analysis of various nuclear facilities. He has been supervising the radiological safety aspects of particle accelerators of DAE. He has been associated with the R&D work related to radiation safety aspects of accelerators and accelerator-driven systems, as well as related nuclear data generation and evaluation. He has carried out development of dosimetric techniques for high energy neutrons, high and very low energy gammas. He has worked in the field of computational radiation physics, using Monte Carlo simulations, non-linear optimizations and random set theory. He has done theoretical simulations related to cosmic ray muon radiography. He has been engaged in the probabilistic safety analysis of high energy, high current accelerators and accelerator driven systems. He has about 80 publications in international journals.

For Limited Circulation Only

Printed & Published by :

Dr. A.V.R. Reddy, Secretary, Indian Association of Nuclear Chemists and Allied Scientists (IANCAS)
(Registration No. MAH 232/1984 GBBSD) on the behalf of IANCAS, C/o. Radiochemistry Division,
Bhabha Atomic Research Centre, Mumbai 400 085.

Printed at

Perfect Prints, 22/23, Jyoti Industrial Estate, Nooribaba Dargah Road, Thane 400 601.
Tel. : (022) 2534 1291 Telefax : (022) 2541 3546, E-mail : perfectprints@gmail.com

Edited by

Dr. R.V. Kamat, Fuel Chemistry Division,
Bhabha Atomic Research Centre, Mumbai 400 085.